TESIS DE LA UNIVERSIDAD DE ZARAGOZA
2023
87

Álvaro Montesinos Joven

Dynamics of almond (Prunus amygdalus (L.) Batsch, syn P. dulcis (Mill.)) tree architecture and scion/rootstock interaction

Director/es
Grimplet, Jerome Bruno
Rubio Cabetas, María José

ISSN 2254-7606

Prensas de la Universidad
Universidad Zaragoza

ISSN 2254-7606

Universidad Zaragoza
1542

Tesis Doctoral

DYNAMICS OF ALMOND (PRUNUS AMYGDALUS (L.) BATSCH, SYN P. DULCIS (MILL.)) TREE ARCHITECTURE AND SCION/ROOTSTOCK INTERACTION

Autor

Álvaro Montesinos Joven

Director/es

Grimplet, Jerome Bruno
Rubio Cabetas, María José

UNIVERSIDAD DE ZARAGOZA
Escuela de Doctorado

Programa de Doctorado en Bioquímica y Biología Molecular

2022

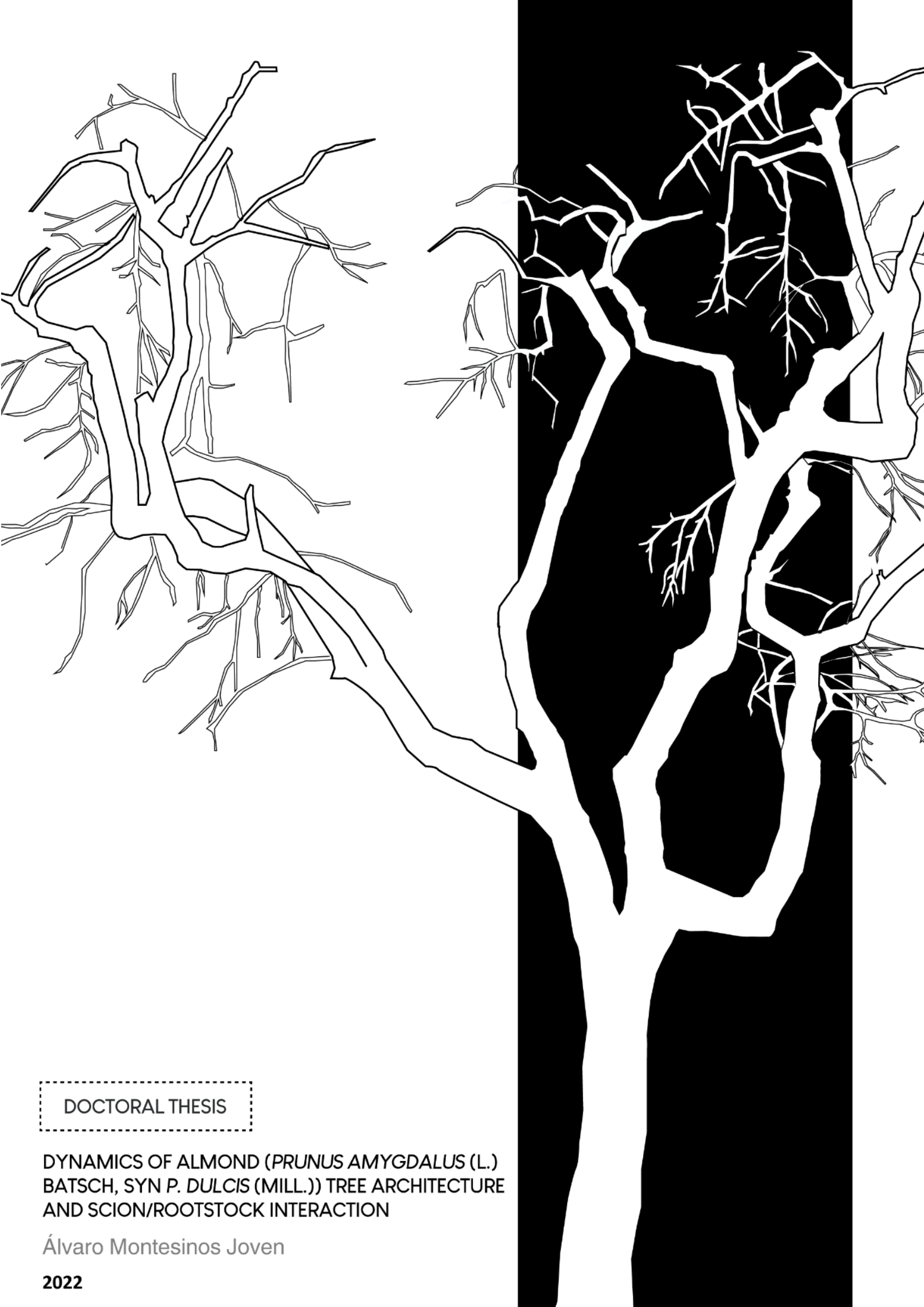

DOCTORAL THESIS

DYNAMICS OF ALMOND (*PRUNUS AMYGDALUS* (L.) BATSCH, SYN *P. DULCIS* (MILL.)) TREE ARCHITECTURE AND SCION/ROOTSTOCK INTERACTION

Álvaro Montesinos Joven

2022

Universidad de Zaragoza
Facultad de Ciencias

Centro de Investigación y Tecnología
Agroalimentaria de Aragón

DOCTORAL THESIS

DYNAMICS OF ALMOND (*PRUNUS AMYGDALUS* (L.) BATSCH, SYN *P. DULCIS* (MILL.)) TREE ARCHITECTURE AND SCION/ROOTSTOCK INTERACTION

Presentada por Álvaro Montesinos Joven para optar al grado de doctor por la Universidad de Zaragoza

Programa de Doctorado en Bioquímica y Biología Molecular

Dirigida por:

Dra. María José Rubio Cabetas y Dr. Jérôme Grimplet

Zaragoza, diciembre de 2021

Agradecimientos

Después de cuatro años y una pandemia, hay muchas personas, en el CITA y fuera, a las que me gustaría agradecer por su inestimable ayuda y apoyo, tanto profesional como personal.

Para empezar, quisiera agradecer a la Dra. María José Rubio Cabetas por confiar en mi desde el primer momento para realizar esta tesis. Gracias Mariajo, por tu guía y por darme la libertad y el espacio para poder desarrollar iniciativa propia como científico y como persona.

Gracias al Dr. Jérôme Grimplet por haber sido el mejor director que uno podría esperar y por todo lo que he podido aprender con él. Aunque bromeemos al respecto, tienes todo mi respeto y estima. Jérôme, sin ti esta tesis no habría salido adelante.

A la Dra. María Luisa Peleato por su cercanía y disponibilidad como tutora.

I am grateful to Dr. Chris Dardick, which it was a truly pleasure working with, for his mentoring during my stage at the USDA and his collaboration in the Chapter 2. In addition, I want to thank Lala and Mark for their hospitality, making me feel at home.

To Dr. Grant Thorp for his collaboration in Chapter 3 and all that he shared and taught us, which was essential to carry out Chapter 4 too.

A Agromillora Group por suministrarnos tanto material vegetal como necesitasemos y más, con el que se llevaron a cabo los capítulos 3, 4, 5 y 6. A Joan y Cristina por su amabilidad siempre que les visitamos en sus instalaciones.

A Bea. Solo hemos compartido despacho al principio y al final, pero siempre he podido contar con tu consejo y ayuda durante esta tesis. Muchas gracias.

A José Miguel y Mayte, por ejercer de chofers y por su apoyo en el trabajo de campo, y a Pepe Jaime, por aguantar estoicamente el frío conmigo. También a José Ángel, por estar siempre disponible ante cualquier duda en el laboratorio. Y al resto de personal de la unidad, por haber construido un ambiente laboral saludable en el que apetezca estar. Lo que tenemos ni es fácil ni es tan común. Igualmente, al CITA y a su dirección por haberme acogido en sus instalaciones.

A todas las personas con las que he coincidido en la sala de becarios, tanto ahora (aunque me hagáis sentir más viejo de lo que ya me siento) como en el pasado, por conseguir que apetezca levantarse a las 6:30 para "trabajar". En especial a Patri, Brenda e Inés. También agradecer a todos los compañeros tanto del CITA como de Aula Dei por compartir cenas, excursiones y

partidos de pádel. Y por supuesto a mi compi Irene. Gracias por sacarme a pasear y ayudarme a mantener la poca cordura que me queda.

A Sara, por hacer más llevaderas tantas mañanas de sueño y tantos momentos de aburrimiento en el despacho. Espero seguir vivo cuando finalmente presentes tu tesis. Y a mi mejor no-amigo, Alejandro. Qué decir. Gracias por todas las horas que hemos pasado juntos, en el CITA y fuera.

A Rocío, por diseñar la portada. Y por aparecer en mi vida.

Y para finalizar, a mis padres. Por todo. Por convertirme en la persona que soy hoy. Por haber fomentado mi curiosidad. Por haberme apoyado siempre. Y por estar ahí cada día. Gracias. Ser vuestro hijo sigue siendo lo mejor que me ha pasado en la vida.

Financiación

Este trabajo ha sido financiado por los proyectos RTA-2014-00062, RTI2018-094210-R-I00 y FPI-INIA2016 CPD2016-0056 de la Agencia Estatal de Investigación (MCIN/AEI/10.13039/501100011033) y el Grupo de Investigación A12 del Gobierno de Aragón.

Index

Table index

Figure index

Abstract

Almond (*Prunus amygdalus* (L.) Batsch, syn *P. dulcis* (Mill.)) economic relevance has surged in recent years, especially in the Iberian Peninsula and in Mediterranean countries. In Spain, almond production has raised significantly during the last years. Nevertheless, while being the first country in area dedicated to almond orchards, in terms of production is still far behind the USA. Hence, new planting systems are under way in the Mediterranean area, which require cultivars and rootstocks that display an upright habit, productive branching and low vigor. Thus, understanding the biological processes that shape the tree three-dimensional shape has become of great importance in recent years. Tree architecture comprises the sum of all the features that define the tree structure and ultimately the productive canopy. This trait is affected by several inputs, from environmental factors to others related to the orchard management like pruning, nutrition and the rootstock choice. The objective of this work is to characterize the physiological and molecular basis of almond tree architecture, and the effect that the scion/rootstock interaction might have in such regulation. The involvement of the IGT family in the genetic diversity of tree habit was analyzed in a set of almond cultivars and wild species. Though its control of branch and root angle has been characterized in some species, no correlation was found in our study between the genetic polymorphism and expression of the IGT family and the diversity in tree habit. The complexity of tree architecture as a trait, involving several aspects of tree development, it has made necessary to develop a comprehensive and quantitative phenotyping protocol, which can be associated to other molecular approaches. Seven parameters were selected as relevant descriptors of tree architecture and the effect of the rootstock genotype on its variability. Using this protocol, we studied the effect in thrity scion/rootstock combinations, resulting from six commercial almond cultivars grafted onto five interspecific hybrid rootstocks. Traits associated to apical dominance and bud outgrowth were significantly influenced by the rootstock. Meanwhile, cultivars presenting especially strong (‘Isabelona’) or weak (‘Lauranne’) phenotype of apical dominance were less affected. This effect is transmitted to shoot formation, with the production of immediate (sylleptic) shoots being altered by the rootstock genotype. We observed differential expression of genes in samples from the scion shoot tips only in cases where these traits were influenced by the rootstock (as it happened with the cultivar ‘Diamar’). These genes were related to bud outgrowth, meristem differentiation, cell division, cell wall reorganization or nutrient uptake. While scion/rootstock interaction is crucial to determine the scion architecture, the cultivar can also influence the rootstock development. We reported a prevalence of genes differentially expressed associated to hormonal regulation, nitrogen availability or root development, proving that, as expected, the scion could also modify the rootstock expression profile. This highlights the importance of considering the effect of both the scion and the rootstock on each other in the regulation of the highly complex trait that is almond tree architecture.

Resumen

La importancia económica del almendro (*Prunus amygdalus* (L.) Batsch, syn *P. dulcis* (Mill.)) ha crecido en los últimos años, especialmente en la península ibérica y países mediterráneos, y en España, la producción ha aumentado significativamente. Sin embargo, aunque es el primer país en área dedicada a su cultivo, está todavía muy lejos de EEUU en términos de producción de almendra. Por ello, se han introducido nuevos sistemas de cultivo en el área mediterránea, que requieren de variedades con un hábito erecto, ramificaciones productivas y un bajo vigor. Debido a esto, ha adquirido relevancia comprender que procesos biológicos modulan la estructura tridimensional del árbol. Todas las características que la definen se engloban en el término arquitectura del árbol, la cual está regulada por varios factores, desde ambientales hasta otros relacionados con el manejo del cultivo, como la poda, los nutrientes o la elección del patrón. El objetivo de este trabajo es caracterizar los factores fisiológicos y moleculares que regulan la arquitectura del almendro, así como el efecto en la misma de la comunicación entre variedad y patrón. La participación de la familia IGT en la diversidad del hábito de crecimiento fue analizada en un conjunto de variedades de almendro y especies silvestres. Aunque en varias especies se ha descrito que regula el ángulo de las ramas y raíces, en almendro, no se ha encontrado ninguna correlación entre la variabilidad de esta familia de genes y la diversidad en hábito. La complejidad de la arquitectura del árbol, involucrando múltiples aspectos del desarrollo del árbol, ha hecho necesario establecer un protocolo de fenotipado cuantitativo enfocado a estudios moleculares. Siete parámetros fueron seleccionados como descriptores de la arquitectura del árbol y del efecto del patrón en su variabilidad. Con estos analizamos el efecto de la interacción entre variedad y patrón en treinta combinaciones con seis variedades comerciales y cinco híbridos interespecíficos. Se observó que el patrón tenía una influencia significativa en los parámetros asociados a la dominancia apical. Por otro lado, variedades con fenotipos extremos de dominancia apical (alta, 'Isabelona', o baja, 'Lauranne') se veían menos afectadas. Este efecto se transmite a la formación de ramas, viéndose alterada la producción de ramas inmediatas (silépticas) por el genotipo del patrón. Solo se observó expresión diferencial de genes en ápices de ramas en individuos de 'Diamar', donde existía una influencia fenotípica del patrón. Estos genes están asociados a la formación de brotes, la diferenciación de meristemos, la división celular, la reorganización de la pared celular o la captación de nutrientes. Mientras que la interacción entre variedad y patrón influye en la arquitectura de la variedad, también la variedad puede afectar al desarrollo del patrón. Observamos una prevalencia de genes expresados diferencialmente asociados a la regulación hormonal, la disponibilidad de nitrógeno o el desarrollo radicular, demostrando que la variedad puede igualmente modificar el perfil molecular del patrón. Esto ratifica la importancia de considerar el efecto mutuo que tienen variedad y patrón en la regulación de un rasgo tan complejo como la arquitectura del almendro.

1. GENERAL INTRODUCTION

1.1. Origin and taxonomy of almond trees

Almond trees (*Prunus amygdalus* (L.) Batsch, syn *P. dulcis* (Mill.)) belong to the genus *Prunus* L., subfamily Amygdaloideae, family Rosaceae. *Prunus* is one of the main cultivated angiosperm's genus, constituted by more than 400 different species, although less than 100 are considered of agronomic importance. Among them, we can find species of such relevance as peach (*P. persica* (L.) Batsch), apricot (*P. armeniaca* L.), japanese (*P. salicina* Lindl.) and european plum (*P. domestica* L.), or cherry (*P. avium* L.). Most extended classification is formed by five different subfamilies: Amygdalus (L.) Focke (almond and peach trees), Cerasus Pers (cherry trees), *Prunus* [=Prunuophara Focke] (plum and apricot trees), Laurocerasus Koehne and Padus (Moench) Koehne. Almond and peach wild species like *P. bucharica* (Korsh.) Fetdsch., *P. kuramica* (Korsh.), *P. webbii* (Spach) Vieh., *P. kotschii* (*A. kotschii* Boiss.), *P. davidiana* (Carr.) or *P. mira* Koehne kov et. Kpst are often used as ornamental trees or as rootstocks, either grafting directly onto them or being used as parents in interspecific hybrid crosses. These species are typically used because they are a good reservoir of natural genetic resistance to biotic and abiotic stresses (Kole, 2011; Socias i Company et al., 2017, 2012).

Almond trees first originated in arid, mountainous terrains, with dry climatic conditions, located in Central Asia (Gradziel, 2017; Socias i Company et al., 2012). A wide number of close species and variations have been described in western China and Mongolia, and in the north of the Balkan Peninsula (Das et al., 2011). Almond domestication occurred in Central Asia approximately five thousand years ago. Later, almond seeds were carried to the Mediterranean region, extending its culture around Europe, where further hybridization took place (Gradziel, 2017). Almond was introduced in California during the 16th and 17th century by Spanish colons (Das et al., 2011; Socias i Company et al., 2017, 2012). Shortly after, it was imported to other regions with Mediterranean climate, such as Western Australia or South Africa (Wirthensohn and Iannamico, 2017).

1.2. Economic significance of almond trees

Almond is one of the most relevant *Prunus* crops, being second in area dedicated after peach and nectarines, with 2,126,304 ha in 2019 (FAOSTAT, 2021). Spain is the second almond producer, only after the USA. A total of 3,497,148 t were produced worldwide in 2019, of which USA produced 1,936,840 t, Spain 340,420 t, and Iran was third with 177,015 t (FAOSTAT, 2021) (Figure 1.1). Other countries with significant almond production were Turkey, Australia or Morocco. Moreover, Spain is the country with more area intended to almond orchards, 687,230 ha in 2019, even above USA, which destined 477,530 ha (FAOSTAT, 2021).

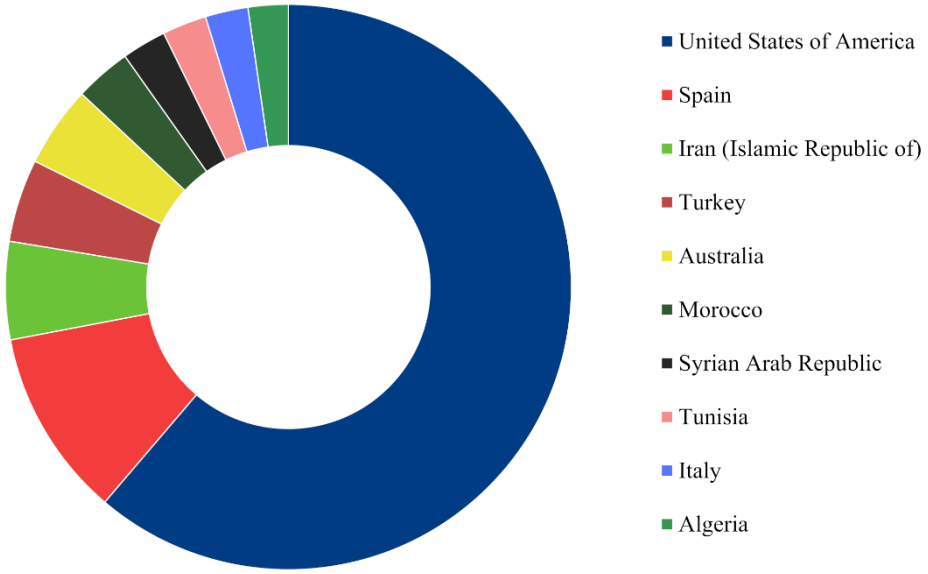

Figure 1.1. Percentage of almond production for the top ten global producers. Data extracted from FAOSTAT (http://www.fao.org/faostat/en/#home, accessed October 8, 2021).

Almond production has grown immensely in Spain in recent years, to the point of almost duplicating its production from 2016 to 2019 (Figure 1.2). Current estimates predict a further increase of almond production in Spain, from 121,600 t of kernel in 2020 to 205,000 t of kernel in 2025 (Iglesias et al., 2021). This growth is due to the establishment of new orchards in recent years, the improvement in their handling, from the pruning to the advances in machinery, and the development of new cultivars and rootstocks. Andalusia is the main almond producer, with 161,546 t in 2019, followed by Aragon, 74,688 t, and Castilla-La Mancha, 74,452 t (MAPA, 2021).

1.3. Development of new almond orchards

Although Spain dedicates considerably more surface to almond orchards than USA, its almond production is substantially inferior (Figure 1.1). This is due to Spain conditions, with dryer and almost desertic climatic conditions, while water availability in the San Joaquin and Sacramento valleys in California, where the majority of almond orchards are located in the USA, is rather superior.

However, in the last decades changes have occurred in the Mediterranean Basin and more specifically in Spain. New planting system have been developed, allowing higher plants per ha while incorporating method for more sustainable cultural practices in order to increase the yield (Rubio-Cabetas et al., 2017; Socias i Company et al., 2009). These new orchards also need new pruning methods of almond trees and maintenance to better adapt to the conditions required. The ideotype cultivar should be of reduced vigor with upright habit and homogeneous branching

occupying less space, since it is a major limitation. Cultivars presenting these genetic characteristics would reduce training and pruning, diminishing therefore the amount of labor and inputs into the orchard as well.

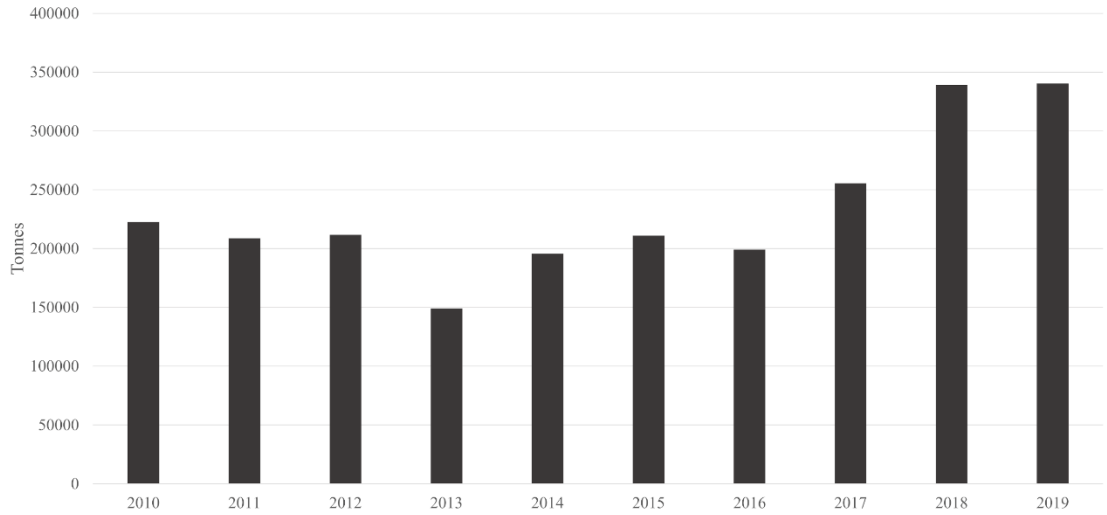

Figure 1.2. Evolution of almond production in Spain from 2010 to 2019. Data extracted from MAPA (https://www.mapa.gob.es/es/estadistica/temas/estadisticas-agrarias/agricultura/superficies-producciones-anuales-cultivos/, accessed October 8, 2021).

Other characteristics have acquired relevancy in almond cultivar breeding lately (Bielsa et al., 2021a). It started from self-compatibility and late blooming, which commercial cultivars already exist (Socias i Company and Felipe, 2007, Socias i Company et al., 2015, 2008), to traits related to root knot nematode rootstock resistance (Felipe et al., 2009), waterlogging tolerance (Rubio-Cabetas et al., 2018) or drought tolerance (Bielsa et al., 2021b, 2019, 2018). In addition, there has been an increasing attention on improving almond nutritional quality, quantifying the presence of tocopherols or monophenols in almond cultivars (Moreno-Gracia et al., 2021). Besides, developing cultivars that have natural resistance to disease, either in the cultivar or the rootstock, have become a point of interest recently (Vahdati et al., 2021). However, the primary focus on the development of rootstocks continues to be vigor control. To that extent, commercial dwarfing rootstock have been introduced in recent years, such as the Rootpac® series (Pinochet, 2010). In the end, new cultivars and rootstocks developed to adapt to new planting system with more trees per ha should also conserve other characteristics of interest, like self-compatibility, late blooming and disease resistances.

1.4. Molecular and physiological regulation of plant architecture

Plant architecture is a complex trait regulated by an extensive network of interactions, involving physiological, metabolic and molecular processes. The elevated complexity of this trait

makes it difficult to unravel the pivotal aspects behind the whole variability found in plants. Although there are other mechanisms involved in the regulation of plant shape, hormonal response is the central regulator, with a vast response of hormones carrying out different processes, from plant development to branching control (Barbier et al., 2019; Rameau et al., 2015; B. Wang et al., 2018).

Auxin is considered the main regulator of plant architecture. It is involved in multiple pathways, but substantially in apical dominance regulation. This hormone is synthesized in the apex, mainly in the leaves, and later, auxin is transported to the roots using specific protein channels, inhibiting the formation of bud outgrowth trough the plant, and hence promoting the axis growth (Adamowski and Friml, 2015; Dierck et al., 2018, 2016a; Korasick et al., 2013; Leyser, 2017). Strigolactones (SLs) act as auxin second messengers in the control of apical dominance, inhibiting bud outgrowth (Bennett et al., 2016; Dierck et al., 2016b; Dun et al., 2012; Shinohara et al., 2013; Waldie et al., 2014). Moreover, SLs participate in other developmental processes such as cell elongation (de Saint Germain et al., 2013). Cytokinins (CKs) have the opposite effect in apical dominance, promoting bud outgrowth (Dun et al., 2012; Waldie and Leyser, 2018). CKs also promote growth in earlier phases of development, including meristem maintenance (Kieber and Schaller, 2018; Neil Emery and Kisiala, 2020). Gibberellic acid (GA) has been extensively considered the main regulator of plant growth, being involved in internode formation or cell elongation (Binenbaum et al., 2018; Hedden and Thomas, 2012). Brassinosteroids (BRs) act in several regulatory mechanisms, promoting growth and affecting branch formation (Chen et al., 2017; Wei and Li, 2016). Abscisic acid (ABA) is a core regulator of stress responses. It has been described inhibiting growth and plant development (Yao and Finlayson, 2015). A similar function has been described for salicylic acid (SA) or jasmonic acid (JA), other hormones involved in defense mechanisms or stress response (Heinrich et al., 2013; Rivas-San Vicente and Plasencia, 2011). Concerning non-hormonal mechanisms, carbohydrate availability have been characterized as an essential regulator of bud outgrowth (Mason et al., 2014; Stokes et al., 2013). Nutrients or amino acids availability also affect the capability of the plant to promote growth (Jong et al., 2014; Xu et al., 2015).

1.5. Defining almond tree architecture

Tree architecture refers to the three-dimensional structure presented by the tree, both in its aerial part and in its roots. Studies to date have been mostly limited to the aerial part of the tree, while disregarding roots due to the inherent difficulties associated to its examination. However, some advancement in the three-dimensional structure of roots have been made (Danjon and Reubens, 2008; Svane et al., 2019; Tracy et al., 2020; Wasson et al., 2012).

Therefore, aerial organs are the main focus of tree architectural analysis. The architectural model can be decomposed in four major features: (i) growth pattern; (ii) branching pattern; (iii) the morphological differentiation of axes; (iv) the sexual differentiation of meristems. The basic unit of tree construction is the metamer or phytomere, which is composed by a node, its leaves and axillary buds plus the subtending internode (Costes et al., 2006; Hallé et al., 1978). The fate of the buds of each metamer is going to define the final overall tree structure.

Growth pattern comprise traits like trunk vigor or tree height. They are affected by processes involving cell elongation or cell wall formation (Costes et al., 2006). Moreover, the availability of resources is an important factor, as it is the root system established. Several features of the tree structure are defined by the branching pattern. They can go from bud outgrowth happening or not, to what type of growth happens (rhythmic or continuous), what kind of branch is formed (proleptic or sylleptic) or where in the axis the shoots are formed (acrotonic, mesotonic or basotonic) (Barthélémy and Caraglio, 2007). The development of these features is controlled primarily by apical dominance, although several other physiological and molecular processes take part, as for example light availability (Casal, 2012; Finlayson et al., 2010; Hill and Hollender, 2019; Hollender and Dardick, 2015). Besides branching pattern, branching angle is also an important feature in defining the ultimate tree structure. This trait is controlled essentially by gravitropism and light perception. Gravitropism controls the orientation of the plant growth in response to the gravitational vector, either growing against if it is an aerial part, or in its direction in the roots (Gerttula et al., 2015; Groover, 2016; Hollender and Dardick, 2015; Su et al., 2017). The growth direction of branches can also be affected by light perception, leading shoots to where light is accessible (Casal, 2012).

Given the structural complexity developed by an adult tree, a detailed quantitative measurement is a herculean task. Nevertheless, trees use to repeat their architecture unit to conform their definitive structure in a process called reiteration (Barthélémy and Caraglio, 2007). Thus, only the two or three first years of the tree or shoot development are analyzed, predicting the outcome from those assessments. The juxtaposition of all these processes makes it difficult to assess tree architecture regulation and which aspects are crucial for the final shape. This is even more challenging when we acknowledge the reality of a typical almond orchard, since we must consider that the phenotype depends of two different individuals, the scion and the rootstock, and the interaction between them.

1.6. Scion/rootstock interaction

Traditionally in almond orchads, cultivars are typically grafted onto a commercial rootstock. Those are responsible of the nutrient uptake and the tolerance to diseases. Although

rooted almond cultivars are nowadays also considered, these are limited to rain fed areas. So that, in sustainable almond orchard under irrigation conditions, the effect on the phenotype by both the scion and the rootstock must be taken into account considering tree architecture, and also how these two genetically different plant systems interact.

Scion/rootstock interaction has been depicted not only occurring in the grafting site, but also affecting on long distances (Aloni et al., 2010; Gaut et al., 2019; Warschefsky et al., 2016). Certain hormone profiles of the rootstock can be imported to the scion, and hormones synthetized in the roots such as SLs can affect the development of aerial traits. The same effect is expected to exist in the opposite direction, with hormones synthetized in the scion affecting the metabolism and molecular profile of the rootstock. Also sRNA and mRNA have been described to be able to move from the rootstock to the scion, unveiling a whole new area of rootstock control of the scion regulation (Bhogale et al., 2014; Kudo and Harada, 2007).

The knowledge about the effect of scion/rootstock interaction in tree architecture is yet limited and almost non-existent at a molecular level. In fruit trees, most studies have been carried out in *Malus* × *domestica*, studying rootstock impact on scion height or trunk diameter (Foster et al., 2017, 2015; Tworkoski and Fazio, 2015). Rootstock influence on scion vigor has also been reported in *Prunus* species (Balducci et al., 2019; Ben Yahmed et al., 2016; Lordan et al., 2019). On the contrary, although molecular studies have been performed in the graft union (Gautier et al., 2019; Pina et al., 2017; Rasool et al., 2020), remarkably little is known about how the scion influences the rootstock phenotype.

1.7. New techniques in plant breeding

Historically, efforts in plant breeding extended through long periods of time, needing more than a decade to establish a new cultivar. Improvement of molecular techniques made possible to screen genetically for desired traits in almond populations (Badenes et al., 2016; Rubio-Cabetas et al., 2014). The use of these molecular approaches has reduced remarkably the timeline in selection and plant breeding. Techniques used in past years for marker-assisted selection (MAS) in almond comprised the use of quantitative trait loci (QTL) analysis or association mapping (AM) (Font i Forcada et al., 2017).

In the last decade, the decreasing of sequencing prices and development of new molecular techniques has allowed to shift these approaches to the analysis of single nucleotide polymorphisms (SNPs), gaining tremendous amount of genomic information (Levy and Boone, 2019). Moreover, this reduction in prices have contributed to several Rosaceae genomes being released (Jung et al., 2019). For almond, two cultivars have been recently sequenced *de novo*. The

first almond genome was published for the cultivar ‘Lauranne’ (Sánchez-Pérez et al., 2019). This sequence has a total length of 246 Mb, and it is divided in 4,078 scaffolds, 2,572 of them organized in eight pseudomolecules with 27,817 genes. Almost at the same time it was published the genome of the almond cultivar ‘Texas’ (Alioto et al., 2020). It has a total length of 227.6 Mb, which a 91% is organized in eight pseudomolecules with 27,969 protein-coding genes and 6,747 non-coding genes. The recent publication of the almond genome has allowed performing genome wide associations studies (GWAS) in almond populations, which have been up to now focus on nut traits (Di Guardo et al., 2021; Pavan et al., 2021). Close species to almond like peach have benefited of having a published genome earlier and more genomic studies have been published, analyzing several traits (Elsadr et al., 2019; Guo et al., 2020; Li et al., 2021; Liu et al., 2015; Mas-Gómez et al., 2021; Tan et al., 2021).

Furthermore, this decreasing of prices has extended to other techniques as RNA-Seq, allowing as studying complete gene expression profiles in an extended number of individuals. Transcriptome analysis in almond has been focus in various relevant traits, like drought response, flowering period, self-incompability or cold tolerance (Bielsa et al., 2018; Gómez et al., 2019; Guo et al., 2021; Hosseinpour et al., 2018; Prudencio et al., 2020). This bulk of genomic information requires us to obtain also a large amount of phenotypic data. Since a substantial number of individuals must be analyzed, phenotyping protocols must be simple and allow quick data collection. Otherwise, when studying complex traits like tree architecture, the task would be too laborious to carry out.

1.8. Thesis objectives

The general objective of this thesis is to characterize the underlining physiological and molecular basis of almond tree architecture regulation, and how this is affected by the scion/rootstock interaction. This can be divided in three sub-objectives:

1. Analyze different scion/rootstock combinations with several parameters to phenotype the aerial tree architecture traits and develop a comprehensive phenotyping protocol.

2. Characterize the molecular basis encoding the different tree architecture phenotypes in multiple almond cultivars and scion/rootstock combinations.

3. To establish the crosstalk between the scion and the rootsock at the molecular level to explain the variability of the tree architecture.

2. POLYMORPHISMS AND GENE EXPRESSION IN THE ALMOND IGT FAMILY ARE NOT CORRELATED TO VARIABILITY IN GROWTH HABIT IN MAJOR COMMERCIAL ALMOND CULTIVARS

Montesinos, Á., Dardick, C., Rubio-Cabetas, M. J., and Grimplet, J. (2021) Polymorphisms and gene expression in the almond IGT family are not correlated to variability in growth habit in major commercial almond cultivars. *PLoS ONE* 16: e0252001. doi:10.1371/journal.pone.0252001.

Abstract

Almond (*Prunus amygdalus* (L.) Batsch, syn *P. dulcis* (Mill.)) breeding programs aimed at selecting cultivars adapted to intensive orchards have recently focused on the optimization of tree architecture. This multifactorial trait is defined by numerous components controlled by processes such as hormonal responses, gravitropism and light perception. Gravitropism sensing is crucial to control the branch angle and therefore, the tree habit. A gene family, denominated IGT family after a shared conserved domain, has been described as involved in the regulation of branch angle in several species, including rice (*Oryza sativa*) and *Arabidopsis thaliana*, and even in fruit trees like peach (*P. persica* (L.) Batsch). Here we identified six members of this family in almond: *LAZY1*, *LAZY2*, *TAC1*, *DRO1*, *DRO2* and *IGT-like*. After analyzing their protein sequences in forty-one almond cultivars and wild species, little variability was found, pointing a high degree of conservation in this family. To our knowledge, this is the first effort to analyze the diversity of IGT family proteins in members of the same tree species. Gene expression was analyzed in fourteen cultivars of agronomical interest comprising diverse tree habit phenotypes. Only *LAZY1*, *LAZY2* and *TAC1* were expressed in almond shoot tips during the growing season. No relation could be established between the expression profile of these genes and the variability observed in the tree habit. However, some insight has been gained in how *LAZY1* and *LAZY2* are regulated, identifying the *IPA1* almond homologues and other transcription factors involved in hormonal responses as regulators of their expression. Besides, we have found various polymorphisms that could not be discarded as involved in a potential polygenic origin of regulation of architectural phenotypes. Therefore, we have established that neither the expression nor the genetic polymorphism of IGT family genes are correlated to diversity of tree habit in currently commercialized almond cultivars, with other gene families contributing to the variability of these traits.

2.1. Introduction

In the last decade, more intensive almond (*Prunus amygdalus* (L.) Batsch, syn *P. dulcis* (Mill.)) orchards have become the predominant model in the Mediterranean areas, in order to increase productivity and to reduce labor cost (Socias i Company et al., 2009). Under this scenario, there is a growing interest in developing almond cultivars more adapted to mechanical pruning and presenting a natural branching that reduces pruning cost to achieve the desired tree structure. In consequence, optimized cultivars need to have low vigor, reasonable branching and an upright overall architecture.

Tree architecture is a highly complex trait defined by the sum of phenotypic components that influence the three-dimensional shape of the tree. It involves growth direction, growth rhythm, branching mode, position of the branches, the sexual differentiation of meristems and the length of axillary shoots (Costes et al., 2006). Tree architecture is affected by environmental parameters such as light perception, gravity sensing, sugar availability or nutrients supply that take part in the plant physiological and hormonal regulation (Hearn, 2016; Hill and Hollender, 2019; Hollender and Dardick, 2015).

Two physiological processes that affect the plant architecture are apical dominance and lateral bud outgrowth. Auxins act as the principal factor in the control of apical dominance. This hormone is synthesized at the apical leaves and transported throughout the plant, inhibiting lateral bud outgrowth. It promotes strigolactone (SL) biosynthesis, which is able to translocate to the bud and stop bud outgrowth (Barbier et al., 2019; Bennett et al., 2016). Cytokinins (CKs) act antagonistically to SLs, promoting shoot apical meristem (SAM) differentiation and therefore bud outgrowth (Dun et al., 2012; Tanaka et al., 2006). Sugar availability has also been described as a positive regulator of bud outgrowth (Barbier et al., 2015; Mason et al., 2014). These processes are essential for shaping the plant structure, although the overall tree habit, which is defined by the relative angle of the branches, is essentially regulated by two responses: light perception and gravitropism.

Light perception regulates both the growth and the direction of lateral branches. It is based on the ratio between red light and far red light (R:FR), captured by phytochrome photoreceptors phyA and phyB. When the R:FR is low, phyA is activated while phyB is inhibited, which sets off the inhibition of bud outgrowth, redistributing the auxin flux and focusing plant efforts in the growth of the primary axis (Casal, 2012; Finlayson et al., 2010; Rausenberger et al., 2012; Reddy and Finlayson, 2014).

Gravitropism is the main regulator of the branching angle. Its regulation occurs in specific cells called statocytes, where organelles containing large starch grains, called amyloplasts, act as gravity sensors (Walker and Sack, 1990). These organelles sediment in the direction of the gravitational vector, triggering a signal which involves the opening of ion channels and the reorganization of the cytoskeleton (Berut et al., 2018; Kolesnikov et al., 2016; Leitz et al., 2009). This response leads to a relocation of auxin carriers PIN3 and PIN7 changing the direction of the auxin flux, which provokes a differential growth and a curvature in the opposing direction of the gravitational vector (Band et al., 2012; Kleine-Vehn et al., 2010; Schüler et al., 2015).

LAZY1 has been described extensively as an influential factor in the control of plant architecture since its characterization in *Oryza sativa* (rice) as a regulator of tiller angle in agravitropic mutants (Abe et al., 2004; Li et al., 2007; Yoshihara an Iino, 2007). Orthologs of this gene were found in *Arabidopsis thaliana* and *Zea mays* (maize), leading to the characterization of the same family in these species (Dong et al., 2013; Howard et al., 2014; Yoshihara et al., 2013). This family also includes *DRO1*, which was initially reported as an influential factor of root architecture in rice (Guseman et al., 2017; Uga et al., 2013). *LAZY1* is related to *TAC1*, which is also involved in plant architecture regulation. *TAC1* was first identified in rice mutants with increased tiller angle, and it has also been characterized in Arabidopsis (Dardick et al., 2013; Yu et al., 2007). *TAC1* differs from the rest of the family, denominated IGT family, in its lack of an EAR-like conserved domain denominated CCL domain located in the C-terminal region, which consists of fourteen aminoacids (Dardick et al., 2013; Nakamura et al., 2019). This conserved region is essential for the function and subcellular localization of IGT proteins. Since *LAZY1* and *TAC1* promote opposite phenotypes, and due to the lack of the CCL conserved domain, *TAC1* has been proposed as a negative regulator of *LAZY1* activity, in an upstream capacity (Dardick et al., 2013; Nakamura et al., 2019; Sasaki and Yamamoto, 2015). However, the specific mechanism of the interaction between *LAZY1* and *TAC1* interaction is yet to be discovered (Hollender et al., 2020).

The involvement of IGT family genes in gravitropism has been described in Arabidopsis and rice, acting as mediators between the sedimentation of statoliths gravity sensors and the relocation of auxin PIN carriers (Dardick et al., 2013; Taniguchi et al., 2017; Yoshihara and Spalding, 2017; Zhang et al., 2018). Although a direct interaction with the phyA-phyB system is yet to be discovered, *TAC1* expression is influenced by the light perception regulator *COP1*, which would provide for integration between light and gravity responses (Waite and Dardick, 2018).

The analysis of the mutation *br* in *P. persica* (L.) Batsch (peach), which is related to vertically oriented growth of branches, led to the annotation of an ortholog of *TAC1* (Dardick et

al., 2013). Further studies have described the involvement of *TAC1* in auxin response mechanisms within different branching genotypes in peach, proving that the mechanisms involved in the control of the growth habit are conserved to a certain point in *Prunus* species (Hollender et al., 2018; Tworkoski et al., 2015).

A total of six members of the IGT family have been found in almond: *LAZY1*, *LAZY2*, *DRO1*, *DRO2*, *IGT-like* and *TAC1*. With the exception of *TAC1*, all of them have the five conserved regions described in Arabidopsis (Nakamura et al., 2019). In this study, we carried out a genomic comparison for these six genes in forty-one almond cultivars and wild species with different growth habit phenotypes. Moreover, we analyzed the gene expression of the IGT family members in fourteen selected cultivars and searched for variants in their promoter region. Posteriorly, *LAZY1* and *LAZY2* promoters were inspected to identify regulatory elements (REs) associated to transcription factors (TFs) that could be involved in the regulation of *LAZY1* and *LAZY2*. Twenty-one TFs were selected due to its described function or its presence in growing shoot tips in previous studies and the analysis of their gene expression was carried out.

2.2. Materials and Methods

2.2.1. Almond tree populations

Forty-one cultivars and wild species (Supplementary Data 2.1; Annex2), whose genome had been previously obtained as part of the almond sequencing consortium (Alioto et al., 2020) were selected to perform the comparative analysis of the IGT family protein sequences (Supplementary Data 2.2; Annex 2). From these, twenty-seven cultivars were phenotyped for growth habit (Supplementary Data 2.1; Annex 2), using a scale from 1 to 5 according UPOV (Interantional Union for the Protection of New Varieties of Plants) guidelines: 1 = upright (< 60º), 2 = somewhat upright (60º - 80º), 3 = semi-open (80º - 100º), 4 = open (100º - 120º), 5 = weeping (> 120º) (Felipe, 2000). Fourteen cultivars of agronomical interest were selected to analyze the gene expression of the IGT family members. Ten out of these fourteen were chosen to analyze the expression of twenty-one transcription factors (Table 2.1).

2.2.3. Comparative genomics

The cultivar genomes were assembled against the *P. dulcis* 'Texas' Genome v2.0 (Alioto et al., 2020) (https://www.rosaceae.org/analysis/295). Adapter sequences were removed by processing the raw reads sequences of the forty-one cultivars with Trimmomatic v0.36.6 (Bolger et al., 2014). Alignments were performed using the Bowtie2 package (Galaxy Version 2.3.4.3) (Langmead and Salzberg, 2012; Langmead et al., 2009). Variant calling to detect SNPs was

performed with the FreeBayes package (Galaxy Version 1.1.0.46-0) (Garrison et al., 2012). SNPs were filtered with the PLINK package (Galaxy Version 2.0.0) (Chang et al., 2015; Purcell et al., 2007) using the following parameters: read depth (DP) = 10; alternated allele observation count (AO) = 0.2. Promoter regions of the IGT family members were analyzed up to 2,000 bp upstream the start codon. All procedures were carried out using the Galaxy platform.

Table 2.1. List of cultivars selected for the gene expression analysis of the IGT family members.

Cultivar	Tree habit
'Forastero' (FOR)	Upright
'Bartre' (BAR)	Upright
'Ferragnes' (FER)	Somewhat upright
'Garfi' (GAR)	Somewhat upright
Garnem® (GN)	Somewhat upright
'Diamar' (DIA)	Somewhat upright
'Marinada' (MAN)	Somewhat upright
'Soleta' (SOL)	Semi-open
'Marcona' (MAC)	Semi-open
'Vairo' (VAI)	Semi-open
'Isabelona' (ISA)	Semi-open
'Vialfas' (VIA)	Semi-open
'Guara' (GUA)	Open
'Desmayo Largueta' (DLA)	Weeping

The ten cultivars in bold were posteriorly chosen to study the expression of transcriptions factors associated to *LAZY1* and *LAZY2* promoters. Overall tree habit phenotype for each cultivar is described categorically according UPOV (Interantional Union for the Protection of New Varieties of Plants) guidelines.

2.2.4. Phylogenetic tree

The evolutionary history was inferred by using the Maximum Likelihood method and Poisson correction model (Zuckerkandl and Pauling, 1965). The tree with the highest log likelihood (-5,447.29) is shown. Initial tree(s) for the heuristic search were obtained automatically by applying Neighbor-Join and BioNJ algorithms to a matrix of pairwise distances estimated using a JTT model, and then selecting the topology with superior log likelihood value. This analysis involved 252 amino acid sequences. There were a total of 424 positions in the final dataset. Evolutionary analyses were conducted in MEGA X (Kumar et al., 2018).

2.2.5. Quantitative real-time PCR (qPCR)

Tissue samples for the fourteen selected cultivars were gathered at the same day from adult trees at the end of summer (late August), when one-year old branches were developed, while maintaining an active growth. Cultivars were kept at an experimental orchard in Centro de

Investigación y Tecnología Agroalimentaria de Aragón (CITA) (41°43'29.4" N 0°48'27.3" W). Five cm of the tip from one-year old lateral branches were collected. Each biological replicate consisted of three tips from the same tree. RNA extraction was performed from these samples using the CTAB method described previously (Meisel et al., 2005) with some modifications (Chang et al., 1993; Salzman et al., 1999; Zeng and Yang, 2002). Extracted RNA was quantified using a NanoDrop® ND-1000 UV-vis spectrophotometer (NanoDrop Technologies, Wilmington, DE, USA). RNA integrity was verified by electrophoresis on a 1% agarose gel. RNA samples (2,500 ng) were reverse transcribed with SuperScript III First-Strand Synthesis System (Thermo Fisher Scientific, https://www.thermofisher.com) in a total volume of 21 μL according to the manufacturer's instructions. qPCR was performed using the Superscript III Platinum SYBR Green qRT-PCR Kit (Thermo Fisher Scientific, https://www.thermofisher.com). Each reaction was run in triplicate. Primers for the IGT family members were designed using the respective QUIAGEN CLC Genomics Workbench tool (QUIAGEN, https://digitalinsights.qiagen.com/). Actin primers were used as an internal control to normalize expression (Hosseinpour et al., 2018). The reactions were performed using a 7900 DNA sequence detector (Thermo Fisher Scientific, https://www.thermofisher.com). In ten out of the previous fourteen cultivars (Table 2.1), an expression analysis for selected TFs was performed in SGIker, UPV/EHU (Bizkaia, Spain) using a 48*48 Fluidigm array. Primer for the selected TFs were designed using the online tool Primer3Plus (Untergasser et al., 2007) (http://www.bioinformatics.nl/cgi-bin/primer3plus/primer3plus.cgi). Reactions were carried out using the Fluidigm BioMark HD Nanofluidic qPCR System combined with a GE 48*48 Dynamic Arrays (Fluidigm, https://www.fluidigm.com) and detection through EvaGreen fluorochrome (Bio-Rad Laboratories, https://www.bio-rad.com). CTs were obtained with Fluidigm Real-Time PCR Analysis Software version 4.1.3 (Fluidigm, https://www.fluidigm.com).

2.2.6. Promoter analysis

The promoter sequences of *LAZY1* and *LAZY2* genes, 1,500–1,800 bp upstream of the start codon, were analyzed in search of regulatory *cis*-elements. PlantCARE (Lescot et al., 2002) (http://bioinformatics.psb.ugent.be/webtools/plantcare/html/) and New PLACE (Higo et al., 1999) (https://www.dna.affrc.go.jp/PLACE) were used to identify putative cis-elements and their correspondent binding factors.

2.2.7. Statistical Analysis

Three biological replicates from different branches of the same tree were used. All the statistical analysis was carried out in R (https://cran.r-project.org/). Analysis of significance for

expression analysis was performed using a Kruskal-Wallis H test and comparison between means was performed with a Nemenyi test using the PMCMR R package (Pohlert, 2014).

2.3. Results and Discussion

2.3.1. Almond IGT family members

Six IGT family members were found in almond using BLASTp to search homologues from peach sequences. The peach nomenclature (Waite and Dardick, 2021) was kept for almond: *LAZY1* (Prudul26A025589), *LAZY2* (Prudul26A030030), *DRO1* (Prudul26A032079), *DRO2* (Prudul26A028716), *IGT-like* (Prudul26A033016) and *TAC1* (Prudul26A020993). The phylogenetic analysis also revealed that LAZY1 and LAZY2 peptide sequences are closely related, as well as DRO1 and DRO2. TAC1 is more similar to the rest of the members than IGT-like even without the CCL domain (Figure 2.1, Supplementary Data 2.2; Annex 2). Although little is known about IGT-like function, the high variability could suggest a less-essential activity, or at least less selective pressure on its amino acid sequence. DRO1 and DRO2 are the most conserved members among cultivars; DRO1 shares the same protein sequence for all the different cultivars and wild species (Figure 2.1, Supplementary Data 2.2; Annex 2). Despite the fact that polymorphisms are observed trough the different cultivars, overall, the protein sequences of the IGT Family members are highly conserved, hinting to an essential role in tree architecture regulation (Figure 2.1, Supplementary Data 2.2; Annex 2).

2.3.2. IGT family protein sequence

IGT family proteins share five conserved regions in Arabidopsis, with the exception of TAC1, which lacks the CCL domain in the 3' terminal, which comprise region V (Figure 2.2). While Regions I, II and V are remarkably conserved, regions III and IV differed more between members, which might indicate that their preservation is not as essential to keep their activity (Nakamura et al., 2019). Furthermore, functional analysis in transgenic rescue experiments involving AtLAZY1 have shown that even proteins with mutated residues in these two regions are able to rescue the *Atlazy1* branch angle phenotype (Yoshihara and Spalding, 2020). In almond, a similar display of conserved regions can be seen, with Regions I, II and V extremely conserved while more variability is observed in Regions III and IV (Figure 2.2). The high degree of conservation that these regions keep throughout plant species highlights its importance in plant regulation.

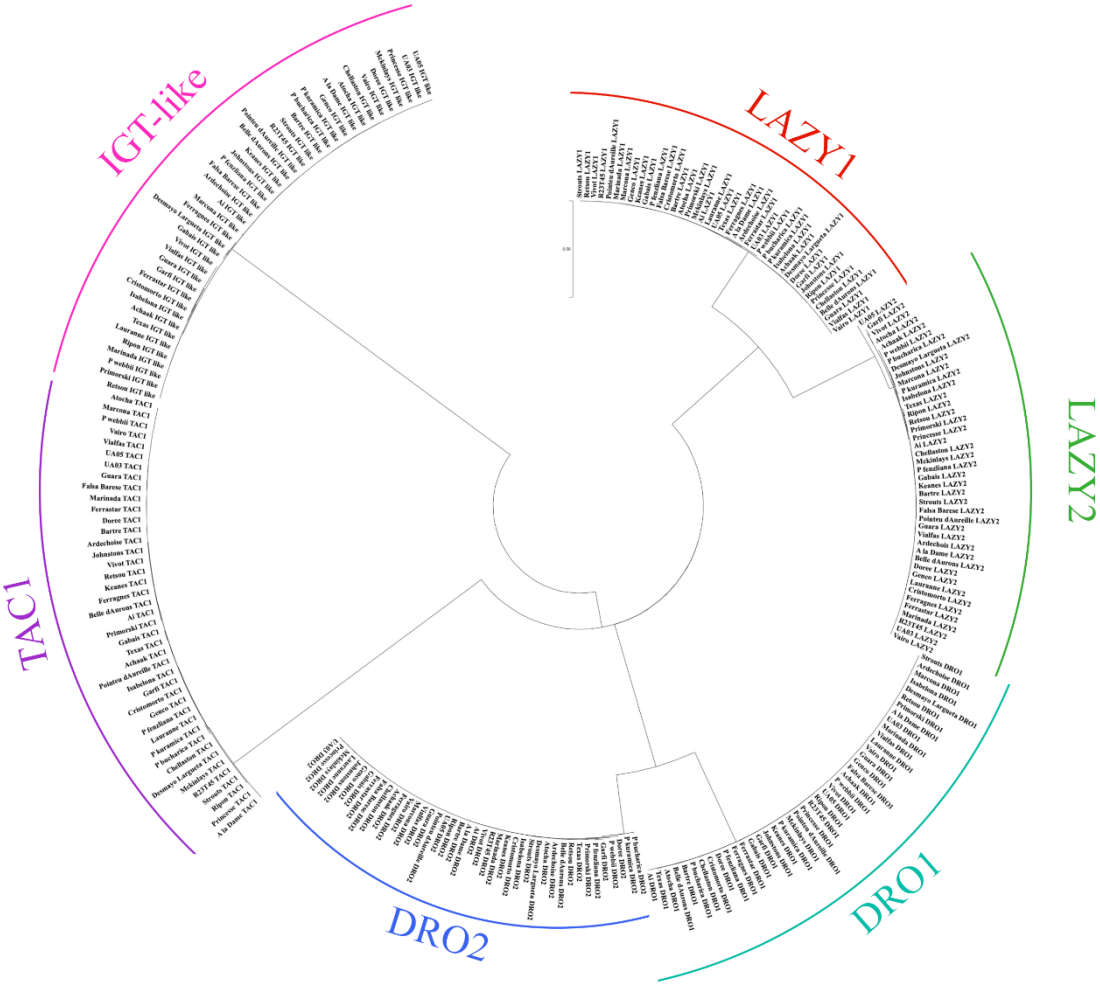

Figure 2.1. Phylogenetic tree of the six IGT family in forty-one cultivars and almond wild species. Cultivars are separated into groups by IGT family protein. Only variants in homozygosis were used for tree building. Names and recorded phenotype of each cultivar and wild species are available in Supplementary Data 2.1 (Annex 2), while protein sequences can be found in Supplementary Data 2.2 (Annex 2).

Both LAZY1 and LAZY2 present mutated residues located in conserved regions in several cultivars and wild species. LAZY1 presents a mutation in Region I, I7 is replaced by a methionine (Table 2.2). Yoshihara and Spalding (2020) reported that individuals with the residues 6 to 8 mutated showed significantly reduced ability to rescue the *atlazy1* branch angle defect nor they were able to mobilize the protein correctly to the plasma membrane in Arabidopsis. Therefore, this region seems to be essential for the correct functionality of the signal peptide. However, AtLAZY1 also presents a methionine in this position on the functional protein and the residue can be found mutated in other members of the IGT family, while W6, probably the indispensable residue, is conserved throughout the members of the family, both in Arabidopsis and almond. This fact would explain why the I7M mutation in homozygosis is not correlated with the observed overall tree habit amongst cultivars (Table 2.2). Several cultivars present a mutation in the Region IV of LAZY2, replacing R293 for a glycine, although no relation with their

phenotype was established. As described by Nakumara et al. (2019), conservation of Region IV is not required to maintain protein functionality.

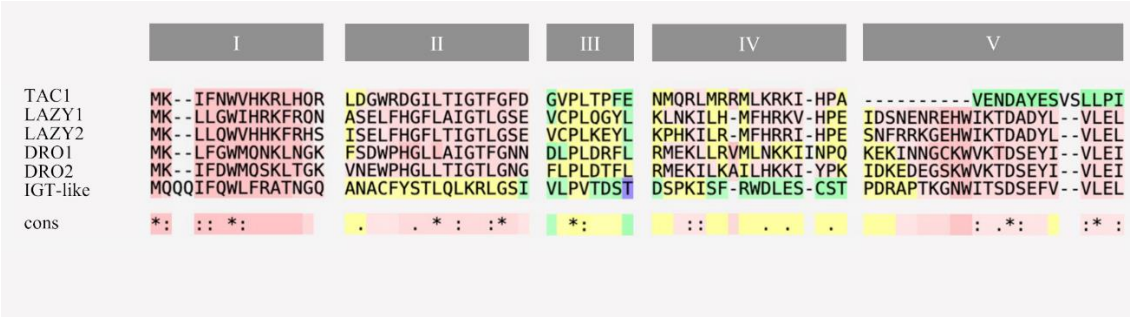

Figure 2.2. Amino acid sequence alignment of the five conserved regions between members of the IGT Family in almond. Sequence alignment analysis was performed using T-COFFEE (Notredame et al., 2000). Red indicates higher levels of conservation. Sequences from 'Texas' cultivar were used as model (Supplementary Data 2.2; Annex 2).

A repetitive region of aspartic residues in TAC1 has been previously described as influential in the protein functionality. Differences in their length may lead to effects in the tree architecture; those who have long runs of aspartic acid residues presented upright phenotypes. Additional residues could affect the functionality or stability of the protein (Hollender et al., 2018). Two different mutations can be observed in our almond cultivars. While a number of cultivars carry the insertion of an additional Asp residue, a deletion of four Asp amino acids can be observed in the wild species *P. bucharica*. Nonetheless, in both cases the mutations are presented only in heterozygosis, thus, this might explain why no phenotypic variations are observed (Table 2.2). No mutations in conserved regions were observed for DRO1 and DRO2. This lack of alterations in their sequence can be explained because *DRO1* and *DRO2*, unlike *LAZY1* and *LAZY2*, are described to act mainly in roots (Uga et al., 2013). Yet, cultivars are predominantly selected by other aerial traits, such as fruit quality or yield, not existing any artificial selection of favored polymorphisms for tree architecture. The high variability observed in the IGT-like protein sequence combined with unknown function hinders the possibility to discern if any mutated amino acid could affect its activity. After an *in-silico* analysis using PROVEAN (Choi and Chan, 2015) and SNAP platforms (Rostlab, https://www.rostlab.org/) other SNPS and indels were highlighted as possible effectors of phenotypic variance. These were marked as deleterious by these online tools, though their effects were limited to a single codon change, deletion or insertion (Table 2.2). Moreover, no relation between these mutations and the described phenotypes was observed.

It was not possible to establish a relation between the sequence variants and the diversity in overall tree habit, even though mutations in conserved regions were detected in LAZY1 and LAZY2 (Table 2.2), which correlate with previous studies indicating a relatively highly conserved

structure for these proteins (Nakamura et al., 2019; Taniguchi et al., 2017). In other species, mutations altering the phenotype produced a truncated protein or altered entire exons affecting protein functionality (Waite and Dardick, 2021). In our case, there are mutations modifying the protein sequence, though, none of them seem to lead to significant phenotypic impacts. In other herbaceous species, these mutations lead to severe effects in cell wall structure that might be even more severe in tree, such as making the individuals that present these variants to be non-viable (Waite and Dardick, 2021). However, the difference in tree architecture might be related to quantitative variation of gene expression. To assess this, the expression of IGT family members was analyzed for a group of fourteen selected cultivars, in order to discover if the phenotypic differences could be due to its expression profile.

Table 2.2. List of mutations of interest whether by their localization or by their predicted outcome.

Protein	Mutation	Prediction	Cultivars presenting the variant
LAZY1	I7M	Neutral	'Bartre' (1), 'Marinada' (2), **'Garfi' (2)**, **'Achaak' (2)**, 'Atocha' (2), **'Princesse' (2)**, ***P. kuramica* (2)**, 'Lauranne' (3), 'Marcona' (3), **'Vialfas' (3)**, 'Vivot' (3), **'Vairo' (3)**, 'Retsou' (3), **'Chellaston' (3)**, **'Isabelona' (3)**, ***P. bucharica* (3)**, **'Guara' (4)**, 'Primorski' (4), 'Cristomorto' (4), 'Ai' (4), **'Belle d'Aurons' (4)**, 'Genco' (4), 'Pointeu d'Aurielle' (4), **'Desmayo Largueta' (5)**
LAZY1	P18Q	Deleterious, codon change	'Lauranne' (3), 'Vialfas' (3), 'Vairo' (3), 'Chellaston' (3), 'Guara' (4), 'Ai' (4), 'Belle d'Aurons' (4)
LAZY1	I182_G184del	Deleterious, codon deletion	***P. bucharica* (3)**
LAZY2	A134E	Deleterious, codon change	'Bartre' (1), 'Ardechoise' (2), **'Garfi' (2)**, **'Atocha' (2)**, 'Princesse' (2), 'Lauranne' (3), 'Vialfas' (3), **'Vivot' (3)**, 'Retsou' (3), 'Guara' (4), 'Primorski' (4),' Belle d'Aurons' (4), 'Genco' (4**)**
LAZY2	R293G	Deleterious, codon change	'Bartre' (1), 'Achaak' (2), **'Marcona' (3)**, 'Chellaston' (3), 'Isabelona' (3), 'Ai' (4), *P. webbii* (4), **'Desmayo Largueta' (5)**
TAC1	D105_D108del	Neutral	*P. bucharica* (3)
TAC1	D108_E109insD	Deleterious, codon insertion	'Bartre' (1), 'Marinada' (2), 'Ardechoise' (2), 'Achaak' (2), 'Ferragnes' (2), 'Princesse' (2), *P. kuramica* (2), 'Marcona' (3), 'Vialfas' (3), 'Vivot' (3), 'Vairo' (3), 'Retsou' (3), 'Chellaston' (3), *P. bucharica* (3), 'Guara' (4), 'Primorski' (4), 'Ai' (4), 'Belle d'Aurons' (4), 'Pointeu d'Aureille' (4), *P. webbii* (4), 'Desmayo Largueta' (5)

Only cultivars presenting the mutation are reported. Overall tree habit description is displayed after each cultivar: (1) = Upright, (2) = Somewhat upright, (3) = Semi-open, (4) = Open, (5) = Weeping. Cultivars in bold present the mutation in both alleles. Complete protein sequences for LAZY1, LAZY2 and TAC1 can be found in Supplementary Data 2.2 (Annex 2). All found variants are listed in Supplementary Data 2.3 (Annex 2).

2.3.3. Expression profiling of IGT Family members in selected almond cultivars

The expression levels of the six IGT family members were analyzed in shoot tips of fourteen almond cultivars on late August (Table 2.1). Expression analysis could provide an estimation of the protein activity. Previous studies in peach have shown than *LAZY1* and *TAC1* expression patterns are similar and both genes are expected to be coordinately regulated (Dardick et al., 2013; Hollender et al., 2020; Tworkoski et al., 2015). Since *TAC1* is believed to act antagonistically to *LAZY* activity, it could be that high levels of *LAZY1* or *LAZY2* expression were influenced by high levels of *TAC1* expression, or vice versa. Furthermore, in poplar (*Populus trichocarpa*), *TAC1* overexpression has been linked to broad-crown trees, while *LAZY1* expression remained constant through both narrow-crown and broad-crown trees (Xu et al., 2017). Therefore, we used the *LAZY1*/*TAC1* and *LAZY2*/*TAC1* expression ratio as a descriptor of *LAZY1* and *LAZY2* molecular activity (Figure 2.3).

LAZY1/*TAC1* and *LAZY2*/*TAC1* did show differences in their ratio profile between cultivars. *LAZY1*/*TAC1* was found to have a higher ratio in Garnem® shoot tips, while upright cultivars 'Bartre' and 'Ferragnes' had the lowest levels of *LAZY1*/*TAC1* ratio. Other cultivars like 'Garfi', 'Vialfas' and 'Vairo' also presented relatively elevated *LAZY1*/*TAC1* ratios (Figure 2.3A). Highest levels of *LAZY2*/*TAC1* expression ratio were found in 'Garfi' and 'Vialfas', although the ratio in 'Garfi' was almost 2-fold higher. Unlike 'Garfi', *LAZY2* was not overexpressed in 'Vialfas' compared to the rest of cultivars, yet its lower levels of *TAC1* could indicate an imbalance in the *LAZY2*/*TAC1* ratio and, therefore, a higher *LAZY2* activity. 'Marcona' and 'Vairo' presented the lowest levels of the *LAZY2*/*TAC1* ratio (Figure 2.3B). It was not possible to find any transcripts of *DRO2* and *IGT-like*, while *DRO1* expression was only detected in a reduced number of cultivars. This result is not unexpected, since *DRO* genes have been described acting mainly in root tissues (Uga et al., 2013).

Garnem® is the only selection that is not a scion cultivar, but rather a hybrid peach x almond rootstock (Felipe, 2009). It has been described that the effect of IGT family members can vary within *Prunus* species, e.g., *TAC1* silencing in plum (*P. domestica*) mimicking the pillar peach genotype leads to more acute effects on tree architecture (Hollender et al., 2018). The peach genetic background in Garnem® could explain why the *LAZY1*/*TAC1* ratio levels are significantly higher compared to the rest of the analyzed genotypes. 'Garfi', the mother genotype of Garnem® shows a similar tree habit phenotype but different expression pattern. In 'Garfi', *LAZY1*/*TAC1* ratio is moderate and *LAZY2*/*TAC1* is elevated when compared with the rest of cultivars (Figure 2.3). However, 'Garfi' expression levels, while being higher than most cultivars, are quite similar for both members of the IGT family, presenting similar absolute values both ratios.

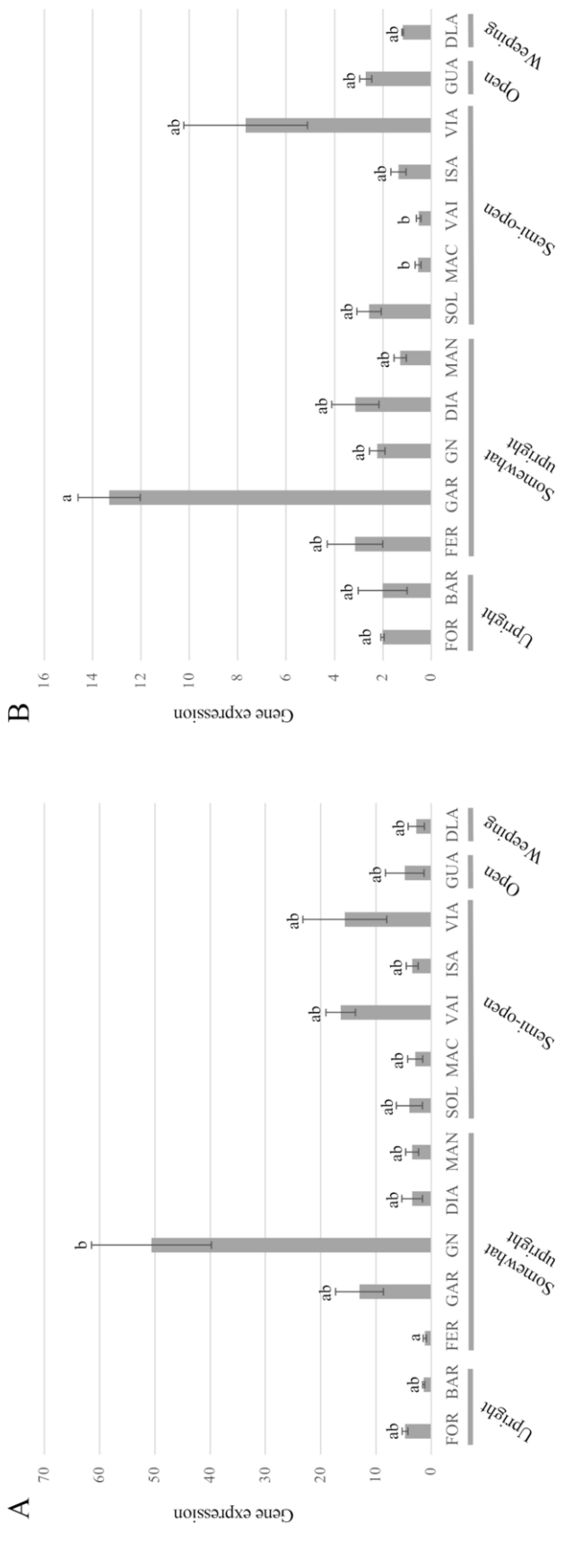

Figure 2.3. Expression analysis of IGT family genes in fourteen cultivars of interest. A, Ratio of relative gene expression between *LAZY1* and *TAC1*. **B,** Ratio of relative gene expression between *LAZY2* and *TAC1*. Cultivars abbreviatures are as follows: 'Forastero' (FOR), 'Bartre' (BAR), 'Ferragnes' (FER), 'Garfi' (GAR), Garnem® (GN), 'Diamar' (DIA), 'Marinada' (MAN), 'Soleta' (SOL), 'Marcona' (MAC), 'Vairo' (VAI), 'Isabelona' (ISA), 'Vialfas' (VIA), 'Guara' (GUA), 'Desmayo Largueta' (DLA). Letters above each bar indicate significance group, derived from Nemenyi's Test.

Although significant differences in gene expression were found on branches that presented vegetative growth, it was not possible to establish a correlation between expression levels and overall tree habit in these cultivars. Both 'Garfi' and Garnem® present an upright architecture, which would be tied to an expected predominance of *LAZY* expression. However, trees with more erect habits as 'Forastero' and 'Bartre' showed low or basal levels of *LAZY*/*TAC1* ratios. Expression levels of both *LAZY1* and *TAC1* in *P. persica* have been described to be related to seasonal changes, being higher in April (Tworkoski et al., 2015). However, they are expected to be expressed in any growing and active tissue (Dardick et al., 2013). In Mediterranean areas, almond displays vegetative growth through late spring to end of summer (Felipe, 2000); hence presenting an active growth in its shoot tips during this period. Even though high levels of *LAZY1* and *LAZY2* are presented exclusively in upright cultivars, it does not appear to be the only factor in shaping the almond tree habit, since cultivars with lower ratios present a more upright phenotype. It is possible that the ratio values changes are too low to observe an effect in the phenotype. In poplar, differences that led to a contrasting phenotype were at least an order of magnitude higher to those observed here (Xu et al., 2017). Though high similarity has been reported between peach and almond genomes (Alioto et al., 2020; Goonetilleke et al., 2018), we did not observe in our set of cultivars the effect on the phenotype that has been described in peach (Dardick et al., 2013; Hollender et al., 2018, Tworkoski et al., 2015). The lack of correlation observed in the studied phase between gene expression and phenotype accompanied by the same case observed with their protein sequence hints to the IGT family may have suffered little to no selection at all in commercial almond orchards (Table 2.2, Figure 2.2). Not being unexpected since, until recently, almond breeding has been focused on improving traits related to either flowering or the fruit (Gradziel, 2017). Thus, other regulatory pathways must be involved in the establishment of the overall tree habit.

2.3.4. Analysis of variants in *LAZY1* and *LAZY2* promoter regions

Although it is not possible to establish any clear correlation between diversity in tree habit and the expression levels of the IGT family members, the difference in *LAZY1* and *LAZY2* expression between the related 'Garfi' and Garnem® gives us a unique opportunity to study in detail the mechanisms involved in regulating their gene expression. Since these two selections present different expression profiles while their sequences are highly similar, divergences in their promoter region and their transcription factors (TFs) binding capabilities could explain the contrast in expression.

Promoter regions of *LAZY1*, *LAZY2* and *TAC1* were analyzed in search of variants within regulatory elements (REs) that might impact their expression and their respective ratios. Two

mutations that could explain the differences observed in their expression profile were found in *LAZY1* and only one in *LAZY2* (Table 2.3). No significant variants were encountered in the *TAC1* promoter region.

Table 2.3. List of variants that correlate with the differences observed in gene expression affecting Regulatory Elements (REs) and their Transcription Factors (TFs) associated.

Gene	Position	RE	TF	Sequence	Alternative	Cultivars presenting the variant
LAZY1	Pd01:20652273	ABRE	*ABI3*	GCCATTTGTC	GCCATTCGTC	'Bartre' (1), **'Ferragnes' (2)**, 'Marinada' (2), 'Soleta' (3), 'Marcona' (3)
LAZY1	Pd01:20652273	E-Box	*RAVL1*	GCCATTTGTC	GCCATTCGTC	'Bartre' (1), **'Ferragnes' (2)**, 'Marinada' (2), 'Soleta' (3), 'Marcona' (3)
LAZY1	Pd01:20652307	TGGGCY-motif	*IPA1*	AGCCCA	GGCCCA	'Bartre' (1), **Garnem® (2)**, **'Isabelona' (3)**, 'Guara' (4), 'Desmayo Largueta' (5)
LAZY2	Pd03:23958144	GTAC-motif	*IPA1*	GATAAGC	GATAAG	'Forastero' (1), 'Bartre' (1), **'Garfi' (2)**, Garnem® (2), 'Diamar' (2), **'Soleta' (3)**, **'Vialfas' (3)**

Only cultivars presenting the mutation are reported. Overall tree habit description is displayed after each cultivar: (1) = Upright, (2) = Somewhat upright, (3) = Semi-open, (4) = Open, (5) = Weeping. Cultivars in bold present the mutation in both alleles. All mutations in promoter sequences can be found in Supplementary Data 2.4 (Annex 2).

Both *LAZY1* and *LAZY2* promoter regions presented a variant within a RE which is associated to the TF *IPA1* (Table 2.3), also known as *SPL9* in Arabidopsis and *SPL14* in rice. *IPA1* has been previously related with the regulation of shoot branching, acting predominantly repressing gene expression, though it has been described to also act in a promoting manner in few cases (Jiao et al., 2010; Miura et al., 2010). In Arabidopsis, it has been reported that *IPA1* downregulates genes involved in responses related to auxin signaling (Lu et al., 2013). While *LAZY1* promoter region presents the variant in a TGGGCY motif, *LAZY2* has a mutated GTAC motif (Table 2.3). *IPA1* has been described to interact with both motifs, and more specifically, directly with the second one (Lu et al., 2013). Due to the nature of *IPA1* activity, it would be conceivable that it is acting in a repressive fashion. Therefore, if a mutation obstructs its binding to a RE, *LAZY1* and *LAZY2* would predictably be overexpressed. The mutations described might fit with this predicted outcome, especially in the *LAZY1* promoter region, where Garnem® presented the mutation, which displayed a remarkable high *LAZY1*/*TAC1* ratio due to an overexpression of *LAZY1* (Table 2.3, Figure 2.3). 'Garfi' also presented a mutation in the *LAZY2* promoter, which could be linked to its elevated *LAZY2*/*TAC1* ratio, though similar levels are observed in *LAZY1*/*TAC1* ratio where no mutation was described (Table 2.3, Figure 2.3). Nevertheless, other cultivars also present the variant in this RE without showing high ratio values, indicating that the mutation does not affect gene expression by itself, possibly being affected by other factors, i.e., *IPA1* expression level, protein activity or the interaction of other TFs.

Another mutation of interest was found in the *LAZY1* promoter region, affecting an E-box element, which has been described as a binding region of the transcription factor *RAVL1* (Table 2.3). The mutation exists in several selected varieties and is present in homozygosis in the cultivar 'Ferragnes' (Table 2.3), whose *LAZY1*/*TAC1* ratio was low (Figure 2.3). In rice, *RAVL1* has been described directly promoting genes involved in BRs and ethylene (ET) responses, acting in diverse metabolic processes (Xuan et al., 2017; Zhu et al., 2018). BRs act promoting branching and shoot growth (Rameau et al., 2015). The involvement of *RAVL1* in regulating *LAZY1* and therefore, gravity response, would place this gene at the crossover between both responses. Moreover, an ABRE element described as a binding region for the TF *ABI3* could be also altered by the same mutation. Nevertheless, *ABI3* is mainly involved in ABA signaling and predominantly in processes related to seed germination (Dekkers et al., 2016).

The mutations described in *LAZY1* and *LAZY2* promoter might explain the differences in their gene expression through cultivars. In particular, a mutation within a RE related to the TF *IPA1* in the *LAZY1* promoter may cause the high *LAZY1*/*TAC1* ratio observed in Garnem®. Other mutations could also affect the expression profile, though more knowledge is needed to characterize their effect.

2.3.5. Analysis of expression *IPA1* homologues in almond

Due to its possible involvement in the regulation of *LAZY1* and *LAZY2* expression, a BLASTp search for IPA1 homologues in almond was conducted using atIPA1. Three *IPA1* homologues were found: *IPA1-like 1* (Prudul26A025211), *IPA1-like 2* (Prudul26A009750) and *IPA1-like 3* (Prudul26A016898). No non-synonymous mutations were found for any of the homologues. The expression levels of the three genes were analyzed in the shoot tips previously collected at the end of summer, in ten of the previous fourteen cultivars.

The expression profile through the ten cultivars was relatively stable for the three genes. Cultivars 'Vairo', 'Marinada' and 'Diamar' presented the highest expression levels (Figure 2.4). However, significant differences were only found in *IPA1-like 2*, which is overexpressed in 'Vairo' and repressed in 'Garfi'. In all three homologues, 'Garfi' presented low expression levels compared with the rest of cultivars. A similar profile can be observed in 'Vialfas' (Figure 2.4). As it is mentioned before, *IPA1* has been previously described acting as a repressor (Jiao et al., 2010; Lu et al., 2013; Miura et al., 2010). Therefore, the relative high ratio observed in both *LAZ1*/*TAC1* and *LAZY2*/*TAC1* in 'Garfi' might be associated with low *IPA1* activity. Although 'Vialfas' high *LAZY2*/*TAC1* ratio was mostly explained by *TAC1* repression, a similar phenomenon could underlie its profile. Nonetheless, no REs associated to *IPA1* were found in the analysis of the *TAC1* promoter.

Garnem® showed similar expression levels than other cultivars for all three *IPA1* homologues, while displaying a remarkably high *LAZY1*/*TAC1* ratio. This overexpression could be caused by the mutation previously described in the *LAZY1* promoter, affecting a regulatory element associated to *IPA1* regulatory activity (Table 2.3). The mutation could disrupt *IPA1* interaction with the *LAZY1* promoter, and hence preventing *LAZY1* inhibition (Figures 2.3 and 2.4). Since no alterations were found in the *LAZY2* promoter, *IPA1* would be able to repress its expression, leading to the lower *LAZY2*/*TAC1* ratio observed in Garnem®.

IPA1 homologues seem to act redundantly, presenting a similar expression profile for the three genes. As it can be observed in 'Garfi' and 'Vialfas', low expression levels may be behind high *LAZY1*/*TAC1* and *LAZY2*/*TAC1* ratios. Therefore, confirming *IPA1* genes as candidate repressors of *LAZY1* and *LAZY2* activity in almond.

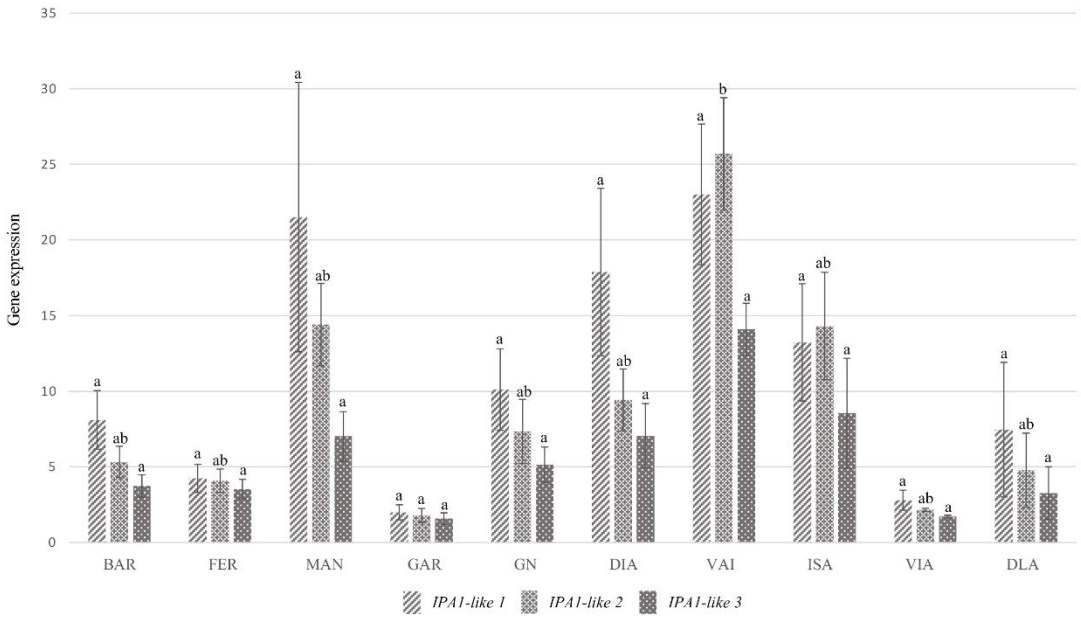

Figure 2.4. Expression analysis of *IPA1* homologues in almond. Cultivars abbreviatures are as follows: 'Bartre' (BAR), 'Ferragnes' (FER), 'Marinada' (MAN), 'Garfi' (GAR), Garnem® (GN), 'Diamar' (DIA), 'Vairo' (VAI), 'Isabelona' (ISA), 'Vialfas' (VIA), 'Desmayo Largueta' (DLA). Statistical analysis was performed for each gene separately. Letters above each bar indicate significance group derived from Nemenyi's test.

2.3.6. Regulatory elements (RE) and transcription factors (TFs) in *LAZY1* and *LAZY2* promoter regions

In order to identify TFs that might interact with REs present in *LAZY1* and *LAZY2* promoter regions, these regions were analyzed using New PLACE and PlantCARE online platforms. Twenty-one TFs were selected as preferred candidates, in addition to the previously

described *RAVL1* and *ABI3*, which possible RE variability was noted within the varieties (Table 2.4). A majority of the TFs are involved in light responses and hormonal regulation. Similar functions have been described in the REs of *LAZY1, LAZY2* and *TAC1* in *Malus* × *domestica* (L. Wang et al., 2018).

Table 2.4. Localization in the *LAZY1* and *LAZY2* promoters of identified Transcription Factors (TFs).

Transcription factor	*P. dulcis* ID	Position *LAZY1*	Position *LAZY2*
ABI3	Prudul26A014736		-1,314, -1,166, -882, -878, 85
ARF1	Prudul26A011950	-1,423	-1,138, -474, 222
ARF2	Prudul26A008717	-1,298, -344, -343	
ATAF1	Prudul26A030564	-1,299, -345, -344	
GATA14	Prudul26A008840	-33	-1,569, -129
GBF6	Prudul26A015068	-345	
GTL1	Prudul26A008868	-892, -890	
HB4	Prudul26A018199	-1325, -1152	-1,475, -1,314, -1,102, -882, -878, 85
HB5	Prudul26A009108		-1,246, -1,011, -758, 115
IAA24	Prudul26A021243	-678	
LEAFY	Prudul26A028984	85	
MYC2	Prudul26A013616	-1,474, -1,296, -1,325, -841, -777, -699, -418, -392, -340, -238, -223, -155	-1,413, -908, -672, -304, -284, -164, 404
OBP4	Prudul26A018122	-869, -863	-1,475, -1469, -516
PCL1	Prudul26A032278		-1,139, -744, -743
phyA	Prudul26A016497		-559
RAP2.2	Prudul26A031706	-1,454, -1,420, -1,374, -1,370, -1,290, -1,203, -1,120, -1,111, -1,046, -1,023, -1,019, -954, -802, -768, -719, -643, -518, -445, -420, -394, -361, -308, -291, -287, -269, -212, -180, -176, -112, -84, -35, -28, -18, 43, 58, 63, 75, 144, 280, 326'	-1,619, -1,564, -1,267, -1,257, -1,232, -1,113, -1105, -1069, -982, -975, -967, -949, -916, -894, -861, -747, -704, -692, -647, -604, -544, -502, -490, -483, -470, -416, -400, -384, -355, -353, -344, -289, -278, -257, -218, -211, -207, -195, -172, -124, -99, -82, -70, -64, -58, -51, -47, -18, 46, 149, 204, 296, 343, 385, 410
RAP2.3	Prudul26A030616	-1036, 8	-1,090, -236
RAVL1	Prudul26A026729	-779, -157, 87, 85	-1,439, -1,277, 402, 402, 402, 403
SGR5	Prudul26A008399	-1,426	
TGA1	Prudul26A032960	-1,168	-58
WUS	Prudul26A011412		82

Position is displayed as relative to the start codon.

Several TFs are involved in auxin responses. While *ARF1* REs are present in both promoter regions, *ARF2* and *IAA24* REs only are found in *LAZY1* promoter; all of them act as mediators in the auxin signaling pathway (Guilfoyle et al., 2015; Leyser, 2018; Li et al., 2016; Luo et al., 2018; Okushima et al., 2005; Vert et al., 2008). Other hormone regulatory pathways are represented among the TFs selected. *RAP2.2* and *RAP2.3* belong to the Group VII of ERF (Ethylene Response Factors) and are involved in various stress responses (Hinz et al., 2010; Nakano et al., 2006; Papdi et al., 2015; Rubio-Cabetas et al., 2018). *RAP2.2* REs can be found extensively repeated through both promoter regions. *LAZY2* promoter exhibits REs for *HB5*, a positive regulator of ABA and GA responses, and *WUS* a promotor of meristem proliferation in response to ET and auxin (Johannesson et al., 2003; Shi et al., 2018; Stamm et al., 2017). The

ATAF1 RE, that falls within the *LAZY1* promoter, is a key regulator of biotic and abiotic stress pathways, promoting ABA biosynthesis and regulating carbon metabolism genes or inducing the expression of genes involved in salt stress and detoxification responses (Garapati et al., 2015; Jensen et al., 2013; Liu et al., 2016; Zhao et al., 2018). Both promoters have REs for the TF *OBP4*, which is a negative regulator of cell expansion and root growth in response to ABA (Ramirez-Parra et al., 2017; Rymen et al., 2017; Xu et al., 2016). *GBF6*, with a RE in *LAZY1* promoter, is repressed by sucrose and acts as a mediator between carbohydrates regulation and amino acid metabolism (Ma et al., 2011). Sugars have been described as an essential part of branch outgrowth (Mason et al., 2014). *TGA4*, with a RE described in both promoters, acts as a regulatory factor that mediate nitrate responses and induce root hair development in Arabidopsis roots (Alvarez et al., 2014; Canales et al., 2017). Light response TFs were also included in the selection. Both *LAZY1* and *LAZY2* promoters present a site for *MYC2* and *HB4*, which are involved in R:FR regulation and shade avoidance response (Kazan and Manners, 2013; Sorin et al., 2009). *PCL1 (*RE found in *LAZY2* promoter), is involved in the circadian clock (Helfer et al., 2011; Onai and Ishiura, 2005). *GT-1*, found in both promoters, and its family member *GTL1*, only in *LAZY1*, have been described to modulate various metabolic processes in response to light perception (Kaplan-Levy et al., 2012). *LAZY2* promoter presents a RE associated to the photoreceptor *phyA*, core regulator of the R:FR ratio light perception (Casal, 2012; Finlayson et al., 2010; Rausenberger et al., 2011; Reddy and Finlayson, 2014). REs for *GATA14*, a zing finger TF belonging to the GATA family, are found in both promoters. GATA family of TFs have been described to integrate growth and light perception in several species (An et al., 2020; Luo et al., 2010). Although *LAZY1* and *LAZY2* have been primarily described as regulators of gravity responses, a lack of known TFs related to gravity perception or responses was found. Only *SGR5*, involved in early stages of shoot gravitropism, could be found in the *LAZY1* promoter (Morita et al., 2006). *LAZY1* promoter present a RE for *LEAFY*, which is a central regulator of inflorescence development (Schultz and Haughn, 1991). Flower development and tree architecture has been previously linked in studies in *Malus* × *domestica* (Foster et al., 2014). Between the TFs identified, there are a prevalence of genes related to several hormones. This points to IGT family genes being affected by numerous regulatory processes, as it could be expected hence their predicted role in a complex trait like tree habit. Gene expression was analyzed for these twenty-one TFs, not observing a connection between their levels and the previously reported *LAZY1*/*TAC1* and *LAZY2*/*TAC1* ratios (Supplementary Data 2.5; Annex 2). In any case, this TFs collection influence gene expression and act in regulatory pathways differently, therefore, the lack of a wide correlation might be expected.

2.4. Conclusions

IGT family proteins are highly conserved in almond, especially within the five conserved regions and a limited number of variations found across all cultivars. Though no correlation with architectural phenotypes was observed, LAZY1 and LAZY2 did exhibit mutations with an expected impact on their functionality. In addition, despite differences in their expression profile, there was no direct relation between the overall tree habit and their expression. Although IGT family members are known to play a role in tree growth habit in other species, we do not see evidence of their influence in tree habit variability for a considerable number of almond cultivars. This is probably because no loss-of-function mutation has been selected in the set of forty-one studied major commercial almond cultivar that favor this trait, while those correlating with phenotype observed in other species alter significantly the protein structure. Until recently, tree habit has not been an influential trait in almond breeding and these types of mutations were probably never selected. Furthermore, several of the mutations found in almond cultivars are present in heterozygosis, hence they could alter the phenotype if appeared in homozygosis and be a foundation for possible future breeding efforts. Anyway, there are many mechanisms leading to different tree habit, and even though *LAZY1* and *LAZY2* are not discriminant in current almond commercial cultivars, other families of genes must be involved in the regulation of almond tree habit. However, important aspects of the regulation of the IGT family in almond have been characterized. TFs *IPA1-like 1*, *IPA1-like 2*, *IPA1-like 3* seems to play a role in the regulation of *LAZY1* and *LAZY2* expression in addition to other TFs involved in hormonal regulation and light perception. In conclusion, almond tree habit depends on numerous factors, which outlines the necessity to better characterize the regulation of this trait and molecular mechanisms behind it both in almond orchards and other fruit trees.

3. PHENOTYPING ALMOND ROOTSTOCK FOR ARCHITECTURAL TRAITS INFLUENCED BY ROOTSTOCK CHOICE

Montesinos, Á., Thorp, G., Grimplet, J., and Rubio-Cabetas, M. (2021). Phenotyping Almond Orchards for Architectural Traits Influenced by Rootstock Choice. *Horticulturae* 7, 159. doi: 10.3390/horticulturae7070159.

Abstract

The cropping potential of almond (*Prunus amygdalus* (L.) Batsch, syn *P. dulcis* (Mill.)) cultivars is determined by their adaptation to edaphoclimatic and environmental conditions. The effects of scion/rootstock interaction on vigor have a decisive impact on this cropping success. Intensively planted orchards with smaller less vigorous trees present several potential benefits for increasing orchard profitability. While several studies have examined rootstock effects on tree vigor, it is less clear how rootstocks influence more specific aspects of tree architecture. The objective of this current study was to identify which architectural traits of commercially important scion cultivars are influenced by rootstock and which of these traits can be useful as descriptors of rootstock performance in breeding evaluations. To do this, six almond cultivars of commercial significance were grafted onto five hybrid rootstocks, resulting in thirty combinations that were measured after their second year of growth. We observed that rootstock choice mainly influenced branch production, but the effects were not consistent across the different scion/rootstock combinations evaluated. This lack of consistency in response highlights the importance of the unique interaction between each rootstock and its respective scion genotype.

3.1. Introduction

Since its development, reported around 1,800 BCE, grafting has been a crucial part of the propagation process for tree and vine crops (Mudge et al., 2009). As well as conferring traits of agronomic interest to trees in the orchard, the use of grafting and clonal rootstocks has facilitated the independent selection of scion and rootstock traits, thus improving breeding techniques. Rootstocks can be selected for relevant root system traits, including conferring resistance to pathogens such as root knot nematodes, endowing tolerance of alkaline and calcareous soils and promoting higher yields in non-irrigated soils (Rubio-Cabetas et al., 2017). Rootstocks can also influence scion phenotype such as fruit quality, yield, flowering time and tree vigor (Albacete et al., 2015; Aloni et al., 2010; Foster et al., 2015; Martínez-Ballesta et al., 2010; Warschefsky et al., 2016).

Nowadays, clonal rootstocks are utilized in numerous fruit and nut species of economic significance (Warschefsky et al., 2016). Their usage is widespread in almond (*Prunus amygdalus* (L.) Batsch, syn *P. dulcis* (Mill.)) orchards, and varieties are generally graft-compatible with both almond and peach (*P. persica* (L.) Batsch) rootstocks and their interspecific hybrids (Felipe, 2009; Rubio-Cabetas et al., 2017). In the last decade, several new dwarfing rootstocks have been developed, conferring low and medium vigor to establish new more intensive and sustainable cropping systems.

Due to their global significance as a major tree fruit crop, rootstock effects on scion vigor have mostly been studied in apple (*Malus* × *domestica*). In these studies, rootstock effects have mainly been described in generic vigor-related parameters such as scion height, trunk diameter, shoot length and frequency of branching (Tworkoski and Fazio, 2009; Tworkoski and Miller, 2007). Apple dwarfing rootstocks can also stimulate flowering in young trees, which indirectly affects shoot production and shoot vigor (Seleznyova et al., 2008). Young apple trees on dwarfing rootstocks form more floral buds and thus more axillary bourse shoots compared with the more vigorous terminal shoots produced from purely vegetative buds. Rootstock involvement in more specific aspects of tree architecture is less clear, and there is often a lack of consistency in responses among different cultivars, which highlights the importance of scion/rootstock interactions (Tworkoski and Miller, 2007; van Hooijdonk et al., 2010). While previous studies with almond have described rootstock effects on vigor in generic terms (Balducci et al., 2019; Lordan et al., 2019), knowledge of rootstock influence on more specific architectural traits and their wider influence over almond tree architecture is still limited.

First introduced by Hallé et al. (1978), architectural analysis of trees provided a way to analyze the dynamics of plant development that is applicable to any species. The architectural

tree models developed from this work are based on four major features: (i) temporal growth pattern; (ii) branching pattern; (iii) morphological differentiation of axes; and (iv) sexual differentiation of meristems (Costes et al., 2006). A total of twenty-three different architectural models were found in nature from all possible combinations of these features (Hallé et al., 1978).

Temporal growth patterns predominantly have two features: rhythmic vs. continuous growth and determinate vs. indeterminate growth (Barthélémy and Caraglio, 2007). Continuous growth is a rare phenomenon and is not observed in Rosaceae species, whose shoots alternate periods of active growth and rest (Costes et al., 2014). Determinate growth refers to the abortion or transformation of the terminal bud into a specialized structure (Costes et al., 2006). If the apical meristem maintains indefinitely its function, then growth is indeterminate. Branching is a key aspect in defining tree structure. An axillary meristem may develop into a shoot at the same time as the extension of the parent axis, without a period of rest or dormancy, to form a sylleptic shoot (Costes et al., 2006). Otherwise, the axillary meristem remains inactive and only develops into a shoot after a period of rest or dormancy, forming a proleptic shoot. Rhythmic (zonal) branching is constituted by groups of branched nodes followed by a succession of unbranched nodes. Diffuse branching is when shoots are disposed uniformly along the main axis (Hallé, 2001). Determinate and indeterminate growth patterns can lead to two different branching patterns, sympodial and monopodial, respectively (Barthélémy and Caraglio, 2007). Sympodial growth is when continued growth of the primary axis occurs via successive growth of axillary buds in subterminal positions, while monopodial growth occurs via continued extension of a single terminal meristem or bud (Costes et al., 2006). The sum of all these features constitutes the architectural tree model.

Markovian models have been used to build general models for describing tree structure (Durand et al., 2005). These methods analyze tree architecture as a succession of zones with a different proportion of node types whose arrangement is defined by transition probabilities, using branches as the study subject (Costes et al., 2006; Costes and Guédon, 2002; Guédon et al., 2001; Seleznyova et al., 2002). This approach has been applied to almond under different circumstances (Negrón et al., 2013, 2014a, 2014b). Although these models are useful for describing and visualizing repetitive patterns in tree architecture and branching formation, they are difficult to incorporate into genomic analyses, such as genome-wide association studies (GWAS). Therefore, accurate and objective measurements are needed. There have been few advancements in the analysis of these kinds of quantitative traits focused on their heritability or on the influence of the environment (Migault et al., 2017; Segura et al., 2008, 2006). Recently, high-throughput phenotyping technologies such as T-LiDAR have been used in apple orchards to identify different architectural groups (Coupel-Ledru et al., 2019). However, these methods fall short in describing the physiology and control processes determining tree shape and architecture or in distinguishing

the nuanced changes that exist between different scion/rootstcok combinations. Furthermore, there are considerable difficulties in measuring a substantial number of architectural traits in enough individuals in large trees modified by pruning. It is easier to record these traits of interest on young, unpruned trees.

The objective of the research presented here was to identify which architectural traits of the scion cultivar are influenced by rootstock genotype and which of these traits can be used as reliable descriptors of rootstock performance in breeding evaluations. We did this by characterizing the genotype-specific effects of a selection of rootstocks on the architecture of a range of important scion cultivars.

3.2. Materials and Methods

3.2.1. Plant material and growth conditions

For the experiment, six almond cultivars of agronomic interest were grafted onto five different commercial rootstocks, resulting in thirty different combinations. The scion cultivars selected were 'Isabelona' (syn. 'Belona'), 'Soleta', 'Guara', 'Vialfas', 'Diamar' (syn. 'Mardía') and 'Lauranne'. All are important commercial cultivars in Spain. The rootstocks were selected to represent a range of vigor responses in the grafted scion: 'GN-8', 'Densipac' (Rootpac® 20), 'Nanopac' (Rootpac® 40), 'Replantpac' (Rootpac® R) and Garnem® (GN15). All were hybrid rootstocks from different origins. Garnem® and 'GN-8' are both almond × peach (*P. amygdalus* (L.) Batsch, syn *P. dulcis* (Mill.). × *P. persica* (L.) Batsch) hybrid rootstocks, while the three others came from the commercial Rootpac® series including Rootpac® 40 (*P. amygdalus* (L.) Batsch, syn *P. dulcis* (Mill.). × *P. persica* (L.) Batsch), Rootpac® 20 (*P. cerasifera* × *P. besseyi*) and Rootpac® R (*P. cerasifera* × *P. amygdalus* (L.) Batsch, syn *P. dulcis* (Mill.)). Grafted plants were supplied by the Agromillora Iberia S.L. nursery in 2018 (Barcelona, Spain). Trees were planted during October 2018 at the Centro de Investigación y Tecnología Agroalimentaria de Aragón (CITA) experimental orchard El Vedado Bajo el Horno (Zuera, Zaragoza, 41º51'46.5'' N 0º39'09.2'' W). Trees were planted as a single stem and supported by a wooden stake. Trees were then left without pruning so that they could express their natural growth habit unaltered. Conventional orchard practices were used for weed control and drip irrigation. Soil type was calcareous with pH around 7–8.

3.2.2. Architectural traits

Data collection was carried out during winter 2020 after two growing seasons from ninety trees with three trees per scion/rootstock combination (Figure 3.1). In total, twenty-four

parameters were considered as possible descriptors of tree architecture, divided into four categories: tree vigor, branching quantity and vigor, branching distribution and branching angle (Table 3.1). In this context, the primary growth axis of the tree was referred to as the trunk with axillary shoots forming directly on the trunk during the first season's growth. A branch was regarded as a second-order structure comprising multiple axillary shoots present during the second season's growth. The tree vigor category included five parameters. Total trunk length (Length) and number of internodes (Nb_IN) were determined from the graft union to the apex of the tree, and average internode length (IN_L) was calculated from those two measures. Trunk diameter was measured at both 20 mm above the graft union (d_Base) and 20 mm (d_Top) below the apex of the tree. Vigor was also recorded as branch diameter measured both at the base (B_dBase) and at the apex (B_dTop) of each branch along the trunk. Seven parameters were included in the branch quantity category. The total number of branches formed directly on the trunk (Nb_B) was recorded, as it was the number of axillary shoots formed on these branches (B_NbAS). Three categories of shoot length were used to describe branching frequency along the trunk; these categories were short (< 100 mm), medium (100 – 200 mm) and long (> 200 mm), denoted as Nb_sB, Nb_mB and Nb_lB, respectively. The ratio of branches by trunk length (BbyL) and trunk internodes (BbyIN) were calculated. The branch distribution category included the internode in which each branch was positioned along the trunk. Also determined from this value was the mean distribution of branches along the trunk (Dist_B), as well as the percentage of shoots in each third of the trunk from the basal to middle and distal sections (Dist_Down, Dist_Med and Dist_Up, respectively). Branching angle was recorded for branches formed directly on the trunk as the angle relative to the trunk at the base of the branch and at the branch tip. Three categories were used to describe branching angle: upright (< 45º), semi-open (45 – 65º) and open (> 65º), resulting in the following according to their base angle (Base_U, Base_SO and Base_O) and tip angle (Top_U, Top_SO and Top_O). In total, seventeen variables were established directly from measured data, while seven variables were calculated combining some of the initial measurements.

3.2.3. Statystical analysis

All statistical analyses were carried out in the R platform (https://cran.r-project.org/, accessed on 11 June 2021). A two-way ANOVA test was performed using the R stats package in order to establish which of the twenty-four measured parameters described in Table 3.1 were influenced by the rootstock genotype. Although the two-way ANOVA test allowed us to observe the influence on the variability of both the rootstock and the cultivar separately, we limited our focus to the effects of their interaction. Since all data were collected from the scion, the interaction of the two independent variables, rootstock and cultivar, described the extent of rootstock

influence in aerial architectural traits. Parameters were selected as being influenced by rootstock choice when the p-value was lower than 0.1. Pearson's correlation coefficients were computed using the Hmisc R package (https://CRAN.R-project.org/package=Hmisc, accessed on 20 December 2020). Parameters correlating with an r value higher than +0.7 or lower than -0.7 were considered redundant, and a single parameter was conserved for analyses. Principal component analysis (PCA) was carried out using the R stats package with default parameters. The rootstock effect on each individual cultivar was evaluated using an ANOVA test to find significant differences. These were assessed with the Tukey's test ($p < 0.05$) using the agricolae R package (https://CRAN.R-project.org/package=agricolae, accessed on 24 January 2021).

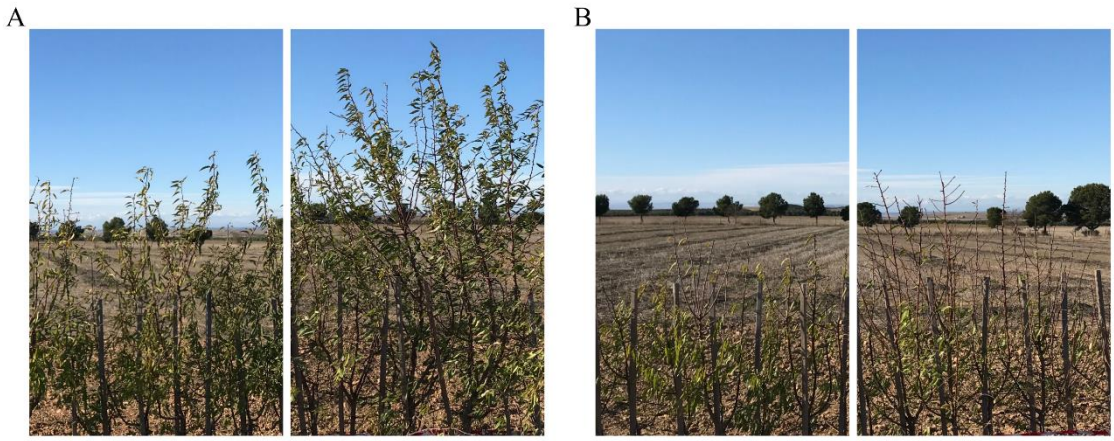

Figure 3.1. Scion/rootstock combinations of two-year-old almond trees show low and high vigor responses. A, 'Guara' grafted onto 'GN-8' (left) and Garnem® (right) rootstocks. **B,** 'Diamar' grafted onto 'GN-8' (left) and Garnem® (right) rootstocks.

3.3. Results

3.3.1. Rootstock influence in trait variability

Out of the twenty-four starting parameters described in Table 3.1, fifteen of these had a p-value lower than 0.1, and of these, eleven had a p-value lower than 0.05 (Table 3.2). Four scion vigor variables were identified as affected by the rootstock choice: Nb_IN, Length, IN_L and d_Top. However, a lack of scion/rootstock interaction was observed for the diameter at the base of the scion (d_Base), which is equivalent to the trunk cross sectional area (TCSA), even though it could be expected that a more vigorous rootstock should have an effect on this trait. No influence was observed for the vigor parameters measured on the branches, such as B_dBase and B_dTop. All traits representing branch quantity were identified as influenced by the rootstock, suggesting that branching may be strongly affected by rootstock selection. Branch distribution parameters were predominately affected by rootstock genotype, with the exception of Dist_Med. Rootstock did not appear to affect branching angle, since only Top_SO might be characterized as

being influenced by the rootstock. All fifteen parameters with a p-value lower than 0.1 were considered as possibly influenced by the rootstock and were used in further analyses.

Table 3.1. Parameters used to quantify aspects of almond tree architecture and the corresponding formula if parameters were calculated from other traits.

Type	Parameter	Formula	Trunk	Branches
Vigor	Number of internodes		Nb_IN	
	Length (mm)		Length	
	Average lenght of internodes (mm)	Length/Nb_IN	IN_L	
	Base diameter (mm)		d_Base	B_dBase
	Apex diameter (mm)		d_Top	B_dTop
Branch quantity	Number of branches		Nb_B	B_NbAS
	Ratio of branches by trunk internodes	Nb_B/Nb_IN	BbyIN	
	Ratio of branches by trunk length	Nb_B/Length	BbyL	
	Number of short branches (< 100 mm)		Nb_sB	
	Number of medium branches (100 – 200 mm)		Nb_mB	
	Number of long branches (> 200 mm)		Nb_lB	
Branch distribution	Mean distribution of branches trough the trunk	SUM(IN)/Nb_IN	Dist_B	
	Percentage of branches in the 1st third of the trunk	NbDown/Nb_B	Dist_Down	
	Percentage of branches in the 2nd third of the trunk	NbMed/Nb_B	Dist_Med	
	Percentage of branches in the 3rd third of the trunk	NbTop/Nb_B	Dist_Up	
Branching habit	Number of upright branches measured at the base (< 45º)		Base_U	
	Number of semiopen branches measured at the base (45º – 65º)		Base_SO	
	Number of open branches measured at the base (> 65º)		Base_O	
	Number of upright branches measured at the apex (< 45º)		Top_U	
	Number of semiopen branches measured at the apex (45º – 65º)		Top_SO	
	Number of open branches measured at the apex (> 65º)		Top_O	

Data were measured on the primary growth axis (trunk) or axillary branches of two-year-old almond trees for thirty scion/rootstock combinations.

3.3.2. Identification of relevant parameters and interaction between them

Different categories correlation values between parameters were analyzed in a two-part approach. Firstly, variables belonging to the same category with a correlation value higher than +0.7 or lower than -0.7 were considered redundant, and a unique representative parameter was selected. Secondly, correlation values above +0.32 or below -0.32 between traits classified among different categories were contemplated as possible interrelated architectural processes.

Vigor parameters Length and Nb_IN were highly correlated, r = 0.899 (Table 3.3), which is not unexpected, since a longer main axis is expected to present a higher number of internodes. In addition, both variables were also negatively correlated with d_Top above the threshold. Length, as well as IN_L, were selected as descriptors of tree vigor

For branch quantity parameters, BbyL and BbyIN presented a correlation value of +0.887 (Table 3.3). Both depended on the number of branches (Table 3.1), describing similar aspects of the phenotype. Despite BbyL having a lower p-value (Table 3.2), BbyIN was chosen as a branch quantity descriptor because it also described the potentiality of a given node to become a branch. Nb_sB and Nb_mB were positively correlated with Nb_B, presenting an $r > 0.7$ (0.722 and 0.801, respectively) (Table 3.3). Therefore, the amount of short and medium shoots (Nb_sB and Nb_mB) might depend primarily on the total number of branches. The number of long shoots (Nb_lB) appeared to be more independent of the total number of branches, $r = 0.397$. Thus, Nb_lB was kept with Nb_B as a branch quantity descriptor. Finally, B_NbAS, did not show correlation values above the 0.7 threshold with any other parameter, and so, with no reason to discard it, the B_NbAS parameter was added to the list of branch quantity descriptors.

Table 3.2. Analysis of the effects of thirty almond scion/rootstock combinations on variability in architectural traits as affected by scion and rootstock genotype and the interaction between the two.

	Trait	Cultivar	Rootstock	Cultivar × Rootstock Interaction
Vigor	Nb_IN	2.21E-06	0.726	**4.21E-07**
	Length	0.00263	0.23671	**4.01E-05**
	IN_L	3.87E-10	0.000153	**0.080919**
	d_Base	4.06E-10	7.32E-06	0.168
	d_Top	8.29E-05	0.28228	**0.00696**
	B_dBase	8.74E-08	0.00189	0.23873
	B_dTop	0.0986	0.0686	0.1342
Branch quantity	Nb_B	0.00037	1.14E-12	**0.01043**
	BbyIN	0.000152	1.20E-07	**0.001294**
	BbyL	0.001262	8.53E-07	**0.000649**
	B_NbAS	7.93E-09	0.00547	**0.05479**
	Nb_sB	3.47E-05	0.00036	**0.05135**
	Nb_mB	0.00208	8.33E-07	**0.01555**
	Nb_lB	0.00634	1.65E-09	**0.00814**
Branch distribution	Dist_B	0.00256	0.08757	**0.00303**
	Dist_Down	0.249	0.7719	**0.0288**
	Dist_Med	0.4682	0.0288	0.2746
	Dist_Up	0.0127	0.0116	**0.0169**
Branching habit	Base_U	0.7449	0.0541	0.9252
	Base_SO	0.182	0.0156	0.6591
	Base_O	0.0643	2.96E-05	0.3477
	Top_U	0.00336	7.06E-07	0.11616
	Top_SO	0.2424	0.3178	**0.0845**
	Top_O	0.0247	7.55E-07	0.6563

Refer to Table 3.1 for abbreviations. Significant variability ($p < 0.1$) for the Cultivar × Rootstock interaction according to the two-way ANOVA test are in bold.

Table 3.3. Pearson's correlation coefficients of variables comparing thirty almond scion/rootstock combinations, classified by which aspect of almond tree architecture they affect and selected by rootstock influence.

		Vigor				Branch quantity							Branch distribution			Branching habit
		Nb_IN	Length	IN_L	d_Top	Nb_B	BbyIN	BbyL	B_NbAS	Nb_sB	Nb_mB	Nb_lB	Dist_B	Dist_Down	Dist_Up	Top_SO
Vigor	Nb_IN	1.000														
	Length	**0.899**	1.000													
	IN_L	-0.306	0.078	1.000												
	d_Top	**-0.707**	**-0.711**	0.075	1.000											
Branch quantity	Nb_B	*0.323*	0.246	-0.169	-0.229	1.000										
	BbyIN	*-0.587*	*-0.563*	0.233	*0.472*	*0.437*	1.000									
	BbyL	*-0.490*	*-0.591*	-0.177	*0.445*	*0.489*	**0.887**	1.000								
	B_NbAS	*-0.483*	*-0.485*	0.067	*0.501*	-0.268	0.215	0.165	1.000							
Branch vigor	Nb_sB	*0.458*	*0.366*	-0.224	*-0.351*	**0.722**	0.084	0.148	*-0.394*	1.000						
	Nb_mB	0.257	0.219	-0.161	-0.234	**0.801**	0.281	*0.361*	-0.225	*0.359*	1.000					
	Nb_lB	-0.214	-0.220	0.122	0.260	*0.397*	*0.616*	*0.547*	0.211	-0.155	0.186	1.000				
Branch distribution	Dist_B	*-0.656*	*-0.672*	0.084	*0.622*	-0.088	*0.452*	*0.409*	*0.393*	-0.124	-0.113	0.113	1.000			
	Dist_Down	*0.540*	*0.579*	-0.026	*-0.480*	-0.041	*-0.434*	*-0.398*	-0.262	0.031	-0.031	-0.112	**-0.796**	1.000		
	Dist_Up	*-0.596*	*-0.580*	0.140	*0.602*	-0.174	*0.362*	0.308	*0.372*	-0.210	-0.190	0.128	**0.914**	*-0.584*	1.000	
Branching habit	Top_SO	0.121	0.088	-0.045	-0.034	-0.016	-0.010	0.000	-0.072	-0.050	0.035	-0.007	0.022	-0.078	0.030	1.000

Refer to Table 3.1 for abbreviations. Parameters with an r value higher than +0.7 or lower than -0.7 between members of the same category are in bold.

For branch distribution parameters, both Dist_Down and Dist_Up were highly correlated with Dist_B, r = -0.796 and r = 0.914, respectively (Table 3.3). Since Dist_B describes the overall distribution of branches along the trunk and not their concentration in a single part of the main axis, it was taken as the unique branch distribution descriptor. As it was the only branching angle parameter at this point, conferring therefore little descriptive value, Top_SO was excluded from subsequent analyses. In summary, seven parameters were selected as representative of three different categories: Length, IN_L, Nb_B BbyIN, B_NbAS, Nb_lB and Dist_B.

Correlations between parameters belonging to different categories were also studied to identify possible interactions. The vigor parameter Length was correlated with the branch quantity traits BbyIN and B_NbAS and with the branch distribution variable Dist_B, indicating a potential interaction between the height of the main axis and these parameters. Furthermore, BbyIN was positively correlated with the branch distribution trait Dist_B (Table 3.3).

3.3.3. Analysis of rootstock and cultivars of interest

Scion/rootstock combinations affected tree height (Length), but the effect was not consistent across the different rootstocks or scion cultivars. For example, 'Isabelona' or 'Diamar' trees grafted onto Rootpac® 20, a low vigor rootstock, were taller when compared with the other rootstocks in this study, while 'Soleta' and 'Vialfas' trees on Rootpac® 20 were shorter (Table 3.4). Moreover, 'Isabelona' and 'Vialfas' trees grafted on Garnem® rootstock, a high vigor rootstock, were taller when compared with trees grafted with the other rootstocks in this study, while 'Diamar' and 'Soleta' trees on Garnem® rootstock were smaller. 'Lauranne' trees were smaller than the other scion cultivars across all rootstocks with the exception of Rootpac® R. The trunks of 'Lauranne' trees on Rootpac® R rootstock were twice the height of 'Lauranne' trees on the other rootstocks. Internode length (IN_L) was similar across all scion/rootstock combinations, with only a few cultivars grafted onto the dwarfing rootstock 'GN-8' showing significant low IN_L values (Table 3.4).

Branching quantity traits were substantially affected by rootstock choice in our cultivars of interest. When grafted onto Garnem® rootstock, the number of branches (Nb_B) was significantly higher on 'Guara', 'Isabelona' and 'Vialfas' trees compared with trees on the dwarfing rootstocks 'GN-8' and Rootpac® 20. Likewise, branching frequency, the number of branches per node (BbyIN), was less when cultivars were grafted onto Rootpac® 20 and 'GN-8'. Combinations with both Rootpac® 40 and Rootpac® R also produced more branches through all scion cultivars (Table 3.4).

Table 3.4. Analysis of the seven non-redundant variables in the thirty scion/rootstock combinations, comparing by rootstock choice.

		'Lauranne'	'Guara'	'Isabelona'	'Diamar'	'Soleta'	'Vialfas'
Length (mm)	Garnem®	353 a	707 a	800 ab	323 c	357 b	1190 a
	'GN-8'	223 a	453 a	443 b	820 ab	847 a	313 d
	Rootpac® 20	317 a	923 a	1053 a	1053 a	373 b	380 cd
	Rootpac® 40	317 a	720 a	450 b	607 bc	730 a	697 b
	Rootpac® R	690 a	717 a	623 ab	687 b	597 ab	653 bc
IN_L (mm)	Garnem®	19.0 a	16.7 a	12.4 a	17.0 a	11.0 a	12.8 ab
	'GN-8'	11.0 b	14.5 a	12.1 a	15.9 a	10.6 a	9.2 b
	Rootpac® 20	18.8 a	18.5 a	11.0 a	17.6 a	13.1 a	15.1 a
	Rootpac® 40	16.2 a	14.8 a	12.2 a	15.0 a	12.7 a	12.3 ab
	Rootpac® R	16.7 a	15.8 a	11.3 a	14.0 a	13.9 a	11.9 ab
Nb_B	Garnem®	9.0 ab	15.3 a	22.3 a	8.7 ab	14.7 a	18.0 a
	'GN-8'	4.0 b	3.3 b	8.0 b	5.7 b	10.3 a	8.7 bc
	Rootpac® 20	5.3 ab	2.7 b	4.7 b	2.7 b	6.3 a	7.7 c
	Rootpac® 40	12.0 a	8.7 ab	8.0 b	7.0 ab	12.0 a	16.7 ab
	Rootpac® R	11.3 a	12.0 ab	13.0 ab	15.0 a	15.3 a	11.7 abc
BbyIN	Garnem®	0.481 ab	0.382 a	0.359 a	0.452 a	0.456 a	0.193 a
	'GN-8'	0.199 b	0.191 a	0.292 a	0.107 c	0.130 b	0.242 a
	Rootpac® 20	0.331 ab	0.070 a	0.048 a	0.043 c	0.232 ab	0.295 a
	Rootpac® 40	0.608 a	0.247 a	0.288 a	0.183 bc	0.209 ab	0.294 a
	Rootpac® R	0.365 ab	0.268 a	0.232 a	0.303 ab	0.362 ab	0.211 a
Nb_lB	Garnem®	5.3 ab	4.7 a	6.3 a	7.7 a	6.3 a	4.3 a
	'GN-8'	3.0 b	2.3 a	1.7 a	3.3 b	4.0 ab	2.7 ab
	Rootpac® 20	3.3 ab	1.0 a	1.3 a	0.7 b	1.7 b	3.0 ab
	Rootpac® 40	7.0 a	3.3 a	2.7 a	1.7 b	3.7 ab	3.7 a
	Rootpac® R	4.7 ab	4.7 a	1.7 a	2.7 b	4.0 ab	0.7 b
B_NbAS	Garnem®	5.2 a	2.7 a	0.5 a	1.3 a	2.8 a	0.4 a
	'GN-8'	7.1 a	1.3 a	0.5 a	0.1 a	0.9 a	2.4 a
	Rootpac® 20	3.5 a	1.0 a	0.0 a	0.3 a	1.6 a	0.2 a
	Rootpac® 40	1.2 a	0.5 a	0.8 a	0.0 a	1.7 a	0.1 a
	Rootpac® R	2.2 a	0.7 a	0.3 a	0.0 a	2.2 a	0.1 a
Dist_B	Garnem®	0.58 a	0.61 a	0.53 a	0.69 a	0.58 ab	0.46 a
	'GN-8'	0.64 a	0.60 a	0.48 a	0.22 b	0.37 b	0.72 a
	Rootpac® 20	0.69 a	0.59 a	0.39 a	0.35 b	0.79 a	0.74 a
	Rootpac® 40	0.59 a	0.40 a	0.52 a	0.44 b	0.49 b	0.47 a
	Rootpac® R	0.63 a	0.50 a	0.51 a	0.44 b	0.57 ab	0.47 a

Refer to Table 3.1 for abbreviations. Assessed with Tukey's test. Values within columns followed by the same letter were not significantly different ($p < 0.05$).

There were more long shoots on scion cultivars grafted onto Garnem® rootstock compared with the other rootstocks (Table 3.4). A similar effect was detected with trees grafted onto Rootpac® 40, but not as consistently across the different scion cultivars as with Garnem®. Cultivars grafted onto 'GN-8' and Rootpac® 20 showed the opposite phenotype, with few long shoots. Despite no significant differences being observed in the number of secondary branches (B_NbAS), cultivars 'Lauranne', 'Soleta' or 'Guara' presented a higher tendency to develop second order branches (Table 3.4).

Only ‘Diamar’ and ‘Soleta’ displayed significant differences of Dist_B between rootstocks combinations. Otherwise, there were no consistent trends observed across the scion/rootstock combinations. (Table 3.4).

3.3.4. Principal component analysis of scion/rootstock combinations

Once the representative parameters were defined, a principal component analysis (PCA) was carried out in order to observe if scion/rootstock combinations grouped together significantly. These analyses showed that 62.5% of the variability could be explained by the first two components (Dim1 and Dim2), while the other components explained a maximum of around 10% of the variability. Thus, only these first two components were taken into consideration.

No clear clusters of samples were observed with the same rootstocks in the PCA since there was a clear effect of the scion genotype. However, most of the combinations with low vigor rootstocks Rootpac® 20 and ‘GN-8’ were located together below the x-axis (Figure 3.2A). Meanwhile, combinations with Garnem® were positioned above the remaining rootstock combinations in the PCA. Rootpac® R and Rootpac® 40 rootstock combinations were scattered through the plot between these two groups. Cultivars did not sort in a noteworthy way, even though a certain separation could be recognized between combinations with ‘Lauranne’ and the rest of cultivars, while ‘Isabelona’ was in the opposite extreme of the grouped cultivars (Figure 3.2B). Length and branch quantity parameters have opposing influence in the components, being the cause behind the differential distribution of rootstock combinations (Figure 3.2C).

3.4. Discussion

Combinations of five rootstocks and six scion varieties were compared in this study to identify a set of representative parameters of tree architecture influenced by rootstock choice. In the first instance, twenty-four parameters comprising four trait categories (Table 3.1) were sorted by how their variability was affected by scion/rootstock interaction (Table 3.2). Then, a Pearson’s correlation test was performed for the fifteen remaining parameters to identify highly correlated parameters from the same category and non-redundant variables. Correlations between parameters from different categories were also analyzed without eliminating parameters (Table 3.3). Only seven variables were selected after this step, and we studied how the scion/rootstock combinations affected these seven parameters and how different almond cultivars were affected by the rootstock (Table 3.4). Finally, these seven variables were submitted to a principal component analysis (PCA) to observe differential distributions of scion/rootstock combinations (Figure 3.2).

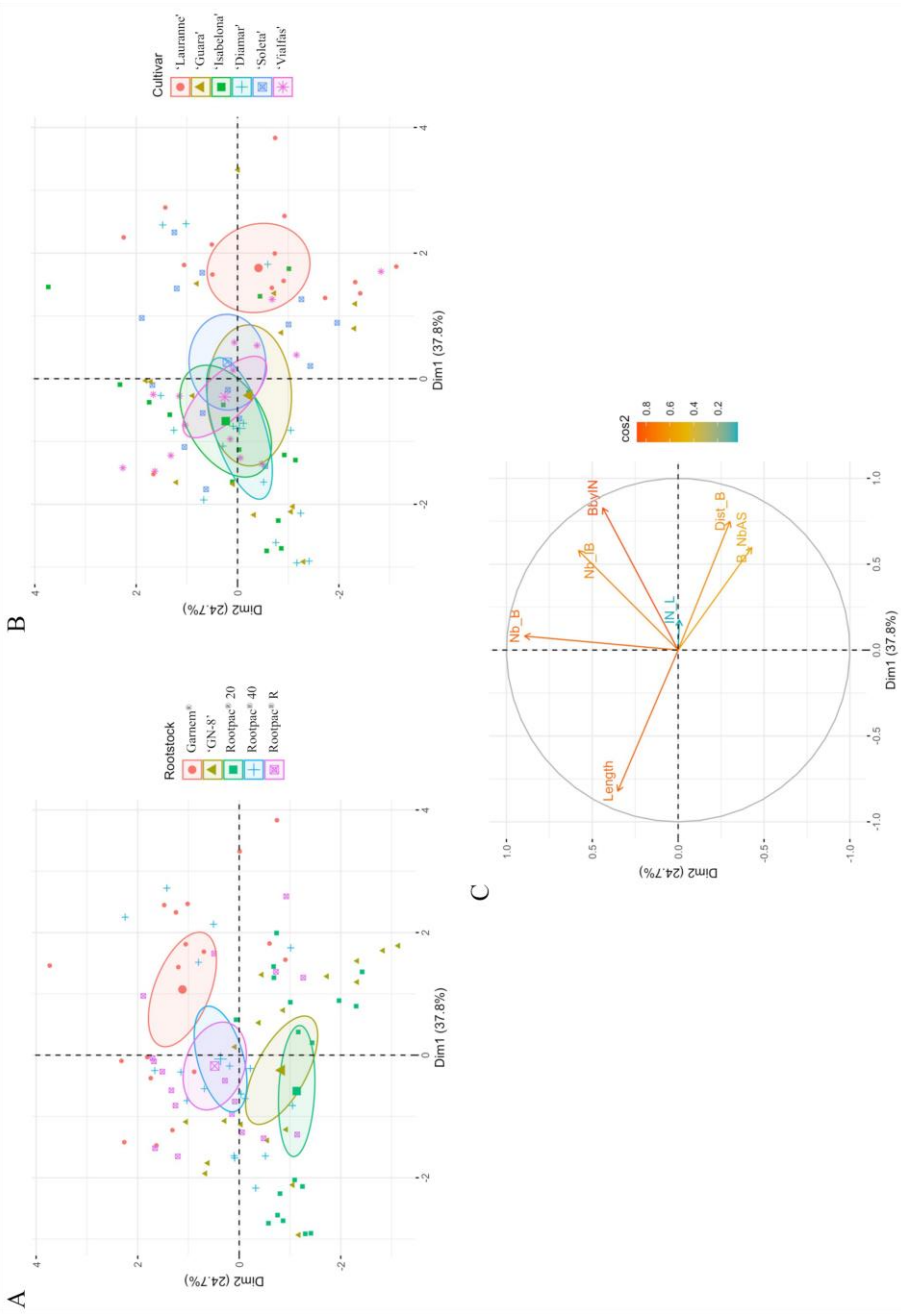

Figure 3.2. Principal component analysis (PCA) of seven non-redundant variables of thirty almond scion/rootstock combinations. A, Distribution of scion/rootstock combinations classified by rootstock choice as categorical variable with the first two components (Dim1 and Dim2) with concentration ellipses for each rootstock. **B,** Distribution of scion/rootstock combinations classified by cultivar choice as categorical variable with the first two components (Dim1 and Dim2) with concentration ellipses for each cultivar. **C,** Distribution of the seven non-redundant variables with the first two components (Dim1 and Dim2). Contribution of each parameter to the components is colored from blue to red. Data were collected from 2-year-old trees. Refer Table 1 for abbreviations

The seven parameters selected represented only three of the trait categories. Two of the parameters, Length and IN_L, belong to the category vigor. Branch quantity was represented by four different parameters Nb_B, B_NbAS. Nb_lB and BbyIN. Finally, Dist_B acts as unique representative of the branch distribution category. Practically no influence of the scion/rootstock interaction was detected in the branching angle category. It is of interest that the parameter IN_L and similar variables to Nb_B and B_NbAS were found to be relevant descriptors of apple tree architecture when selected by their genetic variability (Segura et al., 2006).

A shared trend was observed in the parameters influenced by rootstock genotype, with the majority of traits involved in processes related to the control of branching. It was observed that scion/rootstock combinations were primarily distributed differentially as a function of two opposing traits (Figure 3.2C). The Length parameter presented a negative value for the Dim1 axis, while all branch quantity (Nb_B, BbyIN, B_NbAS, Nb_lB) parameters had positive values in the Dim1 axis. Moreover, Length was negatively correlated with BbyIN and B_NbAS (Table 3.3).

Apical meristem maintenance and branching control are driven by the apical dominance exerted by the apex. Apical dominance refers to the suppression of axillary bud outgrowth during and/or after extension of the parent shoot, reducing the number of sylleptic and/or proleptic shoots, respectively. Gradziel (2012) has described this feature to classify primary and secondary branching patterns in almond. Apical dominance is controlled by the terminal apical meristem on the parent shoot and by the apical meristems of subordinate axillary shoots (Cline, 1991; Dun et al., 2006; Hollender and Dardick, 2015). Auxin is regarded as the main regulator of apical dominance, while other factors and hormones have been described as participating in branching regulation (Barbier et al., 2019; Casal, 2012; de Jong et al., 2014; Dun et al., 2012; Mason et al., 2014; Pereira-Netto et al., 2009; Rameau et al., 2015; Kieber and Schaller, 2018; Waldie et al., 2014; B. Wang et al., 2018; Xu et al., 2015). Specifically, strigolactones (SLs) are a crucial regulator of plant architecture (Napoli et al., 1996; Simons et al., 2007). Application of SL analogs has been proven able to reduce branching in tree species such as olive (*Olea europaea*) (Chesterfield et al., 2020).

Depending on the strength of apical dominance present, we can observe opposing phenotypes as described by Gradziel (2012). If apical dominance is strong, due to the cultivar or the rootstock effect or both, dormancy is imposed, affecting branch quantity parameters and producing low BbyIN, Nb_B and B_NbAS values, while the apical meristem would continue its growth resulting in high Length values. In contrast, with weak apical dominance, the repression of axillary buds is reduced, and more branches will develop, described by high values in branch quantity parameters. Sylleptic shoots are generally formed in the lower portion of the parent shoot, while proleptic shoots are mainly formed from subterminal buds, immediately below the shoot

apex, which is consistent with the positive correlation we found between Length and Dist_Down (Table 3.3). While the redistribution of resources to the formation of these lateral shoots may be expected to slow the growth of the main axis, resulting in determinate growth and low Length values, this effect appears to be mainly constrained to the formation of proleptic shoots formed after a period of rest. This would explain the negative correlation we found between Length and Dist_Up. Furthermore, while the presence of medium (Nb_mB) and short shoots (Nb_sB) correlates with the total number of shoots (Nb_B), we found the development of long shoots (Nb_lB) to be more independent. This is due to the existence of few long shoots, appearing more predominantly in combination with low apical dominance, but not necessarily in those with more branches (Table 3.4).

There is evidence from studies in peach that within the same genotype, rapid extension of the parent axis is associated with weak apical dominance and thus, a high number of sylleptic axillary shoots (Génard et al., 1994). Hence, in our study we often found more branches (Nb_B) with the more vigorous rootstocks than with the less vigorous rootstocks (Table 3.4). Rootpac® 20 and 'GN-8' can be described as dwarfing rootstocks, and their effects on the TCSA have been measured, proving a suppressing influence on tree vigor compared with more vigorous rootstock such as Garnem® and Rootpac® 40 (Ben Yahmed et al., 2016; Lordan et al., 2019). We did not record a strong influence of parameters related to trunk diameter, such as d_Base (Table 3.2). Instead we found a stronger relationship between rootstock vigor and shoot production (Nb_B).We observed that Rootpac® 20 and 'GN-8' seemed to favor apical dominance, not promoting the formation of branches and maintaining an active apical meristem. In contrast, Garnem® appeared to negatively affect apical dominance, forming numerous branches, including long shoots (Nb_lB) and ceasing main axis growth earlier than other rootstocks (Table 3.4). It is possible that this growth response is a forerunner of the strong basitonic growth habit evident in commercial almond orchards. A less intense, but similar effect, can be observed when grafted onto Rootpac® 40. Rootpac® R presented a medium phenotype, with numerous branches but maintaining an active main axis (Table 3.4). This distribution can be observed in the PCA, where Rootpac® 20 and 'GN-8' were diametrically opposed to Garnem®, with Rootpac® 40 and Rootpac® R between them (Figure 3.2A).

Cultivars grafted onto 'GN-8' showed shorter internodes than when grafted onto more vigorous rootstocks, such as Garnem® or Rootpac® 40 (Table 3.4). Internode elongation, which is mainly regulated by gibberellic acid (GA), has been described as being influenced by rootstock genotype (Hearn, 2016; Tworkoski and Miller, 2007). However, SLs are also known to affect internode elongation independent of GA (de Saint Germain et al., 2013).

While there is ample evidence of rootstocks having a strong effect on scion tree architecture, the scion itself plays an essential part in branching regulation. Both 'Diamar' and 'Isabelona' showed a similar phenotype when grafted onto Rootpac® 20, favoring apical dominance, resulting in high Length values and reduced branching, observed through all branch quantity parameters. However, once grafted onto Garnem®, only 'Isabelona' was able to maintain an active apical meristem, while 'Diamar' ceased growth of the main axis earlier (Table 3.4). The cultivar 'Lauranne' presented a typical low apical dominance phenotype, developing an elevated number of both branches (BbyIN) and axillary shoots (B_NbAS) and reduced trunk length when grafted onto almost every rootstock (Table 3.4). Rootpac® R was the only exception, promoting the formation of short horizontal branches (Nb_B) but maintaining an active main axis (Length) (Table 3.4).

While almond trees in commercial orchards show strong basitonic branching with strong lower limbs dominating the growth of the trunk, at the branch level, new shoot growth can predominate from basal, middle or distal sections of the parent shoot (basitonic, mesotonic and acrotonic branching, respectively) (Costes et al., 2014; Negrón et al., 2013). Dist_B, which measures branching distribution, is negatively correlated with Length and positively with BbyIN, connecting apical dominance and branch positioning (Table 3.3). A desirable ideotype might present the axillary shoots equally distributed through the axis, as described by Gradziel (2012), presenting intermediate values for Dist_B, instead of being accumulated in a few internodes. Low apical dominance cultivar 'Lauranne' had consistent high Dist_B values (Table 3.4). In these combinations, the apical meristem ceases its growth early and long branches from the current season's growth form in the upper part of the trunk. 'Guara' presented a comparable phenotype to 'Lauranne', although the formation of branches from the current season's growth was more impaired by dwarfing rootstocks such as 'GN-8' and Rootpac® 20. A similar effect can be observed when cultivars are grafted onto Garnem® (Table 3.4). 'Soleta' displayed significant differences of Dist_B between rootstock combinations, presenting high values when grafted onto Rootpac® 20. However, this combination also presented a reduced number of long shoots (Table 3.4). Thus, the high Dist_B values might be due also to the accumulation of a few short branches in the apex, not descriptive of a lack of apical dominance.

Although they are not distributed as clearly as in the rootstocks comparison, there is a certain degree of separation between some of the cultivars in the PCA. 'Lauranne' combinations were mildly distanced from the rest of the cultivar combinations. Combinations with 'Isabelona' as the cultivar are located predominantly in the opposite extreme, yet closer to the rest of combinations (Figure 3.2B). Apical dominance seems to be heavily influenced by rootstock choice in some cultivars, such as 'Diamar' or 'Soleta', but not in those that present a stronger

control of this feature, such as 'Lauranne'. A similar phenomenon can be observed with 'Isabelona', where the rootstock effect is more diluted (Table 3.4). Hence, this illustrates the importance of a correct choice of rootstock when deciding what scion cultivar should be selected for field production.

3.5. Conclusions

Seven parameters were selected as descriptors of rootstock influence in almond scion architecture. The choice of rootstock affected scion cultivar architecture, modifying both apical dominance and branch parameters. Garnem® and Rootpac® 20 had an opposite influence on the architecture of the scion, as was observed in parameters such as Length or the number of branches (Nb_B), while mixed results were observed with other rootstocks. However, these processes are regulated by numerous physiological processes, and the final phenotype is not only the result of the interaction between the rootstock and the scion but also the result of rootstock and scion interaction with the environment. Cultivars with a strong or weak display of apical dominance, for example 'Lauranne' and 'Isabelona', were less affected by rootstock influence, while the other scion cultivars in this study were strongly influenced by rootstock choice. This highlights the importance of screening rootstock progeny with a number of scion genotypes, in view of the strong scion/rootstock genotype interactions. Thus, a better understanding of what is happening at the graft union and with other physiological and molecular aspects of scion/rootstock interaction is needed in order to decipher the nuanced changes that determine tree architecture across a range of scion/rootstock combinations.

4. ANALYSIS OF THE ROOTSTOCK EFFECT ON SHOOT FORMATION IN TWO-YEAR OLD ALMOND BRANCHES

Abstract

The implementation of new planting systems in almond (*Prunus amygdalus* (L.) Batsch, syn *P. dulcis* (Mill.)) orchards for more sustainable practices has made tree architecture increasingly relevant as an important trait in plant breeding efforts. Multiple features define the three-dimensional structure of the tree, with shoot production being the most important. Shoots in branch can develop after a period of dormancy (proleptic shoots) or immediately at the same time that the parent shoot (sylleptic shoots). The proportion of proleptic or sylleptic shoots alters the resulting tree architecture, with sylleptic shoots being more numerous in the vigorous trees. Scion/rootstock interaction have been deemed to affect several aspects of the tree architecture. In order to study this effect, we analyzed shoot formation in fifteen scion/rootstock combinations resulting of three almond commercial cultivars grafted onto five interspecific hybrid rootstock. The type of shoot (proleptic or sylleptic) and its internode was collected for two-year old branches in three-year old unpruned plants. Here, we report that different rootstock genotypes can alter shoot production, affecting specially the number of sylleptic shoots formed. More insight of the molecular response is needed to comprehend the biological processes behind these differential phenotypes, which seems to be modulate by apical dominance and apical control.

4.1. Introduction

Several aspects define the three-dimensional structure of the tree. The combination of all these scion phenotype features is called tree architecture, which can be affected by how rootstock interact with the scion (Balducci et al., 2019; Seleznyova et al., 2008; Tworkoski and Fazio, 2015; Tworkoski and Miller, 2007; van Hooijdonk et al., 2010). Scion/rootstock interaction determines multiple aspects of tree development, such as flowering time, fruit quality, yield and the tree vigor, which significantly affects the tree architecture (Albacete et al., 2015; Foster et al., 2015; Martínez-Ballesta et al., 2010; Warschefsky et al., 2016).

Tree architecture is defined by four major features: (i) temporal growth pattern; (ii) branching pattern; (iii) morphological differentiation of axes; and (iv) sexual differentiation of meristems (Costes et al., 2006). One of these four features, branching pattern, is a key part of the definitive three-dimensional structure of the tree. The distribution of branches along the axis largely determines the tree architecture, generating rhythmic branching, when branched nodes are followed by unbranched nodes, or diffuse branching, when branches are established uniformly through the axis (Barthélémy and Caraglio, 2007). Besides, events during the dormancy period of buds also determines the final shape. If the axillary shoot develops while the parent branch is still growing, we are referring to a sylleptic shoot. However, if the bud remains inactive and develops after a period of dormancy, typically in *Prunus* trees in the following growing year, it would produce a proleptic shoot (Barthélémy and Caraglio, 2007; Costes et al., 2014).

The dynamics between proleptic and sylleptic shoot development, and their effect in other architectural traits, like fruit set, have been under study. Presence of these distinct shoots pattern have been analyzed in different almond (*Prunus amygdalus* (L.) Batsch, syn *P. dulcis* (Mill)) cultivars, observing differences that must be dependent of the genotype (Negrón et al., 2013). Moreover, the formation of proleptic and sylleptic shoots has been analyzed under different environment or treatments, like water deficiency or pruning (Negrón et al., 2014a, b). Proleptic and sylleptic shoot production is especially important when determining the tree fruit set. In peach (*P. persica* (L.) Batsch), proleptic shoots present more floral buds than sylleptic shoots, while the latter present a higher number of vegetative buds (Fyhrie et al., 2018). Therefore, the overall proportion of these shoot can alter largely the commercial viability of *Prunus* cultivars, and especially almond trees.

In this study, we analyzed the effect of different hybrid rootstocks on the formation of proleptic and sylleptic shoots in two-year-old almond branches. We observed that the type of shoots can variate between scion/rootstock combinations, confirming that rootstocks may alter

the molecular mechanisms that lead to the choice between dormancy or not, and hence, the production of proleptic or sylleptic shoots.

4.2. Materials and Methods

4.2.1. Tree population

For the experiment, we selected a subset of three almond cultivars from the six previously grafted onto five different commercial rootstocks in a previous experiment (Chapter 3; Montesinos et al., 2021b), resulting in a total of fifteen different combinations. The scion cultivars selected were 'Isabelona' (syn. 'Belona'), 'Guara' and 'Lauranne'. The three are important commercial cultivars in Spain. The rootstocks were selected to represent a range of vigor responses in the grafted scion: 'GN- 8', 'Densipac' (Rootpac® 20), 'Nanopac' (Rootpac® 40), 'Replantpac' (Rootpac® R) and Garnem® (GN15). All were hybrid rootstocks from different origins. Garnem® and 'GN-8' are both almond × peach (*P. amygdalus* (L.) Batsch, syn *P. dulcis* (Mill.). × *P. persica* (L.) Batsch) hybrid rootstocks, while the three others came from the commercial Rootpac® series including Rootpac® 40 (*P. amygdalus* (L.) Batsch, syn *P. dulcis* (Mill.). × *P. persica* (L.) Batsch), Rootpac® 20 (*P. cerasifera* × *P. besseyi*) and Rootpac® R (*P. cerasifera* × *P. amygdalus* (L.) Batsch, syn *P. dulcis* (Mill.)). Grafted plants were supplied by the Agromillora Iberia S.L. nursery in 2018 (Barcelona, Spain). Trees were planted during October 2018 at the Centro de Investigación y Tecnología Agroalimentaria de Aragón (CITA) experimental orchard El Vedado Bajo el Horno (Zuera, Zaragoza, 41º51′46.5″ N 0º39′09.2″ W). Trees were planted as a single stem and supported by a wooden stake. Trees were then left without pruning so that they could express their natural growth habit unaltered. Conventional orchard practices were used for weed control and drip irrigation. Soil type was calcareous with pH around 7–8.

4.2.2. Data collection

Data collection was carried out on two-year-old branches during winter 2021 from 150 trees with ten trees per scion/rootstock combination. Three parameters were collected for a whole branch of each tree. Total branch length (Length) and number of internodes (Nb_IN) were determined from the trunk to the apex of the branch, and average internode length (IN_L) was calculated from those two measures. Fate of each internode of the branch was annotated, distinguishing between blind nodes, proleptic shoots and sylleptic shoots.

4.2.3. Statistical analysis

All statistical analyses were carried out in the R platform (https://cran.r-project.org/). Significant differences in phenotypic data were evaluated using an ANOVA test. These were assessed with a Tukey's test ($p < 0.05$) using the agricolae R package (https://CRAN.R-project.org/package=agricolae).

4.3. Results

4.3.1. Architectural description of two-year-old branches

Three parameters studied as descriptors of almond tree architecture in a previous analysis (Chapter 3; Montesinos et al., 2021b) were measured in two-year-old branches of our fifteen scion/rootstock combinations: Length, Nb_IN and IN_L. These features give us a preliminary idea of the different structures that branches present in each combination. All these parameters were influenced by the rootstock genotype in the current experiment.

Rootstock influence on branch length (Length) was similar for all the cultivars. Scions grafted onto Garnem® always presented longer branches. 'Lauranne' and 'Guara' displayed an intermedium phenotype when grafted onto Rootpac® 40 and Rootpac® R, while combinations with 'GN-8' and Rootpac® 20 showed the lowest Length values, though differences were only significant in 'Guara'. However, only when grafted onto Rootpac® 40, 'Isabelona' showed intermediate values, whereas 'Isabelona' combinations with Rootpac® R presented similar branch length than those with 'GN-8' or Rootpac® 20 (Table 4.1). As expected, we observed that vigorous rootstocks like Garnem® had longer branches than those categorized as dwarfing rootstock like 'GN-8' or Rootpac® 20.

The number of internodes (Nb_IN) in the studied branches presented a similar dynamic than branch length. All cultivars had the highest number of internodes when grafted onto Garnem®, while displaying low Nb_IN when grafted onto 'GN-8'. Rootpac® series rootstocks presented small differences between each other in their influence of Nb_IN. The 'Isabelona'/Rootpac® 40 combinations displayed a reduced number of internodes, while for 'Lauranne', and significantly for 'Guara', Nb_IN values were higher when grafted onto Rootpac® 40 (Table 4.1). However, the two dwarfing rootstocks, 'GN-8' and Rootpac® 20, showed diverse influence on Nb_IN in combinations with 'Isabelona' and 'Guara', both less vigorous than 'Lauranne'. In these, scions grafted onto 'GN-8' had less internodes than those grafted onto Rootpac® 20, pointing to a different way of conferring dwarfism (Table 4.1) and may be related with the vigor itself.

Since both Length and Nb_IN are influenced by rootstock, the mean length of the internodes (IN_L) is also influenced. While 'Isabelona' and 'Guara' were more affected by the rootstock, 'Lauranne' displayed less differences between combinations, maybe due to its higher vigor. In the first two, combinations with Rootpac® 20 had the shortest internodes, whereas combinations with 'GN-8', Rootpac® 40 and Rootpac® R presented intermedium IN_L values. Combinations with Garnem® had the highest IN_L. Surprisingly, 'Lauranne' displayed the longest internodes when grafted onto 'GN-8', whereas when grafted onto 'Garnem', 'Lauranne' had the shortest of all its combinations (Table 4.1).

Table 4.1. Analysis of architectural traits related to vigor in two-year-old branches.

Cultivar	Rootstock	Length	Nb_IN	IN_L
'Isabelona'	Rootpac® 20	824.4 b	63.56 ab	13.1 b
	Rootpac® 40	927.1 ab	61.71 ab	15.0 ab
	Rootpac® R	806.2 b	55.63 ab	14.4 b
	'GN-8'	785.6 b	50.00 b	15.6 ab
	Garnem®	1252.0 a	72.80 a	17.2 a
'Guara'	Rootpac® 20	788.9 c	57.00 ab	13.9 c
	Rootpac® 40	1272.2 bc	69.67 a	18.2 ab
	Rootpac® R	1014.4 bc	50.33 b	19.7 ab
	'GN-8'	831.4 c	50.29 b	16.9 bc
	Garnem®	1408.8 a	66.50 ab	21.3 a
'Lauranne'	Rootpac® 20	951.0 b	55.80 b	17.1 ab
	Rootpac® 40	1238.9 b	77.80 b	16.9 ab
	Rootpac® R	1159.0 b	66.00 b	17.7 b
	'GN-8'	1071.0 b	58.10 b	18.8 a
	Garnem®	1564.0 a	99.30 a	16.1 b

Refer to Table 3.1 for abbreviations. Assessed with Tukey's test. Values within columns followed by the same letter were not significantly different ($p < 0.05$).

4.3.2. Number of proleptic and sylleptic shoots in two-year-old branches

The occurrence of proleptic and sylleptic shoots has an important weight in determining the definitive tree architecture. Here, we reported each node fate in two-year-old branches, distinguishing between blind nodes (when no shoot was present), proleptic shoot (when the shoot was developed after a period of dormancy) and sylleptic shoots (when the shoot was developed while the primary axis, or branch, was growing). Data was collected for the whole branch, after the second year of growth. Hence, while sylleptic shoots are present through the whole branch, data about proleptic shoots need two growth seasons and could only be present on the branch that grew during the first year.

The number of proleptic shoots was influenced by the rootstock, though such influence differed between cultivars. 'Lauranne' and 'Guara' displayed the highest number of proleptic

shoots when grafted onto Garnem®. On the contrary, the 'Isabelona'/Garnem® combination had a markedly reduced number of proleptic shoots (Table 4.2). 'GN-8' effect also varied depending on grafted cultivar. 'Guara'/'GN-8' had a reduced number of proleptic shoots, while 'Isabelona' and 'Lauranne' presented medium values when grafted onto 'GN-8' (Table 4.2). On the other hand, Rootpac® rootstocks showed a similar influence on all cultivars. Combinations with Rootpac® 20 had an elevated number of proleptic shoots, whereas those with Rootpac® 40 presented few proleptic shoots in general. Cultivars grafted onto Rootpac® R displayed an intermedium number of proleptic shoots (Table 4.2).

Table 4.2. Mean number of blind nodes, proleptic shoots and sylleptic shoots in two-year-old branches.

Cultivar	Rootstock	Blind nodes	Proleptic shoots	Sylleptic shoots
'Isabelona'	**Rootpac® 20**	45.89 a	15.00 a	2.67 b
	Rootpac® 40	48.00 a	4.29 b	9.43 b
	Rootpac® R	46.88 a	6.13 b	2.63 b
	'GN-8'	39.79 a	7.11 b	3.11 b
	Garnem®	51.30 a	2.80 b	18.70 b
'Guara'	**Rootpac® 20**	49.89 a	6.67 ab	0.44 c
	Rootpac® 40	53.56 a	3.89 b	12.22 a
	Rootpac® R	41.67 a	5.22 ab	3.44 bc
	'GN-8'	45.71 a	4.14 b	0.43 c
	Garnem®	43.13 a	11.88 a	11.50 bc
'Lauranne'	**Rootpac® 20**	44.00 ab	11.20 a	0.60 c
	Rootpac® 40	62.70 a	6.70 a	8.40 b
	Rootpac® R	53.20 b	9.20 a	3.60 bc
	'GN-8'	43.10 b	6.90 a	8.10 b
	Garnem®	64.90 ab	15.10 a	19.30 a

Assessed with Tukey's test. Values within columns followed by the same letter were not significantly different ($p < 0.05$).

There was not much disparity among cultivars in the influence of rootstocks on the number of sylleptic shoots. In all cultivars, combinations with Garnem® and Rootpac® 40 showed the higher number of sylleptic shoots. On the contrary, cultivars grafted onto Rootpac® 20 presented few to none sylleptic shoots. Combinations with Rootpac® R also displayed a reduced number of sylleptic shoots in all cultivars (Table 4.2). Only with scions grafted onto 'GN-8' we observed differences between cultivars. While 'Isabelona' and 'Guara' had few sylleptic shoots grafted onto this rootstock, 'Lauranne' presented a medium-high value (Table 4.2).

Both proleptic and sylleptic shoot development is influenced by rootstock genotype. Proleptic shoot formation seems to be more dependent on the scion characteristics, whereas the effect of the rootstock on sylleptic shoot production might be more determinant, as it can be seen in the near absence of significant differences between rootstocks in 'Isabelona' and 'Lauranne' for proleptic shoots.

4.3.3. Probability of proleptic and sylleptic shoot formation trough the branch

Proleptic and sylleptic shoots for the ten replicates of each combination were annotated and converted to its relative position in a branch with 100 internodes. A higher presence of them in a zone is represented as a higher probability of developing a shoot in that internode of the hypothetical branch.

As it was reported in Table 4.2, combinations with Rootpac® 20 as rootstock had mostly proleptic shoots, though the distribution of these varied between cultivars. While in 'Isabelona' they were between the start of the branch and the 60th relative internode, in 'Guara' and 'Lauranne' there were throughout the whole axis. Only a few sylleptic shoots were annotated, located in all combinations near the apex (Figure 4.1A, F and L). Scions grafted onto Rootpac® 40 had sylleptic shoots throughout the whole branch. Although there were few differences between cultivars, 'Guara' and 'Lauranne' showed a more similar profile than the one it was observed in 'Isabelona' (Figure 4.1B, G and M). Rootpac® R produce a scion with constant branching all along the axis. In all three cultivars, proleptic shoots, located in the first 50 relative internodes, were replaced by sylleptic branches from the 50th relative internode to the apex. While 'Isabelona' presented sylleptic shoots almost up to the apex, in 'Lauranne' and 'Guara' they were concentrated in a higher number a bit before the end of the branch (Figure 4.1C, H and N).

'GN-8' presented more differences between cultivars than any other rootstock. All of them presented a similar distribution of proleptic shoots, being located in the first 50 relative internodes. However, while 'Guara' displayed almost no sylleptic shoots, 'Isabelona' had a few more, and 'Lauranne' presented sylleptic shoots across the whole branch, especially between the 50th relative internode and the 70th (Figure 4.1D, I and O). Scions grafted onto Garnem® showed opposite distributions to what was observed in 'GN-8'. While all cultivars had a similar distribution of sylleptic shoots, being numerous and more present from the 40th relative internode to the apex of the branch, a difference in proleptic shoots was observed. 'Isabelona' had few sylleptic branches in the first 30 relative internodes, while 'Guara' and 'Lauranne' presented significantly more proleptic shoots in the first 50 relative internodes, and beyond (Figure 4.1E, K and P).

In general, it was observed that distribution of proleptic and sylleptic shoots, though with some few variations, is quite similar for all the combinations with a same rootstock. This highlights the importance of the rootstock in the regulation of shoot development, and therefore the tree architecture.

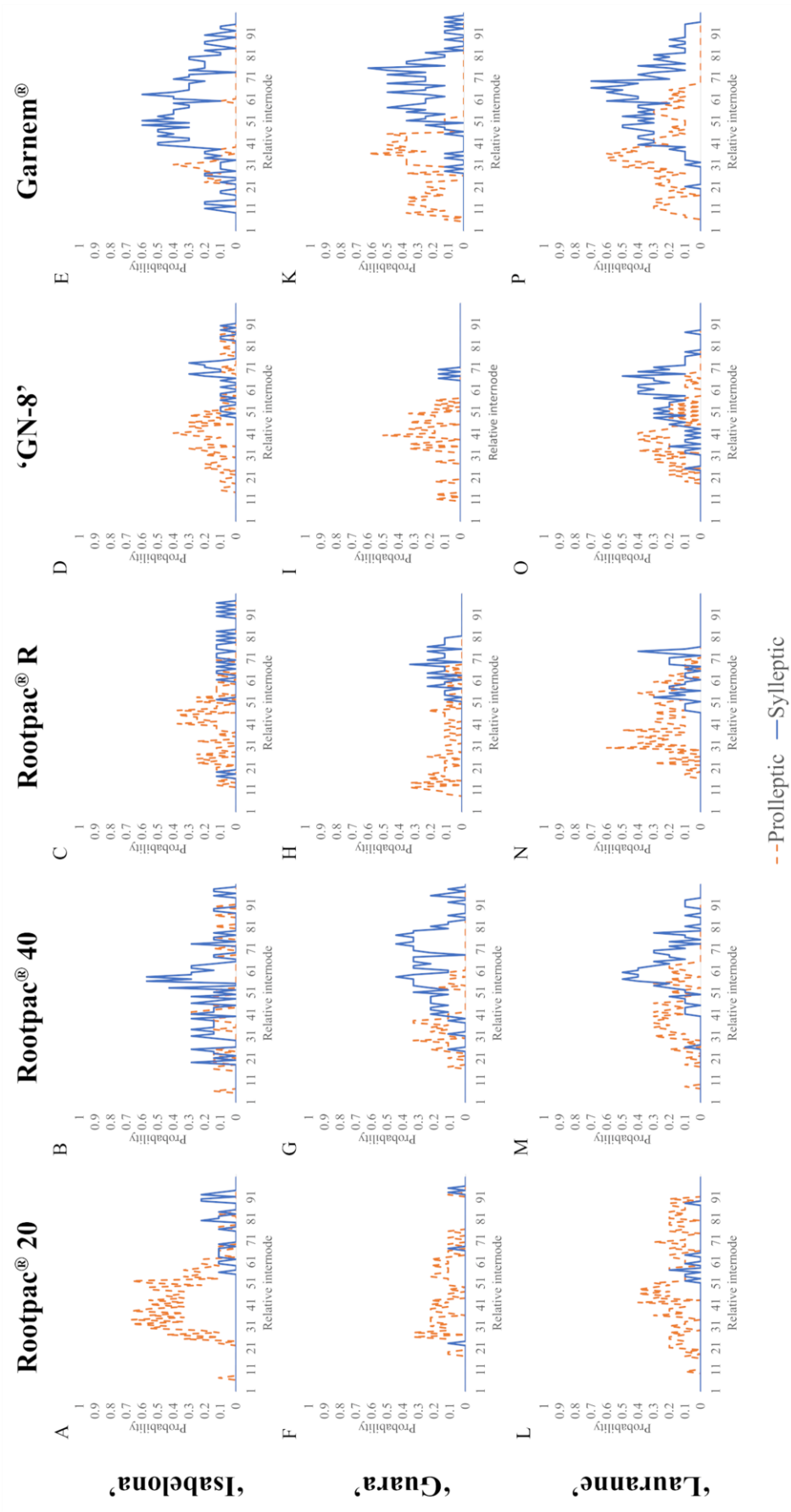

Figure 4.1. Probability of proleptic and sylleptic shoot occurrence in difference scion/rootstock combinations. The probability of proleptic and sylleptic shoot formation in each internode were converted to their relative position and represented in a same branch with 100 internodes for all combinations. Internode 0 refers to the base of the branch and internode 100 refers to the apex.

4.4. Discussion

In this study, we have analyzed the dynamics of two-year-old branches in individuals for which a collection of phenotypic data for architecture characters were obtained previously (Chapter 3; Montesinos et al., 2021b). The initial experiment originally included thirty different combinations of five rootstocks and six cultivars. From these we selected combinations of five rootstocks and three cultivars ('Isabelona', 'Guara' and 'Lauranne') presenting contrasted phenotypes. Here, we have measured certain parameters of two-year-old branches, like its length (Length) or the number and mean length of its internodes (Nb_IN and IN_L). Furthermore, we have studied the number of secondary shoots distinguishing between proleptic and sylleptic shoots. In general, we have observed a similar influence on tree architecture as previously reported, with rootstocks affecting apical dominance and shoot formation in the scion.

Vigor-conferring rootstocks studied previously (Chapter 3; Montesinos et al., 2021b), like Garnem® and Rootpac® 40 affected positively branch length (Table 4.1), as expected. Branch growth is controlled by hormones, gibberellic acid (GA), ethylene (ET) or brassinosteroids (BRs) being essential in its regulation (Hollender et al., 2016; Hollender and Dardick, 2015; J. Liu et al., 2017; Ma et al., 2016). Here, a differential hormonal activity must be exerted by the rootstock, explaining the variations between combinations. Besides, numerous nutrients are captured by the roots and transported to the aerial part, including nitrogen, whose content also affect vigor and branch development (Costa-Broseta et al., 2020; Krouk et al., 2011; Y.Y. Wang et al., 2018). Curiously, dwarfing rootstocks 'GN-8' and Rootpac® 20 present a different effect influencing branch length. Individuals grafted onto 'GN-8' displayed less internodes (Nb_IN) but with a length (IN_L) similar to scions grafted onto non-dwarfing rootstocks like Garnem®. On the contrary, combinations with Rootpac® 20 had a similar number of internodes as the others, but they presented a reduced mean length (13.1, 13.9 and 17.1 mm) (Table 4.1). These differences in internode development may be created by divergences in the scion hormonal profile, which is influenced by the rootstock. Internode elongation has been previously reported being affected by rootstock genotype. This aspect of tree architecture is mainly controlled by GA activity, although other hormones like strigolactones (SL) or BRs take part in it (de Saint Germain et al., 2013; Depuydt and Hardtke, 2011; Zhou et al., 2016; Zhu et al., 2011). This rootstock effect on branches is quite different to what we have observed previously in the trunk, where cultivars grafted onto 'GN-8' displayed shorter internodes than other combinations (Chapter 3; Montesinos et al., 2021b). While this may be contradictory, it reflect the elevated complexity of tree architecture regulation, pointing to the possibility that it exists a differential regulation of internode length according to the position in the tree or the year of growth, maybe related to different hormone gradients. In previous studies in apple (*Malus* × *domestica*) it has been reported that certain

dwarfing rootstocks may or may not affect the first year of shoot growth, while in all cases being affected posteriorly (van Hooijdonk et al., 2011, 2010).

Sylleptic shoot production was correlated to rootstock conferred vigor. Vigor-conferring rootstocks like Rootpac® 40, and specially, Garnem®, promoted the formation of sylleptic shoots (Table 4.2; Figure 4.1C, E, H, K, N and P). On the other hand, proleptic shoots were in a high number in both combinations with the vigor-conferring Garnem® and with the dwarfing rootstocks Rootpac® 20 (Table 4.2; Figure 4.1A, E, F, K, L and P). This contradictory situation may be explained by a combination of apical dominance and vigor effect on shoot development. Apical dominance consists of the shoot apical meristem negative influence on lateral bud outgrowth, favoring the development of the main axis (Hollender and Dardick, 2015; B. Wang et al., 2018). This process may explain why combinations with Rootpac® 20 developed few sylleptic shoots. Sylleptic shoots develop while the main axis, and therefore, vegetative buds are located near the shoot apex, inhibiting its formation. However, in the next year of growth, the shoot apex has distanced itself from dormant buds, releasing them to form proleptic shoots, as we observed in the 'Isabelona'/Rootpac® 20 or 'Lauranne'/Rootpac® 20 combinations (Table 4.2; Figure 4.1A and L). In other cases, like 'Isabelona'/Garnem® or 'Guara'/Rootpac® 40 combinations, we observed a high number of sylleptic shoots and reduced number of proleptic shoots (Table 4.2; Figure 4.1E and G). These phenotypes might be explained by a process denominated apical control, where distal shoots inhibit the formation of new branches (Hollender and Dardick, 2015; Hearn, 2016). In these combinations, sylleptic shoots are produced all over the whole branch, inhibiting the development of proleptic shoots in the next year of growth.

In *Prunus,* sylleptic shoots develop in the basal part of the parent shoot while proleptic shoots do in the apical portion, developing from subterminal buds. Here, in almost all combinations we observed an area of mostly proleptic shoots, followed by sylleptic shoots (Figure 4.1). Though the general cause is simple, since measures were collected from the whole branch and in the second year of growth no proleptic shoots were yet formed, it highlights the fact that in few combinations sylleptic shoots were formed in the first year of growth. This is likely a consequence of both apical dominance and apical control. On one hand, the apical dominance exerted by the own branch inhibits the formation of shoots. On the other hand, the remaining branches of the tree also negatively control the development of new shoots. Only those combinations that conjugate high vigor and weak apical dominance had a rapid extension, where sylleptic shoots were developed in the first year of growth, a process described also in peach (Genard et al., 1994).

Gradziel (2012) described that a desirable almond ideotype may present axillary shoots equally distributed along the axis. Besides, in peach, floral buds are developed in a higher number

in proleptic shoots than in sylleptic shoots (Fyhrie et al., 2018). Therefore, a commercial ideotype should not present a too high number of sylleptic shoots. To avoid this phenotype, combinations of dwarfing rootstocks with weak apical dominance cultivars seems to be the best option. Though scions with strong apical dominance, like 'Isabelona' develop multiple proleptic shoots (Figure 1A-E) when grafted onto dwarfing rootstocks, these combinations typically develop few lateral branches and relocate resources to the main axis (Chapter 3; Montesinos et al., 2021b). On the contrary, combinations of weak apical dominance cultivars, like 'Lauranne', with vigor-conferring rootstock, like Garnem® or Rootpac® 40, naturally develop excessive sylleptic branching (Figure 1N and P) which would force to an exhaustive pruning to have a productive orchard.

4.5. Conclusions

As it happens with other aspects of almond tree architecture, proleptic and sylleptic shoot development is significantly influenced by rootstock genotype. Apical dominance and apical control might have a crucial impact in differences observed between combinations. Though these processes initiate in shoots, they seem to be regulated by signals from the rootstock. Moreover, other processes related to vigor, like hormonal activity or nutrient assimilation, also could play a role in the regulation of bud fate. Therefore, it is a requisite to improve our knowledge in the biological processes that occur at the molecular level to better understand how the scion/rootstock interaction specifically affects the almond tree architecture.

5. IDENTIFICATION OF GENES INVOLVED IN ALMOND SCION TREE ARCHITECTURE INFLUENCED BY ROOTSTOCK GENOTYPE USING TRANSCRIPTOME ANALYSIS

Abstract

The emergence of almond (*Prunus amygdalus* (L.) Batsch, syn *P. dulcis* (Mill.)) intensive and semi-intensive cropping systems has created a necessity for new almond cultivars with vigor and shape adapted to these new circumstances. Hence, it is important to unravel which mechanisms are behind the regulation of the tree three-dimensional structure, or tree architecture, and what factors may play a role, like the rootstock choice. In this study, we have analyzed the rootstock influence in the scion transcriptome, regarding the biological processes that control almond tree architecture. Three commercial almond cultivars were grafted onto three hybrid rootstocks, resulting in nine combinations, whose gene expression in shoot tips were analyzed via RNA-Seq. We report that differences in tree architecture phenotype are correlated with differential expression of genes involved in hormonal and molecular responses associated with the regulation of apical dominance, branch formation, plant growth, cell wall formation or nitrogen assimilation. These results highlight the importance of the rootstock choice in the selection of a desirable scion architecture and in the establishment of almond orchards.

5.1. Introduction

Rootstocks are widely used in numerous fruit and nut orchards (Warschefsky et al., 2016). Its use allows to confer traits of agronomical interest to the cultivars and to independently select favorable traits for scion and rootstock. There are numerous processes where the rootstock influences the scion phenotype, such as tree vigor, yield, flowering time, or fruit quality (Albacete et al., 2015; Aloni et al., 2010; Foster et al., 2015; Martínez-Ballesta et al., 2010; Warschefsky et al., 2016). Almond (*Prunus amygdalus* (L.) Batsch, syn *P. dulcis* (Mill.)) cultivars are graft-compatible with both almond and peach (*P. persica* (L.) Batsch) rootstocks and their interspecific hybrids (Felipe, 2009; Rubio-Cabetas et al., 2017) are widely used in almond orchards.

Among these rootstock effects on the cultivar in various fruit tree species, researchers focused predominantly on scion vigor. Analysis in both apple (*Malus* × *domestica*) and *Prunus* species have described a correlation between rootstock and vigor-related parameters such as scion height or trunk diameter (Balducci et al., 2019; Lordan et al., 2019; Tworkoski and Fazio, 2015; Tworkoski and Miller, 2007). Although the effect in other traits related to tree architecture has been reported in apple cultivars, the interaction is less clear (Seleznyova et al., 2008; Tworkoski and Miller, 2007; van Hooijdonk et al., 2010). In Chapter 3 (Montesinos et al., 2021b), several almond cultivars were grafted onto various hybrid rootstocks and we observed that rootstock influences parameters related to tree architecture like number of shoots or shoot distribution through the trunk. Nevertheless, little to none is known about the effect of the rootstock on the molecular differences that are behind these changes in the scion.

Apical dominance is a crucial regulator of tree architecture. It defines the capacity exerted by the shoot apical meristem (SAM) to repress lateral bud outgrowth, redistributing resources towards the elongation of the main axis (Hollender and Dardick, 2015; B. Wang et al., 2018). Numerous factors are behind the regulation of apical dominance and bud outgrowth with auxins acting as the core regulator, which are predominantly transported throughout the axis by specific efflux and influx carriers, promoting apical dominance (Adamowski and Friml, 2015; Cho and Cho, 2013). Besides, auxin facilitates graft formation, and elevated levels in the rootstock promote callus and vascular cell development, proving that upward transport also happens (Zhai et al., 2021). The exact mechanism by which auxins repress bud outgrowth is yet under scrutiny, but strigolactones (SLs) are proven to act as auxin secondary messengers, inhibiting bud outgrowth (Bennett et al., 2016; Dierck et al., 2016b; Dun et al., 2012; Shinohara et al., 2013; Waldie et al., 2014). Cytokinins (CKs) have the opposite effect, promoting bud outgrowth and shoot branching (Dierck et al., 2016a; Dun et al., 2012; Waldie and Leyser, 2018). Other hormones like gibberellic acid (GA) or brassinosteroids (BRs) are also involved in shoot

development, but their effects are less characterized (Lo et al., 2008; Sun, 2010; Wei and Li, 2016). Sugars have been also described as an important regulator of bud outgrowth, promoting the formation of branches when there is high availability (Mason et al., 2014; Stokes et al., 2013). External stimuli as light perception also controls shoot development via photoreceptors phyA and phyB (Casal, 2012; Holalu and Finlayson, 2017; Reddy and Finlayson, 2014).

Tree vigor is mainly controlled by hormonal response and nutrient availability. GA and BRs are involved in its regulation, primarily promoting cell elongation, although they have been described to stimulate cell proliferation too (Busov et al., 2008; Fridman and Savaldi-Goldstein, 2013; Yamaguchi, 2008). GA activity in cell elongation affect numerous aspects of plant growth, like seed germination, stem elongation, and flower development (Gallego-Bartolomé et al., 2011; Griffiths et al., 2006; Ogawa et al., 2003; White and Rivin, 2000). GA acts connecting external clues such as light perception with molecular regulation of these processes (Alabadí et al., 2008; Filo et al., 2015). Furthermore, deficiencies in GA have been observed to affect tree vigor in several species like poplar, apple, or peach (Hollender et al., 2016; Hollender and Dardick, 2015). CKs and auxins control plant vigor as well, regulating cell proliferation and cell elongation (Busov et al., 2008; Depuydt and Hardtke, 2011; Ma et al., 2016). Nutrient availability is crucial for plant development, and especially nitrogen availability. Hormone synthesis and transport is tightly controlled by nitrogen supply (Krouk et al., 2011). Hence, nitrate acts as a signaling molecule, regulating gene expression, and controlling several developmental processes like root formation, shoot development or flowering (Y. Y. Wang et al., 2018).

In recent years, flowering has been linked with tree architecture. Hormones regulating tree architecture, like auxin or GA, are also part of flowering control, providing a possible crossroad between developmental processes (Srikanth and Schmid, 2011). Studies in Arabidopsis and in woody plants such as apple have proven that important flowering regulators like FLC or FT are involved in shoot development (Foster et al., 2014; Huang et al., 2013; Pin and Nilsson, 2012).

Characterization of all these processes affecting tree architecture using a collection of different rootstocks could help to a better understanding on how they influence scion phenotype. To unravel the molecular mechanisms behind rootstock impact on the cultivar architecture, the transcriptome of nine scion/rootstock combinations, whose effect on scion traits was evaluated in a previous experiment, was sequenced.

5.2. Materials and Methods

5.2.1. Plant materials and growth conditions

For the experiment, a subset of nine scion/rootstock combinations from a trial with thirty combinations was chosen (Chapter 3; Montesinos et al., 2021b), comprising three almond cultivars of agronomic interests which were grafted onto three different commercial rootstocks. The combinations with the following rootstock and scions were selected after analyzing rootstock influence in parameters describing scion architecture: 'Densipac' (Rootpac® 20), 'Nanopac' (Rootpac® 40) and Garnem® (GN15) as rootstocks, and 'Isabelona' (syn. 'Belona'), 'Diamar' (syn. 'Mardía') and 'Lauranne' as cultivars. All rootstocks are hybrids from different origins. Garnem® is an almond × peach (*P. amygdalus* (L.) Batsch, syn *P. dulcis* (Mill.). × *P. persica* (L.) Batsch) hybrid rootstock, while the others came from the commercial RootPac® series: Rootpac® 40 (*P. amygdalus* (L.) Batsch, syn *P. dulcis* (Mill.). × *P. persica* (L.) Batsch) and Rootpac® 20 (*P. cerasifera* × *P. besseyi*). Grafted plants were supplied by the Agromillora Iberia S.L. nursery in 2018 (Barcelona, Spain). Trees were planted during October 2018 at the Centro de Investigación y Tecnología Agroalimentaria de Aragón (CITA) experimental orchard El Vedado Bajo el Horno (Zuera, Zaragoza, 41°51'46.5"N 0°39'09.2"W). Trees were planted as a single axe and supported by a wooden stake. Trees were then left without pruning so that, they could express their natural growth habit unaltered. Conventional orchard practices were used for weed control and drip irrigation. Soil type was calcareous with pH around 7-8.

5.2.2. RNA-Seq analysis

Samples from the nine combinations mentioned were collected from shoot tips of two-year-old branches from three different individuals per combination during summer 2020. RNA extraction was performed from these samples using the CTAB method described previously (Meisel et al., 2005) with some modifications (Chang et al., 1993; Salzman et al., 1999; Zeng and Yang, 2002). Stranded mRNA-Seq analysis was carried out at Centro Nacional de Análisis Genómico (CNAG-CRG) in Barcelona, Spain. Sequencing was performed by an Illumina NovaSeq 6000 System - with > 30 M PE reads per sample and a read length of 2×50bp. FASTQ files were converted with FASTQ Groomer (Galaxy Version 1.1.1) (Blankenberg et al., 2010). Adapter sequences were removed by processing the reads sequences of the twenty-seven individual datasets with Trimmomatic (Galaxy Version 0.38.0) (Bolger et al., 2014). RNA-Seq data alignment was carried out by TopHat (Galaxy Version 2.1.1), with a maximum intron length of 20,000 bp, (D. Kim et al., 2013) on the *P. dulcis* 'Texas' Genome v2.0 (Alioto et al., 2020). Duplicated molecules were located and mate-pairs were confirmed using the MarkDuplicates

(Galaxy Version 2.18.2.2) and FixMateInformation (Galaxy Version 2.18.2.1) Picard tools respectively (http://broadinstitute.github.io/picard). featureCounts (Galaxy Version 1.6.4+galaxy2) was used to measure gene expression (Liao et al., 2014) using the gene annotation *P. dulcis* 'Texas' Genome v2.0 containing 27,044 genes (https://www.rosaceae.org/analysis/295). Differential analysis of count data was performed by edgeR (Galaxy Version 3.24.1) with default settings (Robinson et al., 2009). All procedures were carried out using the Galaxy platform.

5.2.3. RNA-Seq data structural and functional analysis

Principal component analysis (PCA) was carried out using R stats package with default parameters on the gene expression values for all the genes in the nine combinations. Distance between genes was measured using its correspondent function from the R stats package. Hierarchical clustering and correlation networks were performed using the WGCNA package (Langfelder and Horvath, 2008). GO enrichment was carried out using the tool GOEnrichment (Faria, 2017) with p-value cut-off < 0.1 and Benjamin-Hochberg to multiple test correction.

5.3. Results and Discussion

5.3.1. Rootstock influence on scion architecture correlates with differences in gene expression

The phenotypic effect of the rootstock on the nine different scion/rootstock combinations was analyzed previously using the seven architecture parameters, which have been proven to be affected by the rootstock (Chapter 3; Montesinos et al., 2021b). PCA was carried out using these parameters for the subset of combination from this study used for the expression analysis (Figure 5.1A). The first two components explained more than two thirds of the variability, with the first component explaining 51.7%, and the second 24.4%. For two of the cultivars, 'Isabelona' and 'Lauranne', we observed a stronger influence of the cultivar than the rootstock since combinations involving these cultivars can be observed indistinctively clustering together on each side of Figure 5.1A. 'Isabelona' combinations present a strong apical dominance phenotype while those with 'Lauranne' as scion display numerous branching and high vigor. The effect of the rootstock in aerial traits in these two cultivars seems to be limited. However, we observed more diversity between individuals for the 'Isabelona'/Rootpac® 40 combination (Figure 5.1A). Contrarily to these two cultivars, 'Diamar' is more affected by rootstock genotype. When grafted onto Rootpac® 20, which is a dwarfing rootstock, its individuals fall near the high apical dominance, reduced branching such as the combinations involving 'Isabelona'. On the contrary, when grafted onto the vigor-inducing rootstock Garnem®, 'Diamar' combinations clustered with 'Lauranne'

combinations. Although Rootpac® 40 is a more vigor-inducing rootstock compared to Rootpac® 20, it does not reduce apical dominance at the same level than Garnem®. Therefore, 'Diamar'/Rootpac® 40 combinations are between 'Isabelona' and 'Lauranne' combinations, but closest to the former (Figure 5.1A).

A second PCA was carried out, in this case using expression for each gene as variables for the nine combinations (Figure 5.1B). The first two components explained 40% of the variability, with 28.9% and 11.1% of the variability respectively. Data related to each cultivar grouped together. As for phenotypic data, combinations involving both 'Lauranne' and 'Isabelona' did not present any differential distribution involving the rootstock genotype (Figure 1B). As observed for their phenotype data, 'Diamar' combinations presented a contrasted position in the PCA. Individuals grafted onto Rootpac® 20 were clearly separated from individuals grafted onto Garnem® and Rootpac® 40 (Figure 5.1B). Therefore, absence of a rootstock effect in 'Isabelona' and 'Lauranne' combinations seems to be linked to a lack of differential gene expression under these conditions.

A hierarchical clustering was constructed from the RNA-Seq data (Figure 5.2). Data samples were clearly separated according to the scion genotype, which was expected as the samples were taken in this part of the plant and show not only gene expression responding to the rootstock genotype but the global gene expression variation between each genotype. Since these clusters depend on the complete gene expression profile and not only the genes that may affect tree architecture, these results might also be affected by other processes not linked to the observed phenotypes. It is therefore not in the objective of the study to draw conclusions comparing varieties between each other since in these comparisons it is not possible to separate "cultivar effect" from "rootstock effect". For the comparisons intra-cultivar, combinations with 'Lauranne' and 'Isabelona' as cultivars were clearly clustered in one group each with no effect of the rootstocks observed and no differentially expressed gene (DEG). In 'Diamar' we observed a clear separation of samples grafted onto Rootpac® 20 from the others. Transcriptomics data do not allow to clearly separate Garnem® and Rootpac® 40 as opposed to what we observed with the phenotypic data where 'Diamar'/Rootpac® 40 presented an intermediate phenotype between 'Diamar'/Rootpac® 20, that display low vigor and strong apical dominance, and 'Diamar'/Garnem® (Figure 5.2).

On overall, the phenotypic profile of architecture characters is in accordance with the observed data for gene expression in shoot tips, which allow us to assume that the differentially expressed gene in this tissue might be related to differential architecture.

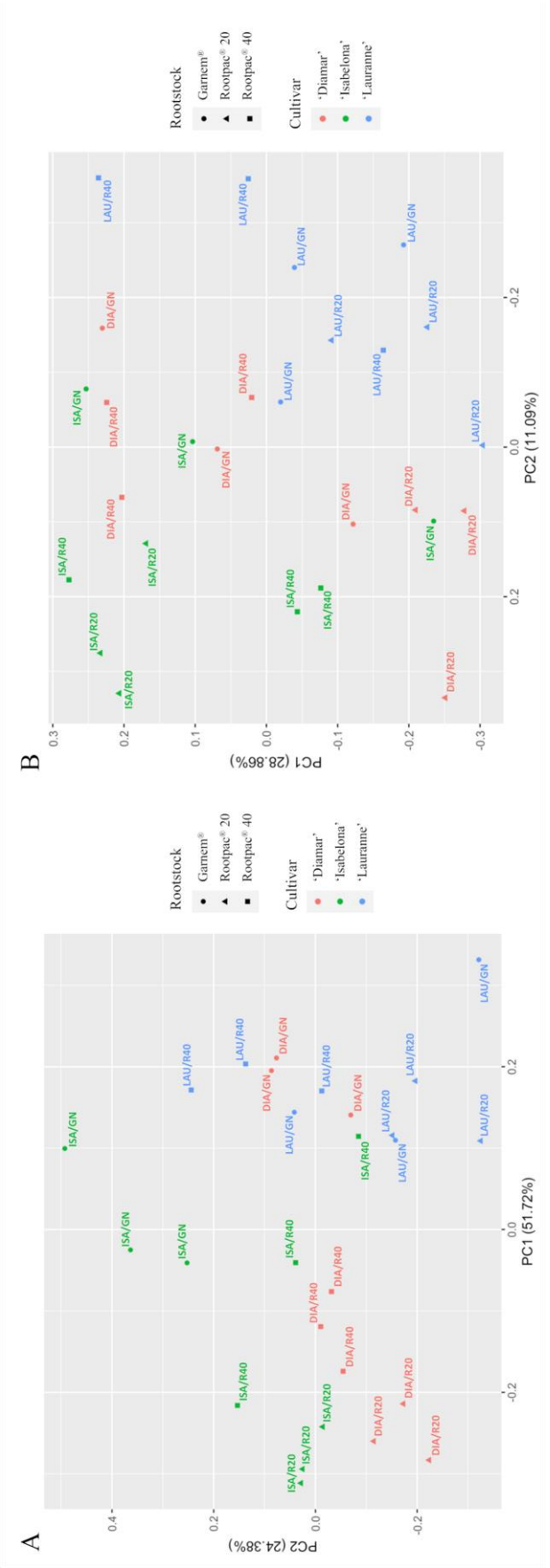

Figure 5.1. Principal component analysis (PCA) of the nine scion/rootstock combinations. A, PCA of the phenotypic data using the seven parameters selected for almond architectural traits in Chapter 3 (Montesinos et al., 2021b). **B**, PCA of the global expression profile data. DIA/GN: 'Diamar'/Garnem®; DIA/R20: 'Diamar'/Rootpac® 20; DIA/R40: 'Diamar'/Rootpac® 40; ISA/GN:'Isabelona'/Garnem®; ISA/R20: 'Isabelona'/Rootpac® 20; ISA/R40: 'Isabelona'/Rootpac® 40; LAU/GN:'Lauranne'/Garnem®; LAU/R20: 'Lauranne'/Rootpac® 20; DIA/R40: 'Lauranne'/Rootpac® 40.

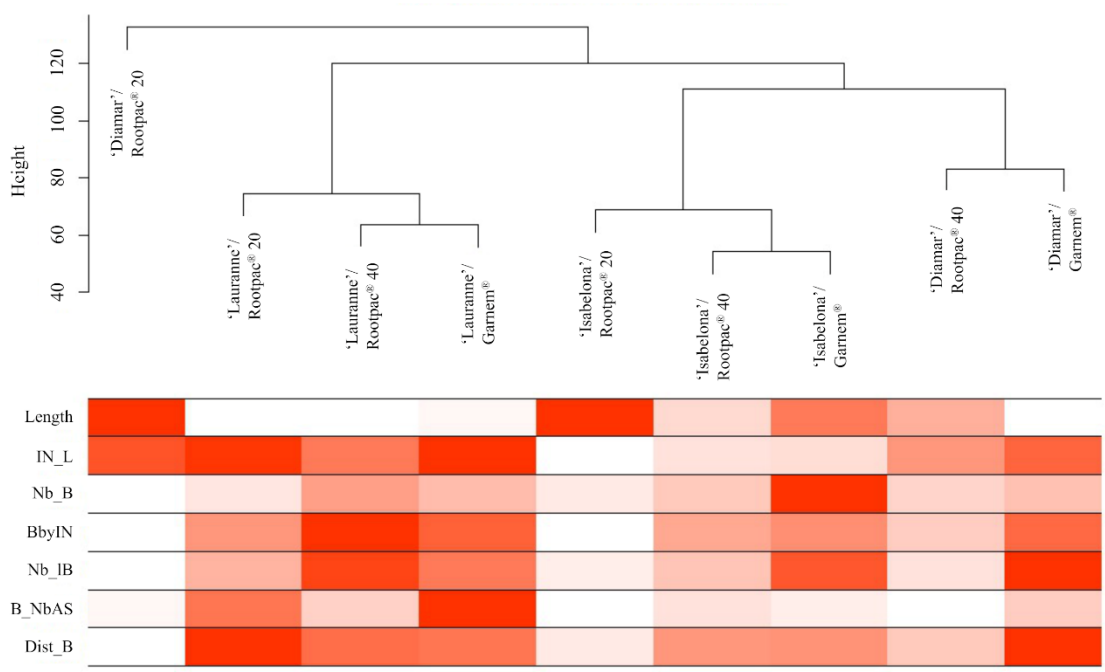

Figure 5.2. Hierarchical clustering of the global transcriptome of the nine scion/rootstock combinations. Intensity of color in the heatmap below the clustering represents the values for each phenotypic trait. Parameters selected from Chapter 3 (Montesinos et al., 2021). Length: trunk length; IN_L: mean length of trunk internodes; Nb_B: number of primary branches; BbyIN: proportion of branches per number of internodes; Nb_lB: number of long branches (> 200 mm); B_NbAS: number of secondary branches per primary branch; Dist_B; distribution of branches through the trunk.

5.3.2. Rootstock differentially affects metabolism genes in 'Diamar' combinations

When comparing the same cultivar grafted onto different rootstocks, 'Lauranne' and 'Isabelona' combinations did not show any DEGs in any comparison (Supplementary Data 5.1, 5.2; Annex 3). As it was previously stated, the reduced rootstock effect on the scion architecture correlates with this absence of differences in gene expression. In the same way that we observed the impact of the rootstock on the scion phenotype, we did observe DEGs in 'Diamar' combinations (Supplementary Data 5.3; Annex 3). In these comparisons, DEGs were only observed when comparing to individuals grafted onto the dwarfing rootstock Rootpac® 20, while we did not observe DEGs between Garnem® and Rootpac® 40. We observed 318 DEGs more expressed with both vigor-inducing rootstocks than with Rootpac® 20 and 137 more expressed in Rootpac® 20. A total of 607 DEGs were found more expressed specifically with Rootpac® 40 than with Rootpac® 20 and 305 more with Rootpac® 20 than with Rootpac® 40. A total of 154 DEGs were detected comparing Garnem® with Rootpac® 20, with 109 DEGs more expressed with Garnem® and 45 with Rootpac® 20 (Figure 5.3).

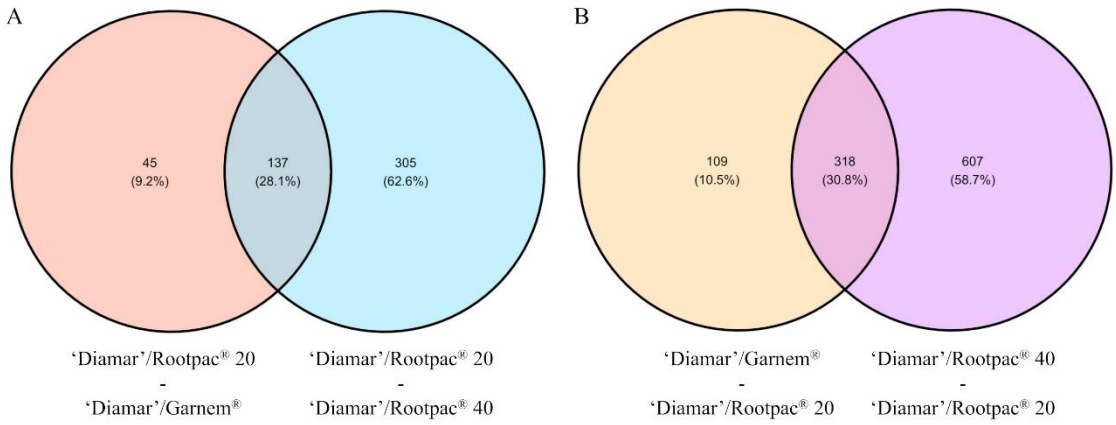

Figure 5.3. Venn diagrams of differentially expressed genes (DEGs) in combinations with 'Diamar' as scion. A, DEGs more expressed in combinations with Rootpac® 20 than with Rootpac® 40 or Garnem®. **B,** DEGs less expressed in combinations with Rootpac® 20 than with Rootpac® 40 or Garnem®.

To characterize the biological processes and molecular functions associated with these DEGs, a GOenrichment analysis was carried out (Figure 5.4). Since the majority of DEGs appeared more expressed in combinations with the vigor-inducing rootstocks Garnem® and Rootpac® 40, we focused on these genes. When analyzing molecular function terms (Figure 5.4A), we observed an enrichment of those related to "catalytic activity" in Garnem® and Rootpac® 40 combinations, especially in the "oxidoreductase activity" category. In both combinations, 'Diamar' presented more vigor than when grafted onto Rootpac® 20, and the enrichment of DEGs belonging to these GO categories is probably due to a higher metabolic activity in the shoot tips of these combinations, which are growing more actively. The term "transmembrane transporter activity" was enriched in individuals grafted onto Garnem® (Figure 5.4A). This might be due to a more active transport of nutrients or hormones linked to active growth (Park et al., 2017; Y. Y. Wang et al., 2018). In individuals grafted onto Rootpac® 40, we observed an enrichment of DEGs belonging to the term "cytoskeletal activity". It is maybe linked to cell division, promoting cell proliferation, or to cell elongation, which could therefore lead to its more vigorous phenotype (Sablowski, 2016).

For terms representing biological processes (Figure 5.4B), we detected an enrichment of DEGs from the term "photosynthesis" in Garnem® combinations. The overrepresentation of these genes might be due to a higher photosynthetic rate that could be linked to the higher vigor displayed by 'Diamar' when grafted onto Garnem®. DEGs characterized with the term "carbohydrate derivative metabolic process" were enriched in individuals grafted onto Garnem®. While a more active metabolism is expected in scions grafted onto a vigor conferring rootstock, like Garnem®; sugars are also an important regulator of branching, and the enrichments of DEGs associated to their pathways may be related to the low apical dominance and numerous branching observed in the 'Diamar'/Garnem® combination (Barbier et al., 2015; Mason et al., 2014).

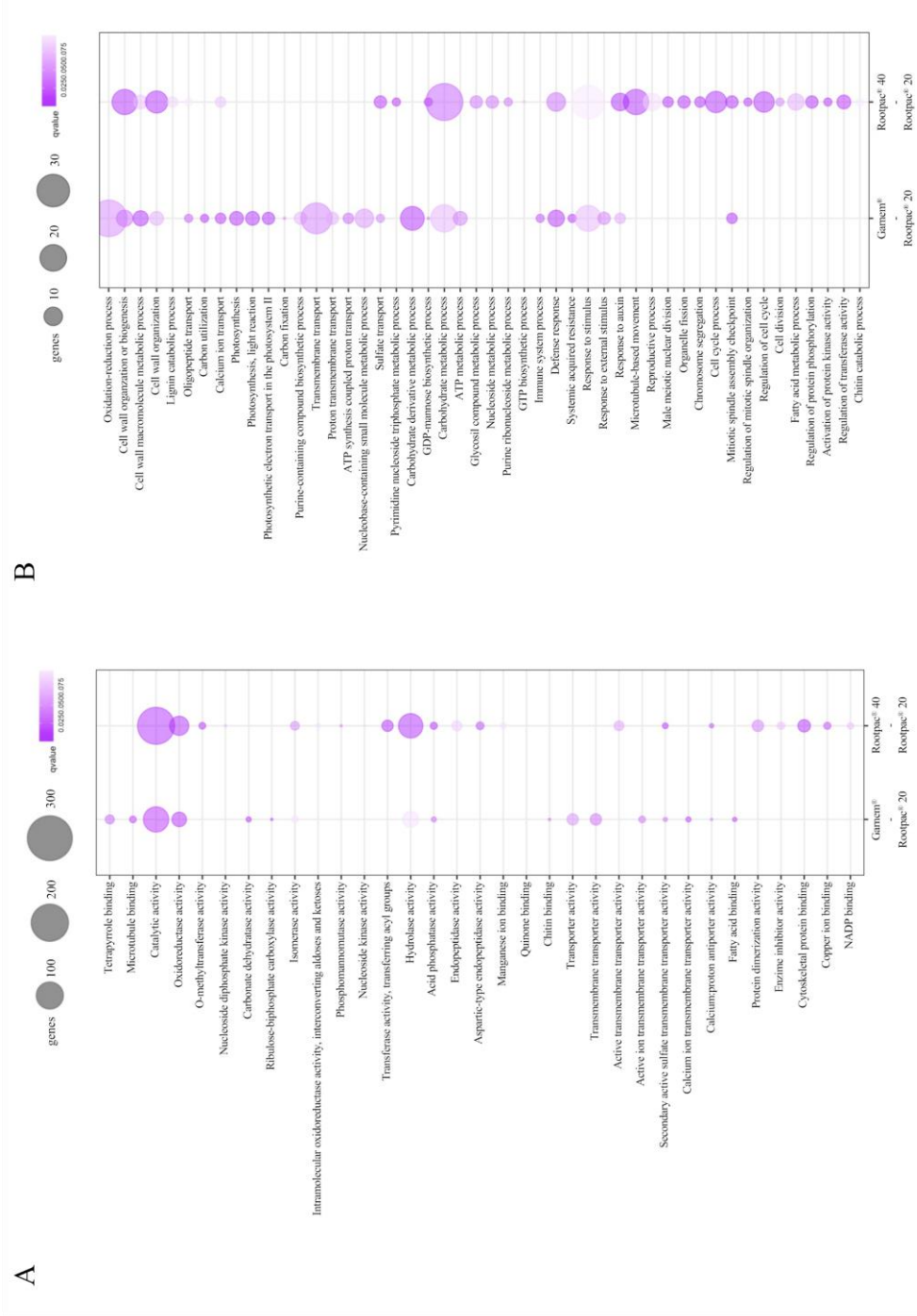

Figure 5.4. GOenrichment of differentially expressed genes (DEGs) in combinations with 'Diamar' as scion. **A,** Molecular function terms for 'Diamar' combinations in which DEGs were less expressed in combinations with Rootpac® 20 than with Rootpac® 40 or Garnem®. **B,** Biological process terms for 'Diamar' combinations in which DEGs were less expressed in combinations with Rootpac® 20 than with Rootpac® 40 or Garnem®.

In both the 'Diamar'/Garnem® and the 'Diamar'/Rootpac® 40 combinations, terms associated with "cell wall organization" were enriched (Figure 5.4B). Similar terms were enriched in previous transcriptomic analysis characterizing rootstock effect in grapevine and citrus (Cochetel et al., 2017; X. Y. Liu et al., 2017). Regulation and reorganization of the cell wall is crucial to allow plant growth, which explain why DEGs related to these processes are upregulated when individuals are grafted onto rootstocks that favor more active growth, like Rootpac® 40 and Garnem® (Cosgrove, 2016; Vaahtera et al., 2019). Several terms associated with cell cycle and cell division are enriched in the 'Diamar'/Rootpac® 40 combination (Figure 4B). This reinforce the notion that growth is upregulated in individuals grafted onto Rootpac® 40 against those grafted onto Rootpac® 20.

In general, we observed an enrichment of terms linked to molecular functions and biological processes in vigor-inducing rootstocks that characterize a more active metabolism, likely due to a more active cell division. Since differences in gene expression are only detected when comparing combinations with vigorous rootstocks to the 'Diamar'/Rootpac® 20 and not between them, it seems that we are looking at a regulation of these processes that explained the low vigor conferred by Rootpac® 20 to the scion.

5.3.3. DEGs associated with promoting apical dominance were upregulated in 'Diamar'/Rootpac® 20

Multiple genes associated to the establishment of apical dominance and the inhibition of bud outgrowth were upregulated in 'Diamar' individuals grafted onto Rootpac® 20. Auxin is the main regulator of these processes, being synthetized in apical leaves and transported through the axis (Barbier et al., 2019). *NF-YA10* (Prudul26A005445) was overexpressed in the 'Diamar'/Rootpac® 20 combination (Table 5.1). *NF-YA10* negatively regulates lateral root density and is likely involved in the regulation of the auxin-signaling regulatory pathway, including indole-3-acetic acid (IAA) biosynthesis by downregulating *YUC2* the enzyme that biosynthesize IAA (Sorin et al., 2014; Zhang et al., 2017). Plants overexpressing *NF-YA10* show reduced IAA content and downregulation of *PIN1* (Zhang et al., 2017). In Arabidopsis, biomass increases through promoting leaf growth and cell expansion and is overexpressed in mature leaves in the expression atlas (Klepikova et al., 2016). In grapevine (*Vitis vinifera*), the tree species with available expression atlas, its orthologue is over expressed in woody stems and in swelling bud (Fasoli et al., 2012). When grafted onto Rootpac® 20, scions present a phenotype with reduced branching and longer branches. Here, *YUC2* expression is too low to give significant data, as expected since IAA is not produced in the observed tissues and *PIN1* expression does not show variation. Hence, *NF-YA10* expression in these shoot tips may be part of a similar regulation in the formation of

branches promoting cell growth or might be a marker of more mature tissues with reduced replication, but its involvement in the auxin pathway is uncertain. *CKX6* (Prudul26A012071) and *CKX7* (Prudul26A024231) were upregulated in 'Diamar'/Rootpac® 20 (Table 5.1). Cytokinin oxidase/dehygrogenase enzimes negatively regulate CKs by inactivating them (Köllmer et al., 2014). Silencing of family members in rice leads to increase branching (Yeh et al., 2015), thus its overexpression when grafted onto Rootpac® 20 may be related to its reduced branching phenotype. Another regulator of CKs, *PAN* (Prudul26A007859), which is associated with shoot control, was also overexpressed in this combination (Table 5.1). PAN is required for normal shoot apical meristem (SAM) development and limits CKs activity, which is a promoter of shoot formation (Maier et al., 2011). Orthologues of *MYB93* (Prudul26A029785) and *DRMH3* (Prudul26A007496), which participate regulating root formation but are also expressed in aerial tissues in Arabidopsis and grapevine (An et al., 2020; Fasoli et al., 2012; Gibbs et al., 2014), were upregulated in 'Diamar'/Rootpac® 20 (Table 5.1).

Table 5.1. Differentially expressed genes (DEGs) associated with apical dominance and shoot formation.

logFC Rootpac® 20 - Garnem®	logFC Rootpac® 20 - Rootpac® 40	*P. dulcis* ID	Gene	GO term	Biological process
1.206		Prudul26A001569	*ABCB15*	GO:0055085	transmembrane transport
3.057		Prudul26A012071	*CKX6*	GO:0009823	cytokinin catabolic process
4.618	4.618	Prudul26A024231	*CKX7*	GO:0009823	cytokinin catabolic process
	1.991	Prudul26A031352	*CLAVATA3*	GO:0048507	meristem development
	1.667	Prudul26A007496	*DRMH3*	GO:0009733	response to auxin
	-4.655	Prudul26A010631	*ESR2*	GO:0009733	response to auxin
-2.090	-1.994	Prudul26A017626	*GH3.6*	GO:0009733	response to auxin
	-2.718	Prudul26A022681	*GSO1*	GO:2000280	regulation of root development
-1.882	-1.903	Prudul26A032023	*IAA16*	GO:0009733	response to auxin
-2.817	-2.527	Prudul26A030184	*IAA4*	GO:0009733	response to auxin
	-1.109	Prudul26A031522	*LAX3*	GO:0060919	auxin influx
	3.466	Prudul26A029785	*MYB93*	GO:1901332	negative regulation of lateral root development
3.372	3.120	Prudul26A005445	*NF-YA10*	GO:0006355	regulation of transcription, DNA-dependent
	1.407	Prudul26A007859	*PAN*	GO:0006355	regulation of transcription, DNA-dependent
-2.237	-2.629	Prudul26A000568	*PAR2*	GO:0009641	shade avoidance
	-2.086	Prudul26A009595	*PIN6*	GO:0055085	transmembrane transport
	1.608	Prudul26A032061	*PIP5K1*	GO:0046854	phosphatidylinositol phosphate biosynthetic process
-2.056	-2.146	Prudul26A005193	*RALFL34*	GO:0019722	calcium-mediated signaling
-1.603	-1.389	Prudul26A015967	*SPL9*	GO:0006355	regulation of transcription, DNA-dependent
	-1.807	Prudul26A024821	*SWEET17*	GO:0008643	carbohydrate transport
	1.124	Prudul26A002767	*VAB*	GO:0009733	response to auxin

Auxin is synthetized in the apex, but to carry out its function it needs to be transported through specific carriers (Adamowski and Friml, 2015; Cho and Cho, 2013; Titapiwatanakun and Murphy, 2009). Three genes involved in promoting auxin transport, and therefore apical

dominance, were upregulated in the 'Diamar'/Rootpac® 20 combination (Table 5.1), whose observed phenotype requires the activation of auxin-mediated growth. *VAB* (Prudul26A002767) encodes an auxin carrier that promotes auxin-mediated plant growth and development (Naramoto and Kyozuka, 2018). PIN proteins play an essential role in auxin distribution (Adamowski and Friml, 2015). Proteins like PIP5K1 (Prudul26A032061) control the formation of clathrin vesicles, mediating the correct polarization of these transporters and the direction of auxin transport. Moreover, double mutants of *PIP5K1* in Arabidopsis present a reduction in apical dominance and develop multiple shoots (Ischebeck et al., 2013). *ABCB15* (Prudul26A001569) has also been linked to auxin transport, but little is known about its effect in plan architecture (Kaneda et al., 2011).

Rootpac® 20 effect in 'Diamar' architecture is characterized by a reduced number of branches and high apical dominance. Here, we saw an upregulation of mechanisms favoring auxin transport, which promotes apical dominance, while genes linked to the inactivation of CK, which promotes branch formation, are overexpressed.

5.3.4. DEGs associated with shoot formation were downregulated in 'Diamar'/Rootpac® 20

CKs act in opposition to auxins, favoring bud outgrowth and shoot formation (Dun et al., 2012). The GH3 family is a large group of genes involved in auxin homeostasis, but also in the synthesis of other hormones, such as jasmonic acid (JA) and salicylic acid (SA) (Fu et al., 2011; Z. Zhang et al., 2007). A member of this family, *GH3.6* (Prudul26A017626), was downregulated in the 'Diamar'/Rootpac® 20 combination (Table 5.1). *GH3.6* has been described to be CK-dependent and to promote meristem development in roots, being also overexpressed in shoot apex in Arabidopsis (Pierdonati et al., 2019; Tian et al., 2019). Similar expression profiles were observed for *ESR2* (Prudul26A010631), *RALFL34* (Prudul26A005193) and *GSO1* (Prudul26A022681) (Table 5.1). As it happens with *GH3.6*, *RALFL34* and *GSO1* have been described participating in root development while being overexpressed in shoot apex and inflorescences (Murphy et al., 2016; Racolta et al., 2014; Schmid et al., 2005). Therefore, its expression in the shoot apex could be linked to the presence of fewer branches in scions grafted onto Rootpac® 20. *ESR2* is a promoter of shoot formation and cell division in response to CKs (Ikeda et al., 2006).

Auxin carriers not only maintain the auxin flux to favor apical dominance, but also can shape plant architecture by redistributing the auxin stream (Sauer et al., 2013). Two transporters engaged in this mechanism are less expressed in the 'Diamar'/Rootpac® 20 combination (Table

1), likely provoking an inhibition of branch formation in this combination. *PIN6* (Prudul26A009595) can adopt different polar localizations and transports auxin in a directional manner (Simon et al., 2016). *PIN6* localization and expression is mediated through phosphorylation in the plasma membrane and the endoplastic reticulum which influence auxin homeostasis and stem elongation (Ditengou et al., 2018). Besides, overexpression *PIN6* mutants display reduced apical dominance and improved root and shoot development (Cazzonelli et al., 2013). Similarly, *LAX3* (Prudul26A031522) overexpression in legumes produces multiple secondary branches, while KO mutants present less branches (Revalska et al., 2015).

Apart from its transport, auxin activity is controlled by numerous auxin response proteins, some of which are downregulated in the scions grafted onto Rootpac® 20 (Table 5.1). AUX/IAA proteins repress the expression of auxin response genes in absence of auxin. *IAA16* (Prudul26A032023) has been described limiting auxin responses and its KO mutants show a reduction in the number of lateral roots in Arabidopsis (Rinaldi et al., 2012). Although its effect in bud outgrowth regulation is unclear, *IAA4* (Prudul26A030184) acts oppositely to auxin (Zhang et al., 2020). *SPL9* (Prudul26A015967) has been observed to act regulating shoot branching, as both repressor and promoter (Jiao et al., 2010; Lu et al., 2013; Miura et al., 2010).

Sugars have been characterized to be a part of bud outgrowth positive regulation (Mason et al., 2014). *SWEET17* (Prudul26A024821) was less expressed in 'Diamar'/Rootpac® 20 (Table 5.1). *SWEET17* acts mobilizing fructose and glucose content (Chardon et al., 2013; Guo et al., 2014). Light availability also affects branching control (Casal, 2012; Finlayson et al., 2010). *PAR1* and *PAR2* play a negative role in the shade avoidance syndrome, acting downstream of *COP1* and being repressed by *phyA* (Bou-Torrent et al., 2008; Zhou et al., 2014). PAR2 (Prudul26A000568) was downregulated in the 'Diamar'/Rootpac® 20 combination (Table 5.1), matching with its repression by *phyA*, which arrest bud outgrowth (Finlayson et al., 2010; Rausenberger et al., 2011).

While auxin activity inhibits branch formation, other processes like CK activity, sugar content or light perception may favor shoot formation. We observed a downregulation in 'Diamar'/Rootpac® 20 of genes involved in auxin homeostasis, as with the rest of mechanisms that promote branch formation.

5.3.5. DEGs involved in plant growth were affected by rootstock in 'Diamar' combinations

GA has been largely known as the growth hormone. Its synthesis and activity are related to active growth and high vigor (Binenbaum et al., 2018; Hedden and Thomas, 2012).

Downregulation of genes involved in GA regulation was characterized in dwarfing rootstocks in citrus (X. Y. Liu et al., 2017). We found various genes associated to GA regulation downregulated in the low vigor 'Diamar'/Rootpac® 20 combination (Table 5.2). *YAB1* (Prudul26A023379) is a GA responsive gene, which is part of a regulatory feedback that control GA levels, being overexpressed when GA levels are high and, thus, repressing its biosynthesis (Dai et al., 2007). Another member of the same family, *YAB5* (Prudul26A020640), presented a similar expression profile. *GASA6* (Prudul26A023277) is thought to be a positive regulator of GA-dependent processes, which affect growth positively. It is also up-regulated by numerous growth hormones (Qu et al., 2016). *GASA4* (Prudul26A028475), which is expressed in meristematic regions, promotes growth and development in response to GA (Roxrud et al., 2007; Rubinovich and Weiss, 2010). *ACL5* (Prudul26A020015) is a crucial part of internode elongation and shoot growth, probably acting downstream of GA responses (Hanzawa et al., 1997). *GASA1* (Prudul26A015013), *GASA9* (Prudul26A011751) or *GAST1* (Prudul26A010439) have been described inhibiting GA response (Zhang and Wang, 2008). Therefore, they could be acting here in a feedback regulatory way, being less expressed in combinations with the dwarfing rootstock Rootpac® 20, and expectedly, with lower levels of GA (Table 5.2).

On the other hand, two genes affecting GA biosynthesis were more expressed in 'Diamar'/Rootpac® 20 combination (Table 5.2). *GA2OX8* (Prudul26A017080) participates in the GA biosynthetic pathway deactivating bioactive GA, while *DAG1* inhibits GA biosynthesis genes (Gabriele et al., 2010; Liu et al., 2021; Zhou et al., 2012). A homologue of this gene in citrus, *GA2OX1*, was also upregulated when grafted onto dwarfing rootstocks (X. Y. Liu et al., 2017). Therefore, the low vigor observed in combinations with Rootpac® 20 as rootstock compared to those with Rootpac® 40 or Garnem® may be in part due to reduced GA activity.

Genes related to other hormonal responses were downregulated when grafted onto the dwarfing Rootpac® 20 rootstock (Table 5.2). *NCED5* (Prudul26A009189) participates in maintaining basal abscisic acid (ABA) levels, which are necessary to promote plant growth (Frey et al., 2012). *CAX3* (Prudul26A005365) participates in Ca^{2+} transport and interacts with auxin response, promoting growth and development (Cheng et al., 2005; Cho et al., 2012). The EXORDIUM family is a group of genes that are involved in BR-mediated responses (Coll-Garcia et al., 2004; Schröder et al., 2011). A member of this family, *EXL5* (Prudul26A006427), was less expressed in the 'Diamar'/Rootpac® 20 combination, which might indicate lower BR activity in scions grafted onto dwarfing rootstocks (Table 5.2).

Light response is an important regulator of plant growth (Casal, 2012; Molas and Kiss, 2009; Yadav et al., 2020). Several homologues to the auxin-induced gene *SAUR50*

(Prudul26A025556, Prudul26A030325, Prudul26A003964) were downregulated when grafted onto the dwarfing rootstock Rootpac® 20 (Table 5.2). *SAUR50* promotes cell expansion and is positively regulated by light (J. Wang et al., 2020). A similar expression profile was presented by other genes associated to light responses (Table 5.2). *NPH3* (Prudul26A025913) and *RPT2* (Prudul26A012618), which act linking phototropism and auxin response, modifying polar auxin transport and promoting growth (Christie et al., 2018; Wan et al., 2012). Oppositely, *SAUR36* (Prudul26A006348) and *ARF16* (Prudul26A009326), which have been described to inhibit cell elongation in response to light or auxin (Dai et al., 2021; Hou et al., 2013), were found being upregulated in 'Diamar'/Rootpac® 20.

Table 5.2. Differentially expressed genes (DEGs) associated with plant growth and vigor.

logFC Rootpac® 20 - Garnem®	logFC Rootpac® 20 - Rootpac® 40	*P. dulcis* ID	Gene	GO term	Biological process
	-2.270	Prudul26A020015	*ACL5*	GO:0006596	polyamine biosynthetic process
	1.216	Prudul26A009326	*ARF16*	GO:0009733	response to auxin
	-1.781	Prudul26A005365	*CAX3*	GO:0006816	calcium ion transport
-1.328		Prudul26A012411	*CAX3*	GO:0006816	calcium ion transport
1.495	1.360	Prudul26A022494	*DAG1*	GO:0006355	regulation of transcription, DNA-dependent
-2.236	-2.443	Prudul26A027852	*ELP*	GO:0009664	plant-type cell wall organization
	-1.387	Prudul26A006427	*EXL5*	GO:0009741	response to brassinosteroid
4.683	5.777	Prudul26A026745	*EXLB1*	GO:0019953	sexual reproduction
	-1.718	Prudul26A015374	*EXT2*	GO:0009664	plant-type cell wall organization
	-2.103	Prudul26A005909	*FBL17*	GO:0051302	regulation of cell division
2.889	2.909	Prudul26A017080	*GA2OX8*	GO:0009686	gibberellin biosynthetic process
-2.966	-3.663	Prudul26A015013	*GASA1*	GO:0009739	response to gibberellin
	-2.087	Prudul26A028475	*GASA4*	GO:0009739	response to gibberellin
-2.386	-2.373	Prudul26A023277	*GASA6*	GO:0009740	gibberellic acid mediated signaling pathway
-1.388	-1.854	Prudul26A011751	*GASA9*	GO:0009739	response to gibberellin
-3.149	-3.656	Prudul26A010439	*GAST1*	GO:0009739	response to gibberellin
	-1.712	Prudul26A009189	*NCED5*	GO:0009688	abscisic acid biosynthetic process
	-1.137	Prudul26A025913	*NPH3*	GO:0009638	phototropism
-1.179	-1.459	Prudul26A012618	*RPT2*	GO:0009638	phototropism
	1.539	Prudul26A006348	*SAUR36*	GO:0009733	response to auxin
	-1.820	Prudul26A025556	*SAUR50*	GO:0009733	response to auxin
-2.051	-2.751	Prudul26A030325	*SAUR50*	GO:0009733	response to auxin
	-3.812	Prudul26A003964	*SAUR50*	GO:0009733	response to auxin
	-1.298	Prudul26A023379	*YAB1*	GO:1902183	regulation of shoot apical meristem development
	-1.881	Prudul26A020640	*YAB5*	GO:1902183	regulation of shoot apical meristem development

In a tissue level, cell proliferation and cell elongation define plant growth. Some effectors of cell proliferation were less expressed in the least vigorous 'Diamar'/Rootpac® 20 combination (Table 5.2). *FBL17* (Prudul26A005909) is a crucial regulator of the cell cycle, targeting a negative regulator and hence, promoting cell division (Gusti et al., 2009). Loss-of-function mutants display reduced growth due to decreased cell proliferation, being necessary to keep meristem activity (Noir et al., 2015). *ELP* (Prudul26A027852) and *EXT2* (Prudul26A015374) are homologues of

EXT1, whose expression is correlated to tip growth in roots, maybe with a function also in shoot tips (Bucher et al., 2002).

Rootpac® 20 is a dwarfing rootstock, conferring reduced vigor to 'Diamar' when grafted. Here, we observed a general downregulation of diverse processes promoting growth in the Diamar'/Rootpac® 20 combination. Specially, we have seen that GA regulation is affected by the rootstock.

5.3.6. DEGs associated with cell wall formation and reorganization were downregulated in combinations with dwarfing rootstock Rootpac® 20

The cell wall defines the ultimate shape of the plant cell, restricting its capacity to elongate or divide (Cosgrove, 2016). Hence, for plants to grow and develop, it is necessary that cells carry out a remodeling of the cell wall. There were multiple genes associated with cell wall reorganization that were downregulated in the 'Diamar'/Rootpac® 20 combination (Table 5.3). They present reduced vigor, and thus, there is a lower need to reshape the cell wall favoring cell division or cell elongation in preparation of mitosis. *EXP1* (Prudul26A014459), *EXP3* (Prudul26A015151), *EXP8* (Prudul26A032368, Prudul26A002026), *EXP15* (Prudul26A028987) and *EXPB3* (Prudul26A000148) are all members of the expansin family, which acts mediating cell wall loosening, allowing then cell expansion (Cosgrove, 2015; Otulak-Kozieł, 2020; Ramakrishna et al., 2019). LRR-extensin proteins like *LRX4* (Prudul26A018014) are part of the cell wall formation and deficiencies in this gene family leads to reduced plant growth (Draeger et al., 2015). *WAT1* (Prudul26A027004) is a vacuolar protein that facilitates auxin transport, involved in secondary cell wall formation. Its downregulation might be related to a complex difference in regulation of auxin homeostasis between combinations. Besides, mutants in Arabidopsis present an important reduction of the wall thickness (Ranocha et al., 2013).

The plant cell wall is formed by numerous components, whose regulation affects cell wall formation and reorganization (Cosgrove, 2016; Meents et al., 2018; Voiniciuc et al., 2018). Various DEGs related to the positive regulation of these processes displayed less expression when 'Diamar' was grafted onto Rootpac® 20 (Table 5.3). More vigor entails tissue growth and a more active cell wall metabolism and reorganization. Lignification is a crucial aspect of the secondary cell wall formation, with laccases like *LAC11* (Prudul26A000315, Prudul26A0016089 and *LAC17* (Prudul26A010009, Prudul26A019505) playing an important role in assuring proper cell structure, controlling lignin deposition (Berthet et al., 2011; Q. Liu et al., 2018; Ranocha et al., 2002; Zhao et al., 2013). *4CLL9* (Prudul26A016569) is a regulator of lignin biosynthesis, both promoting and repressing it (H. Liu et al., 2017). Cell wall hemicellulose is formed by several

molecules, including xyloglucans, which in case of cell wall reorganization are hydrolyzed or remodeled (Park and Cosgrove, 2015). *XTH5* (Prudul26A009872), *XTH6* (Prudul26A002835) and *XTH8* (Prudul26A000404) are involved in loosening the cell wall, allowing cell elongation (Liu et al., 2007; Muñoz and Calderini, 2015; Takahashi et al., 2021). *CSLC5* (Prudul26A026490, Prudul26A005669) is part of the xyloglucan biosynthetic pathway, while *TBL19* (Prudul26A012896, Prudul26A009187, Prudul26A011091) controls xylan acetylation (Gao et al., 2017; Kim et al., 2020).

Table 5.3. Differentially expressed genes (DEGs) associated with cell wall formation and cell wall reorganization.

logFC Rootpac® 20 - Garnem®	logFC Rootpac® 20 - Rootpac® 40	*P. dulcis* ID	Gene	GO term	Biological process
	-2.810	Prudul26A016569	*4CLL9*	GO:0009809	lignin biosynthetic process
	-1.234	Prudul26A007846	*AXS2*	GO:0009226	nucleotide-sugar biosynthetic process
	-1.802	Prudul26A026119	*CSLB4*	GO:0030244	cellulose biosynthetic process
-1.186		Prudul26A023496	*CSLC5*	GO:0071555	cell wall organization
-1.508		Prudul26A005669	*CSLC5*	GO:0071555	cell wall organization
-1.369		Prudul26A026490	*CSLC5*	GO:0071555	cell wall organization
	-1.965	Prudul26A019715	*CSLD3*	GO:0030244	cellulose biosynthetic process
-2.291	-2.939	Prudul26A014459	*EXP1*	GO:0009664	plant-type cell wall organization
-3.251	-3.793	Prudul26A028987	*EXP15*	GO:0009664	plant-type cell wall organization
	-1.438	Prudul26A015151	*EXP3*	GO:0009664	plant-type cell wall organization
-4.175	-5.214	Prudul26A032368	*EXP8*	GO:0009664	plant-type cell wall organization
	-2.896	Prudul26A002026	*EXP8*	GO:0009664	plant-type cell wall organization
-2.101	-2.412	Prudul26A000148	*EXPB3*	GO:0009828	plant-type cell wall loosening
-2.530	-3.596	Prudul26A015935	*FLA9*	GO:0009834	plant-type secondary cell wall biogenesis
	-1.888	Prudul26A000195	*GRF4*	GO:0006355	regulation of transcription, DNA-dependent
	-2.307	Prudul26A000315	*LAC11*	GO:0009809	lignin biosynthetic process
	-3.653	Prudul26A001608	*LAC11*	GO:0009809	lignin biosynthetic process
	-2.197	Prudul26A010009	*LAC17*	GO:0009809	lignin biosynthetic process
	-2.716	Prudul26A019505	*LAC17*	GO:0009809	lignin biosynthetic process
	-1.162	Prudul26A018014	*LRX4*	GO:0009664	plant-type cell wall organization
	-1.471	Prudul26A021520	*PME3*	GO:0042545	cell wall modification
	-1.297	Prudul26A004552	*PME34*	GO:0042545	cell wall modification
	-1.675	Prudul26A029274	*PME54*	GO:0042545	cell wall modification
	-2.214	Prudul26A018663	*PMR5*	GO:0042545	cell wall modification
-1.825	-2.057	Prudul26A012896	*TBL19*	GO:1990937	xylan acetylation
-2.411	-2.674	Prudul26A009187	*TBL19*	GO:1990937	xylan acetylation
-2.367		Prudul26A011091	*TBL19*	GO:1990937	xylan acetylation
	-1.042	Prudul26A027004	*WAT1*	GO:0010315	auxin efflux
	-2.644	Prudul26A009872	*XTH5*	GO:0010411	xyloglucan metabolic process
-2.472		Prudul26A002835	*XTH6*	GO:0010411	xyloglucan metabolic process
-2.327	-2.671	Prudul26A000404	*XTH8*	GO:0010411	xyloglucan metabolic process

Cellulose and pectins are major cell wall components and their synthesis and organization are a crucial aspect of cell wall formation (Meents et al., 2018; Saffer, 2018). FLA proteins, like FLA9 (Prudul26A015935), are associated with wood formation, affecting secondary cell wall formation and structure (He et al., 2019; Wang et al., 2015). They participate in the organization of cell wall polysaccharides like cellulose and pectins, with mutants presenting reduced cellulose

content (E. Liu et al., 2020). *CSLD3* (Prudul26A019715) plays a role in the cellulose biosynthetic pathway (Park et al., 2011; J. Yang et al., 2020). Although its specific role is yet to be characterized, *CSLB4* (Prudul26A026119) seems to be also required for cellulose biosynthesis (Youngs et al., 2007). *GRF4* (Prudul26A000195) positively regulates cellulose biosynthesis and biomass accumulation, controlling *MYB61* transcription. A member of its family in citrus has been characterized being more expressed in vigor-inducing rootstocks (Gao et al., 2020; X. Y. Liu et al., 2017). *PMR5* (Prudul26A018663) is a member of the TBL family, participating in pectin acetylation (Chiniquy et al., 2019). Pectin methylesterases like *PME3* (Prudul26A021520) and *PM34* (Prudul26A004552, Prudul26A029274) affect cell wall composition and cell expansion (Kohorn et al., 2014).

When grafted onto Rootpac® 20, 'Diamar' displayed a broad downregulation of mechanisms involved in cell wall formation and reorganization compared to vigor-conferring rootstocks combinations. Lower expression in this combination may be associated with a less active metabolism, likely due to a less active cell division, which causes a reduced need of cell wall modifications.

5.3.7. Nitrogen metabolism was less active in the 'Diamar'/Rootpac® 20 combination

Nitrogen assimilation is vital for plant growth and development as it is an indispensable nutrient for the mechanisms involved in tree vigor (Krouk et al., 2011). Rootstock effect in nitrogen assimilation has been described in grapevine, where changes in nitrogen content affect the expression profile of genes in dwarfing rootstocks (Cochetel et al., 2017). *NIR1* (Prudul26A012711) and *NIA1* (Prudul26A000078) perform two crucial successive steps in nitrate assimilation, converting NO in assimilable molecules for the plant metabolism (Solomonson and Barber, 1990; Tanaka et al., 1994). Deficiencies in these genes lead to severely impaired growth (Costa-Broseta et al., 2020). *TIP2;3* (Prudul26A020819) mediates NH_3 transport and is upregulated under conditions of high nitrogen availability (Loqué et al., 2005). These three genes were downregulated in the 'Diamar'/Rootpac® 20 combination, evidencing that nitrogen metabolism is less active in scions grafted onto dwarfing rootstocks (Table 5.4). Various homologues to the *NRT1.1* (Prudul26A015004, Prudul26A008539 and Prudul26A010496) transporter were also less expressed when grafted onto Rootpac® 20 (Table 5.4). *NRT1.1* carriers participate in the regulation of architecture processes like root branching, slowing down their development in response to auxin, which they seem able to transport (Krouk et al., 2010; W. Wang et al., 2020). While this function would not match the observed phenotype, since individuals grafted onto Rootpac® 40 or Garnem® displayed reduced apical dominance and

numerous branches in comparison to those grafted onto Rootpac® 20, a different regulatory function in the nitrogen metabolism cannot be discarded for these homologues.

Nitrogen availability is crucial for tree growth and development. Here we detected a downregulation of genes involved in nitrogen assimilation and transport in the reduced vigor 'Diamar'/Rootpac® 20 combination.

Table 5.4. Differentially expressed genes (DEGs) associated with nitrogen assimilation and flowering meristem development.

logFC Rootpac® 20 - Garnem®	logFC Rootpac® 20 - Rootpac® 40	*P. dulcis* ID	Gene	GO term	Biological process
	2.340	Prudul26A017389	*AGL19*	GO:0010048	vernalization response
-1.036	-1.588	Prudul26A005648	*CIB1*	GO:0009908	flower development
2.533	3.217	Prudul26A019427	*DAM5*	GO:0009910	negative regulation of flower development
	-1.465	Prudul26A020430	*EDH2*	GO:0032956	regulation of actin cytoskeleton organization
2.008	2.082	Prudul26A006108	*FD*	GO:0009909	regulation of flower development
1.140	2.335	Prudul26A024273	*NF-YA3*	GO:0006355	regulation of transcription, DNA-dependent
	-1.484	Prudul26A000078	*NIA1*	GO:0042128	nitrate assimilation
-3.863	-2.553	Prudul26A012711	*NIR*	GO:0042128	nitrate assimilation
-1.383		Prudul26A015004	*NRT1*	GO:0010167	response to nitrate
	-3.581	Prudul26A008539	*NTL1*	GO:0055085	transmembrane transport
-1.527	-1.773	Prudul26A010496	*NTL1*	GO:0055085	transmembrane transport
	2.011	Prudul26A030680	*SIP1*	GO:0005975	carbohydrate metabolic process
	-2.655	Prudul26A021958	*TFL1*	GO:0009910	negative regulation of flower development
	-8.809	Prudul26A020819	*TIP2;3*	GO:0055085	transmembrane transport
	-2.140	Prudul26A010866	*WNK6*	GO:0006468	protein phosphorylation

5.3.8. Characterization of DEGs associated with meristem differentiation in 'Diamar' combinations

Flowering has been previously linked to the regulation of tree architecture, though the relation between them is not clearly characterized (Foster et al., 2014; Seleznyova et al., 2008). We observed mixed results, with genes promoting and repressing flowering being more expressed in both combinations with the dwarfing rootstock Rootpac® 20 and the vigor-inducing rootstocks Rootpac® 40 and Garnem®. Various flowering inductors were less expressed when grafted onto Rootpac® 20 (Table 5.4). *EDH2* (Prudul26A020430) promotes flowering transition and its inactivation leads to extremely late flowering (Matsubara et al., 2008). *CIB1* (Prudul26A005648) activates *FT* transcription, thus regulating flowering positively (Y. Liu et al., 2018). Nevertheless, the flowering repressor *TFL1* (Prudul26A021958) was downregulated in 'Diamar'/Rootpac® 20 (Table 5.4). *TFL1* acts antagonistically of *FT*, repressing flowering and increasing vegetative growth (Moraes et al., 2019). The effect of *TFL1* in growth, promoting it, may concur with the

reduced vigor observed in the 'Diamar'/Rootpac® 20 combination compared with 'Diamar'/Rootpac® 40. A gene encoding a homologue of *DAM5* (Prudul26A019427) was upregulated in the 'Diamar'/Rootpac® 20 combination (Table 5.4). *DAM5* and *DAM6* participate in flowering regulating negatively bud dormancy release (Q. Wang et al., 2020). Several flowering inductors were also upregulated in the 'Diamar'/Rootpac® 20 combination (Table 5.4). *FD* (Prudul26A006108) performs a pivotal step in flowering development, being required for *FT* activity, which regulates directly forming a complex (Collani et al., 2019; Wigge et al., 2005). Upstream of this step, *NF-YA3* (Prudul26A024273) interacts with the flowering regulator *CO*, positively affecting floral organ development (Fornari et al., 2013; Su et al., 2018). Lastly, *SIP1* (Prudul26A030680) and *AGL19* (Prudul26A017389) have been described to promote early flowering in respond to light signaling (Jiang et al., 2018; Kang et al., 2015; W. Kim et al., 2013).

Given these results, it is unclear how genes associated to flowering interact with the regulatory pathways involved in tree architecture. Instead of an overall interaction between these two biological processes, it is possible that individual genes carry out specific function that affect both pathways.

5.4. Conclusions

Tree architecture is dependent of numerous processes such as light perception, gravity sensing, sugar availability or nutrient supply that take part in the tree physiological and hormonal regulation. Rootstock interaction with the scion may transform how cultivars respond to the same environmental cues. Previous studies had described how rootstock effect can alter scion architecture traits like number of branches or axis height in tree species, including almond. After carrying out a transcriptome analysis in nine cultivar/rootstock combinations, we report the biological processes that are affected by scion/rootstock interaction (Figure 5.5) potentially responsible of architecture variability. While expression profile of cultivars with strong scion phenotypes is not significatively altered by the rootstock, cultivars whose phenotype is affected by rootstock present a modification of their expression profile. Regulation of hormones involved in apical dominance and branch formation, like auxin and CKs, are influenced by the rootstock. Moreover, mechanisms associated to vigor control, such as GA response or nitrogen assimilation, were shown to also be affected by the rootstock, being limited when grafted onto dwarfing rootstocks. Rootstock interaction can also modify cell wall formation and reorganization, being less active in combinations with dwarfing rootstocks. In conclusion, described effects on scion architecture correlate with significatively differences in the transcriptome of those combinations, affecting several hormonal responses and molecular mechanisms.

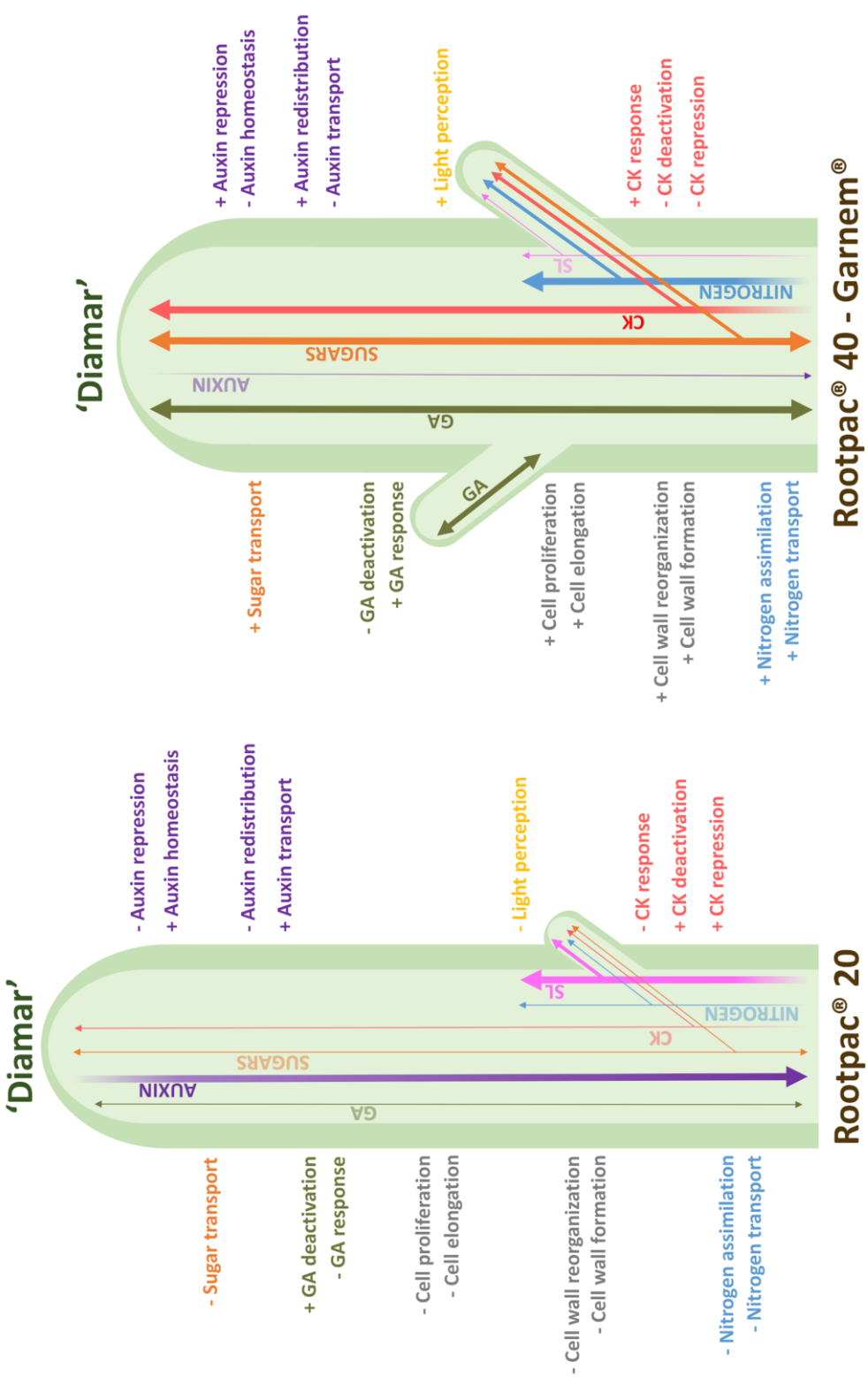

Figure 5.5. Schematic representation of hormonal regulation in 'Diamar' combinations. + indicates upregulation, while – indicates downregulation. Arrows in upward direction indicate root origin, while arrows in downward direction indicate apical origin. GA: Gibberelic Acid; CK: Citokinin; SL: Strigolactone.

6. CHARACTERIZATION OF ALMOND SCION/ROOTSTOCK COMMUNICATION IN CULTIVAR AND ROOTSTOCK TISSUES

Abstract

Rootstock genotype determines multiple aspects of the scion development, including the scion three-dimensional structure, or tree architecture. Thus, rootstock choice is an important factor in the establishment of new almond (*Prunus amygdalus* (L.) Batsch, syn *P. dulcis* (Mill.)) planting systems, which demand cultivars whose vigor and shape adapt to these new requirements. However, if the rootstock genotype is able to alter scion development, it is likely that the scion genotype affects the rootstock performance. Here, we carried out a transcriptomic analysis of the scion/rootstock interaction in young trees, focusing on the scion effect in the rootstock molecular response. Two comercial almond cultivars were grafted onto two hybrid rootstocks, resulting in four combinations, whose gene expression in both scion and rootstock tissue was analyzed via RNA-Seq. We observed that, in fact, the scion genotype has an impact on the rootstock expression profile, affecting the expression of genes associated with hormonal regulation, root development and light signalling. Hence, scion/rootstock communication has a pivotal role in the development of both scion and rootstock, accentuating the importance of a correct choice when establishing new almond orchards.

6.1. Introduction

In modern orchards, rootstocks are used both to select specific root system traits and to confer traits of agronomic interest to trees and fruits (Warschefsky et al., 2016; Rubio-Cabetas et al., 2017). These effects on scion development have been described in numerous trees species; ranging from tree vigor to yield or fruit quality (Albacete et al., 2015; Aloni et al., 2010; Foster et al., 2015; Martínez-Ballesta et al., 2010; Warschefsky et al., 2016). Recently, molecular approaches have been carried out in woody plant species to describe how these effects happen at the molecular level (López-Hinojosa et al., 2021; Ou et al., 2015). In a recent study where almond commercial cultivars were grafted onto hybrid rootstocks, a differential expression of genes associated to hormones involved in the regulation of apical dominance, branch formation and vigor control was observed, while genes related to cell wall reorganization and formation were also affected (Chapter 5).

The analysis of the scion effect on the rootstock has been limited to the graft formation, analyzing the processes that happens in the moment of that vascular union, leading to vascular regeneration and the establishment of the graft junction (Melnyk et al., 2018; Wulf et al., 2019). However, little is known about how the scion can modulate the phenotypes displayed by the rootstock, from nutrient assimilation to pathogen resistance or root development (Li et al., 2016). These traits might be affected differently depending which scion cultivar is grafted onto them.

Rootstock development is controlled by various phytohormones, which have roles in regulating cell elongation, cell division and cell differentiation (Motte et al., 2019; Takatsuka and Umeda, 2014). As it happens with the aerial part of the plant, auxin has an important role in regulating diverse processes in roots, like root patterning, cell division and cell elongation (Ding and Friml, 2010; Overvoorde et al., 2010; Petersson et al., 2009; Saini et al., 2013). Strigolactones (SLs) act in consonance with auxin, controlling lateral root formation and root-hair elongation, while mediating root responses to environment changes (Jiang et al., 2016; Koltai, 2011; Sun et al., 2014). Cytokinins (CKs) promote root cell differentiation and cell division in various root tissues and inhibits lateral root formation in opposition to auxin (Jing and Strader, 2019; J. Liu et al., 2017; Márquez et al., 2019; Saini et al., 2013). Gibberellic acid (GA) is involved in maintaining root cell proliferation and cell elongation in the meristem while arresting lateral root formation (Gou et al., 2010; Ubeda-Tomás et al., 2008; Yaxley et al., 2001). Brassinosteroids (BRs) play a crucial role in controlling the root meristem activity, also participating in the regulation of lateral root initiation or root cell elongation (Li et al., 2020; Wei and Li, 2016). Ethylene (ET) modulates the meristem maintenance, promoting cell division; whilst opposing auxin in lateral root formation (Lewis et al., 2011; Qin et al., 2019).

Light signaling can also control plant development through different mechanisms. In plants, the circadian clock regulates several developmental processes in response to light changes, from seed germination, to hypocotyl elongation, root growth or flowering (Farré, 2012; Inoue et al., 2018). Carbohydrate metabolism and nutrient assimilation are also linked to the regulation of the circadian clock (Sanchez and Kay, 2016). The shade avoidance response also regulates plant growth which is based on the ratio between red light and far red light (R:FR), captured by phytochrome photoreceptors phyA and phyB. Changes in this ratio provoke a redistribution in the auxin flux, changing the direction and activity of the plant growth (Casal, 2012; Finlayson et al., 2010; Holalu and Finlayson, 2017; Rausenberger et al., 2011; Reddy and Finlayson, 2014).

In this study, we have analyzed both the rootstock influence on the scion and the scion influence on the rootstock at the transcriptional response level. We grafted two commercial almond cultivars with opposite architecture and vigor characteristics onto two peach × almond hybrid rootstocks for a total of four combinations. Our goal was to identify which biological processes and molecular responses were affected above and below the graft site.

6.2. Materials and Methods

6.2.1. Plant material and growth conditions

For the experiment, two almond commercial cultivars, 'Isabelona' and 'Lauranne' were grafted onto two hybrid rootstocks, Garnem®, a commercial rootstock, and 'GN-8', a new selection, obtaining four different combinations. Both rootstocks are almond × peach *(Prunus amygdalus* (L.) Batsch, syn *P. dulcis* (Mill.). × *P. persica* (L.) Batsch) hybrid rootstocks. The two cultivars were selected because the weak influence that the rootstock displays in their apical dominance and branch formation phenotype (Chapter 3; Montesinos et al., 2021b). Grafted plants were supplied by the Agromillora Iberia S.L. nursery in 2020 (Barcelona, Spain). Plants were kept in a nursery shortly until sample collection at the Centro de Investigación y Tecnología Agroalimentaria de Aragón (CITA), where conventional orchard practices were applied.

6.2.2. Phenotypic data collection

Phenotypic data was collected for ten replicates of each of the four combinations, before sample collection. Three parameters related to vigor were measured: scion axe length (Length), scion trunk diameter (d_Scion) and rootstock trunk diameter (d_Rootstock). Length was determined from the graft union. d_Scion and d_Rootstock were quantified using a caliper, measuring from 20 mm above and 20 mm below of the graft union respectively.

6.2.3. RNA-Seq analysis

Samples from the four combinations mentioned were collected from 50 mm below and above the graft union of three different individuals per combination during summer 2020. RNA extraction was performed from these samples using the CTAB method described previously (Meisel et al., 2005) with some modifications (Chang et al., 1993; Salzman et al., 1999; Zeng and Yang, 2002). Stranded mRNA-Seq analysis was carried out at Centro Nacional de Análisis Genómico (CNAG-CRG) in Barcelona, Spain. Sequencing was performed by an Illumina NovaSeq 6000 System - with > 30 M PE reads per sample and a read length of 2×50bp. FASTQ files were converted with FASTQ Groomer (Galaxy Version 1.1.1) (Blankenberg et al., 2010). Adapter sequences were removed by processing the reads sequences of the 27 individual datasets with Trimmomatic (Galaxy Version 0.38.0) (Bolger et al., 2014). RNA-Seq data alignment was carried out by TopHat (Galaxy Version 2.1.1), with a maximum intron length of 1,000 bp, (D. Kim et al., 2013) on the *P. dulcis* 'Texas' Genome v2.0 (Alioto et al., 2020). Duplicated molecules were located and mate-pairs were confirmed using the MarkDuplicates (Galaxy Version 2.18.2.2) and FixMateInformation (Galaxy Version 2.18.2.1) Picard tools respectively (http://broadinstitute.github.io/picard). featureCounts (Galaxy Version 1.6.4+galaxy2) was used to measure gene expression (Liao et al., 2014) using the gene annotation *P. dulcis* 'Texas' Genome v2.0 containing 27044 genes (https://www.rosaceae.org/analysis/295). Differential analysis of count data was performed by edgeR (Galaxy Version 3.24.1) with default settings (Robinson et al., 2009). All procedures were carried out using the Galaxy platform.

6.2.4. Statistical analysis

All statistical analyses were carried out in the R platform (https://cran.r-project.org/). Significant differences in phenotypic data were evaluated using an ANOVA test to find. These were assessed with a Tukey's test ($p < 0.05$) using the agricolae R package (https://CRAN.R-project.org/package=agricolae). Principal component analysis (PCA) was carried out using R stats package with default parameters on the gene expression values for the all the genes in the four combinations.

6.3. Results and Discussion

6.3.1. 'Isabelona' and 'Lauranne' vigor was influenced by the rootstock

Tree architecture data was collected for the four combinations, 'Isabelona'/Garnem®, 'Isabelona'/'GN-8', 'Lauranne'/Garnem® and 'Lauranne'/'GN-8' (Figure 6.1). Since trees were too young to have developed any branches, only trunk length (Length) and the diameter of both

the scion (d_Scion) and the rootstock (d_Rootstock) was measured. Due to the intrinsic difficulties of its measurement, no data was collected of the root architecture.

Figure 6.1. Scion/rootstock combinations showed differences in vigor response. From left to right: 'Isabelona'/'GN-8', 'Isabelona'/Garnem®, 'Lauranne'/'GN-8' and 'Lauranne'/Garnem®.

In a previous study with thirty different scion/rootstock combinations (Chapter 3; Montesinos et al., 2021b), we reported that 'Isabelona' displayed reduced vigor paired with strong apical dominance, which resulted in a phenotype with reduced branching and long trunks. On the contrary, 'Lauranne' presented high vigor and weak apical dominance, resulting in numerous branching and a shortening of the trunk. Here, combinations with 'Lauranne' as scion presented higher Length values, and hence, longer trunks (Table 6.1, Figure 6.1). In this case, trees are in their first year of growth, so there are no branches yet that compete with the main axis growth. As a result, 'Lauranne' more vigor leads to higher Length values. Regarding the rootstocks, Garnem® effect as a vigorous rootstock was present on both cultivars, presenting higher Length values than when grafted onto the dwarfing rootstock 'GN-8' (Table 6.1, Figure 6.1).

Trunk diameter (d_Scion) is typically used as a vigor measure, normally presented as TCSA (Trunk Cross Sectional Area). As it happened with Length values, 'Lauranne' presented higher d_Scion values than 'Isabelona'. Besides, cultivars grafted onto Garnem® had also higher d_Scion values than when grafted onto 'GN-8' (Table 6.1). However, we did not observe a significant difference in the rootstock diameters (d_Rootstock), though mean values were slightly lower with 'Isabelona' (Table 6.1).

Table 6.1. Analysis of architectural traits related to vigor in one-year-old scion/rootstock combinations.

Cultivar	Rootstock	Length (mm)	d_Scion (mm)	d_Rootstock (mm)
'Isabelona'	**'GN-8'**	210 a	2.63 a	4.25 a
	Garnem®	260 b	3.25 ab	4.36 a
'Lauranne'	**'GN-8'**	310 c	2.97 ab	4.50 a
	Garnem®	400 d	3.32 b	4.56 a

Assessed with Tukey's test. Values within columns followed by the same letter were not significantly different ($p < 0.05$).

The observed phenotype differences seem to depend mostly on the vigor that each combination displays. Though is likely that the biological processes that will shape the specific tree architecture of each combination are already developed and their phenotypic effects are not yet visible in these one-year-old plants.

6.3.2. Rootstock only influenced gene expression in combinations with 'Isabelona'

We reported in Chapter 5 that the lack of phenotypical differences observed in both 'Lauranne' and 'Isabelona' when grafted onto different rootstocks were correlated with a lack of differentially expressed genes (DEGs). However, in this experiment, 'Lauranne' and 'Isabelona' were selected because of that consistent scion phenotype, expecting that they could influence rootstock transcriptome. In addition, we analyzed the gene expression in the scion in order to determine if the rootstock influences gene expression at an early development stage (Supplementary Data 6.1; Annex 4).

A PCA was carried out using expression for each gene as variables for the four combinations, with the first (PC1; 33.2% of variability explained) and third (PC3; 11.8%) component selected to represent the data (Figure 6.2). As we observed previously in Chapter 5, combinations with 'Lauranne' as scion were not differentiated according to rootstock, grouping together (Figure 6.2). However, we did observe that gene expression in combinations with 'Isabelona' is influenced by the rootstock. These individuals could be separated in two groups in the PCA, depending on whether they were grafted onto Garnem® or 'GN-8'.

Looking at the global picture of gene expression by functional categories, we performed a GO enrichment analysis but due to the low number of genes we did not obtained significant categories. However, we found a similar molecular response to what we observed in previous analysis of almond scion-rootstock combinations (Chapter 5). When grafted onto the vigor-conferring rootstock Garnem®, 'Isabelona' displayed several DEGs overexpressed involved in auxin regulation, mostly in a repressive manner. Besides, DEGs promoting CKs or GA activity or repressing abscisic acid (ABA) response were also overexpressed in these combinations (Supplementary Data 6.2; Annex 4). Therefore, Garnem® influence hormonal regulation here in

a similar manner to what we observed before, with auxin responses being downregulated, hence reducing apical dominance (Barbier et al., 2019; Hill and Hollender, 2019). Moreover, as it happened previously, we found overexpression of DEGs involved in processes associated with active growth, like cell proliferation and cell expansion, or promoting nitrogen and sugar assimilation (Supplementary Data 6.2; Annex 4).

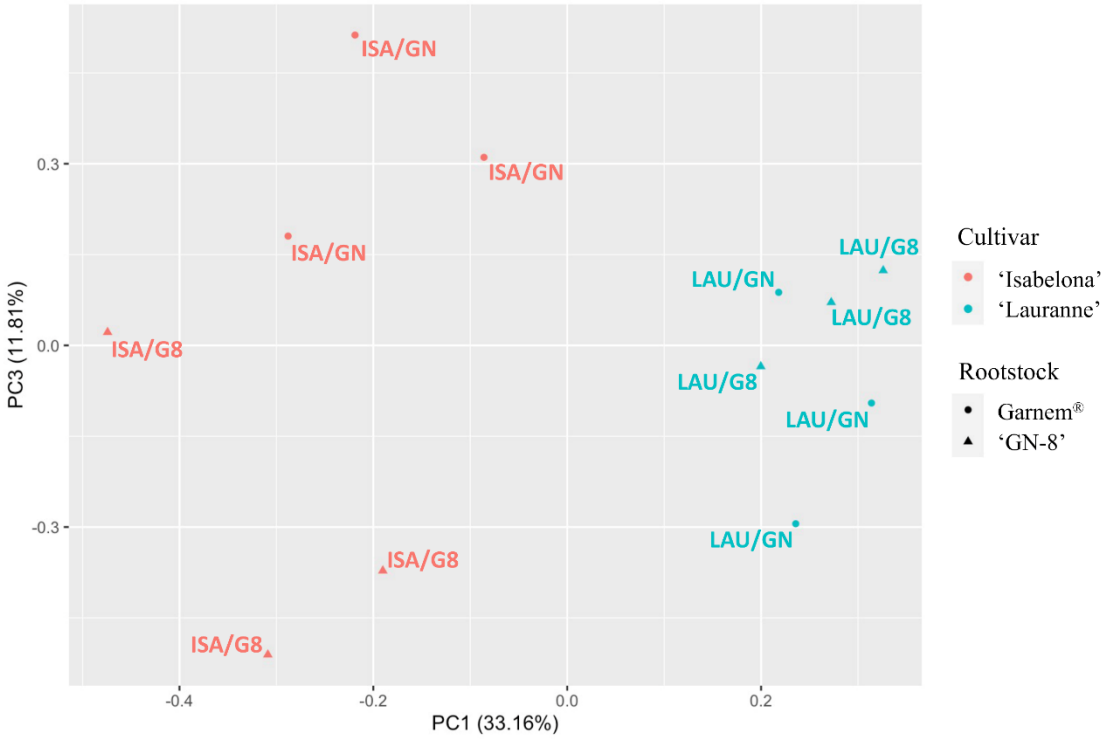

Figure 6.2. Principal component analysis (PCA) of the global expression profile data from cultivar samples of the four scion/rootstock combinations. ISA/GN: 'Isabelona'/Garnem®; ISA/G8: 'Isabelona'/'GN-8'; LAU/GN: 'Lauranne'/Garnem®; LAU/G8: 'Lauranne'/'GN-8'.

Diversely, genes related to ET regulation were overexpressed when 'Isabelona' was grafted onto the dwarfing rootstock 'GN-8' (Supplementary Data 6.2; Annex 4). Contrary to what happened when grafted onto Garnem®, DEGs related to low nitrogen or sugar content were upregulated (Supplementary Data 6.2: Annex 4). However, some genes involved in cell wall reorganization were overexpressed (Supplementary Data 6.2; Annex 4), while in Chapter 5, several genes associated with this process were upregulated in combinations with vigor-conferring rootstocks.

In general, although the effects in the phenotype are not yet visible, we observed a similar expression profile to what has been previously described, with auxin responses downregulated in combinations with a vigor-inducing rootstock, while branching and growth are upregulated in combinations with Garnem®.

6.3.3. Scion/rootstock interaction in almond affected rootstock molecular profile

The cultivar effect of commercial almond cultivars 'Lauranne' and 'Isabelona' on the rootstock development was analyzed in a vigorous rootstock like Garnem®, and a dwarfing rootstock such as 'GN-8' (Supplementary Data 6.3; Annex 4). We carried out a PCA using the expression of each gene as variables for the four different scion/rootstock combinations. The first two components explained 50.1% of the variability, while none of the other variables explained more than a 10%. PC1 and PC2 explained 32.6% and 17.6% of the variability respectively. In the PCA, there was a clear separation between the four different combinations (Figure 6.3). Combinations with Garnem® as rootstock are in the lower-left corner while combinations with 'GN-8' are in the upper-right corner. Therefore, there is a clear effect of the rootstock and it can be observed in the gene expression, with individuals clearly segregating depending on which scion, 'Lauranne' or 'Isabelona', is grafted onto them (Figure 6.3).

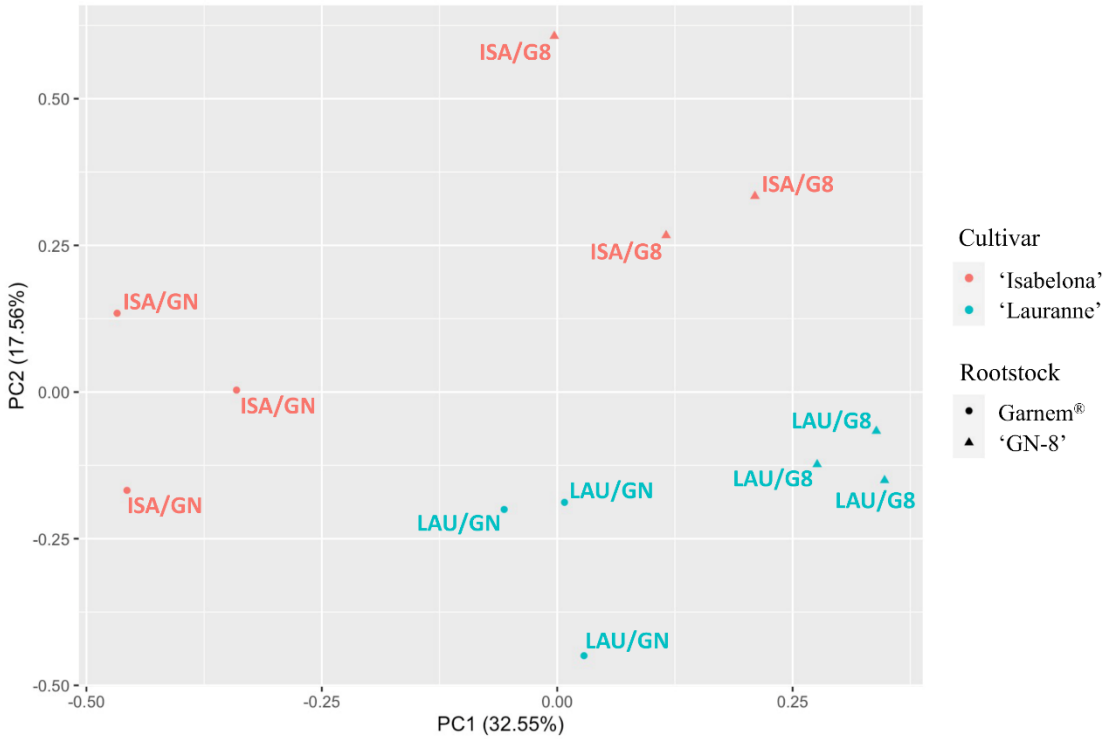

Figure 6.3. Principal component analysis (PCA) of the global expression profile data from rootstock samples of the four scion/rootstock combinations. ISA/GN: 'Isabelona'/Garnem®; ISA/G8: 'Isabelona'/'GN-8'; LAU/GN: 'Lauranne'/Garnem®; LAU/G8: 'Lauranne'/'GN-8'.

A total of 168 DEGs were overexpressed in combinations with 'Isabelona' as scion respective to those with 'Lauranne', of which 100 appeared in the combination with Garnem® and 52 in combination with 'GN-8', while only 16 DEGs were in both combinations (Figure 6.4A). A similar display was observed with DEGs that were underexpressed when 'Isabelona' was the scion. A total of 71 DEGs appeared only in Garnem®, while 74 DEGs were found in 'GN-8'. A total of 34 DEGs were present in both rootstocks (Figure 6.4B).

Therefore, while both Garnem® and 'GN-8' expression profiles are influenced by the scion that is grafted onto them, responses seem to be specific for each rootstock; at least regarding which specific genes are involved. In any case, that does not mean that the regulatory pathways affected by the scion influence are not similar.

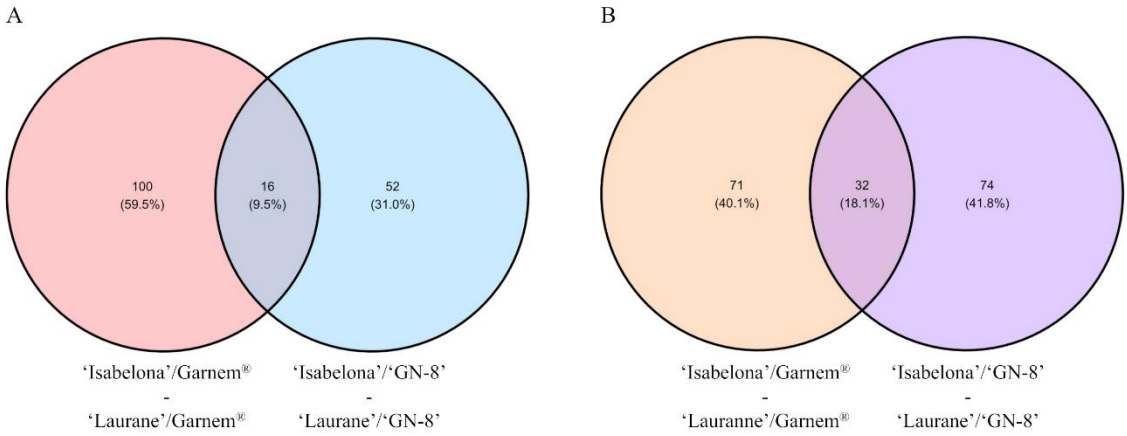

Figure 6.4. Venn diagrams of differentially expressed genes (DEGs) for the four scion/roostock combinations. A, DEGs more expressed in combinations with 'Isabelona' as scion than with 'Lauranne'. **B,** DEGs less expressed in combinations with 'Isabelona' as scion than with 'Lauranne'.

6.3.4. DEGs associated with hormonal regulation were influenced by the cultivar in rootstock tissue

We have seen that changes in hormonal response prompted by a different rootstock affect the almond scion architecture, modifying the number of branches or the growth of the main axis. Therefore, it is likely that the grafted scion also has an effect on the rootstocks, triggering different mechanisms that could affect the rootstock properties. This reciprocal effect has been already described in other species regarding different traits (regulation of rootstock responses to low Pi and phloem sap metabolites) (Gautier et al., 2021; Tietel et al., 2020). Here, we reported that hormonal response is affected by the scion, presumably leading to changes in the root architecture. Although samples were collected from the rootstock trunk, we expect that the variation of the dynamics of hormone flux found there affect the rest of the root system.

Contrary to its function in shoots, auxin has been described to promote the formation of lateral roots (Ding and Friml, 2010; Overvoorde et al., 2010; Petersson et al., 2009; Saini et al., 2013). Various DEGs involved positively in auxin response were downregulated when 'Isabelona' was the scion in Garnem® (Table 6.2). *BUD2* (Prudul26A013026) is an auxin inducible member of the SAMDC family, playing a part in mechanisms promoted by auxin, like apical dominance and root branching (Cui et al., 2010; Ge et al., 2006). *IAR3* (Prudul26A016337) releases IAA from its conjugate form, regulating the free levels of auxin (Davies et al., 1999; Widemann et al., 2013). *ZIFL1* (Prudul26A023995) positively regulates polar auxin transport,

favoring processes like lateral root development (Remy et al., 2013). On the other hand, *GH3.6* (Prudul26A017626), a negative regulator of auxin levels (Pierdonati et al., 2019; Z. Zhang et al., 2007), appeared overexpressed in combinations with 'Isabelona' as scion (Table 6.2). Here, the fact that auxin processes are downregulated in combinations with 'Isabelona' as scion hints to that rootstocks with this cultivar may have a conducible environment to develop less lateral roots. Whereas, rootstocks with 'Lauranne' as scion could develop an increased number of lateral roots, which would correlate to higher substrate availability and therefore affect their vigor and aerial branching phenotype (Chapter 3; Montesinos et al., 2021b).

Table 6.2. Differentially expressed genes (DEGs) associated with hormonal regulation.

logFC 'Isabelona'/Garnem® - 'Lauranne'/Garnem®	logFC 'Isabelona'/'GN-8' - 'Lauranne'/'GN-8'	*P. dulcis* ID	Gene	GO term	Biological process
	1.003	Prudul26A011001	*ACO*	GO:0009693	ethylene biosynthetic process
	-1.243	Prudul26A007830	*ACO*	GO:0009693	ethylene biosynthetic process
1.404		Prudul26A030744	*BAS1*	GO:0055114	oxidation-reduction process
	-1.197	Prudul26A013026	*BUD2*	GO:0006557	S-adenosylmethioninamine biosynthetic process
1.228		Prudul26A008430	*bZIP58*	GO:0006355	regulation of transcription, DNA-templated
1.755		Prudul26A017801	*CKX5*	GO:0009823	cytokinin catabolic process
	1.106	Prudul26A028543	*CVIF2*	GO:0043086	negative regulation of catalytic activity
	1.014	Prudul26A016230	*CVIF2*	GO:0043086	negative regulation of catalytic activity
	-1.434	Prudul26A017398	*CYP94C1*	GO:0009611	response to wounding
	1.295	Prudul26A002650	*ERF12*	GO:0009873	ethylene-activated signaling pathway
	1.232	Prudul26A022504	*ERF12*	GO:0009873	ethylene-activated signaling pathway
-2.000	-2.949	Prudul26A000689	*GA2OX8*	GO:0009686	gibberellin biosynthetic process
	1.358	Prudul26A017626	*GH3.6*	GO:0010252	auxin homeostasis
-5.950		Prudul26A016337	*IAR3*	GO:0009850	auxin metabolic process
1.007		Prudul26A016134	*LOL1*	GO:0034052	positive regulation of plant-type hypersensitive response
1.821		Prudul26A022418	*MAX1*	GO:0016117	carotenoid biosynthetic process
	-1.005	Prudul26A005107	*RCA*	GO:0050790	regulation of catalytic activity
1.102		Prudul26A028381	*SPL8*	GO:0030154	cell differentiation
-1.640		Prudul26A006492	*SWEET2*	GO:0008643	carbohydrate transport
-1.176		Prudul26A023995	*ZIFL1*	GO:0010540	basipetal auxin transport

GA acts mostly in opposition to the auxin response, inhibiting lateral root formation while promoting cell elongation and proliferation in the central root (Ubeda-Tomás et al., 2008; Yaxley et al., 2001). Three genes related positively to GA activity were found to be upregulated in

rootstock tissues in combinations with 'Isabelona' as the scion (Table 6.2). *LOL1* (Prudul26A016134) and *bZIP58* (Prudul26A008430) modulate GA levels, favoring its activity and acting in numerous pathways regulated by this hormone (Wu et al., 2014). *SPL8* (Prudul26A028381) can act both in a positive or negative manner, although has been described to negatively affect root elongation in Arabidopsis (Y. Zhang et al., 2007). On the other hand, *GA2OX8* (Prudul26A000689) is downregulated in combinations with 'Isabelona' (Table 6.2). GA2OX8 catalyzes the deactivation of active GA, hence reducing its levels and activity (Liu et al., 2021; Zhou et al., 2012). In general, genes related to increased GA levels are upregulated in rootstocks when 'Isabelona' is the scion. This could lead to the elongation of the central root, in a similar manner of what we observed in the scion, while inferior expression of GA responses in combinations with 'Lauranne' would favor the development of numerous lateral roots.

ET response was also be affected by the scion. 1-Aminocyclopropane-1-Carboxylic Acid Oxidase (*ACO)* carries out a crucial step in ET biosynthesis, controlling ET production (Houben and Van de Poel, 2019; Ruduś et al., 2013). Homologues of this gene (Prudul26A011001, Prudul26A007830) were found both upregulated and downregulated in 'Isabelona'/'GN-8' combinations (Table 6.2). *ERF12* has been described to participate in floral transition and seed dormancy in response to ethylene, being activated by its presence (Chandler and Werr, 2020; J. Li et al., 2019). Here, two homologues (Prudul26A002650, Prudul26A022504) where upregulated when 'Isabelona' was grafted onto 'GN-8' (Table 6.2). ET acts opposing auxin effect in lateral root formation (Lewis et al., 2011; Qin et al., 2019), which matches the reduced auxin response that has been reported in combinations with 'Isabelona'. BRs have an opposite function to ET, favoring the initiation of lateral roots (X. Li et al., 2019; Wei and Li, 2016). BAS1 (Prudul26A030744), an enzyme that catalyzes BR inactivation (Neff et al., 1999), is overexpressed in Garnem® when 'Isabelona' is the scion (Table 6.2).

Scion also influenced the expression of genes involved in other hormonal responses. *CKX5* (Prudul26A017801) was overexpressed in the 'Isabelona'/Garnem® combination (Table 6.2). Being a CK dehydrogenase, CKX5 participates in degrading CKs (Ha et al., 2012). *MAX1* (Prudul26A022418), which is part of the SL biosynthetic pathway (Booker et al., 2005; Challis et al., 2013), is also upregulated when Garnem® had 'Isabelona' as scion (Table 6.2). Jasmonic acid (JA) is typically activated in stress responses (Ruan et al., 2019). *CYP94C1* (Prudul26A017398) carries out the oxidative inactivation of this hormone (Bruckhoff et al., 2016). This gene was less expressed in the 'Isabelona'/'GN-8' combination too, hinting to a negative regulation of growth in this combination (Table 6.2). Finally, a couple of genes related to sugar availability were affected by the scion. Two *CVIF2* homologues (Prudul26A028543, Prudul26A016230) were overexpressed in the 'Isabelona'/'GN-8' combination (Table 2). *CVIF2*

might regulate sucrose cleaving, therefore negatively affecting plant sugar levels (W. Yang et al., 2020). *RCA* (Prudul26A005107), which was downregulated with 'Isabelona' as scion (Table 6.2), promotes RuBisCO activity and therefore sugar production (Portis et al., 2008). Moreover, the sugar transporter *SWEET2* (Prudul26A006492), which is especially active in roots (Chen et al., 2015), was also less expressed when 'Isabelona' was the scion. Therefore, 'Isabelona' seems to influence negatively sugar production in roots, which might lead to a reduction in the formation of roots.

In conclusion, the presence of a different scion affects the hormonal response in the rootstock. In this case, we observed that rootstocks with 'Isabelona' as scion present an hormonal setting that should inhibit the formation of lateral roots, while those with 'Lauranne' as scion are prompted to develop more lateral roots.

6.3.5. Root development and root cell wall reorganization are negatively influenced by 'Isabelona'

Root architecture is regulated by numerous genes that mediate the formation of the primary root and others, like lateral roots or adventitious roots (Eshel and Beeckman, 2013). Though samples were collected from below the grafting site in 'GN-8' and Garnem® rootstocks, we would expect that changes in the expression profile would condition the behavior of other parts of the rootstock.

Two inhibitors of lateral root formation were overexpressed in combinations with 'Isabelona' (Table 6.3). *AGL79* (Prudul26A020939) acts as a repressor of lateral root development (Gao et al., 2018). While not affecting lateral root initiation, *LRP1* (Prudul26A023724) does affect its progression. Its overexpression in Arabidopsis reduced the number of lateral roots (Singh et al., 2020). *IAA4* (Prudul26A024452) is also overexpressed in the 'Isabelona'/Garnem® combination (Table 6.3). *IAA4* acts in opposition to auxin response, inhibiting the formation of adventitious roots (Zhang et al., 2020). Therefore, there is an upregulation of processes that lead to reduce lateral root formation when 'Isabelona' is the scion. Moreover, two homologues of *FIP37* (Prudul26A025382, Prudul26A011653) were highly overexpressed in the 'Isabelona'/Garnem® combination (Table 6.3). *FIP37* effect in meristem development has been mostly described in shoots, but it acts preventing meristem proliferation and therefore bud outgrowth (Shen et al., 2016). A similar function is carried out by *TSO1* (Song et al., 2000; W. Wang et al., 2018). Here, we found a homologue of this gene, *TCX2* (Prudul26A017201), being downregulated when 'Isabelona' was the scion (Table 6.3).

'Lauranne' has been proved to be a more vigorous scion than 'Isabelona'. Here, we also observed several genes involved in cell proliferation being downregulated in the rootstock in combinations with 'Isabelona' (Table 6.3). *ERF3* (Prudul26A005381) promotes cell division and cell elongation of the root meristem (Zhao et al., 2015). *SKP2A* (Prudul26A008007) is a regulator of cell proliferation, promoting cell division in lateral root primordium, whose degradation is stimulated by auxin (Jurado et al., 2010, 2008). Two homologues of *SNAK2* (Prudul26A014041, Prudul26A015706) were found. *SNAK1* has been described to promote cell division in response to external stimuli (Nahirñak et al., 2019, 2012). *SnRK1* is involved in repressing growth in response to low energy supplies (Baena-González and Hanson, 2017). Here, a member of its family, *KING1* (Prudul26A009950), was upregulated in the 'Isabelona'/Garnem® combination (Table 6.3).

Table 6.3. Differentially expressed genes (DEGs) associated with root development and root cell wall reorganization.

logFC 'Isabelona'/Garnem® - 'Lauranne'/Garnem®	logFC 'Isabelona'/'GN-8' - 'Lauranne'/'GN-8'	*P. dulcis* ID	Gene	GO term	Biological process
-1.023		Prudul26A020211	*4CLL6*	GO:0006744	ubiquinone biosynthetic process
	-1.627	Prudul26A014215	*4CLL9*	GO:0000272	polysaccharide catabolic process
1.094		Prudul26A020939	*AGL79*	GO:0006355	regulation of transcription, DNA-templated
	-1.062	Prudul26A005381	*ERF3*	GO:0072659	protein localization in plasma membrane
-1.265	1.319	Prudul26A009806	*EXPL1*	GO:0019953	sexual reproduction
3.089		Prudul26A025382	*FIP37*	GO:0010073	meristem maintenance
3.072		Prudul26A011653	*FIP37*	GO:0010073	meristem maintenance
	1.468	Prudul26A000195	*GRF4*	GO:0006355	regulation of transcription, DNA-templated
	-1.032	Prudul26A031613	*GUX3*	GO:0045492	xylan biosynthetic process
1.180		Prudul26A024452	*IAA4*	GO:0009733	response to auxin
1.174		Prudul26A009950	*KING1*	GO:0042128	nitrate assimilation
	1.024	Prudul26A023724	*LRP1*	GO:0048364	root development
1.334	1.832	Prudul26A008528	*MYB103*	GO:0006355	regulation of transcription, DNA-templated
-1.300		Prudul26A012897	*MYB20*	GO:1901141	regulation of lignin biosynthetic process
-1.074		Prudul26A014014	*ROL1*	GO:0071555	cell wall organization
	-1.022	Prudul26A008007	*SKP2A*	GO:0010311	lateral root formation
-1.694		Prudul26A014041	*SNAK2*	GO:0006952	defense response
	-1.850	Prudul26A015706	*SNAK2*	GO:0006952	defense response
	-3.009	Prudul26A007951	*TBL19*	GO:0045492	xylan biosynthetic process
	-1.001	Prudul26A014994	*TBL29*	GO:0045492	xylan biosynthetic process
-1.405		Prudul26A017201	*TCX2*	GO:0006355	regulation of transcription, DNA-templated

The regulation of several components that are part of the cell wall, like lignins, xyloglucans or pectins, is essential in the control of cell wall formation and cell wall reorganization (Cosgrove, 2016; Meents et al., 2018; Voiniciuc et al., 2018). Numerous genes associated to their synthesis or transport were downregulated in combinations with 'Isabelona' compared to those with 'Lauranne' as the scion (Table 6.3). Members of the 4CL family like *4CLL6* (Prudul26A020211) and *4CLL9* (Prudul26A014215) are part of the phenylpropanoid metabolism pathway, participating in lignin biosynthesis (H. Liu et al., 2017). The MYB transcription factor, *MYB20* (Prudul26A012897), promotes the lignin biosynthesis pathway (Geng et al., 2020). However, another MYB TF linked to lignin biosynthesis, *MYB103* (Prudul26A008528), was overexpressed in combinations with 'Isabelona' as scion (Ohman et al., 2013). *GUX3* (Prudul26A031613) is involved in xylan modification while *TBL19* (Prudul26A007951) and *TBL29* (Prudul26A014994) participate in xylan acetylation (Gao et al., 2017; Grantham et al., 2017; Mortimer et al., 2015). These modifications are crucial to ensure xylan function and cell wall strength. Knockout mutants of *ROL1* (Prudul26A014014) produce aberrant pectin structure which leads to reduced elongation growth, highlighting a role for *ROL1* in cell wall reorganization (Ringli et al., 2008; Schumacher et al., 2021). Nevertheless, some genes associated also to cell wall formation were found to be upregulated when 'Isabelona' was the scion (Table 6.3). *GRF4* (Prudul26A000195) promotes cellulose biosynthesis in a response involving *MYB61* transcription factor (Gao et al., 2020). *EXPL1* (Prudul26A009806) is associated to cell wall remodeling in response to auxin and lateral root initiation (Ramakrishna et al., 2019). Contradictorily, *EXPL1* was overexpressed in 'GN-8', while being downregulated in the 'Isabelona'/Garnem® combination (Table 6.3). This could mean a differential response for this gene depending on which rootstock is affected by the scion, maybe linked to the fact that 'GN-8' is a prominently less vigorous rootstock than Garnem®.

In general, processes related to root formation or active tissue growth like cell wall reorganization were downregulated when 'Isabelona' was the scion, expecting that these combinations should present a root system with fewer lateral roots. This response is in line with the hormonal status reported previously, that favored root formation in rootstocks with 'Lauranne' as scion, and not in those with 'Isabelona'.

6.3.6. DEGs associated with light responses are affected by cultivar in rootstock tissue

Light regulates numerous processes related to plant development, and several pathways are involved in growth control (Molas and Kiss, 2009; Yadav et al., 2020). Light availability mediates the formation of lateral branches, through several responses like shade avoidance (Casal, 2012; Finlayson et al., 2010). In the root, we observed an upregulation of genes involved in

responses related to reduced light in combinations that had 'Isabelona' as scion, with *ABR* (Prudul26A020068) being overexpressed and several homologues of *phyE* (Prudul26A014761, Prudul26A002019) and *UVR8* (Prudul26A018495, Prudul26A003343, Prudul26A011979) downregulated (Table 6.4). *ABR* is involved in ABA responses and it is induced by light deprivation (Su et al., 2016). *phyE* regulates responses to low R/FR, in consonance with *phyB* (Devlin et al., 1998). The photoreceptor *UVR8* mediates the signal produced by UV-B that inhibits shade avoidance responses (Sharma et al., 2019). Auxin and light responses are tightly integrated, affecting tree architecture (Keuskamp et al., 2010). Two inhibitors of auxin response affected by light were overexpressed in combinations with 'Isabelona' (Table 6.4). *NPH3* (Prudul26A013341) participates in an auxin feedback response, modifiying auxin transport in response to phototropism (Wan et al., 2012). *RVE7* (Prudul26A019438) is a member of the same family of *RVE1*, which modulates plant growth through repression of auxin levels (Rawat et al., 2009). 'Lauranne', which shows numerous branching, is expected not to be affected as acutely by light availability than 'Isabelona', which displays reduced branching. Here, this effect is more prevalent in Garnem®, while 'GN-8' is less affected by the scion light perception. This could be caused by the higher vigor presented by Garnem®, being more influenceable by changes that favor growth.

Table 6.4. Differentially expressed genes (DEGs) associated with light responses and circadian clock regulation

logFC 'Isabelona'/Garnem® - 'Lauranne'/Garnem®	logFC 'Isabelona'/'GN-8' - 'Lauranne'/'GN-8'	*P. dulcis* ID	Gene	GO term	Biological process
1.899		Prudul26A020068	*ABR*	GO:0009733	response to auxin
1.596		Prudul26A024462	*COL6*	GO:0006355	regulation of transcription, DNA-templated
-1.751	-1.054	Prudul26A016707	*GI*	GO:0042752	regulation of circadian rhythm
1.061		Prudul26A014609	*JMJD5*	GO:0042752	regulation of circadian rhythm
-1.542		Prudul26A026608	*MDL1*	GO:0055114	oxidation-reduction process
1.368		Prudul26A013341	*NPH3*	GO:0009638	phototropism
-1.339		Prudul26A014761	*phyE*	GO:0009585	red, far-red light phototransduction
-1.364		Prudul26A002019	*phyE*	GO:0009585	red, far-red light phototransduction
-1.453		Prudul26A027917	*PRR7*	GO:0007623	circadian rhythm
1.009		Prudul26A019438	*RVE7*	GO:0007623	circadian rhythm
-1.078		Prudul26A018495	*UVR8*	GO:0009649	entrainment of circadian clock
-1.078	-1.042	Prudul26A003343	*UVR8*	GO:0009649	entrainment of circadian clock
-1.798	-1.143	Prudul26A011979	*UVR8*	GO:0009649	entrainment of circadian clock

The circadian clock, which is controlled by light, between other environmental responses, regulates numerous processes in plant development, including root growth (Farré, 2012; Inoue et al., 2018; Sanchez and Kay, 2016). We detected a mixed pattern of expression profiles of genes

involved in circadian clock regulation. *COL6* (Prudul26A024462) and *JMJD5* (Prudul26A014609) were overexpressed in the 'Isabelona'/Garnem® combination (Table 6.4). CO-like genes are light responsive genes under circadian clock control and affecting circadian rhythms (Chia et al., 2008; Ledger et al., 2001). *JMJD5* is integrated in various responses regulated by circadian period, including flowering regulation (Jones et al., 2019). On the other hand, the circadian clock regulator *GI* (Prudul26A016707) was downregulated in combinations with 'Isabelona' (Table 6.4). This gene participates in regulating daily *CO* expression and in activating *FT* expression, being controlled by light (Sawa et al., 2007; Sawa and Kay, 2011; Song et al., 2014). While we do not observe any concrete trend in the influence of the scion in the circadian clock regulation, it seems clear that these processes can be affected by the interaction between scion and rootstock.

6.4. Conclusions

Interaction between scion and rootstock in almond trees occur in both directions, also influencing the scion the rootstock development. Here, we identified multiple biological processes being differentially affected depending which almond cultivar was grafted. Between these, we describe genes involved in hormonal regulation, root development, cell wall reorganization, light perception and circadian clock regulation (Figure 6.5). This influence seems to have a feedback effect in the development of the scion. We report that cultivars displaying more vigor like 'Lauranne' influence positively root development, including lateral root formation. This would favor the capture of nutrients by the radicular system and, in consequence, would promote scion growth, resulting in the vigorous phenotype that 'Lauranne' presents when compared to 'Isabelona'. Therefore, choosing the correct scion/rootstock combination is essential to the success of the orchard. In intensive systems, the rootstock effect in tree vigor depends not only on its genotype, but also the scion is determinant in root development, and hence, tree growth.

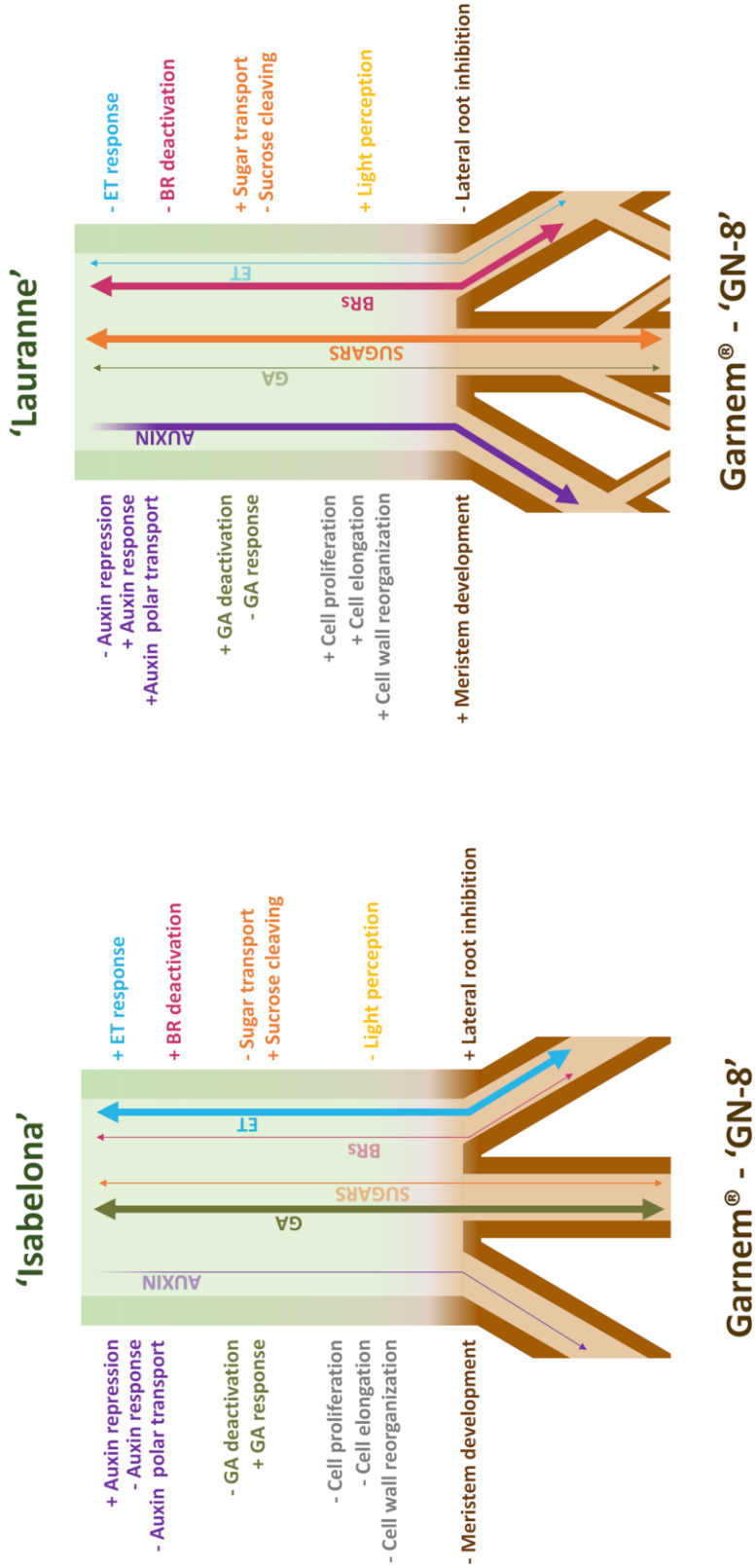

Figure 6.5. Schematic representation of the scion effect in the rootstock hormonal regulation. + indicates upregulation, while – indicates downregulation. Arrows only in downward direction indicate apical origin. GA: Gibberelic acid; BRs: Brassinosteroids; ET: Ethylene

.

7. GENERAL DISCUSSION

Modern almond (*Prunus amygdalus* (L.) Batsch, syn *P. dulcis* (Mill.)) planting systems require not only high fruit quality, but also new agronomical traits concerning tree characteristics, like reduced vigor or a narrow canopy. Moreover, to reduce costs associated with crop maintenance, it would be beneficial that almond scion developed these ideotypes naturally, diminishing the labor necessary to accommodate them in new efficient planting systems. Tree architecture is comprised by all the traits that define the three-dimensional structure of the scion. This encompasses tree vigor, branch formation, tree habit or flowering differentiation. Consisting then of numerous quantitative parameters, tree architecture can be considered as a remarkably complex trait. Likewise, a vast number of biological processes and hormonal responses defines its molecular regulation. Consequently, deciphering how tree architecture is regulated needs of a broad approach. In this doctoral thesis, we have determined how to phenotype almond tree architecture to facilitate its molecular study. We have also analyzed which biological processes are of major importance in the phenotypical differences observed. Moreover, we have begun to unravel the dynamics between scion and rootstock interaction, which are substantial in determining not only the vigor but also the whole architecture of the adult tree.

7.1. Phenotyping almond trees for tree architectural data

Tree architecture was first introduced by Hallé et al. (1978) to analyze the dynamics of tree spatial development. This was posteriorly expanded, identifying the main factors behind tree architecture (Barthélémy and Caraglio, 2007; Costes et al., 2006). Divided in four major features, our interest was primed to two of them: branching pattern and morphological differentiation of axes.

In our first attempt to characterize the molecular basis behind tree architecture, and specifically tree habit, we utilized general descriptors of the canopy, distinguishing between five types of tree habit described by UPOV (International Union for the Protection of New Varieties of Plants) (upright, somewhat upright, semiopen, open and weeping) that described the overall tree (Chapter 2; Montesinos et al., 2021a). This approach was proven limited for molecular approaches. Firstly, tree habit is more complex than the depiction of the overall tree habit, depending not only on the orientation that individual branches present, but also on of the characteristics of which branches growth and with what vigor. Secondly, qualitative non-continuous descriptors are not objective, depending on the person who measure them. Thirdly, only five categories are quite reductive for all the shapes that almond branches can lead to formed. Consequently, we landed at the conclusion that for detecting which molecular responses are associated with tree architecture, we needed a more robust and quantitative phenotype protocol.

To that goal, we tested twenty-four quantitative parameters in Chapter 3 (Montesinos et al., 2021b). This set of parameters was divided in four categories: vigor, branch quantity, branch distribution and branching habit. Detailed phenotypic data of architectural traits is only achievable in young trees (or branches), while in trees older that three-years-old is not feasible to collect this data due to the sheer complexity of their structure. Our interest was focused on which parameters were influenced by rootstock genotype, given than in almond orchards the rootstock is a crucial aspect of the scion development. We detected that vigor (though not those related to Trunk Cross-Sectional Area), branch quantity and branch distribution parameters were clearly influenced by rootstock. Otherwise, branching habit seems to depend on the scion primarily, not being affected the branch angle by the rootstock. Besides, we observed a negative correlation between vigor (Length) and branch quantity (BbyIN and B_NbAS) parameters, which is explained by the strength of apical dominance. Trees with a strong apical dominance effect move resources to the main axis, being this larger and displaying a reduced number of shoots. On the contrary, trees that present weak apical dominance, relocate resources to new shoots, developing a higher number of them, which finally arrest the growth of the main axis, leading to a shorter trunk or central branch.

To better comprehend the dynamics of shoot formation in almond trees, and the influence that the rootstock genotype exerts on them, in Chapter 4 we studied the formation of secondary shoots in two-year-old branches. We distinguished between two types of shoots, depending on whether they grew immediately or after a period of dormancy. They are denominated sylleptic and proleptic shoots respectively (Barthélémy and Caraglio, 2007). Sylleptic and proleptic shoots formation was previously studied in diverse conditions in almond and peach (*P. persica* (L.) Batsch) trees (Fyhrie et al., 2018; Negrón et al., 2015, 2014a, b; Prats-Llinàs et al., 2019). Here, we observed that their formation, while depending on the cultivar, was also clearly influenced by rootstock genotype. Concordantly with results in Chapter 3 (Montesinos et al., 2021b), we detected a prevalence of sylleptic shoots in combinations with reduced apical dominance.

7.2. Molecular regulation of tree architecture in almond trees

At the phenotype level, tree architecture is a complex trait comprehend by multiple parameters. Equally, its molecular regulation depends on multiple interconnected pathways that are modulated by endogenous elements like hormones, but also by exogenous elements like nutrient availability, light perception, or gravitropism.

In Chapter 2 (Montesinos et al., 2021a), a first effort was made to characterize the molecular basis behind tree architecture analyzing a family of six genes, denominated the IGT family. This family has been associated with the regulation of tree habit in peach (Dardick et al., 2013; Guseman et al., 2017; Hollender et al., 2018; Waite and Dardick, 2021). Moreover, its

members have been extensively characterized in *Arabidopsis thaliana* and *Oryza sativa*, connecting gravitational perception with the relocation of auxin carriers (Hollender et al., 2020; Nakamura et al., 2019; Taniguchi et al., 2017; Yoshihara and Spalding, 2020; Zhang et al., 2018). In our study, we analyzed the sequence of forty-one almond cultivars and wild species, to evaluate if there was an association between differences observed in overall tree habit and their corresponding protein sequence. Although there were variants in most of the IGT family members, including mutations in highly conserved regions, no correlation with the described phenotypes was observed. Furthermore, we studied the expression in shoot tips of the IGT family members in a subset of fourteen almond commercial cultivars, finding that only three were expressed (*LAZY1*, *LAZY2* and *TAC1*). Again, we did not detect any correlation with their overall tree habit, though there were differences in gene expression between cultivars. This variance gave us an opportunity to analyze the regulation of IGT family genes. We found two mutations in the promotor sequences of *LAZY1* and *LAZY2* correlated to differences in gene expression. The region was identified as a possible binding site of the TF *IPA1*. A posterior gene expression analysis of three *IPA1* homologues confirmed that it was a likely regulator of *LAZY1* and *LAZY2* expression. In definitive, though we did improve our understanding of the IGT family regulation, tree architecture, at least in almond, is likely to be regulated by multiple biological processes, not only a single gene family, and hence a wider approach is needed to understand it.

To this purpose, we carried out an RNA-Seq analysis of shoot tips in three cultivars grafted each onto three hybrid rootstocks (Chapter 5). We observed several biological processes involved in the regulation of tree architecture. Predominantly, we noted that genes associated with apical dominance and bud outgrowth were expressed differentially in comparisons where they were phenotypical differences, such as 'Diamar' grafted onto Rootpac® 20 against 'Diamar' grafted onto Rootpac® 40 or Garnem®. Apical dominance is regulated by various hormones, but its central regulator is auxin, acting positively (Barbier et al., 2019; Hollender and Dardick, 2015; B. Wang et al., 2018). In Chapters 5 and 6, we observed several genes involved in auxin regulation to be correlated with differences in the phenotype, like *NF-YA10*, *PIN6*, *VAB* or *IAA6*. Citokinins, sugar concentration or nitrogen availability have the opposite effect, favoring branch formation (Krouk et al., 2011; Mason et al., 2014; Waldie and Leyser, 2018; Y. Y. Wang et al., 2018). In accordance, we did report that genes positively associated with these responses were overexpressed when apical dominance was low, such as *CKX6*, *CKX7*, *SWEET17* or *NRT1.1*.

Apart from biological processes associated with branch formation, we also detected differentialy expressed genes (DEGs) that were associated with vigor and plant growth. Gibberellic acid (GA) is the main hormone controlling plant growth, favoring cell proliferation and elongation (Busov et al., 2008; Hedden and Thomas, 2012). We observed multiple genes

involved in its pathway, such as *YAB1*, *GASA6*, *GA2OX8* or *DAG1*, being correlated with phenotypically differences in vigor. Likewise, we also noticed genes associated to cell division and cell elongation being more expressed in more vigorous scion/rootstock combinations, like *FBL17* or *ELP*. Because of this higher rate of growth, in Chapter 5 we found an overexpression of genes associated with cell wall formation and cell wall reorganization, as for example various *EXP*, *LAC* or *XTH* genes. Augmented growth requires the reorganization of the cell wall, allowing cell elongation and cell division (Cosgrove, 2016; Meents et al., 2018).

7.3. Dynamics of scion/rootstock interaction in almond combinations

Rootstock genotype affects considerably the development of multiple scion features (Warschefsky et al., 2016). Tree architecture is no exception to this, and the effect of the rootstock in the scion were both observed at the phenotype and at the molecular level.

Although rootstocks always exert some influence in the scions that are grafted onto them, not all cultivars are equally influenced by rootstock genotype. We described in Chapter 3 (Montesinos et al., 2021b) that cultivars with prevalent apical dominance phenotype like 'Isabelona' (strong apical dominance) and 'Lauranne' (weak apical dominance), were not as affected by the rootstock genotype as other cultivars, like 'Diamar' or 'Soleta'. In these cases, rootstocks significantly altered their development, promoting longer trunks (Length) and reduced branching (Nb_B, BbyIN, B_NbAS) in combinations with Rootpac® 20, or limited main axis growth and numerous branching in combinations with Rootpac® 40 and Garnem®.

Likewise, in Chapter 5 we confirmed that the lack of influence in the phenotype that exists in combinations with 'Isabelona' and 'Lauranne' was correlated with a lack of DEGs. However, when 'Diamar' was the scion, we detected differences in gene expression, as we reported diversity in the scion tree architecture of these combinations. The exact mechanism by which the rootstock translates its signals to the scion is yet to be uncover in higher clarity. Given the differences in genes associated to hormonal responses, it seems likely that hormone transport from the roots plays an essential role in modifying the scion response. Furthermore, nutrients captured and transported from the roots, specifically nitrogen, also appear to have an important role in affecting the scion development. Recent studies have also highlighted the fact that even mRNA and small RNAs are involved in this communication in multiple species, travelling long distances and affecting other aspects of tree development, although their study was outside of the scope of this thesis (W. Liu et al., 2020; Yang et al., 2015).

While the rootstock effect on the scion, although in a reduced extent, had been previously described, the effect of the scion on the rootstock development had not attracted much interest

until now. However, as the rootstock seemingly transport hormones and other signals to the scion affecting its development; it was logical to assume that the same occurs in the opposite direction. In Chapter 6, after an RNA-Seq analyses of rootstock tissue, we studied the differences in the transcriptome of hybrid rootstocks Garnem® and 'GN-8' with the cultivars 'Isabelona' and 'Lauranne' grafted onto them. As it happened with the scion previously, we observed that different scions can alter the molecular response in the rootstock, affecting genes related both to hormonal response, like *GH3.6*, *GA2OX8*, *ACO* or *CKX5*, and to other processes associated with plant growth, such as *4CLL* or *TBL* genes. Furthermore, we detected that the scion can alter the expression of genes related to lateral root formation, such as *LRP1*, *AGL79* or *SKP2A*. This means that the scion is a determinant part in the formation of the root architecture in almond trees, and hence the ability of the tree to obtain nutrients and resources. Thus, it is apparent that the communication in both directions between scion and rootstock matters significatively to the development of the adult tree, and that understanding how each cultivar interacts with each rootstock is essential to obtain combinations that accomplish our requirements.

8. CONCLUSIONS

1. Variability of the six IGT family members protein sequences among almond cultivars is not correlated with differences observed in overall tree habit phenotype. Expression levels of the IGT family members *LAZY1*, *LAZY2* and *TAC1* in shoot tips are not correlated either with tree habit variability.

2. We have identified twenty-one transcriptions factors that seem to participate in regulating the expression of *LAZY1* and *LAZY2*. *IPA1* homologues have been identified as a candidate regulator of IGT family expression levels.

3. Seven of the twenty-one parameters analyzed to describe almond tree architecture were selected as descriptors of rootstock influence on scion tree architecture. They described the length of the trunk, the sized of the internodes, the amount of branching, its vigor and its distribution through the main axis. All of them were tightly connected to apical dominance

4. Dwarfing rootstocks like Rootpac® 20 or 'GN-8' had a positive effect on the scion apical dominance, and therefore favored the growth of the main axis. On the opposite, Garnem® promoted the formation of branches in the scion by relocating resources to its development.

5. Not all cultivars behave equally to the same rootstock. 'Isabelona' and 'Lauranne' were less influenced by rootstock genotype, presenting remarkably high and low apical dominance phenotypes, respectively.

6. Rootstock genotype affected shoot type formation, modifying predominantly the occurrence of sylleptic shoots, while proleptic shoot formation was less affected by rootstock choice. Garnem® and Rootpac® 40 promoted the development of sylleptic shoots in almond cultivars.

7. The transcriptome of cultivars with extreme apical dominance phenotypes like 'Isabelona' and 'Lauranne' were not significantly altered by rootstock genotype. Otherwise, cultivars that were affected phenotypically by the rootstock, like 'Diamar', also presented differentialy expressed genes when grafted onto different rootstocks.

8. Expression of genes associated with hormonal responses involved in apical dominance were differentially affected by rootstock genotype in 'Diamar' combinations. Scions grafted onto Rootpac® 20 displayed an upregulation of processes that favor auxin activity and a downregulation of those that repress it.

Meanwhile, processes associated positively with cytokinin activity, light perception, sugar transport or nitrogen availability, which favor branch formation, were downregulated in scions grafted onto Rootpac® 20, respective to those grafted onto Garnem® or Rootpac® 40.

9. When grafted onto Garnem® or Rootpac® 40, 'Diamar' showed an overexpression of genes associated with vegetative development, like gibberellic acid activity, cell proliferation or cell elongation. In consequence, genes related to cell wall formation and cell wall reorganization were upregulated in these combinations.

10. Expression levels in the rootstock were influenced by cultivar genotype. Genes associated with root formation and root development in combinations with 'Lauranne' as scion were upregulated, compared to those with 'Isabelona', in both Garnem® and 'GN-8'. Biological processes related to light response, like circadian clock regulation, were also affected by the scion.

9. CONCLUSIONES

1. La variabilidad entre variedades de almendro en la secuencia de proteínas de los seis miembros de la familia IGT no esta correlacionada con las diferencias fenotípicas observadas en el hábito global del árbol. La expresión relativa en apices de ramas de los miembros de la familia IGT *LAZY1*, *LAZY2* y *TAC1* tampoco esta correlacionada con la variabilidad fenotípica en el hábito del árbol.

2. Hemos identificado veintiun factores de transcripción que podrían participar regulando la expresión de *LAZY1* y *LAZY2*. Homólogos del gen *IPA1* homologuos han sido identificados como candidatos de reguladores de la expresión de los miembros de la familia IGT.

3. Siete de los veintiun parámetros analizados para describer la arquitectura del almendro fueron seleccionados como descriptores de la influencia del patrón en la arquitectura de la variedad. Estos describen la longitud del tronco, el tamaño de los entrenudos, la cantidad de ramas, su vigor y su distribución en el eje principal. Todos ellos estaban conectados estrechamente a la dominancia apical.

4. Patrones enanizantes como Rootpac® 20 o 'GN-8' tuvieron un efecto positivo en la dominancia ápical ejercida por la variedad, y por tanto favorecen el crecimiento del eje principal. Por el contrario, Garnem® promovió la formación de ramas en la variedad, relocalizando recursos para su desarrollo.

5. No todas las variedades se comportan de la misma injertadas en un mismo patrón. 'Isabelona' y 'Lauranne' fueron menos influenciadas por el genotipo del patrón, presentando una dominancia apical marcadamente elevada y reducida respectivamente.

6. El tipo de rama producida se ve afecta por el genotipo del patrón, modificando la formación de ramas silépticas, y afectando en menor medida la formación de ramas prolépticas. Garnem® y Rootpac® 40 promovieron el desarrollo de ramas silépticas en las variedades de almendro.

7. El transcriptoma de variedades que presentaban fenotipos extremos de dominancia apical, como 'Isabelona' y 'Lauranne', no fue alterado significativamente por el genotipo del patrón. Sin embargo, variedades que estaban afectadas fenotípicamente por el patrón, como 'Diamar', sí presentaron genes diferencialmente expresados con diferentes patrón.

8. La expresión de genes asociados a la respuesta hormonas e involucrados en la dominancia apical estuvo diferencialmente afectada por el genotipo del patrón en las combinaciones con 'Diamar'. Individuos injertados en Rootpac® 20 mostraron una regulación positiva de procesos que favorecen la actividad de las auxinas y una regulación negativa de aquellos que reprimen su actividad. A su vez, los procesos asociados positivamente con la actividad de las citoquininas, la percepción de la luz, el transporte de azúcares o la presencia de nitrógeno, los cuales favorecen la formación de las ramas, estaban regulados negativamente en individuos injertados en Rootpac® 20 en comparación con aquellos injertados en Garnem® o Rootpac® 40.

9. 'Diamar', injertado en Garnem® o Rootpac® 40, presentó sobreexpresión de genes asociados con el desarrollo vegetativo, como aquellos relacionado con la actividad de las giberelinas, la proliferación celular o la elongación celular. En consecuencia, genes relacionados con la formación y reorganización de la pared celular también se vieron sobreexpresados en estas combinaciones.

10. La expresión de genes en el patrón se vió afectada por el genotipo de la variades, sobreexpesandose genes asociados la fomación y desarrollo de raíces en las combinaciones con 'Lauranne', respecto a aquellas con 'Isabelona'. También se vieron afectados procesos relacionados con la percepción de luz, incluída la respuesta circadiana.

10. BIBLIOGRAPHY

Abe, K., Takahashi, H., and Suge, H. (2004). Graviresponding sites in shoots of normal and lazy rice seedlings. *Physiol. Plant* 92, 371–374. doi: 10.1111/j.1399-3054.1994.tb08823.x.

Adamowski, M., and Friml, J. (2015). PIN-Dependent Auxin Transport: Action, Regulation, and Evolution. *Plant Cell Online* 27, 20–32. doi:10.1105/tpc.114.134874.

Alabadí, D., Gallego-Bartolomé, J., Orlando, L., García-Cárcel, L., Rubio, V., Martínez, C., et al. (2008). Gibberellins modulate light signaling pathways to prevent Arabidopsis seedling de-etiolation in darkness. *Plant J.* 53, 324–335. doi:10.1111/j.1365-313X.2007.03346.x.

Albacete, A., Martínez-Andújar, C., Martínez-Pérez, A., Thompson, A. J., Dodd, I. C., and Pérez-Alfocea, F. (2015). Unravelling rootstock×scion interactions to improve food security. *J. Exp. Bot.* 66, 2211–2226. doi:10.1093/jxb/erv027.

Alioto, T., Alexiou, K. G., Bardil, A., Barteri, F., Castanera, R., Cruz, F., et al. (2020). Transposons played a major role in the diversification between the closely related almond and peach genomes: results from the almond genome sequence. *Plant J.* 101, 455–472. doi:10.1111/tpj.14538.

Aloni, B., Cohen, R., Karni, L., Aktas, H., and Edelstein, M. (2010). Hormonal signaling in rootstock-scion interactions. *Sci. Hortic. (Amsterdam).* 127, 119–126. doi:10.1016/j.scienta.2010.09.003.

Alvarez, J. M., Riveras, E., Vidal, E. A., Gras, D. E., Contreras-López, O., Tamayo, K. P., et al. (2014). Systems approach identifies TGA1 and TGA4 transcription factors as important regulatory components of the nitrate response of Arabidopsis thaliana roots. *Plant J.* 80, 1–13. doi:10.1111/tpj.12618.

An, H., Zhang, J., Xu, F., Jiang, S., and Zhang, X. (2020). Transcriptomic profiling and discovery of key genes involved in adventitious root formation from green cuttings of highbush blueberry (Vaccinium corymbosum L.). *BMC Plant Biol.* 20, 1–14. doi:10.1186/s12870-020-02398-0.

Badenes, M. L., Fernández i Martí, A., Ríos, G., Rubio-Cabetas, M. J. (2016). Application of genomic technologies to the breeding of trees. *Front. Genet*. 7, 1–13. doi:10.3389/fgene.2016.00198.

Baena-González, E., and Hanson, J. (2017). Shaping plant development through the SnRK1–TOR metabolic regulators. *Curr. Opin. Plant Biol.* 35, 152–157. doi:10.1016/j.pbi.2016.12.004.

Balducci, F., Capriotti, L., Mazzoni, L., Medori, I., Albanesi, A., Giovanni, B., et al. (2019). The rootstock effects on vigor, production and fruit quality in sweet cherry (Prunus avium L.). *J. Berry Res.* 9, 249–265. doi:10.3233/JBR-180345.

Band, L. R., Wells, D. M., Larrieu, A., Sun, J., Middleton, A. M., French, A. P., et al. (2012). Root gravitropism is regulated by a transient lateral auxin gradient controlled by a tipping-point mechanism. *Proc. Natl. Acad. Sci. USA* 109, 4668–4673. doi: 10.1073/pnas.1201498109

Barbier, F. F., Dun, E. A., Kerr, S. C., Chabikwa, T. G., and Beveridge, C. A. (2019). An Update on the Signals Controlling Shoot Branching. *Trends Plant Sci.* 24, 220–236. doi:10.1016/j.tplants.2018.12.001.

Barbier, F. F., Lunn, J. E., and Beveridge, C. A. (2015). Ready, steady, go! A sugar hit starts the race to shoot branching. *Curr. Opin. Plant Biol.* 25, 39–45. doi:10.1016/j.pbi.2015.04.004.

Barthélémy, D., and Caraglio, Y. (2007). Plant architecture: A dynamic, multilevel and comprehensive approach to plant form, structure and ontogeny. *Ann. Bot.* 99, 375–407. doi:10.1093/aob/mcl260.

Ben Yahmed, J., Ghrab, M., and Ben Mimoun, M. (2016). Eco-physiological evaluation of different scion-rootstock combinations of almond grown in Mediterranean conditions. *Fruits* 71, 185–193. doi:10.1051/fruits/2016003.

Bennett, T., Liang, Y., Seale, M., Ward, S., Müller, D., and Leyser, O. (2016). Strigolactone regulates shoot development through a core signalling pathway. *Biol. Open*, bio.021402. doi:10.1242/bio.021402.

Berthet, S., Demont-Caulet, N., Pollet, B., Bidzinski, P., Cézard, L., Le Bris, P., et al. (2011). Disruption of LACCASE4 and 17 results in tissue-specific alterations to lignification of Arabidopsis thaliana stems. *Plant Cell* 23, 1124–1137. doi:10.1105/tpc.110.082792.

Berut, A., Chauvet, H., Legue, V., Moulia, B., Pouliquen, O., and Forterre, Y. (2018). Gravisensors in plant cells behave like an active granular liquid. *Proc. Natl. Acad. Sci. USA* 115, 5123–5128 . doi: 10.1073/pnas.1801895115.

Bhogale, S., Mahajan, A. S., Natarajan, B., Rajabhoj, M., Thulasiram, H. V., and Banerjee, A.K. (2014). MicroRNA156: A potential graft-transmissible microrna that modulates plant

architecture and tuberization in Solanum tuberosum ssp. andigena. *Plant Physiol.* 164, 1011–1027. doi:10.1104/pp.113.230714.

Bielsa, B., Hewitt, S., Reyes-Chin-Wo, S., Dhingra, A., and Rubio-Cabetas, M. J. (2018). Identification of water use efficiency related genes in "Garnem" almond-peach rootstock using time-course transcriptome analysis. *PLoS One* 13, 1–24. doi:10.1371/journal.pone.0205493.

Bielsa, B., Montesinos, Á., Espiau, M. T., Ansón, J. M., Jaime, S. J., Laya, D., et al. (2021a). Mejora genética del almendro: pasado, presente y futuro. *Agricultura* 1047, 48–55.

Bielsa, B., Sanz, M., and Rubio-Cabetas, M. J. (2019). Uncovering early response to drought by proteomic, physiological and biochemical changes in the almond × peach rootstock "Garnem." *Funct. Plant Biol.* 46, 994–1008. doi:10.1071/FP19050.

Bielsa, B., Sanz, M. Á., and Rubio-Cabetas, M. J. (2021b). 'Garnem'and Myrobalan 'P. 2175': Two Different Drought Responses and Their Implications in Drought Tolerance. *Horticulturae* 7, 299. doi:10.3390/horticulturae7090299.

Binenbaum, J., Weinstain, R., and Shani, E. (2018). Gibberellin Localization and Transport in Plants. *Trends Plant Sci.* 23, 410–421. doi:10.1016/j.tplants.2018.02.005.

Blankenberg, D., Gordon, A., Von Kuster, G., Coraor, N., Taylor, J., Nekrutenko, A., et al. (2010). Manipulation of FASTQ data with galaxy. *Bioinformatics* 26, 1783–1785. doi:10.1093/bioinformatics/btq281.

Bolger, A. M., Lohse, M., and Usadel, B. (2014). Trimmomatic: A flexible trimmer for Illumina sequence data. *Bioinformatics* 30, 2114–2120. doi:10.1093/bioinformatics/btu170.

Booker, J., Sieberer, T., Wright, W., Williamson, L., Willett, B., Stirnberg, P., et al. (2005). MAX1 encodes a cytochrome P450 family member that acts downstream of MAX3/4 to produce a carotenoid-derived branch-inhibiting hormone. *Dev. Cell* 8, 443–449. doi:10.1016/j.devcel.2005.01.009.

Bou-Torrent, J., Roig-Villanova, I., Galstyan, A., and Martínez-García, J. F. (2008). PAR1 and PAR2 integrate shade and hormone transcriptional networks. *Plant Signal. Behav.* 3, 453–454. doi:10.4161/psb.3.7.5599.

Bruckhoff, V., Haroth, S., Feussner, K., König, S., Brodhun, F., and Feussner, I. (2016). Functional characterization of CYP94-genes and identification of a novel jasmonate catabolite in flowers. *PLoS One* 11, 1–26. doi:10.1371/journal.pone.0159875.

Bucher, M., Brunner, S., Zimmermann, P., Zardi, G. I., Amrhein, N., Willmitzer, L., et al. (2002). The expression of an extensin-like protein correlates with cellular tip growth in tomato. *Plant Physiol.* 128, 911–923. doi:10.1104/pp.129.3.1417.

Busov, V. B., Brunner, A. M., and Strauss, S. H. (2008). Genes for control of plant stature and form. *New Phytol.* 177, 589–607. doi: 10.1111/j.1469-8137.2007.02324.x.

Canales, J., Contreras-López, O., Álvarez, J. M., and Gutiérrez, R. A. (2017). Nitrate induction of root hair density is mediated by TGA1/TGA4 and CPC transcription factors in Arabidopsis thaliana. *Plant J.* 92, 305–316. doi:10.1111/tpj.13656.

Casal, J. J. (2012). Shade Avoidance. *Arab. B.* 10, e0157. doi:10.1199/tab.0157.

Cazzonelli, C. I., Vanstraelen, M., Simon, S., Yin, K., Carron-Arthur, A., Nisar, N., et al. (2013). Role of the Arabidopsis PIN6 Auxin Transporter in Auxin Homeostasis and Auxin-Mediated Development. *PLoS One* 8. doi:10.1371/journal.pone.0070069.

Challis, R. J., Hepworth, J., Mouchel, C., Waites, R., and Leyser, O. (2013). A role for More Axillary Growth1 (MAX1) in evolutionary diversity in strigolactone signaling upstream of MAX2. *Plant Physiol.* 161, 1885–1902. doi:10.1104/pp.112.211383.

Chandler, J. W., and Werr, W. (2020). A phylogenetically conserved APETALA2/ETHYLENE RESPONSE FACTOR, ERF12, regulates Arabidopsis floral development. *Plant Mol. Biol.* 102, 39–54. doi:10.1007/s11103-019-00936-5.

Chang, C. C., Chow, C. C., Tellier, L. C. A. M., Vattikuti, S., Purcell, S. M., and Lee, J. J. (2015). Second-generation PLINK: Rising to the challenge of larger and richer datasets. *Gigascience* 4, 1–16. doi: 0.1186/s13742-015-0047-8.

Chang, S., Puryear, J., and Cairney, J. (1993). A simple and efficient method for isolating RNA from pine trees. *Plant Mol Biol Rep* 11, 113–116. doi:10.1007/BF02670468.

Chardon, F., Bedu, M., Calenge, F., Klemens, P. A. W., Spinner, L., Clement, G., et al. (2013). Leaf fructose content is controlled by the vacuolar transporter SWEET17 in Arabidopsis. *Curr. Biol.* 23, 697–702. doi:10.1016/j.cub.2013.03.021.

Chen, H. Y., Huh, J. H., Yu, Y. C., Ho, L. H., Chen, L. Q., Tholl, D., et al. (2015). The Arabidopsis vacuolar sugar transporter SWEET2 limits carbon sequestration from roots and restricts Pythium infection. *Plant J.* 83, 1046–1058. doi:10.1111/tpj.12948.

Chen, J., Nolan, T. M., Ye, H., Zhang, M., Tong, H., Xin, P., et al. (2017). Arabidopsis WRKY46, WRKY54, and WRKY70 Transcription Factors Are Involved in Brassinosteroid-Regulated Plant Growth and Drought Responses. *The Plant Cell* 29, 1425–1439. doi:10.1105/tpc.17.00364.

Cheng, N. H., Pittman, J. K., Shigaki, T., Lachmansingh, J., LeClere, S., Lahner, B., et al. (2005). Functional association of Arabidopsis CAX1 and CAX3 is required for normal growth and ion homeostasis. *Plant Physiol.* 138, 2048–2060. doi:10.1104/pp.105.061218.

Chesterfield, R. J., Vickers, C. E., and Beveridge, C. A. (2020). Translation of Strigolactones from Plant Hormone to Agriculture: Achievements, Future Perspectives, and Challenges. *Trends Plant Sci.* 25, 1087–1106. doi:10.1016/j.tplants.2020.06.005.

Chia, T. Y. P., Müller, A., Jung, C., and Mutasa-Göttgens, E. S. (2008). Sugar beet contains a large CONSTANS-LIKE gene family including a CO homologue that is independent of the early-bolting (B) gene locus. *J. Exp. Bot.* 59, 2735–2748. doi:10.1093/jxb/ern129.

Chiniquy, D., Underwood, W., Corwin, J., Ryan, A., Szemenyei, H., Lim, C. C., et al. (2019). PMR5, an acetylation protein at the intersection of pectin biosynthesis and defense against fungal pathogens. *Plant J.* 100, 1022–1035. doi:10.1111/tpj.14497.

Cho, D., Villiers, F., Kroniewicz, L., Lee, S., Seo, Y. J., Hirschi, K. D., et al. (2012). Vacuolar CAX1 and CAX3 influence auxin transport in guard cells via regulation of apoplastic pH. *Plant Physiol.* 160, 1293–1302. doi:10.1104/pp.112.201442.

Cho, M., and Cho, H.-T. (2013). The function of ABCB transporters in auxin transport. *Plant Signal. Behav.* 8, 642-54. doi:10.4161/psb.22990.

Choi, Y., and Chan, A. P. (2015). PROVEAN web server: A tool to predict the functional effect of amino acid substitutions and indels. *Bioinformatics* 31, 2745–2747. doi:10.1093/bioinformatics/btv195.

Christie, J. M., Suetsugu, N., Sullivan, S., and Wada, M. (2018). Shining light on the function of nph3/rpt2-like proteins in phototropin signaling. *Plant Physiol.* 176, 1015–1024. doi:10.1104/pp.17.00835.

Cline, M. G. (1991). Apical dominance. *Bot. Rev.* 57, 318–358. doi:10.1007/BF02858771.

Cochetel, N., Escudié, F., Cookson, S. J., Dai, Z., Vivin, P., Bert, P. F., et al. (2017). Root transcriptomic responses of grafted grapevines to heterogeneous nitrogen availability depend on rootstock genotype. *J. Exp. Bot.* 68, 4339–4355. doi:10.1093/jxb/erx224.

Coll-Garcia, D., Mazuch, J., Altmann, T., and Müssig, C. (2004). EXORDIUM regulates brassinosteroid-responsive genes. *FEBS Lett.* 563, 82–86. doi:10.1016/S0014-5793(04)00255-8.

Collani, S., Neumann, M., Yant, L., and Schmid, M. (2019). FT modulates genome-wide DNA-binding of the bZIP transcription factor FD. *Plant Physiol.* 180, 367–380. doi:10.1104/pp.18.01505.

Cosgrove, D. J. (2015). Plant expansins: Diversity and interactions with plant cell walls. *Curr. Opin. Plant Biol.* 25, 162–172. doi:10.1016/j.pbi.2015.05.014.

Cosgrove, D. J. (2016). Plant cell wall extensibility: Connecting plant cell growth with cell wall structure, mechanics, and the action of wall-modifying enzymes. *J. Exp. Bot.* 67, 463–476. doi:10.1093/jxb/erv511.

Costa-Broseta, Á., Castillo, M., and León, J. (2020). Nitrite reductase 1 is a target of nitric oxide-mediated post-translational modifications and controls nitrogen flux and growth in arabidopsis. *Int. J. Mol. Sci.* 21, 1–13. doi:10.3390/ijms21197270.

Costes, E., Crespel, L., Denoyes, B., Morel, P., Demene, M.-N., Lauri, P.-E., et al. (2014). Bud structure, position and fate generate various branching patterns along shoots of closely related Rosaceae species: a review. *Front. Plant Sci.* 5, 1–11. doi:10.3389/fpls.2014.00666.

Costes, E., and Guédon, Y. (2002). Modelling branching patterns on 1-year-old trunks of six apple cultivars. *Ann. Bot.* 89, 513–524. doi:10.1093/aob/mcf078.

Costes, E., Lauri, P.-E., and Regnard, J. L. (2006). Analyzing Fruit Tree Architecture: Implications for Tree Management and Fruit Production. *Hort. Rev.* 32, 1–61. doi:10.1002/9780470767986.ch1.

Coupel-Ledru, A., Pallas, B., Delalande, M., Boudon, F., Carrié, E., Martinez, S., et al. (2019). Multi-scale highthroughput phenotyping of apple architectural and functional traits in

orchard reveals genotypic variability under contrasted watering regimes. *Hortic. Res.* 6, 1–15. doi:10.1038/s41438-019-0137-3.

Cui, X., Ge, C., Wang, R. Wang, H., Chen, W., Fu, Z., Jiang, X. et al. (2010). The *BUD2* mutation affects plant architecture through altering cytokinin and auxin responses in *Arabidopsis*. *Cell Res* 20, 576–586. doi:10.1038/cr.2010.51.

Dai, M., Zhao, Y., Ma, Q., Hu, Y., Hedden, P., Zhang, Q., et al. (2007). The rice YABBY1 gene is involved in the feedback regulation of gibberellin metabolism. *Plant Physiol.* 144, 121–133. doi:10.1104/pp.107.096586.

Dai, X., Lu, Q., Wang, J., Wang, L., Xiang, F., and Liu, Z. (2021). MiR160 and its target genes ARF10, ARF16 and ARF17 modulate hypocotyl elongation in a light, BRZ, or PAC-dependent manner in Arabidopsis: miR160 promotes hypocotyl elongation. *Plant Sci.* 303, 110686. doi:10.1016/j.plantsci.2020.110686.

Danjon, F., and Reubens, B. (2008). Assessing and analyzing 3D architecture of woody root systems, a review of methods and applications in tree and soil stability, resource acquisition and allocation. *Plant Soil* 303, 1–34. doi:10.1007/s11104-007-9470-7.

Dardick, C., Callahan, A., Horn, R., Ruiz, K. B., Zhebentyayeva, T., Hollender, C., et al. (2013). PpeTAC1 promotes the horizontal growth of branches in peach trees and is a member of a functionally conserved gene family found in diverse plants species. *Plant J.* 75, 618–630. doi:10.1111/tpj.12234.

Das, B., Ahmed, N., and Singh, P. (2011). Prunus diversity-early and present development: a review. *Int. J. Biodivers. Conserv.* 3, 721–734. doi: 10.5897/ijbcx11.003

Davies, R. T., Goetz, D. H., Lasswell, J., Anderson, M. N., and Bartel, B. (1999). IAR3 encodes an auxin conjugate hydrolase from Arabidopsis. *Plant Cell* 11, 365–376. doi:10.1105/tpc.11.3.365.

de Saint Germain, A., Ligerot, Y., Dun, E. A., Pillot, J.-P., Ross, J. J., Beveridge, C. A., et al. (2013). Strigolactones Stimulate Internode Elongation Independently of Gibberellins. *Plant Physiol.* 163, 1012–1025. doi:10.1104/pp.113.220541.

Dekkers, B. J. W., He, H., Hanson, J., Willems, L. A. J., Jamar, D. C. L., Cueff, G., et al. (2016). The Arabidopsis Delay of Germination 1 gene affects Abscisic Acid Insensitive 5 (ABI5) expression and genetically interacts with ABI3 during Arabidopsis seed development. *Plant J.* 85, 451–465. doi:10.1111/tpj.13118.

Depuydt, S., and Hardtke, C. S. (2011). Hormone signalling crosstalk in plant growth regulation. *Curr. Biol.* 21, R365–R373. doi:10.1016/j.cub.2011.03.013.

Devlin, P. F., Patel, S. R., and Whitelam, G. C. (1998). Phytochrome E influences internode elongation and flowering time in arabidopsis. *Plant Cell* 10, 1479–1487. doi:10.1105/tpc.10.9.1479.

Dierck, R., De Keyser, E., De Riek, J., Dhooghe, E., Van Huylenbroeck, J., Prinsen, E., et al. (2016a). Change in auxin and cytokinin levels coincides with altered expression of branching genes during axillary bud outgrowth in chrysanthemum. *PLoS One* 11, 1–30. doi:10.1371/journal.pone.0161732.

Dierck, R., Dhooghe, E., Van Huylenbroeck, J., De Riek, J., De Keyser, E., and Van Der Straeten, D. (2016b). Response to strigolactone treatment in chrysanthemum axillary buds is influenced by auxin transport inhibition and sucrose availability. *Acta Physiol. Plant.* 38, 1–11. doi:10.1007/s11738-016-2292-6.

Dierck, R., Leus, L., Dhooghe, E., Huylenbroeck, J. Van, and Riek, J. De (2018). Branching gene expression during chrysanthemum axillary bud outgrowth regulated by strigolactone and auxin transport. *Plant Growth Regul.* 86, 23-36. doi:10.1007/s10725-018-0408-2.

Di Guardo, M., Farneti, B., Khomenko, I., Modica, G., Mosca, A., Distefano, G., et al. (2021). Genetic characterization of an almond germplasm collection and volatilome profiling of raw and roasted kernels. *Hortic. Res*. 8, 1–19. doi:10.1038/s41438-021-00465-7.

Ding, Z., and Friml, J. (2010). Auxin regulates distal stem cell differentiation in Arabidopsis roots. *Proc. Natl. Acad. Sci. U. S. A.* 107, 12046–12051. doi:10.1073/pnas.1000672107.

Ditengou, F. A., Gomes, D., Nziengui, H., Kochersperger, P., Lasok, H., Medeiros, V., Paponov, I. A. et al. (2018). Characterization of auxin transporter PIN 6 plasma membrane targeting reveals a function for PIN 6 in plant bolting. *New Phyto.* 217, 1610–1624. doi:10.1111/nph.14923.

Dong, Z., Jiang, C., Chen, X., Zhang, T., Ding, L., Song, W., et al. (2013). Maize LAZY1 mediates shoot gravitropism and inflorescence development through regulating auxin transport, auxin signaling, and light response. *Plant Physiol.* 163, 1306–1322. doi: 10.1104/pp.113.227314.

Draeger, C., Ndinyanka Fabrice, T., Gineau, E., Mouille, G., Kuhn, B. M., Moller, I., et al. (2015). Arabidopsis leucine-rich repeat extensin (LRX) proteins modify cell wall composition and influence plant growth. *BMC Plant Biol.* 15, 1–11. doi:10.1186/s12870-015-0548-8.

Dun, E. A., Ferguson, B. J., and Beveridge, C. A. (2006). Apical dominance and shoot branching. Divergent opinions or divergent mechanisms? *Plant Physiol.* 142, 812–819. doi:10.1104/pp.106.086868.

Dun, E. A., Germain, A. de Saint, Rameau, C., and Beveridge, C. A. (2012). Antagonistic action of strigolactone and cytokinin in bud outgrowth control. *Plant Physiol.* 158, 487–498. doi:10.1104/pp.111.186783.

Durand, J. B., Guédon, Y., Caraglio, Y., and Costes, E. (2005). Analysis of the plant architecture via tree-structured statistical models: The hidden Markov tree models. *New Phytol.* 166, 813–825. doi:10.1111/j.1469-8137.2005.01405.x.

Elsadr, H., Sherif, S., Banks, T., Somers, D., and Jayasankar, S. (2019). Refining the Genomic Region Containing a Major Locus Controlling Fruit Maturity in Peach. *Sci. Rep*. 9, 1–12. doi:10.1038/s41598-019-44042-4.

Eshel, A., and Beeckman, T. (2013). Plant roots: the hidden half. CRC press.

Faria, D. (2017). GOEnrichment. GitHub repository. GitHub. https://github.com/DanFaria/GOEnrichment [Accesed September 8, 2021]

Farré, E. M. (2012). The regulation of plant growth by the circadian clock. *Plant Biol.* 14, 401–410. doi:10.1111/j.1438-8677.2011.00548.x.

Fasoli, M., Dal Santo, S., Zenoni, S., Tornielli, G. B., Farina, L., Zamboni, A., et al. (2012). The grapevine expression atlas reveals a deep transcriptome shift driving the entire plant into a maturation program. *Plant Cell* 24, 3489–3505. doi:10.1105/tpc.112.100230.

Felipe, A.J. (2000). El almendro: El material vegetal. Integrum, Lerida.

Felipe, A. J. (2009). “Felinem”, “Garnem”, and “Monegro” almond x peach hybrid rootstocks. *HortScience* 44, 196–197. doi:10.21273/HORTSCI.44.1.196.

Filo, J., Wu, A., Eliason, E., Richardson, T., Thines, B. C., and Harmon, F. G. (2015). Gibberellin driven growth in elf3 mutants requires PIF4 and PIF5. *Plant Signal. Behav.* 10, 1–9. doi:10.4161/15592324.2014.992707.

Finlayson, S. A., Krishnareddy, S. R., Kebrom, T. H., and Casal, J. J. (2010). Phytochrome regulation of branching in arabidopsis. *Plant Physiol.* 152, 1914–1927. doi:10.1104/pp.109.148833.

Font i Forcada, C., Sánchez-Pérez, R., Eduardo, I., Wu S., Fernández i Martí, Á. (2017). "Molecular breeding and genomics" in Almonds: botany, production and uses, ed. R. Socias i Company, and T. M. Gradziel (CABI, Wallingford, UK), 149–167. doi:10.1079/9781780643540.0149.

Food and Agriculture Organization of the United Nations. (2021). FAOSTAT. http://www.fao.org/faostat/en/#home [Accessed October 8, 2021].

Fornari, M., Calvenzani, V., Masiero, S., Tonelli, C., and Petroni, K. (2013). The Arabidopsis NF-YA3 and NF-YA8 genes are functionally redundant and are required in early embryogenesis. *PLoS One* 8. doi:10.1371/journal.pone.0082043.

Foster, T. M., Celton, J. M., Chagne, D., Tustin, D. S., and Gardiner, S. E. (2015). Two quantitative trait loci, Dw1 and Dw2, are primarily responsible for rootstock-induced dwarfing in apple. *Hortic. Res.* 2, 9. doi:10.1038/hortres.2015.1.

Foster, T. M., McAtee, P. A., Waite, C. N., Boldingh, H. L., and McGhie, T. K. (2017). Apple dwarfing rootstocks exhibit an imbalance in carbohydrate allocation and reduced cell growth and metabolism. *Hortic. Res.* 4. doi:10.1038/hortres.2017.9.

Foster, T. M., Watson, A. E., van Hooijdonk, B. M., and Schaffer, R. J. (2014). Key flowering genes including FT-like genes are upregulated in the vasculature of apple dwarfing rootstocks. *Tree Genet. Genomes* 10, 189–202. doi:10.1007/s11295-013-0675-z.

Frey, A., Effroy, D., Lefebvre, V., Seo, M., Perreau, F., Berger, A., et al. (2012). Epoxycarotenoid cleavage by NCED5 fine-tunes ABA accumulation and affects seed dormancy and drought tolerance with other NCED family members. *Plant J.* 70, 501–512. doi:10.1111/j.1365-313X.2011.04887.x.

Fridman, Y., and Savaldi-Goldstein, S. (2013). Brassinosteroids in growth control: How, when and where. *Plant Sci.* 209, 24–31. doi:10.1016/j.plantsci.2013.04.002.

Fu, J., Yu, H., Li, X., Xiao, J., and Wang, S. (2011). Rice GH3 gene family: Regulators of growth and development. *Plant Signal. Behav.* 6, 570–574. doi:10.4161/psb.6.4.14947.

Fyhrie, K., Prats-Llinàs, M. T., López, G., and DeJong, T. M. (2018). How does peach fruit set on sylleptic shoots borne on epicormics compare with fruit set on proleptic shoots ? *Eur. J. Hortic. Sci.* 83, 3–11. doi:https://doi.org/10.17660/eJHS.2018/83.1.1.

Gabriele, S., Rizza, A., Martone, J., Circelli, P., Costantino, P., and Vittorioso, P. (2010). The Dof protein DAG1 mediates PIL5 activity on seed germination by negatively regulating GA biosynthetic gene AtGA3ox1. *Plant J.* 61, 312–323. doi:10.1111/j.1365-313X.2009.04055.x.

Gallego-Bartolomé, J., Alabadí, D., and Blázquez, M. A. (2011). DELLA-induced early transcriptional changes during etiolated development in arabidopsis thaliana. *PLoS One* 6. doi:10.1371/journal.pone.0023918.

Gao, R., Wang, Y., Gruber, M. Y., and Hannoufa, A. (2018). MiR156/SPL10 modulates lateral root development, branching and leaf morphology in arabidopsis by silencing AGAMOUS-LIKE 79. *Front. Plant Sci.* 8, 1–12. doi:10.3389/fpls.2017.02226.

Gao, Y., He, C., Zhang, D., Liu, X., Xu, Z., Tian, Y., et al. (2017). Two trichome birefringence-like proteins mediate xylan acetylation, which is essential for leaf blight resistance in rice. *Plant Physiol.* 173, 470–481. doi:10.1104/pp.16.01618.

Gao, Y., Xu, Z., Zhang, L., Li, S., Wang, S., Yang, H., et al. (2020). MYB61 is regulated by GRF4 and promotes nitrogen utilization and biomass production in rice. *Nat. Commun.* 11, 1–12. doi:10.1038/s41467-020-19019-x.

Garapati, P., Feil, R., Lunn, J. E., Van Dijck, P., Balazadeh, S., and Mueller-Roeber, B. (2015). Transcription factor arabidopsis activating factor1 integrates carbon starvation responses with trehalosemetabolism. *Plant Physiol.* 169, 379–390. doi:10.1104/pp.15.00917.

Garrison, E., and Marth, G. (2012). Haplotype-based variant detection from short-read sequencing. arXiv:1207.3907 [Preprint]. Available at: https://arxiv.org/abs/1207.3907 (Accessed October 8, 2021).

Gaut, B. S., Miller, A. J., and Seymour, D. K. (2019). Living with Two Genomes: Grafting and Its Implications for Plant Genome-to-Genome Interactions, Phenotypic Variation, and Evolution. *Annu. Rev. Genet.* 53, 195-215. doi:10.1146/annurev-genet-112618-043545.

Gautier, A. T., Chambaud, C., Brocard, L., Ollat, N., Gambetta, G. A., Delrot, S., et al. (2019). Merging genotypes: Graft union formation and scion-rootstock interactions. *J. Exp. Bot.* 70, 805–815. doi:10.1093/jxb/ery422.

Gautier, A. T., Merlin, I., Doumas, P., Cochetel, N., Mollier, A., Vivin, P., et al. (2021). Identifying roles of the scion and the rootstock in regulating plant development and functioning under different phosphorus supplies in grapevine. *Environ. Exp. Bot.* 185, 104405. doi:10.1016/j.envexpbot.2021.104405.

Ge, C., Cui, X., Wang, Y., Hu, Y., Fu, Z., Zhang, D., et al. (2006). BUD2, encoding an S-adenosylmethionine decarboxylase, is required for Arabidopsis growth and development. *Cell Res.* 16, 446–456. doi:10.1038/sj.cr.7310056.

Génard, M., Pagès, L., and Kervella, K. (1994). Relationship between sylleptic branching and components of parent shoot development in the peach tree. *Ann. Bot.* 74, 465–470. doi: 10.1006/anbo.1994.1142.

Geng, P., Zhang, S., Liu, J., Zhao, C., Wu, J., Cao, Y., et al. (2020). MYB20, MYB42, MYB43, and MYB85 regulate phenylalanine and lignin biosynthesis during secondary cell wall formation. *Plant Physiol.* 182, 1272–1283. doi:10.1104/PP.19.01070.

Gerttula, S., Zinkgraf, M., Muday, G. K., Lewis, D. R., Ibatullin, F. M., Brumer, H., et al. (2015). Transcriptional and Hormonal Regulation of Gravitropism of Woody Stems in Populus. *Plant Cell*, tpc.15.00531. doi:10.1105/tpc.15.00531.

Gibbs, D. J., Voß, U., Harding, S. A., Fannon, J., Moody, L. A., Yamada, E., et al. (2014). AtMYB93 is a novel negative regulator of lateral root development in Arabidopsis. *New Phytol.* 203, 1194–1207. doi:10.1111/nph.12879.

Gómez, E. M., Buti, M., Sargent, D. J., Dicenta, F, and Ortega, E. (2019). Transcriptomic analysis of pollen-pistil interactions in almond (Prunus dulcis) identifies candidate genes for components of gametophytic self-incompatibility. *Tree Genet. Genomes* 15, 53. https://doi.org/10.1007/s11295-019-1360-7

Goonetilleke, S. N., March, T. J., Wirthensohn, M. G., Arus, P., Walker, A. R., and Mather, D.E. (2018). Genotyping by Sequencing in Almond: SNP Discovery, Linkage Mapping, and Marker Design. *G3 Genes, Genomes, Genetics*, 8 161–172. doi: 10.1534/g3.117.300376.

Gou, J., Strauss, S. H., Tsai, C. J., Fang, K., Chen, Y., Jiang, X., et al. (2010). Gibberellins regulate lateral root formation in Populus through interactions with auxin and other hormones. *Plant Cell* 22, 623–639. doi:10.1105/tpc.109.073239.

Gradziel, T. M. (2017). “History of cultivation” in Almonds: botany, production and uses, ed. R. Socias i Company, and T. M. Gradziel (CABI, Wallingford, UK), 43–71. doi:10.1079/9781780643540.0043.

Gradziel, T. M. (2012). The utilization of wild relatives of cultivated almond and peach in modifying tree architecture for crop improvement. *Acta Hortic.* 948, 271–278. doi: 10.17660/ActaHortic.2012.948.31.

Grantham, N. J., Wurman-Rodrich, J., Terrett, O. M., Lyczakowski, J. J., Stott, K., Iuga, D., et al. (2017). An even pattern of xylan substitution is critical for interaction with cellulose in plant cell walls. *Nat. Plants* 3, 859–865. doi:10.1038/s41477-017-0030-8.

Griffiths, J., Murase, K., Rieu, I., Zentella, R., Zhang, Z. L., Powers, S. J., et al. (2006). Genetic characterization and functional analysis of the GID1 gibberellin receptors in Arabidopsis. *Plant Cell* 18, 3399–3414. doi:10.1105/tpc.106.047415.

Groover, A. (2016). Gravitropisms and reaction woods of forest trees - evolution, functions and mechanisms. *New Phytol.* 211, 790–802. doi:10.1111/nph.13968.

Guédon, Y., Barthélémy, D., Caraglio, Y., and Costes, E. (2001). Pattern analysis in branching and axillary flowering sequences. *J. Theor. Biol.* 212, 481–520. doi:10.1006/jtbi.2001.2392.

Guilfoyle, T. J. (2015). The PB1 domain in auxin response factor and Aux/IAA proteins: a versatile protein interaction module in the auxin response. *Plant Cell* 27, 33–43. doi:10.1105/tpc.114.132753.

Guo, C., Wei, Y., Yang, B., Ayup, M., Li, N., Liu, J., et al. (2021). Developmental transcriptome profiling uncovered carbon signaling genes associated with almond fruit drop. *Sci. Rep.* 11, 1–12. doi:10.1038/s41598-020-69395-z.

Guo, J., Cao, K., Deng, C., Li, Y., Zhu, G., Fang, W., et al. (2020). An integrated peach genome structural variation map uncovers genes associated with fruit traits. *Genome Biol.* 21(1), 1–19. doi:10.1186/s13059-020-02169-y.

Guo, W. J., Nagy, R., Chen, H. Y., Pfrunder, S., Yu, Y. C., Santelia, D., et al. (2014). SWEET17, a facilitative transporter, mediates fructose transport across the tonoplast of arabidopsis roots and leaves. *Plant Physiol.* 164, 777–789. doi:10.1104/pp.113.232751.

Guseman, J. M., Webb, K., Srinivasan, C., and Dardick, C. (2017). DRO1 influences root system architecture in Arabidopsis and Prunus species. *Plant J.* 89, 1093–1105. doi:10.1111/tpj.13470.

Gusti, A., Baumberger, N., Nowack, M., Pusch, S., Eisler, H., Potuschak, T., et al. (2009). The Arabidopsis thaliana F-box protein FBL17 is essential for progression through the second mitosis during pollen development. *PLoS One* 4. doi:10.1371/journal.pone.0004780.

Ha, S., Vankova, R., Yamaguchi-Shinozaki, K., Shinozaki, K., and Tran, L. S. P. (2012). Cytokinins: Metabolism and function in plant adaptation to environmental stresses. *Trends Plant Sci.* 17, 172–179. doi:10.1016/j.tplants.2011.12.005.

Hallé, F. (2001). "Branching in Plants" in Branching in Nature, ed. V. Fleury, J. F. Gouyet, and M. Léonetti (Springer: Berlin/Heidelberg, Germany), 23–40. doi:10.1007/978-3-662-06162-6_2.

Hallé, F., Oldeman, R. A. A., and Tomlinson, P. B. (1978). "Forests and Vegetation" in Tropical Trees and Forests, ed. F. Hallé, R. A. A. Oldeman, and P. B. Tomlinson (Springer, Berlin, Heidelberg), 332–385. doi:10.1007/978-3-642-81190-6_5.

Hanzawa, Y., Takahashi, T., and Komeda, Y. (1997). ACL5: An Arabidopsis gene required for internodal elongation after flowering. *Plant J.* 12, 863–874. doi:10.1046/j.1365-313X.1997.12040863.x.

Hearn D. J. (2016). "Perennial Growth, Form and Architecture of Angiosperm Trees" in Comparative and Evolutionary Genomics of Angiosperm Trees. Plant Genetics and Genomics: Crops and Models, ed. A. Groover, and Q. Cronk (Springer, Chams), 21, 179–204. doi: 10.1007/7397_2016_25.

He, J., Zhao, H., Cheng, Z., Ke, Y., Liu, J., and Ma, H. (2019). Evolution analysis of the fasciclin-like arabinogalactan proteins in plants shows variable fasciclin-AGP domain constitutions. *Int. J. Mol. Sci.* 20. doi:10.3390/ijms20081945.

Hedden, P., and Thomas, S. G. (2012). Gibberellin biosynthesis and its regulation. *Biochem. J.* 444, 11–25. doi:10.1042/BJ20120245.

Heinrich, M., Hettenhausen, C., Lange, T., Wünsche, H., Fang, J., Baldwin, I.T., et al. (2013). High levels of jasmonic acid antagonize the biosynthesis of gibberellins and inhibit the growth of Nicotiana attenuata stems. *Plant J.* 73, 591–606. doi: 10.1111/tpj.12058.

Helfer, A., Nusinow, D. A., Chow, B. Y., Gehrke, A. R., Bulyk, M. L., and Kay, S. A. (2011). LUX ARRHYTHMO encodes a nighttime repressor of circadian gene expression in the Arabidopsis core clock. *Curr. Biol.* 21, 126–133. doi:10.1016/j.cub.2010.12.021.

Higo, K., Ugawa, Y., Iwamoto, M., and Korenaga, T. (1999). Plant cis-acting regulatory DNA elements (PLACE) database: 1999. *Nucleic Acids Res*. 27, 297–300. doi: 10.1093/nar/27.1.297.

Hill, J. L., and Hollender, C. A. (2019). Branching out: new insights into the genetic regulation of shoot architecture in trees. *Curr. Opin. Plant Biol.* 47, 73–80. doi:10.1016/j.pbi.2018.09.010.

Hinz, M., Wilson, I. W., Yang, J., Buerstenbinder, K., Llewellyn, D., Dennis, E. S., et al. (2010). Arabidopsis RAP2.2: An ethylene response transcription factor that is important for hypoxia survival. *Plant Physiol.* 153, 757–772. doi:10.1104/pp.110.155077.

Holalu, S. V., and Finlayson, S. A. (2017). The ratio of red light to far red light alters Arabidopsis axillary bud growth and abscisic acid signalling before stem auxin changes. *J. Exp. Bot.* 68, 943–952. doi:10.1093/jxb/erw479.

Hollender, C. A., and Dardick, C. (2015). Molecular basis of angiosperm tree architecture. *New Phytol.* 206, 541–556. doi: 10.1111/nph.13204.

Hollender, C. A., Hadiarto, T., Srinivasan, C., Scorza, R., and Dardick, C. (2016). A brachytic dwarfism trait (dw) in peach trees is caused by a nonsense mutation within the gibberellic acid receptor PpeGID1c. *New Phytol.* 210, 227–239. doi:10.1111/nph.13772.

Hollender, C. A., Hill, J. L., Waite, J., and Dardick, C. (2020). Opposing influences of TAC1 and LAZY1 on Lateral Shoot Orientation in Arabidopsis. *Sci. Rep.* 10, 1–13. doi:10.1038/s41598-020-62962-4.

Hollender, C. A., Waite, J. M., Tabb, A., Raines, D., Chinnithambi, S., and Dardick, C. (2018). Alteration of TAC1 expression in Prunus species leads to pleiotropic shoot phenotypes. *Hortic. Res.* 5, 1–9. doi:10.1038/s41438-018-0034-1.

Hosseinpour, B., Sepahvand, S., Aliabad, K. K., Bakhtiarizadeh, M., Imani, A., Assareh, R., et al. (2018). Transcriptome profiling of fully open flowers in a frost-tolerant almond genotype in response to freezing stress. *Mol. Genet. Genomics* 293, 151–163. doi: 10.1007/s00438-017-1371-8.

Hou, K., Wu, W., and Gan, S. S. (2013). SAUR36, a SMALL AUXIN UP RNA gene, is involved in the promotion of leaf senescence in arabidopsis. *Plant Physiol.* 161, 1002–1009. doi:10.1104/pp.112.212787.

Houben, M., and Van de Poel, B. (2019). 1-aminocyclopropane-1-carboxylic acid oxidase (ACO): The enzyme that makes the plant hormone ethylene. *Front. Plant Sci.* 10, 1–15. doi:10.3389/fpls.2019.00695.

Howard, T. P., Hayward, A. P., Tordillos, A., Fragoso, C., Moreno, M. A., Tohme, J., et al. (2014). Identification of the maize gravitropism gene lazy plant1 by a transposon-tagging genome resequencing strategy. *PLoS One* 9. doi: 10.1371/journal.pone.0087053

Huang, X., Ding, J., Effgen, S., Turck, F., and Koornneef, M. (2013). Multiple loci and genetic interactions involving flowering time genes regulate stem branching among natural variants of Arabidopsis. *New Phytol.* 199, 843–857. doi:10.1111/nph.12306.

Iglesias, I., Foles, P., and Oliveira, C. M. (2021). El cultivo del almendro en España y Portugal: Situación, innovación tecnológica, costes, rentabilidad y perspectivas. *Revista de Fruticultura*, 81, 6–49.

Ikeda, Y., Banno, H., Niu, Q. W., Howell, S. H., and Chua, N. H. (2006). The ENHANCER of SHOOT REGENERATION 2 gene in Arabidopsis regulates CUP-SHAPED COTYLEDON 1 at the transcriptional level and controls cotyledon development. *Plant Cell Physiol.* 47, 1443–1456. doi:10.1093/pcp/pcl023.

Inoue, K., Araki, T., and Endo, M. (2018). Circadian clock during plant development. *J. Plant Res.* 131, 59–66. doi:10.1007/s10265-017-0991-8.

Ischebeck, T., Werner, S., Krishnamoorthy, P., Lerche, J., Meijón, M., Stenzel, I., et al. (2013). Phosphatidylinositol 4,5-bisphosphate influences PIN polarization by controlling clathrin-mediated membrane trafficking in Arabidopsis. *Plant Cell* 25, 4894–4911. doi:10.1105/tpc.113.116582.

Jensen, M. K., Lindemose, S., Masi, F. de, Reimer, J. J., Nielsen, M., Perera, V., et al. (2013). ATAF1 transcription factor directly regulates abscisic acid biosynthetic gene NCED3 in Arabidopsis thaliana. *FEBS Open Bio* 3, 321–327. doi:10.1016/j.fob.2013.07.006.

Jiang, L., Matthys, C., Marquez-Garcia, B., De Cuyper, C., Smet, L., De Keyser, A., et al. (2016). Strigolactones spatially influence lateral root development through the cytokinin signaling network. *J. Exp. Bot.* 67, 379–389. doi:10.1093/jxb/erv478.

Jiang, P., Wang, S., Zheng, H., Li, H., Zhang, F., Su, Y., et al. (2018). SIP1 participates in regulation of flowering time in rice by recruiting OsTrx1 to Ehd1. *New Phytol.* 219, 422–435. doi:10.1111/nph.15122.

Jiao, Y., Wang, Y., Xue, D., Wang, J., Yan, M., Liu, G., et al. (2010). Regulation of OsSPL14 by OsmiR156 defines ideal plant architecture in rice. *Nat. Genet.* 42, 541–544. doi:10.1038/ng.591.

Jing, H., and Strader, L. C. (2019). Interplay of auxin and cytokinin in lateral root development. *Int. J. Mol. Sci.* 20. doi:10.3390/ijms20030486.

Johannesson, H., Wang, Y., Hanson, J., and Engström, P. (2003). The Arabidopsis thaliana homeobox gene ATHB5 is a potential regulator of abscisic acid responsiveness in developing seedlings. *Plant Mol. Biol.* 51, 719–729. doi:10.1023/A:1022567625228.

Jones, M. A., Morohashi, K., Grotewold, E., and Harmer, S. L. (2019). Arabidopsis JMJD5/JMJ30 acts independently of LUX ARRHYTHMO within the plant circadian clock to enable temperature compensation. *Front. Plant Sci.* 10, 1–12. doi:10.3389/fpls.2019.00057.

Jong, M. De, Ongaro, V., and Ljung, K. (2014). Auxin and Strigolactone Signaling are Required for Modulation of Arabidopsis Shoot Branching by Nitrogen Supply. *Plant Physiol.* 166, 384–395. doi:10.1104/pp.114.242388.

Jung, S., Lee, T., Cheng, C. H., Buble, K., Zheng, P., Yu, J., et al. (2019). 15 years of GDR: New data and functionality in the Genome Database for Rosaceae. *Nucleic Acids Res*. 47, D1137–D1145. doi:10.1093/nar/gky1000.

Jurado, S., Abraham, Z., Manzano, C., López-Torrejón, G., Pacios, L. F., and del Pozo, C. (2010). The arabidopsis cell cycle F-Box protein SKP2A binds to auxin. *Plant Cell* 22, 3891–3904. doi:10.1105/tpc.110.078972.

Jurado, S., Díaz-Triviño, S., Abraham, Z., Manzano, C., Gutierrez, C., and del Pozo, C. (2008). SKP2A, an F-box protein that regulates cell division, is degraded via the ubiquitin pathway. *Plant J.* 53, 828–841. doi:10.1111/j.1365-313X.2007.03378.x.

Kaneda, M., Schuetz, M., Lin, B. S. P., Chanis, C., Hamberger, B., Western, T. L., et al. (2011). ABC transporters coordinately expressed during lignification of Arabidopsis stems include a set of ABCBs associated with auxin transport. *J. Exp. Bot.* 62, 2063–2077. doi:10.1093/jxb/erq416.

Kang, M. J., Jin, H. S., Noh, Y. S., and Noh, B. (2015). Repression of flowering under a noninductive photoperiod by the HDA9-AGL19-FT module in Arabidopsis. *New Phytol.* 206, 281–294. doi:10.1111/nph.13161.

Kaplan-Levy, R. N., Brewer, P. B., Quon, T., and Smyth, D.R. (2012). The trihelix family of transcription factors–light, stress and development. *Trends Plant Sci.* 17, 163-171. doi: 10.1016/j.tplants.2011.12.002.

Kazan, K., and Manners, J. M. (2013). MYC2: The master in action. *Mol. Plant* 6, 686–703. doi:10.1093/mp/sss128.

Keuskamp, D. H., Pollmann, S., Voesenek, L. A. C. J., Peeters, A. J. M., and Pierik, R. (2010). Auxin transport through PIN-FORMED 3 (PIN3) controls shade avoidance and fitness during competition. *Proc. Natl. Acad. Sci. U. S. A.* 107, 22740–22744. doi:10.1073/pnas.1013457108.

Kieber, J. J., and Schaller, G. E. (2018). Cytokinin signaling in plant development. *Development* 145, 1–7. doi:10.1242/dev.149344.

Kim, D., Pertea, G., Trapnell, C., Pimentel, H., Kelley, H., and Salzberg, S.L. (2013). TopHat2: accurate alignment of transcriptomes in the presence of insertions, deletions and gene fusions. *Genome Biol.* 14, R36. doi: 10.1186/gb-2013-14-4-r36

Kim, S. J., Chandrasekar, B., Rea, A. C., Danhof, L., Zemelis-Durfee, S., Thrower, N., et al. (2020). The synthesis of xyloglucan, an abundant plant cell wall polysaccharide, requires CSLC function. *Proc. Natl. Acad. Sci. U. S. A.* 117, 20316–20324. doi:10.1073/PNAS.2007245117.

Kim, W., Latrasse, D., Servet, C., and Zhou, D. X. (2013). Arabidopsis histone deacetylase HDA9 regulates flowering time through repression of AGL19. *Biochem. Biophys. Res. Commun.* 432, 394–398. doi:10.1016/j.bbrc.2012.11.102.

Kleine-Vehn, J., Leitner, J., Zwiewka, M., Sauer, M., Abas, L., Luschnig, C., et al. (2008). Differential degradation of PIN2 auxin efflux carrier by retromer-dependent vacuolar targeting. *Proc. Natl. Acad. Sci. U. S. A.* 105, 17812–17817. doi:10.1073/pnas.0808073105.

Klepikova, A. V., Kasianov, A. S., Gerasimov, E. S., Logacheva, M. D., and Penin, A. A. (2016). A high resolution map of the Arabidopsis thaliana developmental transcriptome based on RNA-seq profiling. *Plant J.* 88, 1058–1070. doi:10.1111/tpj.13312.

Kohorn, B. D., Kohorn, S. L., Saba, N. J., and Martinez, V. M. (2014). Requirement for pectin methyl esterase and preference for fragmented over native pectins for wall-associated kinase-activated, EDS1/PAD4-dependent stress response in arabidopsis. *J. Biol. Chem.* 289, 18978–18986. doi:10.1074/jbc.M114.567545.

Kole, C. (2011). Wild crop relatives: Genomic and breeding resources: Temperate fruits. Springer-Verlag Berlin Heidelberg. doi:10.1007/978-3-642-16057-8.

Kolesnikov, Y. S., Kretynin, S. V., Volotovsky, I. D., Kordyum, E. L., Ruelland, E., and Kravets, V. S. (2016). Molecular mechanisms of gravity perception and signal transduction in plants. *Protoplasma* 253, 1005. doi:10.1007/s00709-015-0934-y.

Köllmer, I., Novák, O., Strnad, M., Schmülling, T., and Werner, T. (2014). Overexpression of the cytosolic cytokinin oxidase/dehydrogenase (CKX7) from Arabidopsis causes specific changes in root growth and xylem differentiation. *Plant J.* 78, 359–371. doi:10.1111/tpj.12477.

Koltai, H. (2011). Strigolactones are regulators of root development. *New Phytol.* 190, 545–549. doi:10.1111/j.1469-8137.2011.03678.x.

Korasick, D. A., Enders, T. A., and Strader, L. C. (2013). Auxin biosynthesis and storage forms. *J. Exp. Bot.* 64, 2541–2555. doi:10.1093/jxb/ert080.

Krouk, G., Lacombe, B., Bielach, A., Perrine-Walker, F., Malinska, K., Mounier, E., et al. (2010). Nitrate-regulated auxin transport by NRT1.1 defines a mechanism for nutrient sensing in plants. *Dev. Cell* 18, 927–937. doi:10.1016/j.devcel.2010.05.008.

Krouk, G., Ruffel, S., Gutiérrez, R. A., Gojon, A., Crawford, N. M., Coruzzi, G. M., et al. (2011). A framework integrating plant growth with hormones and nutrients. *Trends Plant Sci.* 16, 178–182. doi:10.1016/j.tplants.2011.02.004.

Kudo, H., and Harada, T. (2007). A graft-transmissible RNA from tomato rootstock changes leaf morphology of potato scion. *HortScience* 42, 225–226. doi:10.21273/hortsci.42.2.225.

Kumar, S., Stecher, G., Li, M., Knyaz, C., and Tamura, K. (2018). MEGA X: Molecular evolutionary genetics analysis across computing platforms. *Mol. Biol. Evol.* 35, 1547–1549. doi: 10.1093/molbev/msy096.

Langfelder, P., and Horvath, S. (2008). WGCNA: An R package for weighted correlation network analysis. *BMC Bioinformatics* 9. doi:10.1186/1471-2105-9-559.

Langmead, B., and Salzberg, S. L. (2012). Fast gapped-read alignment with Bowtie 2. *Nat. Methods* 9, 357–9. doi: 10.1038/nmeth.1923.

Langmead, B., Trapnell, C., Pop, M., and Salzberg, S. L. (2009). Ultrafast and memory-efficient alignment of short DNA sequences to the human genome. *Genome Biol*. 10, 1-10. doi: 10.1186/gb-2009-10-3-r25.

Ledger, S., Strayer, C., Ashton, F., Kay, S. A., and Putterill, J. (2001). Analysis of the function of two circadian-regulated CONSTANS-LIKE genes. *Plant J.* 26, 15–22. doi:10.1046/j.1365-313X.2001.01003.x.

Leitz, G., Kang, B. H., and Schoenwaelder, M. E. A. (2009). Statolith sedimentation kinetics and force transduction to the cortical endoplasmic reticulum in gravity-sensing Arabidopsis columella cells. *Plant Cell* 21, 843–860. doi: 10.1105/tpc.108.065052.

Lescot, M., Dehais, P., Thijs, G., Marchal, K., Moreau, Y., Van De Peer, Y., et al. (2002). PlantCARE, a database of plant cis-acting regulatory elements and a portal to tools for in silico analysis of promoter sequences. *Nucleic Acids Res*. 30, 325–7. doi: 10.1093/nar/30.1.325.

Levy, S. E., and Boone, B. E. (2019). Next-Generation Sequencing Strategies. *Cold Spring Harb. Perspect. Med.* 9, a025791. doi:10.1101/cshperspect.a025791.

Lewis, D. R., Negi, S., Sukumar, P., and Muday, G. K. (2011). Ethylene inhibits lateral root development, increases IAA transport and expression of PIN3 and PIN7 auxin efflux carriers. *Development* 138, 3485–3495. doi:10.1242/dev.065102.

Leyser, O. (2017). Auxin Signaling. *Plant Physiol.* 176, 465–479. doi:10.1104/pp.17.00765.

Li, G., Ma, J., Tan, M., Mao, J., An, N., Sha, G., et al. (2016). Transcriptome analysis reveals the effects of sugar metabolism and auxin and cytokinin signaling pathways on root growth and development of grafted apple. *BMC Genomics* 17, 1–17. doi:10.1186/s12864-016-2484-x.

Li, J., Chen, F., Li, Y., Li, P., Wang, Y., Mi, G., et al. (2019). ZmRAP2.7, an AP2 transcription factor, is involved in maize brace roots development. *Front. Plant Sci.* 10, 1–11. doi:10.3389/fpls.2019.00820.

Li, P., Wang, Y., Qian, Q., Fu, Z., Wang, M., Zeng, D., et al. (2007). LAZY1 controls rice shoot gravitropism through regulating polar auxin transport. *Cell. Res.* 17, 402–410. doi: 10.1038/cr.2007.38.

Li, T., Lei, W., He, R., Tang, X., Han, J., Zou, L., et al. (2020). Brassinosteroids regulate root meristem development by mediating BIN2-UPB1 module in Arabidopsis. *PLoS Genet.* 16, 1–27. doi:10.1371/journal.pgen.1008883.

Li, X., Chen, T., Li, Y., Wang, Z., Cao, H., Chen, F., et al. (2019). ETR1/RDO3 regulates seed dormancy by relieving the inhibitory effect of the ERF12-TPL complex on DELAY OF GERMINATION1 expression. *Plant Cell* 31, 832–847. doi:10.1105/tpc.18.00449.

Li, Y., Cao, K., Li, N., Zhu, G., Fang, W., Chen, C., et al. (2021). Genomic analyses provide insights into peach local adaptation and responses to climate change. *Genome Res.* 31, 592–606. doi:10.1101/GR.261032.120.

Liao, Y., Smyth, G. K., and Shi, W. (2014). FeatureCounts: An efficient general purpose program for assigning sequence reads to genomic features. *Bioinformatics* 30, 923–930. doi:10.1093/bioinformatics/btt656.

Liu, B., Zhao, S., Li, P., Yin, Y., Niu, Q., Yan, J., et al. (2021). Plant buffering against the high-light stress-induced accumulation of CsGA2ox8 transcripts via alternative splicing to finely tune gibberellin levels and maintain hypocotyl elongation. *Hortic. Res.* 8, 1–10. doi:10.1038/s41438-020-00430-w.

Liu, E., MacMillan, C. P., Shafee, T., Ma, Y., Ratcliffe, J., van de Meene, A., et al. (2020). Fasciclin-Like Arabinogalactan-Protein 16 (FLA16) Is Required for Stem Development in Arabidopsis. *Front. Plant Sci.* 11, 1–16. doi:10.3389/fpls.2020.615392.

Liu, H., Guo, Z., Gu, F., Ke, S., Sun, D., Dong, S., et al. (2017). 4-Coumarate-CoA ligase-like gene OsAAE3 negatively mediates the rice blast resistance, floret development and lignin biosynthesis. *Front. Plant Sci.* 7, 1–13. doi:10.3389/fpls.2016.02041.

Liu, J., Moore, S., Chen, C., and Lindsey, K. (2017). Crosstalk Complexities between Auxin, Cytokinin, and Ethylene in Arabidopsis Root Development: From Experiments to Systems Modeling, and Back Again. *Mol. Plant* 10, 1480–1496. doi:10.1016/j.molp.2017.11.002.

Liu, Q., Luo, L., and Zheng, L. (2018). Lignins: Biosynthesis and biological functions in plants. *Int. J. Mol. Sci.* 19, 335. doi:10.3390/ijms19020335.

Liu, R., Holik, A. Z., Su, S., Jansz, N., Chen, K., Leong, H. S., et al. (2015). Why weight? Modelling sample and observational level variability improves power in RNA-seq analyses. *Nucleic Acids Res.* 43, e97. doi:10.1093/nar/gkv412.

Liu, W., Xiang, C., Li, X., Wang, T., Lu, X., Liu, Z., et al. (2020b). Identification of long-distance transmissible mrna between scion and rootstock in cucurbit seedling heterografts. *Int. J. Mol. Sci.* 21, 1–22. doi:10.3390/ijms21155253.

Liu, X. Y., Li, J., Liu, M. M., Yao, Q., and Chen, J. Z. (2017). Transcriptome profiling to understand the effect of citrus rootstocks on the growth of "Shatangju" mandarin. *PLoS One* 12, 1–22. doi:10.1371/journal.pone.0169897.

Liu, Y. B., Lu, S. M., Zhang, J. F., Liu, S., and Lu, Y. T. (2007). A xyloglucan endotransglucosylase/hydrolase involves in growth of primary root and alters the deposition of cellulose in Arabidopsis. *Planta* 226, 1547–1560. doi:10.1007/s00425-007-0591-2.

Liu, Y., Li, X., Ma, D., Chen, Z., Wang, J., and Liu, H. (2018). CIB1 and CO interact to mediate CRY 2-dependent regulation of flowering. *EMBO Rep.* 19, 1–10. doi:10.15252/embr.201845762.

Liu, Y., Sun, J., and Wu, Y. (2016). Arabidopsis ATAF1 enhances the tolerance to salt stress and ABA in transgenic rice. *J. Plant Res.* 129, 955–962. doi:10.1007/s10265-016-0833-0.

Lo, S. F., Yang, S. Y., Chen, K. T., Hsing, Y. I., Zeevaart, J. A. D., Chen, L. J., et al. (2008). A novel class of gibberellin 2-oxidases control semidwarfism, tillering, and root development in rice. *Plant Cell* 20, 2603–2618. doi:10.1105/tpc.108.060913.

López-Hinojosa, M., de María, N., Guevara, M. A., Vélez, M. D., Cabezas, J. A., Díaz, L. M., et al. (2021). Rootstock effects on scion gene expression in maritime pine. *Sci. Rep.* 11, 1–16. doi:10.1038/s41598-021-90672-y.

Loqué, D., Ludewig, U., Yuan, L., and Von Wirén, N. (2005). Tonoplast intrinsic proteins AtTIP2;1 and AtTIP2;3 facilitate NH 3 transport into the vacuole. *Plant Physiol.* 137, 671–680. doi:10.1104/pp.104.051268.

Lordan, J., Zazurca, L., Maldonado, M., Torguet, L., Alegre, S., and Miarnau, X. (2019). Horticultural performance of 'Marinada' and 'Vairo' almond cultivars grown on a genetically diverse set of rootstocks. *Sci. Hortic.* 256, 108558. doi:10.1016/j.scienta.2019.108558.

Lu, Z., Yu, H., Xiong, G., Wang, J., Jiao, Y., Liu, G., et al. (2013). Genome-wide binding analysis of the transcription activator IDEAL PLANT ARCHITECTURE1 reveals a complex network regulating rice plant architecture. *Plant Cell* 25, 3743–3759. doi:10.1105/tpc.113.113639.

Luo, J., Zhou, J. J., and Zhang, J.Z. (2018). Aux/IAA gene family in plants: Molecular structure, regulation, and function. *Int. J. Mol. Sci.* 19, 1–17. doi: 10.3390/ijms19010259.

Luo, X. M., Lin, W. H., Zhu, S., Zhu, J. Y., Sun, Y., Fan, X. Y., et al. (2010). Integration of Light- and Brassinosteroid-Signaling Pathways by a GATA Transcription Factor in Arabidopsis. *Dev. Cell* 19, 872–883. doi:10.1016/j.devcel.2010.10.023.

Ma, J., Hanssen, M., Lundgren, K., Hernández, L., Delatte, T., Ehlert, A., et al. (2011). The sucrose-regulated Arabidopsis transcription factor bZIP11 reprograms metabolism and regulates trehalose metabolism. *New Phytol.* 191, 733–745. doi:10.1111/j.1469-8137.2011.03735.x.

Ma, Y., Xue, H., Zhang, L., Zhang, F., Ou, C., Wang, F., et al. (2016). Involvement of Auxin and Brassinosteroid in Dwarfism of Autotetraploid Apple (Malus × domestica). *Sci. Rep.* 6, 1–14. doi:10.1038/srep26719.

Maier, A. T., Stehling-Sun, S., Offenburger, S. L., and Lohmann, J. U. (2011). The bZIP transcription factor PERIANTHIA: A multifunctional hub for meristem control. *Front. Plant Sci.* 2, 1–17. doi:10.3389/fpls.2011.00079.

Márquez, G., Alarcón, M. V., and Salguero, J. (2019). Cytokinin Inhibits Lateral Root Development at the Earliest Stages of Lateral Root Primordium Initiation in Maize Primary Root. *J. Plant Growth Regul.* 38, 83–92. doi:10.1007/s00344-018-9811-1.

Martínez-Ballesta, M. C., Alcaraz-López, C., Muries, B., Mota-Cadenas, C., and Carvajal, M. (2010). Physiological aspects of rootstock-scion interactions. *Sci. Hortic.* 127, 112–118. doi:10.1016/j.scienta.2010.08.002.

Mas-Gómez, J., Cantín, C. M., Moreno, M., Prudencio, Á. S., Gómez-Abajo, M., Bianco, L., et al. (2021). Exploring genome-wide diversity in the national peach (Prunus persica) germplasm collection at cita (zaragoza, Spain). *Agronomy* 11. doi:10.3390/agronomy11030481.

Mason, M. G., Ross, J. J., Babst, B. A., Wienclaw, B. N., and Beveridge, C. A. (2014). Sugar demand, not auxin, is the initial regulator of apical dominance. *Proc. Natl. Acad. Sci. U. S. A.* 111, 6092–6097. doi:10.1073/pnas.1322045111.

Matsubara, K., Yamanouchi, U., Wang, Z. X., Minobe, Y., Izawa, T., and Yano, M. (2008). Ehd2, a rice ortholog of the maize Indeterminate1 gene, promotes flowering by up-regulating Ehd1. *Plant Physiol.* 148, 1425–1435. doi:10.1104/pp.108.125542.

Meents, M. J., Watanabe, Y., and Samuels, A. L. (2018). The cell biology of secondary cell wall biosynthesis. *Ann. Bot.* 121, 1107–1125. doi:10.1093/aob/mcy005.

Meisel, L., Fonseca, B., González, S., Baeza-Yates, R., Cambiazo, V., Campos, R., et al. (2005). A rapid and efficient method for purifying high quality total RNA from peaches (Prunus persica) for functional genomics analyses. *Biol. Res*. 38, 83–8. doi: 10.4067/S0716-97602005000100010.

Melnyk, C. W., Gabel, A., Hardcastle, T. J., Robinson, S., Miyashima, S., Grosse, I., et al. (2018). Transcriptome dynamics at *Arabidopsis* graft junctions reveal an intertissue recognition mechanism that activates vascular regeneration. *Proc. Natl. Acad. Sci. U. S. A.* 115, E2447–E2456. doi:10.1073/pnas.1718263115.

Migault, V., Pallas, B., and Costes, E. (2017). Combining Genome-Wide Information with a Functional Structural Plant Model to Simulate 1-Year-Old Apple Tree Architecture. *Front. Plant Sci.* 7, 1–14. doi:10.3389/fpls.2016.02065.

Ministerio de Agricultura, Pesca y Alimentación. (2021). Superficies y producciones anuales de cultivos. https://www.mapa.gob.es/es/estadistica/temas/estadisticas-agrarias/agricultura/superficies-producciones-anuales-cultivos/ [Accessed October 8, 2021].

Miura, K., Ikeda, M., Matsubara, A., Song, X. J., Ito, M., Asano, K., et al. (2010). OsSPL14 promotes panicle branching and higher grain productivity in rice. *Nat. Genet.* 42, 545–549. doi:10.1038/ng.592.

Molas, M. L., and Kiss, J. Z. (2009). Phototropism and Gravitropism in Plants. *Adv. Bot. Res.* 49, 1–34. doi:10.1016/S0065-2296(08)00601-0.

Montesinos, Á., Dardick, C., Rubio-Cabetas, M. J., and Grimplet, J. (2021a). Polymorphisms and gene expression in the almond IGT family are not correlated to variability in growth habit

in major commercial almond cultivars. *PLoS One* 16, 1–20. doi:10.1371/journal.pone.0252001.

Montesinos, Á., Thorp, G., Grimplet, J., and Rubio-Cabetas, M. (2021b). Phenotyping Almond Orchards for Architectural Traits Influenced by Rootstock Choice. *Horticulturae* 7, 159. doi:10.3390/horticulturae7070159.

Moraes, T. S., Dornelas, M. C., and Martinelli, A. P. (2019). FT/TFL1: Calibrating plant architecture. *Front. Plant Sci.* 10, 97. doi:10.3389/fpls.2019.00097.

Moreno-Gracia, B., Laya, D., Rubio-Cabetas, M. J., and Sanz-García, M. Á. (2021). Study of Phenolic Compounds and Antioxidant Capacity of Spanish Almonds. *Foods* 10, 2334. doi: 10.3390/foods10102334.

Morita, M. T., Sakaguchi, K., Kiyose, S. I., Taira, K., Kato, T., Nakamura, M., et al. (2006). A C2H2-type zinc finger protein, SGR5, is involved in early events of gravitropism in Arabidopsis inflorescence stems. *Plant J.* 47, 619–628. doi:10.1111/j.1365-313X.2006.02807.x.

Mortimer, J. C., Faria-Blanc, N., Yu, X., Tryfona, T., Sorieul, M., Ng, Y. Z., et al. (2015). An unusual xylan in Arabidopsis primary cell walls is synthesised by GUX3, IRX9L, IRX10L and IRX14. *Plant J.* 83, 413–426. doi:10.1111/tpj.12898.

Motte, H., Vanneste, S., and Beeckman, T. (2019). Molecular and environmental regulation of root development. *Annu. Rev. Plant Biol.* 70, 465–488. doi: 10.1146/annurev-arplant-050718-100423.

Mudge, K., Janick, J., Scofield, S., and Goldschmidt, E. E. (2009). A History of Grafting. *Am. Soc. Hortic. Sci.*. 35, 437–493. doi:10.1002/9780470593776.ch9.

Muñoz, M., and Calderini, D. F. (2015). Volume, water content, epidermal cell area, and XTH5 expression in growing grains of wheat across ploidy levels. *F. Crop. Res.* 173, 30–40. doi:10.1016/j.fcr.2014.12.010.

Murphy, E., Vu, L. D., Van Den Broeck, L., Lin, Z., Ramakrishna, P., Van De Cotte, B., et al. (2016). RALFL34 regulates formative cell divisions in Arabidopsis pericycle during lateral root initiation. *J. Exp. Bot.* 67, 4863–4875. doi:10.1093/jxb/erw281.

Nahirñak, V., Almasia, N. I., Fernandez, P. V., Hopp, H. E., Estevez, J. M., Carrari, F., et al. (2012). Potato Snakin-1 gene silencing affects cell division, primary metabolism, and cell wall composition. *Plant Physiol.* 158, 252–263. doi:10.1104/pp.111.186544.

Nahirñak, V., Rivarola, M., Almasia, N. I., Barón, M. P. B., Hopp, H. E., Vile, D., et al. (2019). Snakin-1 affects reactive oxygen species and ascorbic acid levels and hormone balance in potato. *PLoS One* 14, 1–18. doi:10.1371/journal.pone.0214165.

Nakamura, M., Nishimura, T., and Morita, M. T. (2019). Bridging the gap between amyloplasts and directional auxin transport in plant gravitropism. *Curr. Opin. Plant Biol.* 52, 54–60. doi:10.1016/j.pbi.2019.07.005.

Nakano, T., Suzuki, K., Fujimura, T., Shinshi, H. (2006). Genome-wide analysis of the ERF gene family in Arabidopsis and rice. *Plant Physiol.* 140, 411–432. doi: 10.1104/pp.105.073783.

Napoli, C. (1996). Highly branched phenotype of the petunia dad1-1 mutant is reversed by grafting. *Plant Physiol.* 111, 27–37. doi:10.1104/pp.111.1.27.

Naramoto, S., and Kyozuka, J. (2018). ARF GTPase machinery at the plasma membrane regulates auxin transport-mediated plant growth. *Plant Biotechnol.* 35, 155–159. doi:10.5511/plantbiotechnology.18.0312a.

Neff, M. M., Nguyen, S. M., Malancharuvil, E. J., Fujioka, S., Noguchi, T., Seto, H., et al. (1999). Bas1: A gene regulating brassinosteroid levels and light responsiveness in Arabidopsis. *Proc. Natl. Acad. Sci. U. S. A.* 96, 15316–15323. doi:10.1073/pnas.96.26.15316.

Negrón, C., Contador, L., Lampinen, B. D., Metcalf, S. G., Dejong, T. M., Guédon, Y., et al. (2013). Systematic Analysis of Branching Patterns of Three Almond Cultivars with Different Tree Architectures. *J. Am. Soc. Hortic. Sci.* 138, 407–415.

Negrón, C., Contador, L., Lampinen, B. D., Metcalf, S. G., Guédon, Y., Costes, E., et al. (2014a). Differences in proleptic and epicormic shoot structures in relation to water deficit and growth rate in almond trees (Prunus dulcis). *Ann. Bot.* 113, 545–554. doi:10.1093/aob/mct282.

Negrón, C., Contador, L., Lampinen, B. D., Metcalf, S. G., Guédon, Y., Costes, E., et al. (2014b). How different pruning severities alter shoot structure: A modelling approach in young "Nonpareil" almond trees. *Funct. Plant Biol.* 42, 325–335. doi:10.1071/FP14025.

Neil Emery, R. J., and Kisiala, A. (2020). The roles of cytokinins in plants and their response to environmental stimuli. *Plants* 9, 1–4. doi:10.3390/plants9091158.

Noir, S., Marrocco, K., Masoud, K., Thomann, A., Gusti, A., Bitrian, M., et al. (2015). The control of arabidopsis thaliana growth by cell proliferation and endoreplication requires the F-box protein FBL17. *Plant Cell* 27, 1461–1476. doi:10.1105/tpc.114.135301.

Notredame, C., Higgins, D. G., and Heringa, J. (2000). T-Coffee: A novel method for fast and accurate multiple sequence alignment. *J. Mol. Bio.* 302, 205-217. doi: 10.1006/jmbi.2000.4042.

Ogawa, M., Hanada, A., Yamauchi, Y., Kuwahara, A., Kamiya, Y., and Yamaguchi, S. (2003). Gibberellin biosynthesis and response during Arabidopsis seed germination. *Plant Cell* 15, 1591–1604. doi:10.1105/tpc.011650.

Ohman, D., Demedts, B., Kumar, M., Gerber, L., Gorzsas, A., Goeminne, G., et al. (2013). MYB103 is required for FERULATE-5-HYDROXYLASE expression and syringyl lignin biosynthesis in Arabidopsis stems. *Plant J.* 73, 63–76. doi:10.1111/tpj.12018.

Okushima, Y., Mitina, I., Quach, H. L., and Theologis, A. (2005). AUXIN RESPONSE FACTOR 2 (ARF2): A pleiotropic developmental regulator. *Plant J.* 43, 29–46. doi:10.1111/j.1365-313X.2005.02426.x.

Onai, K., and Ishiura, M. (2005). PHYTOCLOCK 1 encoding a novel GARP protein essential for the Arabidopsis circadian clock. *Genes to Cells* 10, 963–972. doi:10.1111/j.1365-2443.2005.00892.x.

Otulak-Kozieł, K., Kozieł, E., Lockhart, B. E., and Bujarski, J. J. (2020). The expression of potato expansin A3 (StEXPA3) and extensin4 (StEXT4) genes with distribution of StEXPAs and HRGPs-extensin changes as an effect of cell wall rebuilding in two types of PVYNTN–Solanum tuberosum interactions. *Viruses* 12, 66. doi: 10.3390/v12010066.

Ou, C., Jiang, S., Wang, F., Tang, C., and Hao, N. (2015). An RNA-Seq analysis of the pear (Pyrus communis L.) transcriptome, with a focus on genes associated with dwarf. *Plant Gene* 4, 69–77. doi:10.1016/j.plgene.2015.08.003.

Overvoorde, P., Fukaki, H., and Beeckman, T. (2010). Auxin control of root development. *Cold Spring Harb. Perspect. Biol.* 2, a001537. doi:10.1101/cshperspect.a001537.

Papdi, C., Pérez-Salamõ, I., Joseph, M. P., Giuntoli, B., Bögre, L., Koncz, C., et al. (2015). The low oxygen, oxidative and osmotic stress responses synergistically act through the ethylene response factor VII genes RAP2.12, RAP2.2 and RAP2.3. *Plant J.* 82, 772–784. doi:10.1111/tpj.12848.

Park, J., Lee, Y., Martinoia, E., and Geisler, M. (2017). Plant hormone transporters: What we know and what we would like to know. *BMC Biol.* 15, 1–15. doi:10.1186/s12915-017-0443-x.

Park, S., Szumlanski, A. L., Gu, F., Guo, F., and Nielsen, E. (2011). A role for CSLD3 during cell-wall synthesis in apical plasma membranes of tip-growing root-hair cells. *Nat. Cell Biol.* 13, 973–980. doi:10.1038/ncb2294.

Park, Y. B., and Cosgrove, D. J. (2015). Xyloglucan and its interactions with other components of the growing cell wall. *Plant Cell Physiol.* 56, 180–194. doi:10.1093/pcp/pcu204.

Pavan, S., Delvento, C., Mazzeo, R., Ricciardi, F., Losciale, P., Gaeta, L., et al. (2021). Almond diversity and homozygosity define structure, kinship, inbreeding, and linkage disequilibrium in cultivated germplasm, and reveal genomic associations with nut and seed weight. *Hortic. Res.* 8, 1–12. doi:10.1038/s41438-020-00447-1.

Pereira-Netto, A. B., Roessner, U., Fujioka, S., Bacic, A., Asami, T., Yoshida, S., et al. (2009). Shooting control by brassinosteroids: Metabolomic analysis and effect of brassinazole on Malus prunifolia, the Marubakaido apple rootstock. *Tree Physiol.* 29, 607–620. doi:10.1093/treephys/tpn052.

Petersson, S. V., Johansson, A. I., Kowalczyk, M., Makoveychuk, A., Wang, J. Y., Moritz, T., et al. (2009). An auxin gradient and maximum in the arabidopsis root apex shown by high-resolution cell-specific analysis of IAA distribution and synthesis. *Plant Cell* 21, 1659–1668. doi:10.1105/tpc.109.066480.

Pierdonati, E., Unterholzner, S. J., Salvi, E., Svolacchia, N., Bertolotti, G., Dello Ioio, R., et al. (2019). Cytokinin-dependent control of GH3 group II family genes in the arabidopsis root. *Plants* 8, 1–9. doi:10.3390/plants8040094.

Pina, A., Cookson, S. J., Calatayud, A., Trinchera, A., and Errea, P. (2017). "Physiological and Molecular Mechanisms Underlying Graft Compatibility" in Vegetable grafting: principles and practices, ed. G., Colla, G., F. Pérez-Alfocea, and D. Schwarz (CABI, Croydon, London, UK), 132–154. doi:10.1079/9781780648972.0000.

Pin, P. A., and Nilsson, O. (2012). The multifaceted roles of FLOWERING LOCUS T in plant development. *Plant Cell Environ.* 35, 1742–1755. doi:10.1111/j.1365-3040.2012.02558.x.

Pinochet, J. (2010). "Replantpac" (Rootpac R), a plum-almond hybrid rootstock for replant situations. *HortScience* 45, 299–301. doi:10.21273/hortsci.45.2.299.

Pohlert, T. (2014). The pairwise multiple comparison of mean ranks package (PMCMR). *R package*, 27, 9.

Portis, A. R., Li, C., Wang, D., and Salvucci, M. E. (2008). Regulation of Rubisco activase and its interaction with Rubisco. *J. Exp. Bot.* 59, 1597–1604. doi:10.1093/jxb/erm240.

Prats-Llinàs, M. T., López, G., Fyhrie, K., Pallas, B., Guédon, Y., Costes, E., et al. (2019). Long proleptic and sylleptic shoots in peach (Prunus persica L. Batsch) trees have similar, predetermined, maximum numbers of nodes and bud fate patterns. *Ann. Bot.* 123, 993–1004. doi:10.1093/aob/mcy232.

Prudencio, Á. S., Hoeberichts, F. A., Dicenta, F., Martínez-Gómez, P., and Sánchez-Pérez, R. (2021). Identification of early and late flowering time candidate genes in endodormant and ecodormant almond flower buds. *Tree Physiol.* 41, 589–605. doi:10.1093/treephys/tpaa151.

Purcell, S., Neale, B., Todd-Brown, K., Thomas, L., Ferreira, M. A. R., Bender, D., et al. (2007). PLINK: A tool set for whole-genome association and population-based linkage analyses. *Am. J. Hum. Genet.* 81, 559–75. doi: 10.1086/519795.

Qin, H., He, L., and Huang, R. (2019). The coordination of ethylene and other hormones in primary root development. *Front. Plant Sci.* 10. doi:10.3389/fpls.2019.00874.

Qu, J., Kang, S. G., Hah, C., and Jang, J. C. (2016). Molecular and cellular characterization of GA-Stimulated Transcripts GASA4 and GASA6 in Arabidopsis thaliana. *Plant Sci.* 246, 1–10. doi:10.1016/j.plantsci.2016.01.009.

Racolta, A., Bryan, A. C., and Tax, F. E. (2014). The receptor-like kinases GSO1 and GSO2 together regulate root growth in arabidopsis through control of cell division and cell fate specification. *Dev. Dyn.* 243, 257–278. doi:10.1002/dvdy.24066.

Ramakrishna, P., Duarte, P. R., Rance, G. A., Schubert, M., Vordermaier, V., Vu, L. D., et al. (2019). EXPANSIN A1-mediated radial swelling of pericycle cells positions anticlinal

cell divisions during lateral root initiation. *Proc. Natl. Acad. Sci. U. S. A.* 116, 8597–8602. doi:10.1073/pnas.1820882116.

Rameau, C., Bertheloot, J., Leduc, N., Andrieu, B., Foucher, F., and Sakr, S. (2015). Multiple pathways regulate shoot branching. *Front. Plant Sci.* 5, 1–15. doi:10.3389/fpls.2014.00741.

Ramirez-Parra, E., Perianez-Rodriguez, J., Navarro-Neila, S., Gude, I., Moreno-Risueno, M. A., and del Pozo, J. C. (2017). The transcription factor OBP4 controls root growth and promotes callus formation. *New Phytol.* 213, 1787–1801. doi:10.1111/nph.14315.

Ranocha, P., Chabannes, M., Chamayou, S., Danoun, S., Jauneau, A., Boudet, A. M., et al. (2002). Laccase down-regulation causes alterations in phenolic metabolism and cell wall structure in poplar. *Plant Physiol.* 129, 145–155. doi:10.1104/pp.010988.

Ranocha, P., Dima, O., Nagy, R., Felten, J., Corratge-Faillie, C., Novak, O., et al. (2013). Arabidopsis WAT1 is a vacuolar auxin transport facilitator required for auxin homoeostasis. *Nat. Commun.* 4, 1–9. doi:10.1038/ncomms3625.

Rasool, A., Mansoor, S., Bhat, K. M., Hassan, G. I., Baba, T. R., Alyemeni, M. N., et al. (2020). Mechanisms Underlying Graft Union Formation and Rootstock Scion Interaction in Horticultural Plants. *Front. Plant Sci.* 11, 1778. doi:10.3389/fpls.2020.590847.

Rausenberger, J., Tscheuschler, A., Nordmeier, W., Wüst, F., Timmer, J., Schäfer, E., et al. (2011). Photoconversion and nuclear trafficking cycles determine phytochrome A's response profile to far-red light. *Cell* 146, 813–825. doi:10.1016/j.cell.2011.07.023.

Rawat, R., Schwartz, J., Jones, M. A., Sairanen, I., Cheng, Y., Andersson, C. R., et al. (2009). REVEILLE1, a Myb-like transcription factor, integrates the circadian clock and auxin pathways. *Proc. Natl. Acad. Sci. U. S. A.* 106, 16883-16888. doi: 10.1073/pnas.0813035106.

Reddy, S. K., and Finlayson, S. A. (2014). Phytochrome B promotes branching in Arabidopsis by suppressing auxin signaling. *Plant Physiol.* 164, 1542–1550. doi:10.1104/pp.113.234021.

Remy, E., Baster, P., Friml, J., and Duque, P. (2013). ZIFL1.1 transporter modulates polar auxin transport by stabilizing membrane abundance of multiple PINs in Arabidopsis root tip. *Plant Signal. Behav.* 8, e25688. doi:10.4161/psb.25688.

Revalska, M., Vassileva, V., Zechirov, G., and Iantcheva, A. (2015). Is the auxin influx carrier LAX3 essential for plant growth and development in the model plants Medicago truncatula, Lotus japonicus and Arabidopsis thaliana? *Biotechnol. Biotechnol. Equip.* 29, 786–797. doi:10.1080/13102818.2015.1031698.

Rinaldi, M. A., Liu, J., Enders, T. A., Bartel, B., and Strader, L. C. (2012). A gain-of-function mutation in IAA16 confers reduced responses to auxin and abscisic acid and impedes plant growth and fertility. *Plant Mol. Biol.* 79, 359–373. doi:10.1007/s11103-012-9917-y.

Ringli, C., Bigler, L., Kuhn, B. M., Leiber, R. M., Diet, A., Santelia, D., et al. (2008). The modified flavonol glycosylation profile in the Arabidopsis rol1 mutants results in alterations in plant growth and cell shape formation. *Plant Cell* 20, 1470–1481. doi:10.1105/tpc.107.053249.

Rivas-San Vicente, M., and Plasencia, J. (2011). Salicylic acid beyond defence: Its role in plant growth and development. *J. Exp. Bot.* 62, 3321–3338. doi:10.1093/jxb/err031.

Robinson, M. D., McCarthy, D. J., and Smyth, G. K. (2009). edgeR: A Bioconductor package for differential expression analysis of digital gene expression data. *Bioinformatics* 26, 139–140. doi:10.1093/bioinformatics/btp616.

Roxrud, I., Lid, S. E., Fletcher, J. C., Schmidt, E. D. L., and Opsahl-Sorteberg, H. G. (2007). GASA4, one of the 14-member Arabidopsis GASA family of small polypeptides, regulates flowering and seed development. *Plant Cell Physiol.* 48, 471–483. doi:10.1093/pcp/pcm016.

Ruan, J., Zhou, Y., Zhou, M., Yan, J., Khurshid, M., Weng, W., et al. (2019). Jasmonic acid signaling pathway in plants. *Int. J. Mol. Sci.* 20, 2479. doi:10.3390/ijms20102479.

Rubinovich, L., and Weiss, D. (2010). The Arabidopsis cysteine-rich protein GASA4 promotes GA responses and exhibits redox activity in bacteria and in planta. *Plant J.* 64, 1018–1027. doi:10.1111/j.1365-313X.2010.04390.x.

Rubio-Cabetas, M. J., Picó, B., Casas, A., and Badenes, M. L. (2014). "Aplicación de la biotecnología en los programas actuales de mejora" in La obtención de variedades: desde la mejora clásica hasta la mejora genética molecular, ed. R. Socias i Company, M. J. Rubio-Cabetas, A. Garcés-Claver, C. Mallor, and J. M. Álvarez (CITA/SECH/SEG, Zaragoza, Spain), 97–137.

Rubio-Cabetas, M. J., Felipe, A. J., and Reighard, G. L. (2017). "Rootstock Development" in Almonds: botany, production and uses, ed. R. Socias i Company, and T. M. Gradziel (CABI, Wallingford, UK), 193–220. doi:10.1079/9781780643540.0209.

Rubio-Cabetas, M. J., Pons, C., Bielsa, B., Amador, M. L., Marti, C., and Granell, A. (2018). Preformed and induced mechanisms underlies the differential responses of Prunus rootstock to hypoxia. *J. Plant Physiol.* 228, 134–149. doi:10.1016/j.jplph.2018.06.004.

Ruduś, I., Sasiak, M., and Kępczyński, J. (2013). Regulation of ethylene biosynthesis at the level of 1-aminocyclopropane-1-carboxylate oxidase (ACO) gene. *Acta Physiol. Plant.* 35, 295–307. doi:10.1007/s11738-012-1096-6.

Rymen, B., Kawamura, A., Schäfer, S., Breuer, C., Iwase, A., Shibata, M., et al. (2017). ABA suppresses root hair growth via the OBP4 transcriptional regulator. *Plant Physiol.* 173, 1750–1762. doi:10.1104/pp.16.01945.

Sablowski, R. (2016). Coordination of plant cell growth and division: collective control or mutual agreement? *Curr. Opin. Plant Biol.* 34, 54–60. doi:10.1016/j.pbi.2016.09.004.

Saffer, A. M. (2018). Expanding roles for pectins in plant development. *J. Integr. Plant Biol.* 60, 910–923. doi:10.1111/jipb.12662.

Saini, S., Sharma, I., Kaur, N., and Pati, P. K. (2013). Auxin: A master regulator in plant root development. *Plant Cell Rep.* 32, 741–757. doi:10.1007/s00299-013-1430-5.

Salzman, R. A., Fujita, T., Zhu-Salzman, K., Hasegawa, P. M., and Bressan, R. A. (1999). An improved RNA isolation method for plant tissues containing high levels of phenolic compounds or carbohydrates. *Plant Mol. Biol. Rep.* 17, 11–17. doi:10.1023/A:1007520314478.

Sánchez-Pérez, R., Pavan, S., Mazzeo, R., Moldovan, C., Aiese Cigliano, R., Del Cueto, J., et al. (2019). Mutation of a bHLH transcription factor allowed almond domestication. *Science* 364, 1095–1098. doi:10.1126/science.aav8197.

Sanchez, S. E., and Kay, S. A. (2016). The plant circadian clock: From a simple timekeeper to a complex developmental manager. *Cold Spring Harb. Perspect. Biol.* 8, a027748. doi:10.1101/cshperspect.a027748.

Sasaki, S., and Yamamoto, K. T. (2015). Arabidopsis LAZY1 is a peripheral membrane protein of which the Carboxy-terminal fragment potentially interacts with microtubules. *Plant Biotechnol.* 32, 103–108. doi: 10.5511/plantbiotechnology.15.0106a.

Sauer, M., Robert, S., and Kleine-Vehn, J. (2013). Auxin: Simply complicated. *J. Exp. Bot.* 64, 2565–2577. doi:10.1093/jxb/ert139.

Sawa, M., and Kay, S. A. (2011). GIGANTEA directly activates Flowering Locus T in Arabidopsis thaliana. *Proc. Natl. Acad. Sci. U. S. A.* 108, 11698–11703. doi:10.1073/pnas.1106771108.

Sawa, M., Nusinow, D. A., Kay, S. A., and Imaizumi, T. (2007). FKF1 and GIGANTEA complex formation is required for day-length measurement in Arabidopsis. *Science* 318, 261–265. doi:10.1126/science.1146994.

Schmid, M., Davison, T. S., Henz, S. R., Pape, U. J., Demar, M., Vingron, M., et al. (2005). A gene expression map of Arabidopsis thaliana development. *Nat. Genet.* 37, 501–506. doi:10.1038/ng1543.

Schröder, F., Lisso, J., and Müssig, C. (2011). Exordium-like1 promotes growth during low carbon availability in arabidopsis. *Plant Physiol.* 156, 1620–1630. doi:10.1104/pp.111.177204.

Schüler, O., Hemmersbach, R., and Böhmer, M. (2015). A Bird's-Eye View of Molecular Changes in Plant Gravitropism Using Omics Techniques. *Front. Plant Sci.* 6, 1176. doi:10.3389/fpls.2015.01176.

Schultz, E. A., and Haughn, G. W. (1991). LEAFY, a homeotic gene that regulates inflorescence development in arabidopsis. *Plant Cell* 3, 771–781. doi:10.1105/tpc.3.8.771.

Schumacher, I., Ndinyanka Fabrice, T., Abdou, M. T., Kuhn, B. M., Voxeur, A., Herger, A., et al. (2021). Defects in Cell Wall Differentiation of the Arabidopsis Mutant rol1-2 Is Dependent on Cyclin-Dependent Kinase CDK8. *Cells* 10, 1–16. doi:10.3390/cells10030685.

Segura, V., Cilas, C., and Costes, E. (2008). Dissecting apple tree architecture into genetic, ontogenetic and environmental effects: Mixed linear modelling of repeated spatial and temporal measures. *New Phytol.* 178, 302–314. doi:10.1111/j.1469-8137.2007.02374.x.

Segura, V., Cilas, C., Laurens, F., and Costes, E. (2006). Phenotyping progenies for complex architectural traits: A strategy for 1-year-old apple trees (Malus x domestica Borkh.). *Tree Genet. Genomes* 2, 140–151. doi:10.1007/s11295-006-0037-1.

Seleznyova, A. N., Thorp, T. G., Barnett, A. M., and Costes, E. (2002). Quantitative analysis of shoot development and branching patterns in Actinidia. *Ann. Bot.* 89, 471–482. doi:10.1093/aob/mcf069.

Seleznyova, A. N., Tustin, D. S., and Thorp, T. G. (2008). Apple dwarfing rootstocks and interstocks affect the type of growth units produced during the annual growth cycle: Precocious transition to flowering affects the composition and vigour of annual shoots. *Ann. Bot.* 101, 679–687. doi:10.1093/aob/mcn007.

Sharma, A., Sharma, B., Hayes, S., Kerner, K., Hoecker, U., Jenkins, G. I., et al. (2019). UVR8 disrupts stabilisation of PIF5 by COP1 to inhibit plant stem elongation in sunlight. *Nat. Commun.* 10, 1–10. doi:10.1038/s41467-019-12369-1.

Shen, L., Liang, Z., Gu, X., Chen, Y., Teo, Z. W. N., Hou, X., et al. (2016). N6-Methyladenosine RNA Modification Regulates Shoot Stem Cell Fate in Arabidopsis. *Dev. Cell* 38, 186–200. doi:10.1016/j.devcel.2016.06.008.

Shi, B., Guo, X., Wang, Y., Xiong, Y., Wang, J., Hayashi, K., et al. (2018). Feedback from Lateral Organs Controls Shoot Apical Meristem Growth by Modulating Auxin Transport. *Dev. Cell* 44, 204–216. doi:10.1016/j.devcel.2017.12.021.

Shinohara, N., Taylor, C., and Leyser, O. (2013). Strigolactone Can Promote or Inhibit Shoot Branching by Triggering Rapid Depletion of the Auxin Efflux Protein PIN1 from the Plasma Membrane. *PLoS Biol.* 11, e1001474. doi:10.1371/journal.pbio.1001474.

Simon, S., Skůpa, P., Viaene, T., Zwiewka, M., Tejos, R., Klíma, P., et al. (2016). PIN6 auxin transporter at endoplasmic reticulum and plasma membrane mediates auxin homeostasis and organogenesis in Arabidopsis. *New Phytol.* 211, 65–74. doi:10.1111/nph.14019.

Simons, J. L., Napoli, C. A., Janssen, B. J., Plummer, K. M., and Snowden, K. C. (2007). Analysis of the DECREASED APICAL DOMINANCE genes of petunia in the control of axillary branching. *Plant Physiol.* 143, 697–706. doi:10.1104/pp.106.087957.

Singh, S., Yadav, S., Singh, A., Mahima, M., Singh, A., Gautam, V., et al. (2020). Auxin signaling modulates LATERAL ROOT PRIMORDIUM1 (LRP1) expression during lateral root development in Arabidopsis. *Plant J.* 101, 87–100. doi:10.1111/tpj.14520.

Socias i Company, R., Alonso, J. M., Kodad, O., and Gradziel, T. M. (2012). "Almond" in Fruit Breeding. Handbook of Plant Breeding, ed. M. Badenes, and D. Byrne (Springer, Boston, MA), 697–728. doi:10.1007/978-1-4419-0763-9_18.

Socias i Company, R., Ansón, J. M., and Espiau, M. T. (2017). "Taxonomy, botany and physiology" in Almonds: botany, production and uses, ed. R. Socias i Company, and T. M. Gradziel (CABI, Wallingford, UK), 1–42. doi:10.1079/9781780643540.0001.

Socias i Company, R., and Felipe, A. J. (2007). 'Belona' and 'Soleta' almonds. *HortScience* 42, 704–706. doi:10.21273/hortsci.42.3.704.

Socias i Company, R., Gómez Aparisi, J., Alonso, J. M., Rubio-Cabetas, M. J., and Kodad, O., (2009). Retos y perspectivas de los nuevos cultivares y patrones de almendro para un cultivo sostenible. *Inf. Tec. Econ. Agrar.* 105, 99–116.

Socias i Company, R., Kodad, O., Alonso, J. M., and Felipe, A. J. (2008). 'Mardía' Almond. *HortScience* 43, 2240–2242. doi:10.21273/HORTSCI.43.7.2240.

Socias i Company, R., Kodad, O., Ansón, J. M., Alonso, J. M. (2015). 'Vialfas' Almond. *HortScience* 50, 1726–1728. doi:10.21273/HORTSCI.50.11.1726.

Solomonson, L. P., and Barber, M. J. (1990). Assimilatory nitrate reductase: Functional properties and regulation. *Annu. Rev. Plant Physiol. Plant Mol. Biol.* 41, 225–253. doi:10.1146/annurev.pp.41.060190.001301.

Song, J. Y., Leung, T., Ehler, L. K., Wang, C., and Liu, Z. (2000). Regulation of meristem organization and cell division by TSO1, an Arabidopsis gene with cysteine-rich repeats. *Development* 127, 2207–2217. doi:10.1242/dev.127.10.2207.

Song, Y. H., Estrada, D. A., Johnson, R. S., Kim, S. K., Lee, S. Y., MacCoss, M. J., et al. (2014). Distinct roles of FKF1, GIGANTEA, and ZEITLUPE proteins in the regulation of constans stability in Arabidopsis photoperiodic flowering. *Proc. Natl. Acad. Sci. U. S. A.* 111, 17672–17677. doi:10.1073/pnas.1415375111.

Sorin, C., Declerck, M., Christ, A., Blein, T., Ma, L., Lelandais-Brière, C., et al. (2014). A miR169 isoform regulates specific NF-YA targets and root architecture in Arabidopsis. *New Phytol.* 202, 1197–1211. doi:10.1111/nph.12735.

Sorin, C., Salla-Martret, M., Bou-Torrent, J., Roig-Villanova, I., and Martínez-García, J. F. (2009). ATHB4, a regulator of shade avoidance, modulates hormone response in Arabidopsis seedlings. *Plant J.* 59, 266–277. doi:10.1111/j.1365-313X.2009.03866.x.

Srikanth, A., and Schmid, M. (2011). Regulation of flowering time: All roads lead to Rome. *Cell. Mol. Life Sci.* 68, 2013–2037. doi:10.1007/s00018-011-0673-y.

Stamm, P., Topham, A. T., Mukhtar, N. K., Jackson, M. D. B., Tomé, D. F. A., Beynon, J. L., et al. (2017). The transcription factor ATHB5 affects GA-mediated plasticity in hypocotyl cell growth during seed germination. *Plant Physiol.* 173, 907–917. doi:10.1104/pp.16.01099.

Stokes, M. E., Chattopadhyay, A., Wilkins, O., Nambara, E., and Campbell, M. M. (2013). Interplay between Sucrose and Folate Modulates Auxin Signaling in Arabidopsis. *Plant Physiol.* 162, 1552–1565. doi:10.1104/pp.113.215095.

Su, H., Cao, Y., Ku, L., Yao, W., Cao, Y., Ren, Z., et al. (2018). Dual functions of ZmNF-YA3 in photoperiod-dependent flowering and abiotic stress responses in maize. *J. Exp. Bot.* 69, 5177–5189. doi:10.1093/jxb/ery299.

Su, M., Huang, G., Zhang, Q., Wang, X., Li, C., Tao, Y., et al. (2016). The LEA protein, ABR, is regulated by ABI5 and involved in dark-induced leaf senescence in Arabidopsis thaliana. *Plant Sci.* 247, 93–103. doi:10.1016/j.plantsci.2016.03.009.

Su, S. H., Gibbs, N. M., Jancewicz, A. L., and Masson, P. H. (2017). Molecular Mechanisms of Root Gravitropism. *Curr. Biol.* 27, R964–R972. doi:10.1016/j.cub.2017.07.015.

Sun, H., Tao, J., Liu, S., Huang, S., Chen, S., Xie, X., et al. (2014). Strigolactones are involved in phosphate- and nitrate-deficiency-induced root development and auxin transport in rice. *J. Exp. Bot.* 65, 6735–6746. doi:10.1093/jxb/eru029.

Sun, T. P. (2010). Gibberellin-GID1-DELLA: A pivotal regulatory module for plant growth and development. *Plant Physiol.* 154, 567–570. doi:10.1104/pp.110.161554.

Svane, S. F., Jensen, C. S., and Thorup-Kristensen, K. (2019). Construction of a large-scale semi-field facility to study genotypic differences in deep root growth and resources acquisition. *Plant Methods* 15, 1–16. doi:10.1186/s13007-019-0409-9.

Takahashi, D., Johnson, K. L., Hao, P., Tuong, T., Erban, A., Sampathkumar, A., et al. (2021). Cell wall modification by the xyloglucan endotransglucosylase/hydrolase XTH19

influences freezing tolerance after cold and sub-zero acclimation. *Plant Cell Environ.* 44, 915–930. doi:10.1111/pce.13953.

Takatsuka, H., and Umeda, M. (2014). Hormonal control of cell division and elongation along differentiation trajectories in roots. *J. Exp. Bot.* 65, 2633–2643. doi:10.1093/jxb/ert485.

Tanaka, M., Takei, K., Kojima, M., Sakakibara, H., and Mori, H. (2006). Auxin controls local cytokinin biosynthesis in the nodal stem in apical dominance. *Plant J.* 45, 1028–1036. doi:10.1111/j.1365-313X.2006.02656.x.

Tanaka, S., Ida, S., Irifune, K., Oeda, K., and Morikawa, H. (1994). Nucleotide sequence of a gene for nitrite reductase from arabidopsis thaliana. *Mitochondrial DNA* 5, 57–61. doi:10.3109/10425179409039705.

Taniguchi, M., Furutani, M., Nishimura, T., Nakamura, M., Fushita, T., Iijima, K., et al. (2017). The Arabidopsis LAZY1 Family Plays a Key Role in Gravity Signaling within Statocytes and in Branch Angle Control of Roots and Shoots. *Plant Cell* 29, 1984–1999. doi:10.1105/tpc.16.00575.

Tan, Q., Li, S., Zhang, Y., Chen, M., Wen, B., Jiang, S., et al. (2021). Chromosome-level genome assemblies of five Prunus species and genome-wide association studies for key agronomic traits in peach. *Hortic. Res.* 8, 1–18. doi:10.1038/s41438-021-00648-2.

Tian, C., Wang, Y., Yu, H., He, J., Wang, J., Shi, B., et al. (2019). A gene expression map of shoot domains reveals regulatory mechanisms. *Nat. Commun.* 10, 1–12. doi:10.1038/s41467-018-08083-z.

Tietel, Z., Srivastava, S., Fait, A., Tel-Zur, N., Carmi, N., and Raveh, E. (2020). Impact of scion/rootstock reciprocal effects on metabolomics of fruit juice and phloem sap in grafted Citrus reticulata. *PloS One*, 15(1), e0227192. doi: 10.1371/journal.pone.0227192.

Titapiwatanakun, B., and Murphy, A. S. (2009). Post-transcriptional regulation of auxin transport proteins: Cellular trafficking, protein phosphorylation, protein maturation, ubiquitination, and membrane composition. *J. Exp. Bot.* 60, 1093–1107. doi:10.1093/jxb/ern240.

Tracy, S. R., Nagel, K. A., Postma, J. A., Fassbender, H., Wasson, A., and Watt, M. (2020). Crop Improvement from Phenotyping Roots: Highlights Reveal Expanding Opportunities. *Trends Plant Sci*. 25, 105–118. doi:10.1016/j.tplants.2019.10.015.

Tworkoski, T., and Fazio, G. (2015). Effects of Size-Controlling Apple Rootstocks on Growth, Abscisic Acid, and Hydraulic Conductivity of Scion of Different Vigor. *Int. J. Fruit Sci.* 15, 369–381. doi:10.1080/15538362.2015.1009973.

Tworkoski, T., and Miller, S. (2007). Rootstock effect on growth of apple scions with different growth habits. *Sci. Hortic.* 111, 335–343. doi:10.1016/j.scienta.2006.10.034.

Tworkoski, T., Webb, K., and Callahan, A. (2015). Auxin levels and MAX1–4 and TAC1 gene expression in different growth habits of peach. *Plant Growth Regul.* 77, 279–288. doi:10.1007/s10725-015-0062-x.

Ubeda-Tomás, S., Swarup, R., Coates, J., Swarup, K., Laplaze, L., Beemster, G. T. S., et al. (2008). Root growth in Arabidopsis requires gibberellin/DELLA signalling in the endodermis. *Nat. Cell Biol.* 10, 625–628. doi:10.1038/ncb1726.

Uga, Y., Sugimoto, K., Ogawa, S., Rane, J., Ishitani, M., Hara, N., et al. (2013). Control of root system architecture by DEEPER ROOTING 1 increases rice yield under drought conditions. *Nat. Genet.* 45, 1097–1102. doi: 10.1038/ng.2725.

Untergasser, A., Nijveen, H., Rao, X., Bisseling, T., Geurts, R., and Leunissen, J. A. M. (2007). Primer3Plus, an enhanced web interface to Primer3. *Nucleic Acids Res*. 35, 71–74. doi: 10.1093/nar/gkm306.

Vaahtera, L., Schulz, J., and Hamann, T. (2019). Cell wall integrity maintenance during plant development and interaction with the environment. *Nat. Plants* 5, 924–932. doi:10.1038/s41477-019-0502-0.

Vahdati, K., Sarikhani, S., Arab, M. M., Leslie, C. A., Dandekar, A. M., Aletà, N., et al. (2021). Advances in Rootstock Breeding of Nut Trees: Objectives and Strategies. *Plants* 10, 2234. doi: 10.3390/plants10112234.

van Hooijdonk, B. M., Woolley, D. J., Warrington, I. J., and Tustin, D. S. (2010). Initial alteration of scion architecture by dwarfing apple rootstocks may involve shoot-root-shoot signalling by auxin, gibberellin, and cytokinin. *J. Hortic. Sci. Biotechnol.* 85, 59–65. doi:10.1080/14620316.2010.11512631.

van Hooijdonk, B. M., Woolley, D. J., Warrington, I. J., and Tustin, D. S. (2011). Rootstocks modify scion architecture, endogenous hormones, and root growth of newly grafted 'Royal Gala'apple trees. *J. Am. Soc. Hortic. Sci*. 136, 93–102. doi:10.21273/JASHS.136.2.93.

Vert, G., Walcher, C. L., Chory, J., and Nemhauser, J. L. (2008). Integration of auxin and brassinosteroid pathways by Auxin Response Factor 2. *Proc. Natl. Acad. Sci. U. S. A.* 105, 9829–9834. doi:10.1073/pnas.0803996105.

Voiniciuc, C., Pauly, M., and Usadel, B. (2018). Monitoring polysaccharide dynamics in the plant cell wall. *Plant Physiol.* 176, 2590–2600. doi:10.1104/pp.17.01776.

Waite, J. M., and Dardick, C. (2018). TILLER ANGLE CONTROL 1 modulates plant architecture in response to photosynthetic signals. *J. Exp. Bot.*, 69, 4935–4944. doi:10.1093/jxb/ery253.

Waite, J. M., and Dardick, C. (2021). The roles of the IGT gene family in plant architecture: past, present, and future. *Curr. Opin. Plant Biol.* 59, 101983. doi:10.1016/j.pbi.2020.101983.

Waldie, T., and Leyser, O. (2018). Cytokinin targets auxin transport to promote shoot branching. *Plant Physiol.* 177, 803–818. doi:10.1104/pp.17.01691.

Waldie, T., McCulloch, H., and Leyser, O. (2014). Strigolactones and the control of plant development: Lessons from shoot branching. *Plant J.* 79, 607–622. doi:10.1111/tpj.12488.

Walker L.M., and Sack F.D. (1990). Amyloplasts as possible statoliths in gravitropic protonemata of the moss Ceratodon purpureus. *Planta* 181, 71–77. doi: 10.1007/BF00202326.

Wan, Y., Jasik, J., Wang, L., Hao, H., Volkmann, D., Menzel, D., et al. (2012). The signal transducer NPH3 integrates the phototropin1 photosensor with PIN2-based polar auxin transport in Arabidopsis root phototropism. *Plant Cell* 24, 551–565. doi:10.1105/tpc.111.094284.

Wang, B., Smith, S. M., and Li, J. (2018). Genetic Regulation of Shoot Architecture. *Annu. Rev. Plant Biol.* 69, 437–468. doi:10.1146/annurev-arplant-042817-040422.

Wang, H., Jiang, C., Wang, C., Yang, Y., Yang, L., Gao, X., et al. (2015). Antisense expression of the fasciclin-like arabinogalactan protein FLA6 gene in Populus inhibits expression of its homologous genes and alters stem biomechanics and cell wall composition in transgenic trees. *J. Exp. Bot.* 66, 1291–1302. doi:10.1093/jxb/eru479.

Wang, J., Sun, N., Zhang, F., Yu, R., Chen, H., Deng, X. W., et al. (2020). SAUR17 and SAUR50 differentially regulate PP2C-D1 during apical hook development and cotyledon opening in arabidopsis. *Plant Cell* 32, 3792–3811. doi:10.1105/tpc.20.00283.

Wang, L., Cai, W., Du, C., Fu, Y., Xie, X., and Zhu, Y. (2018). The isolation of the IGT family genes in Malus × domestica and their expressions in four idiotype apple cultivars. *Tree Genet. Genomes* 14, 1–11. doi:10.1007/s11295-018-1258-9.

Wang, Q., Xu, G., Zhao, X., Zhang, Z., Wang, X., Liu, X., et al. (2020). Transcription factor TCP20 regulates peach bud endodormancy by inhibiting DAM5/DAM6 and interacting with ABF2. *J. Exp. Bot.* 71, 1585–1597. doi:10.1093/jxb/erz516.

Wang, W., Hu, B., Li, A., and Chu, C. (2020). NRT1.1s in plants: Functions beyond nitrate transport. *J. Exp. Bot.* 71, 4373–4379. doi:10.1093/jxb/erz554.

Wang, W., Sijacic, P., Xu, P., Lian, H., and Liu, Z. (2018). Arabidopsis TSO1 and MYB3R1 form a regulatory module to coordinate cell proliferation with differentiation in shoot and root. *Proc. Natl. Acad. Sci. U. S. A.* 115, E3045–E3054. doi:10.1073/pnas.1715903115.

Wang, Y. Y., Cheng, Y. H., Chen, K. E., and Tsay, Y. F. (2018). Nitrate Transport, Signaling, and Use Efficiency. *Annu. Rev. Plant Biol.* 69, 85–122. doi:10.1146/annurev-arplant-042817-040056.

Warschefsky, E. J., Klein, L. L., Frank, M. H., Chitwood, D. H., Londo, J. P., von Wettberg, E. J. B., et al. (2016). Rootstocks: Diversity, Domestication, and Impacts on Shoot Phenotypes. *Trends Plant Sci.* 21, 418–437. doi:10.1016/j.tplants.2015.11.008.

Wasson, A. P., Richards, R. A., Chatrath, R., Misra, S. C., Prasad, S. V. S., Rebetzke, G. J., et al. (2012). Traits and selection strategies to improve root systems and water uptake in water-limited wheat crops. *J. Exp. Bot.* 63, 3485–3498. doi:10.1093/jxb/ers111.

Wei, Z., and Li, J. (2016). Brassinosteroids Regulate Root Growth, Development, and Symbiosis. *Mol. Plant* 9, 86–100. doi:10.1016/j.molp.2015.12.003.

White, C. N., and Rivin, C. J. (2000). Gibberellins and seed development in maize. II. Gibberellin synthesis inhibition enhances abscisic acid signaling in cultured embryos. *Plant Physiol.* 122, 1089–1097. doi:10.1104/pp.122.4.1089.

Widemann, E., Miesch, L., Lugan, R., Holder, E., Heinrich, C., Aubert, Y., et al. (2013). The amidohydrolases IAR3 and ILL6 contribute to jasmonoyl-isoleucine hormone turnover and generate 12-hydroxyjasmonic acid upon wounding in arabidopsis leaves. *J. Biol. Chem.* 288, 31701–31714. doi:10.1074/jbc.M113.499228.

Wigge, P. A., Kim, M. C., Jaeger, K. E., Busch, W., Schmid, M., Lohmann, J. U., et al. (2005). Integration of spatial and temporal information during floral induction in Arabidopsis. *Science* 309, 1056–1059. doi:10.1126/science.1114358.

Wirthensohn, M., and Iannamico, L. (2017). "Almond in the Southern Hemisphere" in Almonds: botany, production and uses, ed. R. Socias i Company, and T. M. Gradziel (CABI, Wallingford, UK), 87–110. doi:10.1079/9781780643540.0087.

Wu, J., Zhu, C., Pang, J., Zhang, X., Yang, C., Xia, G., et al. (2014). OsLOL1, a C2C2-type zinc finger protein, interacts with OsbZIP58 to promote seed germination through the modulation of gibberellin biosynthesis in Oryza sativa. *Plant J.* 80, 1118–1130. doi:10.1111/tpj.12714.

Wulf, K. E., Reid, J. B., and Foo, E. (2019). Auxin transport and stem vascular reconnection - has our thinking become canalized? *Ann. Bot.* 123, 429–439. doi:10.1093/aob/mcy180.

Xu, D., Qi, X., Li, J., Han, X., Wang, J., Jiang, Y., et al. (2017). PzTAC and PzLAZY from a narrow-crown poplar contribute to regulation of branch angles. *Plant Physiol. Biochem.* 118, 571–578. doi:10.1016/j.plaphy.2017.07.011.

Xu, J., Zha, M., Li, Y., Ding, Y., Chen, L., Ding, C., et al. (2015). The interaction between nitrogen availability and auxin, cytokinin, and strigolactone in the control of shoot branching in rice (Oryza sativa L.). *Plant Cell Rep.* 34, 1647–1662. doi:10.1007/s00299-015-1815-8.

Xu, P., Chen, H., Ying, L., and Cai, W. (2016). AtDOF5.4/OBP4, a DOF Transcription Factor Gene that Negatively Regulates Cell Cycle Progression and Cell Expansion in Arabidopsis thaliana. *Sci. Rep.* 6, 1–13. doi:10.1038/srep27705.

Xuan, Y. H., Duan, F. Y., Je, B. Il, Kim, C. M., Li, T. Y., Liu, J. M., et al. (2017). Related to ABI3/VP1-Like 1 (RAVL1) regulates brassinosteroidmediated activation of AMT1;2 in rice (Oryza sativa). *J. Exp. Bot.* 68, 727–737. doi:10.1093/jxb/erw442.

Yadav, A., Singh, D., Lingwan, M., Yadukrishnan, P., Masakapalli, S. K., and Datta, S. (2020). Light signaling and UV-B-mediated plant growth regulation. *J. Integr. Plant Biol.* 62, 1270–1292. doi:10.1111/jipb.12932.

Yamaguchi, S. (2008). Gibberellin metabolism and its regulation. *Annu. Rev. Plant Biol.* 59, 225–251. doi:10.1146/annurev.arplant.59.032607.092804.

Yang, J., Bak, G., Burgin, T., Barnes, W. J., Mayes, H. B., Peña, M. J., et al. (2020). Biochemical and genetic analysis identify CSLD3 as a beta-1,4-glucan synthase that functions during plant cell wall synthesis. *Plant Cell* 32, 1749–1767. doi:10.1105/tpc.19.00637.

Yang, W., Chen, S., Cheng, Y., Zhang, N., Ma, Y., Wang, W., et al. (2020). Cell wall/vacuolar inhibitor of fructosidase 1 regulates ABA response and salt tolerance in Arabidopsis. *Plant Signal. Behav.* 15. doi:10.1080/15592324.2020.1744293.

Yang, Y., Mao, L., Jittayasothorn, Y., Kang, Y., Jiao, C., Fei, Z., et al. (2015). Messenger RNA exchange between scions and rootstocks in grafted grapevines. *BMC Plant Biol.* 15, 1–14. doi:10.1186/s12870-015-0626-y.

Yao, C., and Finlayson, S. A. (2015). Abscisic Acid Is a General Negative Regulator of Arabidopsis Axillary Bud Growth. *Plant Physiol.* 169, 611–626. doi:10.1104/pp.15.00682.

Yaxley, J. R., Ross, J. J., Sherriff, L. J., and Reid, J. B. (2001). Gibberellin biosynthesis mutations and root development in pea. *Plant Physiol.* 125, 627–633. doi:10.1104/pp.125.2.627.

Yeh, S. Y., Chen, H. W., Ng, C. Y., Lin, C. Y., Tseng, T. H., Li, W. H., et al. (2015). Down-Regulation of Cytokinin Oxidase 2 Expression Increases Tiller Number and Improves Rice Yield. *Rice* 8, 1–13. doi:10.1186/s12284-015-0070-5.

Yoshihara, T., and Iino, M. (2007). Identification of the gravitropism-related rice gene LAZY1 and elucidation of LAZY1-dependent and -independent gravity signaling pathways. *Plant Cell Physiol* 48, 678–688. doi: 10.1093/pcp/pcm042.

Yoshihara, T., and Spalding, E. P. (2017). LAZY genes mediate the effects of gravity on auxin gradients and plant architecture. *Plant Physiol.* 175, 959–969. doi:10.1104/pp.17.00942.

Yoshihara, T., and Spalding, E. P. (2020). Switching the direction of stem gravitropism by altering two amino acids in Atlazy1. *Plant Physiol.* 182, 1039–1051. doi:10.1104/pp.19.01144.

Yoshihara, T., Spalding, E. P., and Iino, M. (2013). AtLAZY1 is a signaling component required for gravitropism of the Arabidopsis thaliana inflorescence. *Plant J.* 74, 267–279. doi: 10.1111/tpj.12118.

Youngs H. L., Hamann T., Osborne E., and Somerville C. (2007) “The Cellulose Synthase Superfamily” in Cellulose: Molecular and Structural Biology, eds. R. M. Brown, and I. M. Saxena I.M. (Springer, Dordrecht), 35–48. doi:10.1007/978-1-4020-5380-1_3.

Yu, B., Lin, Z., Li, H., Li, X., Li, J., Wang, Y., et al. (2007). TAC1, a major quantitative trait locus controlling tiller angle in rice. *Plant J.* 52, 891–898. doi:10.1111/j.1365-313X.2007.03284.x.

Zeng, Y., and Yang, T. (2002). RNA isolation from highly viscous samples rich in polyphenols and polysaccharides. *Plant Mol. Biol. Rep.* 20, 417. doi:10.1007/BF02772130.

Zhai, L., Wang, X., Tang, D., Qi, Q., Yer, H., Jiang, X., et al. (2021). Molecular and physiological characterization of the effects of auxin-enriched rootstock on grafting. *Hortic. Res.* 8. 1–13. doi:10.1038/s41438-021-00509-y.

Zhang, M., Hu, X., Zhu, M., Xu, M., and Wang, L. (2017). Transcription factors NF-YA2 and NF-YA10 regulate leaf growth via auxin signaling in Arabidopsis. *Sci. Rep.* 7, 1–9. doi:10.1038/s41598-017-01475-z.

Zhang, N., Yu, H., Yu, H., Cai, Y., Huang, L., Xu, C., et al. (2018). A Core Regulatory Pathway Controlling Rice Tiller Angle Mediated by the LAZY1-Dependent Asymmetric Distribution. 30, 1461–1475. doi:10.1105/tpc.18.00063.

Zhang, S., and Wang, X. (2008). Expression pattern of GASA, downstream genes of DELLA, in Arabidopsis. *Chinese Sci. Bull.* 53, 3839–3846. doi:10.1007/s11434-008-0525-9.

Zhang, Y., Schwarz, S., Saedler, H., and Huijser, P. (2007a). SPL8, a local regulator in a subset of gibberellin-mediated developmental processes in Arabidopsis. *Plant Mol. Biol.* 63, 429–439. doi:10.1007/s11103-006-9099-6.

Zhang, Y., Yang, X., Cao, P., Xiao, Z., Zhan, C., Liu, M., et al. (2020). The bZIP53-IAA4 module inhibits adventitious root development in Populus. *J. Exp. Bot.* 71, 3485–3498. doi:10.1093/jxb/eraa096.

Zhang, Z., Li, Q., Li, Z., Staswick, P. E., Wang, M., Zhu, Y., et al. (2007b). Dual regulation role of GH3.5 in salicylic acid and auxin signaling during arabidopsis-Pseudomonas syringae interaction. *Plant Physiol.* 145, 450–464. doi:10.1104/pp.107.106021.

Zhao, J., Missihoun, T. D., and Bartels, D. (2018). The ATAF1 transcription factor is a key regulator of aldehyde dehydrogenase 7B4 (ALDH7B4) gene expression in Arabidopsis thaliana. *Planta* 248, 1017–1027. doi:10.1007/s00425-018-2955-1.

Zhao, Q., Nakashima, J., Chen, F., Yin, Y., Fu, C., Yun, J., et al. (2013). LACCASE is necessary and nonredundant with PEROXIDASE for lignin polymerization during vascular development in Arabidopsis. *Plant Cell* 25, 3976–3987. doi:10.1105/tpc.113.117770.

Zhao, Y., Cheng, S., Song, Y., Huang, Y., Zhou, S., Liu, X., et al. (2015). The interaction between rice ERF3 and WOX11 promotes crown root development by regulating gene expression involved in cytokinin signaling. *Plant Cell* 27, 2469–2483. doi:10.1105/tpc.15.00227.

Zhou, B., Lin, J., Peng, W., Peng, D., Zhuo, Y., Zhu, D., et al. (2012). Dwarfism in Brassica napus L. induced by the over-expression of a gibberellin 2-oxidase gene from Arabidopsis thaliana. *Mol. Breed.* 29, 115–127. doi:10.1007/s11032-010-9530-1.

Zhou, P., Song, M., Yang, Q., Su, L., Hou, P., Guo, L., et al. (2014). Both PHYTOCHROME RAPIDLY REGULATED1 (PAR1) and PAR2 promote seedling photomorphogenesis in multiple light signaling pathways. *Plant Physiol.* 164, 841–852. doi:10.1104/pp.113.227231.

Zhou, X., Zhang, Z. L., Park, J., Tyler, L., Yusuke, J., Qiu, K., et al. (2016). The ERF11 transcription factor promotes internode elongation by activating gibberellin biosynthesis and signaling. *Plant Physiol.* 171, 2760–2770. doi:10.1104/pp.16.00154.

Zhu, L., Hu, J., Zhu, K., Fang, Y., Gao, Z., He, Y., et al. (2011). Identification and characterization of SHORTENED UPPERMOST INTERNODE 1, a gene negatively regulating uppermost internode elongation in rice. *Plant Mol. Biol.* 77, 475–487. doi:10.1007/s11103-011-9825-6.

Zhu, X. F., Yuan, D. P., Zhang, C., Li, T. Y., and Xuan, Y. H. (2018). RAVL1, an upstream component of brassinosteroid signalling and biosynthesis, regulates ethylene signalling via activation of EIL1 in rice. *Plant Biotechnol. J.* 16, 1399–1401. doi:10.1111/pbi.12925.

Zuckerkandl, E., and Pauling L. (1965). Evolutionary Divergence and Convergence in Proteins. *Evol. Genes Proteins* 97–166. doi: 10.1016/b978-1-4832-2734-4.50017-6.

11. ANNEXES

Annex 1

Abbreviations

ABA: Abscisic acid

AM: Association mapping

BR: Brassinosteroid

CK: Citokinin

DEG: Differentially expressed gene

ET: Ethylene

GA: Gibberellic acid

GWAS: Genome-wide association mapping

IAA: Indole-3-acetic acid

JA: Jasmonic acid

MAS: Marker assisted selection

PCA: Principal component analysis

qPCR: Quantitative real-time PCR

QTL: Quantitative trait loci

RE: Regulatory element

R:FR: Red:Far Red

SAM: Shoot apical meristem

SL: Strigolactone

SNP: Single nucleotide polimorphism

TCSA: Trunk-cross sectional area

TF: Transcription factor

UPOV: International Union for the protection of New Varieties of Plants

Annex 2

Supplementary Data 2.1. List of the forty-one almond cultivars and wild species. Overall tree habit phenotype for each cultivar is described categorically according UPOV (International Union for the protection of New Varieties of Plants) guidelines.

Cultivar	Tree habit
'Bartre'	Upright
'Marinada'	Somewhat upright
'Ardechoise'	Somewhat upright
'Garfi'	Somewhat upright
'Achaak'	Somewhat upright
'Atocha'	Somewhat upright
'Ferragnes'	Somewhat upright
'Princesse'	Somewhat upright
Prunus kuramica	Somewhat upright
'Lauranne'	Semi-open
'Marcona'	Semi-open
'Vialfas'	Semi-open
'Vivot'	Semi-open
'Vairo'	Semi-open
'Retsou'	Semi-open
'Chellastone'	Semi-open
'Isabelona'	Semi-open
Prunus bucharica	Semi-open
'Guara'	Open
'Primorski'	Open
'Cristomorto'	Open
'Ai'	Open
'Belle d'Aurons'	Open
'Genco'	Open
'Pointeu d'Aureille'	Open
Prunus webbii	Open
'Desmayo Largueta'	Weeping
'Mckinlays'	Unknown
'Keanes'	Unknown
'R23T45'	Unknown
'Ripon'	Unknown
'Strouts'	Unknown
'Johnstons'	Unknown
'Doree'	Unknown
'Ferrastar'	Unknown
'A la Dame'	Unknown
'Falsa Barese'	Unknown
'UA03'	Unknown
'UA05'	Unknown
P. fenzliana	Unknown
'Gabais'	Unknown

Supplementary Data 2.2. Protein sequences of the six IGT family members in the forty-one almond cultivars and wild species. First entry of each cultivar or wild species contains homozygous variants while second entry contains both homozygous and heterozygous variants. Due to the extension of this dataset, this information is only available in the extended data.

Supplementary Data 2.3. List of mutations affecting the protein sequence for the forty-one almond cultivars and wild species. HOM: mutation in both alleles; HET: mutation in only one allele. Due to the extension of this dataset, this information is only available in the extended data.

Supplementary Data 2.4. List of mutations affecting the promoter sequence of *TAC1*, *LAZY1* and *LAZY2* for the selected fourteen almond cultivars. HOM: mutation in both alleles; HET: mutation in only one allele. Due to the extension of this dataset, this information is only available in the extended data.

Supplementary Data 2.5. Heatmap of relative gene expression for identified transcription factors (TFs). TFs are separated into three groups, whether they are expected to interact with both promoters or only one of them. Heatmap was constructed in R (https://cran.r-project.org/).

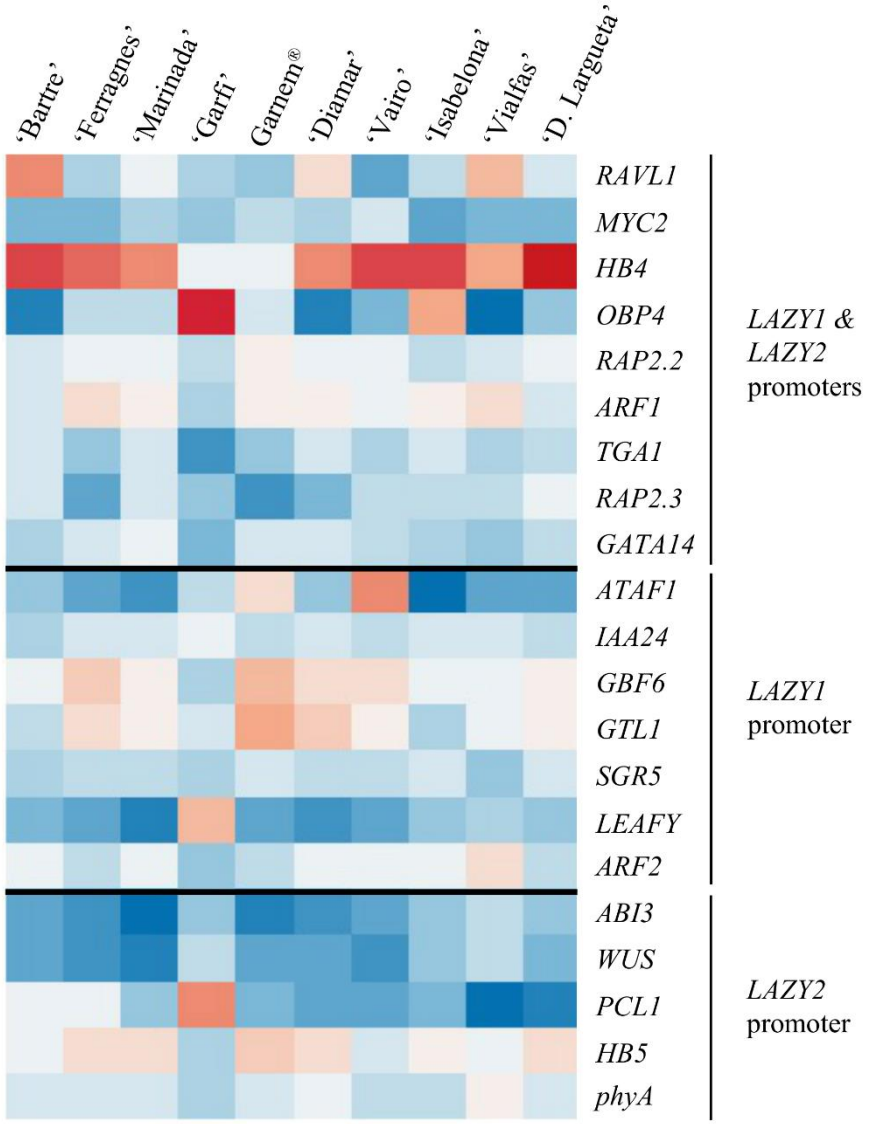

Annex 3

Supplementary Data 5.1. RNA-Seq data from the analysis of the rootsock influence on 'Lauranne'. LAU: 'Lauranne'; R20: Rootpac® 20; R40: Rootpac® 40; GN: Garnem®. Due to the extension of this dataset, this information is only available in the extended data.

Supplementary Data 5.2. RNA-Seq data from the analysis of the rootsock influence on 'Isabelona'. ISA: 'Isabelona'; R20: Rootpac® 20; R40: Rootpac® 40; GN: Garnem®. Due to the extension of this dataset, this information is only available in the extended data.

Supplementary Data 5.1. RNA-Seq data from the analysis of the rootsock influence on 'Diamar'. DIA: 'Diamar'; R20: Rootpac® 20; R40: Rootpac® 40; GN: Garnem®. Due to the extension of this dataset, this information is only available in the extended data.

Annex 4

Supplementary Data 6.1. RNA-Seq data from the analysis of the rootsock influence on the scion. ISA: 'Isabelona'; GN: Garnem®; G8: 'GN-8'; LAU: 'Lauranne'. Due to the extension of this dataset, this information is only available in the extended data.

Supplementary Data 6.2. Differentially expressed genes (DEGs) of interest observed in scion samples from 'Isabelona'.

Supplementary Data 6.3. RNA-Seq data from the analysis of the scion influence on the rootstock. ISA: 'Isabelona'; GN: Garnem®; LAU: 'Lauranne'; G8: 'GN-8'. Due to the extension of this dataset, this information is only available in the extended data.

Annex 5

Montesinos, Á., Dardick, C., Rubio-Cabetas, M. J., and Grimplet, J. (2021) Polymorphisms and gene expression in the almond IGT family are not correlated to variability in growth habit in major commercial almond cultivars. *PLoS ONE* 16: e0252001. doi:10.1371/journal.pone.0252001.

PLOS ONE

RESEARCH ARTICLE

Polymorphisms and gene expression in the almond IGT family are not correlated to variability in growth habit in major commercial almond cultivars

Álvaro Montesinos[1,2], **Chris Dardick**[3], **María José Rubio-Cabetas**[1,2], **Jérôme Grimplet**[1,2]*

1 Centro de Investigación y Tecnología Agroalimentaria de Aragón (CITA), Unidad de Hortofruticultura, Gobierno de Aragón, Avda. Montañana, Zaragoza, Spain, **2** Instituto Agroalimentario de Aragón–IA2 (CITA-Universidad de Zaragoza), Calle Miguel Servet, Zaragoza, Spain, **3** Appalachian Fruit Research Station, United States Department of Agriculture—Agriculture Research Service, Kearneysville, WV, United States of America

* jgrimplet@cita-aragon.es

OPEN ACCESS

Citation: Montesinos Á, Dardick C, Rubio-Cabetas MJ, Grimplet J (2021) Polymorphisms and gene expression in the almond IGT family are not correlated to variability in growth habit in major commercial almond cultivars. PLoS ONE 16(10): e0252001. https://doi.org/10.1371/journal.pone.0252001

Editor: Sara Amancio, Universidade de Lisboa Instituto Superior de Agronomia, PORTUGAL

Received: May 7, 2021

Accepted: September 29, 2021

Published: October 13, 2021

Peer Review History: PLOS recognizes the benefits of transparency in the peer review process; therefore, we enable the publication of all of the content of peer review and author responses alongside final, published articles. The editorial history of this article is available here: https://doi.org/10.1371/journal.pone.0252001

Data Availability Statement: All relevant data are within the manuscript and its Supporting Information files.

Abstract

Almond breeding programs aimed at selecting cultivars adapted to intensive orchards have recently focused on the optimization of tree architecture. This multifactorial trait is defined by numerous components controlled by processes such as hormonal responses, gravitropism and light perception. Gravitropism sensing is crucial to control the branch angle and therefore, the tree habit. A gene family, denominated IGT family after a shared conserved domain, has been described as involved in the regulation of branch angle in several species, including rice and Arabidopsis, and even in fruit trees like peach. Here we identified six members of this family in almond: *LAZY1*, *LAZY2*, *TAC1*, *DRO1*, *DRO2*, *IGT-like*. After analyzing their protein sequences in forty-one almond cultivars and wild species, little variability was found, pointing a high degree of conservation in this family. To our knowledge, this is the first effort to analyze the diversity of IGT family proteins in members of the same tree species. Gene expression was analyzed in fourteen cultivars of agronomical interest comprising diverse tree habit phenotypes. Only *LAZY1*, *LAZY2* and *TAC1* were expressed in almond shoot tips during the growing season. No relation could be established between the expression profile of these genes and the variability observed in the tree habit. However, some insight has been gained in how *LAZY1* and *LAZY2* are regulated, identifying the *IPA1* almond homologues and other transcription factors involved in hormonal responses as regulators of their expression. Besides, we have found various polymorphisms that could not be discarded as involved in a potential polygenic origin of regulation of architectural phenotypes. Therefore, we have established that neither the expression nor the genetic polymorphism of IGT family genes are correlated to diversity of tree habit in currently commercialized almond cultivars, with other gene families contributing to the variability of these traits.

Funding: Research was funded by the grants RTA2014-00062-00-00 (MJRC, JG, AM), RTI-2018-094210-R-100 (MJRC, JG, AM) and FPI-INIA CPD2016-0056 (AM) from the Spanish Research State Agency (AEI) (https://www.ciencia.gob.es/portal/site/MICINN/aei). The funders had no role in study design, data collection and analysis, decision to publish, or preparation of the manuscript.

Competing interests: The authors have declared that no competing interests exist.

Introduction

In the last decade, more intensive almond orchards have become the predominant model in the Mediterranean areas, in order to increase productivity and to reduce labor cost [1]. Under this scenario, there is a growing interest in developing almond cultivars more adapted to mechanical pruning and presenting a natural branching that reduces pruning cost to achieve the desired tree structure. In consequence, optimized cultivars need to have low vigor, reasonable branching and an upright overall architecture.

Tree architecture is a highly complex trait defined by the sum of phenotypic components that influence the three-dimensional shape of the tree. It involves growth direction, growth rhythm, branching mode, position of the branches, the sexual differentiation of meristems and the length of axillary shoots [2]. Tree architecture is affected by environmental parameters such as light perception, gravity sensing, sugar availability or nutrients supply that take part in the plant physiological and hormonal regulation [3–5].

Two physiological processes that affect the plant architecture are apical dominance and the lateral bud outgrowth. Auxins act as the principal factor in the control of apical dominance. This hormone is synthesized at the apical leaves and transported throughout the plant, inhibiting lateral bud outgrowth. It promotes strigolactone (SL) biosynthesis, which is able to translocate to the bud and stop bud outgrowth [6, 7]. Cytokinins (CKs) act antagonistically to SLs, promoting Shoot Apical Meristem (SAM) differentiation and therefore bud outgrowth [8, 9]. Sugar availability has also been described as a positive regulator of bud outgrowth [10, 11]. These processes are essential for shaping the plant structure, although the overall tree habit, which is defined by the relative angle of the branches, is essentially regulated by two responses: light perception and gravitropism.

Light perception regulates both the growth and the direction of lateral branches. It is based on the ratio between red light and far red light (R:FR), captured by phytochrome photoreceptors phyA and phyB. When the R:FR is low, phyA is activated while phyB is inhibited, which sets off the inhibition of bud outgrowth, redistributing the auxin flux and focusing plant efforts in the growth of the primary axis [12–15].

Gravitropism is the main regulator of the branching angle. Its regulation occurs in specific cells called statocytes, where organelles containing large starch grains, called amyloplasts, act as gravity sensors [16]. These organelles sediment in the direction of the gravitational vector, triggering a signal which involves the opening of ion channels and the reorganization of the cytoskeleton [17–19]. This response leads to a relocation of auxin carriers PIN3 and PIN7 changing the direction of the auxin flux, which provokes a differential growth and a curvature in the opposing direction of the gravitational vector [20–22].

LAZY1 has been described extensively as an influential factor in the control of plant architecture since its characterization in *Oryza sativa* (rice) as a regulator of tiller angle in agravitropic mutants [23–25]. Orthologs of this gene were found in *Arabidopsis thaliana* and *Zea mays* (maize), leading to the characterization of the same family in these species [26–28]. This family also includes *DRO1*, which was initially reported as an influential factor of root architecture in rice [29, 30]. *LAZY1* is related to *TAC1*, which is also involved in plant architecture regulation. *TAC1* was first identified in rice mutants with increased tiller angle, and it has also been characterized in Arabidopsis [31, 32]. *TAC1* differs from the rest of the family, denominated IGT family, in its lack of an EAR-like conserved domain denominated CCL domain located in the C-terminal region, which consists of 14 aminoacids [31, 33]. This conserved region is essential for the function and subcellular localization of IGT proteins. Since *LAZY1* and *TAC1* promote opposite phenotypes, and due to the lack of the CCL conserved domain, *TAC1* has been proposed as a negative regulator of *LAZY1* activity, in an upstream capacity [31, 33, 34]. However, the specific mechanism of the interaction between *LAZY1* and *TAC1* interaction is yet to be discovered [35].

The involvement of IGT family genes in gravitropism has been described in Arabidopsis and rice, acting as mediators between the sedimentation of statoliths gravity sensors and the relocation of auxin PIN carriers [33, 36–38]. Although a direct interaction with the phyA-phyB system is yet to be discovered, *TAC1* expression is influenced by the light perception regulator *COP1*, which would provide for integration between light and gravity responses [39].

The analysis of the mutation *br* in *Prunus persica* (peach), which is related to vertically oriented growth of branches, led to the annotation of an ortholog of *TAC1* [31]. Further studies have described the involvement of *TAC1* in auxin response mechanisms within different branching genotypes in peach, proving that the mechanisms involved in the control of the growth habit are conserved to a certain point in *Prunus* species [40, 41].

A total of 6 members of the IGT family have been found in *Prunus dulcis*: *LAZY1*, *LAZY2*, *DRO1*, *DRO2*, *IGT-like*, *TAC1*. With the exception of *TAC1*, all of them have the five conserved regions described in Arabidopsis [33]. In this study we carried out a genomic comparison for these six genes in forty-one almond cultivars and wild species with different growth habit phenotypes. Moreover, we analyzed the gene expression of the IGT family members in fourteen selected cultivars and searched for variants in their promoter region. Posteriorly, *LAZY1* and *LAZY2* promoters were inspected to identify regulatory elements (REs) associated to transcription factors (TFs) that could be involved in the regulation of *LAZY1* and *LAZY2*. Twenty-one TFs were selected due to its described function or its presence in growing shoot tips in previous studies and the analysis of their gene expression was carried out.

Material and methods

Almond tree populations

Forty-one cultivars and wild species (S1 File), whose genome had been previously obtained as part of the almond sequencing consortium [42] were selected to perform the comparative analysis of the IGT family protein sequences (S2 File). From these, twenty-seven cultivars were phenotyped for growth habit (S1 File), using a scale from 1 to 5 according UPOV guidelines: 1 = upright (< 60˚), 2 = somewhat upright (60˚ - 80˚), 3 = semi-open (80˚ - 100˚), 4 = open (100˚ - 120˚), 5 = weeping (> 120˚) [43]. Fourteen cultivars of agronomical interest were selected to analyze the gene expression of the IGT family members. Ten out of these fourteen were chosen to analyze the expression of twenty-one transcription factors (Table 1).

Comparative genomics

The cultivar genomes were assembled against the *P. dulcis* Texas Genome v2.0 [42] (https://www.rosaceae.org/analysis/295). Adapter sequences were removed by processing the raw reads sequences of the 41 cultivars with Trimmomatic v0.36.6 [44]. Alignments were performed using the Bowtie2 package (Galaxy Version 2.3.4.3) [45, 46]. Variant calling to detect SNPs was performed with the FreeBayes package (Galaxy Version 1.1.0.46–0) [47]. SNPs were filtered with the PLINK package (Galaxy Version 2.0.0) [48, 49] using the following parameters: read depth (DP) = 10; alternated allele observation count (AO) = 0.2. Promoter regions of the IGT family members were analyzed up to 2,000 pb upstream the start codon. All procedures were carried out using the Galaxy platform.

Phylogenetic tree

The evolutionary history was inferred by using the Maximum Likelihood method and Poisson correction model [50]. The tree with the highest log likelihood (-5447.29) is shown. Initial tree (s) for the heuristic search were obtained automatically by applying Neighbor-Join and BioNJ

Table 1. List of cultivars selected for the gene expression analysis of the IGT family members.

Cultivar	Tree habit
'Forastero' (FOR)	Upright
'Bartre' (BAR)	Upright
'Ferragnes' (FER)	Somewhat upright
'Garfi' (GAR)	Somewhat upright
'Garnem' (GN)	Somewhat upright
'Diamar' (DIA)	Somewhat upright
'Marinada' (MAN)	Somewhat upright
'Soleta' (SOL)	Semi-open
'Marcona' (MAC)	Semi-open
'Vairo' (VAI)	Semi-open
'Isabelona' (ISA)	Semi-open
'Vialfas' (VIA)	Semi-open
'Guara' (GUA)	Open
'Desmayo Largueta' (DLA)	Weeping

The ten cultivars in bold were posteriorly chosen to study the expression of transcriptions factors associated to *LAZY1* and *LAZY2* promoters. Overall tree habit phenotype for each cultivar is described categorically according UPOV guidelines.

https://doi.org/10.1371/journal.pone.0252001.t001

algorithms to a matrix of pairwise distances estimated using a JTT model, and then selecting the topology with superior log likelihood value. This analysis involved 252 amino acid sequences. There were a total of 424 positions in the final dataset. Evolutionary analyses were conducted in MEGA X [51].

Quantitative real-time PCR (qPCR)

Tissue samples for the fourteen selected cultivars were gathered at the same day from adult trees at the end of summer (late August), when one-year old branches were developed, while maintaining an active growth. Cultivars were kept at an experimental orchard in Centro de Investigación y Tecnología Agroalimentaria de Aragón (CITA) (41˚43'29.4" N 0˚48'27.3" W). Five cm of the tip from one-year old lateral branches were collected. Each biological replicate consisted of three tips from the same tree. RNA extraction was performed from these samples using the CTAB method described previously [52] with some modifications [53–55]. Extracted RNA was quantified using a NanoDrop® ND-1000 UV-vis spectrophotometer (NanoDrop Technologies, Wilmington, DE, USA). RNA integrity was verified by electrophoresis on a 1% agarose gel. RNA samples (2500 ng) were reverse transcribed with SuperScript III First-Strand Synthesis System (Thermo Fisher Scientific, https://www.thermofisher.com) in a total volume of 21 μL according to the manufacturer's instructions. qPCR was performed using the Superscript III Platinum SYBR Green qRT-PCR Kit (Thermo Fisher Scientific, https://www.thermofisher.com). Each reaction was run in triplicate. Primers for the IGT family members were designed using the respective QUIAGEN CLC Genomics Workbench tool (QUIAGEN, https://digitalinsights.qiagen.com/). Actin primers were used as an internal control to normalize expression [56]. The reactions were performed using a 7900 DNA sequence detector (Thermo Fisher Scientific, https://www.thermofisher.com). In ten out of the previous fourteen cultivars (Table 1), an expression analysis for selected transcription factors (TFs) was performed in SGIker, UPV/EHU (Bizkaia, Spain) using a 48*48 Fluidigm array. Primer for the selected transcription factors (TFs) were designed using the online tool Primer3Plus [57]

(http://www.bioinformatics.nl/cgi-bin/primer3plus/primer3plus.cgi). Reactions were carried out using the Fluidigm BioMark HD Nanofluidic qPCR System combined with a GE 48*48 Dynamic Arrays (Fluidigm, https://www.fluidigm.com) and detection through EvaGreen fluorochrome (Bio-Rad Laboratories, https://www.bio-rad.com). CTs were obtained with Fluidigm Real-Time PCR Analysis Software version 4.1.3 (Fluidigm, https://www.fluidigm.com).

Promoter analysis

The promoter sequences of *LAZY1* and *LAZY2* genes, 1500–1800 bp upstream of the start codon, were analyzed in search of regulatory cis-elements. PlantCARE [58] (http://bioinformatics.psb.ugent.be/webtools/plantcare/html/) and New PLACE [59] (https://www.dna.affrc.go.jp/PLACE) were used to identify putative cis-elements and their correspondent binding factors.

Statistical analysis

Three biological replicates from different branches of the same tree were used. All the statistical analysis was carried out in R (https://cran.r-project.org/). Analysis of significance for expression analysis was performed using Kruskal-Wallis H test and comparison between means was performed with a Nemenyi test using the PMCMR R package [60].

Results and discussion

Prunus dulcis IGT family members

Six IGT family members were found in *P. dulcis* using BLASTp to search homologues from *P. persica* sequences. The *P. persica* nomenclature [61] was kept for *P. dulcis*: *LAZY1* (Prudul26A025589), *LAZY2* (Prudul26A030030), *DRO1* (Prudul26A032079), *DRO2* (Prudul26A028716), *IGT-like* (Prudul26A033016) and *TAC1* (Prudul26A020993). The phylogenetic analysis also revealed that LAZY1 and LAZY2 peptide sequences are closely related, as well as DRO1 and DRO2. TAC1 is more similar to the rest of the members than IGT-like even without the CCL domain (Fig 1, S2 File). Although little is known about IGT-like function, the high variability could suggest a less-essential activity, or at least less selective pressure on its amino acid sequence. DRO1 and DRO2 are the most conserved members among cultivars; DRO1 shares the same protein sequence for all the different cultivars and wild species (Fig 1, S2 File). Despite the fact that polymorphisms are observed trough the different cultivars, overall, the protein sequences of the IGT Family members are highly conserved, hinting to an essential role in tree architecture regulation (Fig 1, S2 File).

IGT family protein sequence

IGT family proteins share five conserved regions in Arabidopsis, with the exception of TAC1, which lacks the CCL domain in the 3' terminal, which comprise region V (Fig 2). While Regions I, II and V are remarkably conserved, regions III and IV differed more between members, which might indicate that their preservation is not as essential to keep their activity [33]. Furthermore, functional analysis in transgenic rescue experiments involving AtLAZY1 have shown that even proteins with mutated residues in these two regions are able to rescue the *Atlazy1* branch angle phenotype [62]. In *P. dulcis*, a similar display of conserved regions can be seen, with Regions I, II and V extremely conserved while more variability is observed in Regions III and IV (Fig 2). The high degree of conservation that these regions keep throughout plant species highlights its importance in plant regulation.

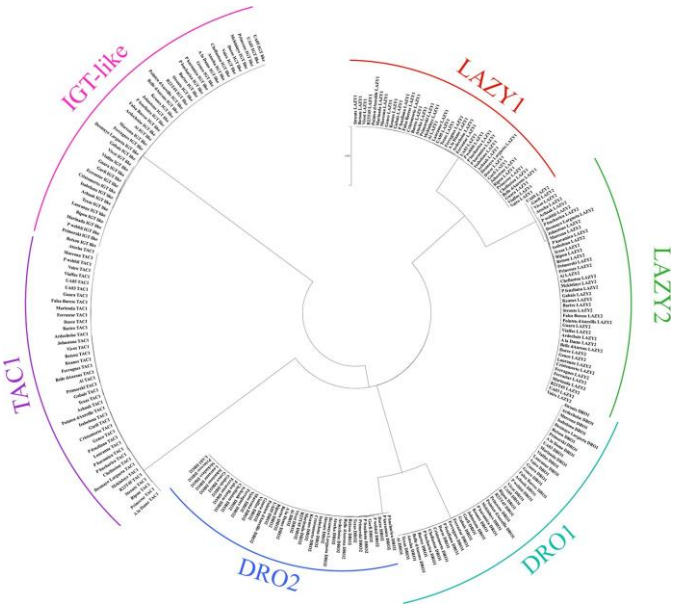

Fig 1. Phylogenetic tree of the six IGT family in forty-one cultivars and almond wild species. Cultivars are separated into groups by IGT family protein. Only variants in homozygosis were used for tree building. Names and recorded phenotype of each cultivar and wild species are available in S1 File, while protein sequences can be found in S2 File.

https://doi.org/10.1371/journal.pone.0252001.g001

Both LAZY1 and LAZY2 present mutated residues located in conserved regions in several cultivars and wild species. LAZY1 presents a mutation in Region I, I7 is replaced by a methionine (Table 2). Yoshihara and Spalding [62] reported that individuals with the residues 6 to 8 mutated showed significantly reduced ability to rescue the *atlazy1* branch angle defect nor they were able to mobilize the protein correctly to the plasma membrane in Arabidopsis. Therefore, this region seems to be essential for the correct functionality of the signal peptide. However, AtLAZY1 also presents a methionine in this position on the functional protein and the residue can be found mutated in other members of the IGT family, while W6, probably the

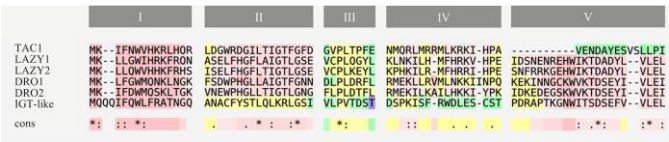

Fig 2. Amino acid sequence alignment of the five conserved regions between members of the IGT Family in *P. dulcis*. Sequence alignment analysis was performed using T-COFFEE [63]. Red indicates higher levels of conservation. Sequences from Texas cultivar were used as model (S2 File).

https://doi.org/10.1371/journal.pone.0252001.g002

Table 2. List of mutations of interest whether by their localization or by their predicted outcome.

Protein	Mutation	Prediction	Cultivars presenting the variant
LAZY1	I7M	Neutral	'Bartre' (1), 'Marinada' (2), **'Garfi' (2)**, **'Achaak' (2)**, 'Atocha' (2), **'Princesse' (2)**, ***P. kuramica* (2)**, 'Lauranne' (3), 'Marcona' (3), **'Vialfas' (3)**, 'Vivot' (3), **'Vairo' (3)**, 'Retsou' (3), **'Chellaston' (3)**, **'Isabelona' (3)**, ***P. bucharica* (3)**, **'Guara' (4)**, 'Primorski' (4), 'Cristomorto' (4), 'Ai' (4), **'Belle d'Aurons' (4)**, 'Genco' (4), 'Pointeu d'Aurielle' (4), **'Desmayo Largueta' (5)**
LAZY1	P18Q	Deleterious, codon change	'Lauranne' (3), 'Vialfas' (3), 'Vairo' (3), 'Chellaston' (3), 'Guara' (4), 'Ai' (4), 'Belle d'Aurons' (4)
LAZY1	I182_G184del	Deleterious, codon deletion	***P. bucharica* (3)**
LAZY2	A134E	Deleterious, codon change	'Bartre' (1), 'Ardechoise' (2), **'Garfi' (2)**, **'Atocha' (2)**, 'Princesse' (2), 'Lauranne' (3), 'Vialfas' (3), **'Vivot' (3)**, 'Retsou' (3), 'Guara' (4), 'Primorski' (4),' Belle d'Aurons' (4), 'Genco' (4)
LAZY2	R293G	Deleterious, codon change	'Bartre' (1), 'Achaak' (2), **'Marcona' (3)**, 'Chellaston' (3), 'Isabelona' (3), 'Ai' (4), *P. webbii* (4), **'Desmayo Largueta' (5)**
TAC1	D105_D108del	Neutral	*P. bucharica* (3)
TAC1	D108_E109insD	Deleterious, codon insertion	'Bartre' (1), 'Marinada' (2), 'Ardechoise' (2), 'Achaak' (2), 'Ferragnes' (2), 'Princesse' (2), *P. kuramica* (2), 'Marcona' (3), 'Vialfas' (3), 'Vivot' (3), 'Vairo' (3), 'Retsou' (3), 'Chellaston' (3), *P. bucharica* (3), 'Guara' (4), 'Primorski' (4), 'Ai' (4), 'Belle d'Aurons' (4), 'Pointeu d'Aureille' (4), *P. webbii* (4), 'Desmayo Largueta' (5)

Only cultivars presenting the mutation are reported. Overall tree habit description is displayed after each cultivar: (1) = Upright, (2) = Somewhat upright, (3) = Semi-open, (4) = Open, (5) = Weeping. Cultivars in bold present the mutation in both alleles. Complete protein sequences for LAZY1, LAZY2 and TAC1 can be found in S2 File. All found variants are listed in S3 File.

https://doi.org/10.1371/journal.pone.0252001.t002

indispensable residue, is conserved throughout the members of the family, both in Arabidopsis and almond. This fact would explain why the I7M mutation in homozygosis is not correlated with the observed overall tree habit amongst cultivars (Table 2). Several cultivars present a mutation in the Region IV of LAZY2, replacing R293 for a glycine, although no relation with their phenotype was established. As described by Nakamura *et al.* [33], conservation of Region IV is not required to maintain protein functionality.

A repetitive region of aspartic residues in TAC1 has been previously described as influential in the protein functionality. Differences in their length may lead to effects in the tree architecture; those who have long runs of aspartic acid residues presented upright phenotypes. Additional residues could affect the functionality or stability of the protein [40]. Two different mutations can be observed in our almond cultivars. While a number of cultivars carry the insertion of an additional Asp residue, a deletion of four Asp amino acids can be observed in the wild species *Prunus bucharica*. Nonetheless, in both cases the mutations are presented only in heterozygosis, thus this might explain why no phenotypic variations are observed (Table 2). No mutations in conserved regions were observed for DRO1 and DRO2. This lack of alterations in their sequence can be explained because *DRO1* and *DRO2*, unlike *LAZY1* and *LAZY2*, are described to act mainly in roots [30]. Yet, cultivars are predominantly selected by other aerial traits, such as fruit quality or yield, not existing any artificial selection of favored polymorphisms for tree architecture. The high variability observed in the IGT-like protein sequence combined with unknown function hinders the possibility to discern if any mutated amino acid could affect its activity. After an in-silico analysis using PROVEAN [64] and SNAP platforms (Rostlab, https://www.rostlab.org/) other SNPS and indels were highlighted as possible effectors of phenotypic variance. These were marked as deleterious by these online tools, though their effects were limited to a single codon change, deletion or insertion (Table 2). Moreover, no relation between these mutations and the described phenotypes was observed.

It was not possible to establish a relation between the sequence variants and the diversity in overall tree habit, even though mutations in conserved regions were detected in LAZY1 and

LAZY2 (Table 2), which correlate with previous studies indicating a relatively highly conserved structure for these proteins [33, 36]. In other species, mutations altering the phenotype produced a truncated protein or altered entire exons affecting protein functionality [61]. In our case, there are mutations modifying the protein sequence, however, none of them seem to lead to significant phenotypic impacts. In other herbaceous species these mutations lead to severe effects in cell wall structure that might be even more severe in tree, such as making the individuals that present these variants to be non-viable [61]. However, the difference in tree architecture might be related to quantitative variation of gene expression. To assess this, the expression of IGT family members was analyzed for a group of fourteen selected cultivars, in order to discover if the phenotypic differences could be due to its expression profile.

Expression profiling of IGT family members in selected almond cultivars

The expression levels of the six IGT family members were analyzed in shoot tips of fourteen almond cultivars on late August (Table 1). Expression analysis could provide an estimation of the protein activity. Previous studies in *P. persica* have shown than *LAZY1* and *TAC1* expression patterns are similar and both genes are expected to be coordinately regulated [31, 35, 41]. Since *TAC1* is believed to act antagonistically to *LAZY* activity, it could be that high levels of *LAZY1* or *LAZY2* expression were influenced by high levels of *TAC1* expression, or vice versa. Furthermore, in poplar (*Populus trichocarpa*), *TAC1* overexpression has been linked to broad-crown trees, while *LAZY1* expression remained constant through both narrow-crown and broad-crown trees [65]. Therefore, we used the *LAZY1*/*TAC1* and *LAZY2*/*TAC1* expression ratio as a descriptor of *LAZY1* and *LAZY2* molecular activity (Fig 3).

LAZY1/*TAC1* and *LAZY2*/*TAC1* did show differences in their ratio profile between cultivars. *LAZY1*/*TAC1* was found to have a higher ratio in 'Garnem' shoot tips, while upright cultivars 'Bartre' and 'Ferragnes' had the lowest levels of *LAZY1*/*TAC1* ratio. Other cultivars like 'Garfi', 'Vialfas' and 'Vairo' also presented relatively elevated *LAZY1*/*TAC1* ratios (Fig 3A). Highest levels of *LAZY2*/*TAC1* expression ratio were found in 'Garfi' and 'Vialfas', although the ratio in 'Garfi' was almost 2-fold higher. Unlike 'Garfi', *LAZY2* was not overexpressed in 'Vialfas' compared to the rest of cultivars, yet its lower levels of *TAC1* could indicate an imbalance in the *LAZY2*/*TAC1* ratio and, therefore, a higher *LAZY2* activity. 'Marcona' and 'Vairo' presented the lowest levels of the *LAZY2*/*TAC1* ratio (Fig 3B). It was not possible to find any

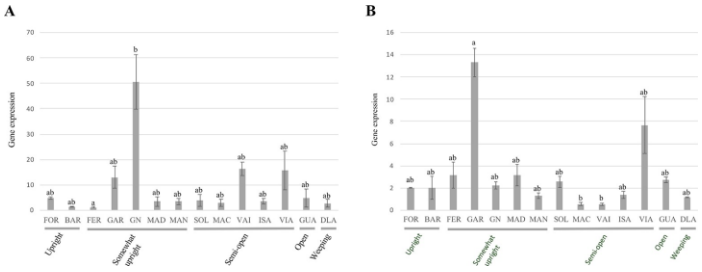

Fig 3. Expression analysis of IGT family genes in fourteen cultivars of interest. A, Ratio of relative gene expression between *LAZY1* and *TAC1*. B, Ratio of relative gene expression between *LAZY2* and *TAC1*. Cultivars abbreviatures are as follows: 'Forastero' (FOR), 'Bartre' (BAR), 'Ferragnes' (FER), 'Garfi' (GAR), 'Garnem' (GN), 'Diamar' (DIA), 'Marinada' (MAN), 'Soleta' (SOL), 'Marcona' (MAC), 'Vairo' (VAI), 'Isabelona' (ISA), 'Vialfas' (VIA), 'Guara' (GUA), 'Desmayo Largueta' (DLA). Letters above each bar indicate significance group, derived from Nemenyi's Test.

https://doi.org/10.1371/journal.pone.0252001.g003

transcripts of *DRO2* and *LAZY-like*, while *DRO1* expression was only detected in a reduced number of cultivars. This result is not unexpected, since *DRO* genes have been described acting mainly in root tissues [30].

'Garnem' is the only selection that is not a scion cultivar, but rather a hybrid peach x almond rootstock [66]. It has been described that the effect of IGT family members can vary within Prunus species, e.g., *TAC1* silencing in plum (*Prunus domestica*) mimicking the pillar peach genotype leads to more acute effects on tree architecture [40]. The peach genetic background in 'Garnem' could explain why the *LAZY1*/*TAC1* ratio levels are significantly higher compared to the rest of the analyzed genotypes. 'Garfi', the mother genotype of 'Garnem' shows a similar tree habit phenotype but different expression pattern. In 'Garfi', *LAZY1*/*TAC1* ratio is moderate and *LAZY2*/*TAC1* is elevated when compared with the rest of cultivars (Fig 3). However, 'Garfi' expression levels, while being higher than most cultivars, are quite similar for both members of the IGT family, presenting similar absolute values both ratios.

Although significant differences in gene expression were found on branches that presented vegetative growth, it was not possible to establish a correlation between expression levels and overall tree habit in these cultivars. Both 'Garfi' and 'Garnem' present an upright architecture, which would be tied to an expected predominance of *LAZY* expression. However, trees with more erect habits as 'Forastero' and 'Bartre' showed low or basal levels of *LAZY*/*TAC1* ratios. Expression levels of both *LAZY1* and *TAC1* in *P. persica* have been described to be related to seasonal changes, being higher in April [41]. However, they are expected to be expressed in any growing and active tissue [31]. In Mediterranean areas, almond displays vegetative growth through late spring to end of summer [43]; hence presenting an active growth in its shoot tips during this period. Even though high levels of *LAZY1* and *LAZY2* are presented exclusively in upright cultivars, it does not appear to be the only factor in shaping the almond tree habit, since cultivars with lower ratios present a more upright phenotype. It is possible that the ratio values changes are too low to observe an effect in the phenotype. In poplar, differences that led to a contrasting phenotype were at least an order of magnitude higher to those observed here [65]. Though high similarity has been reported between peach and almond genomes [42, 67], we did not observe in our set of cultivars the effect on the phenotype that has been described in peach [31, 40, 41]. The lack of correlation observed in the studied phase between gene expression and phenotype accompanied by the same case observed with their protein sequence hints to the IGT family may have suffered little to no selection at all in commercial almond orchards (Table 2, Fig 2). Not being unexpected since, until recently, almond breeding has been focused on improving traits related to either flowering or the fruit [68]. Thus, other regulatory pathways must be involved in the establishment of the overall tree habit.

Analysis of variants in *LAZY1* and *LAZY2* promoter regions

Although it is not possible to establish any clear correlation between diversity in tree habit and the expression levels of the IGT family members, the difference in *LAZY1* and *LAZY2* expression between the related 'Garfi' and 'Garnem' gives us a unique opportunity to study in detail the mechanisms involved in regulating their gene expression. Since these two selections present different expression profiles while their sequences are highly similar, divergences in their promoter region and their transcription factors (TFs) binding capabilities could explain the contrast in expression.

Promoter regions of *LAZY1*, *LAZY2* and *TAC1* were analyzed in search of variants within regulatory elements (REs) that might impact their expression and their respective ratios. Two mutations that could explain the differences observed in their expression profile were found in

Table 3. List of variants that correlate with the differences observed in gene expression affecting Regulatory Elements (REs) and their Transcription Factors (TFs) associated.

Gene	Position	RE	TF	Sequence	Alternative	Cultivars presenting the variant
LAZY1	Pd01:20652273	ABRE	*ABI3*	GCCATTTGTC	GCCATTCGTC	'Bartre' (1), **'Ferragnes' (2)**, 'Marinada' (2), 'Soleta' (3), 'Marcona' (3)
LAZY1	Pd01:20652273	E-Box	*RAVL1*	GCCATTTGTC	GCCATTCGTC	'Bartre' (1), **'Ferragnes' (2)**, 'Marinada' (2), 'Soleta' (3), 'Marcona' (3)
LAZY1	Pd01:20652307	TGGGCY-motif	*IPA1*	AGCCCA	GGCCCA	'Bartre' (1), **'Garnem' (2)**, **'Isabelona' (3)**, 'Guara' (4), 'Desmayo Largueta' (5)
LAZY2	Pd03:23958144	GTAC-motif	*IPA1*	GATAAGC	GATAAG	'Forastero' (1), 'Bartre' (1), **'Garfi' (2)**, 'Garnem' (2), 'Diamar' (2), **'Soleta' (3)**, **'Vialfas' (3)**

Only cultivars presenting the mutation are reported. Overall tree habit description is displayed after each cultivar: (1) = Upright, (2) = Somewhat upright, (3) = Semi-open, (4) = Open, (5) = Weeping. Cultivars in bold present the mutation in both alleles. All mutations in promoter sequences can be found in S4 File.

https://doi.org/10.1371/journal.pone.0252001.t003

LAZY1 and only one in *LAZY2* (Table 3). No significant variants were encountered in the *TAC1* promoter region.

Both *LAZY1* and *LAZY2* promoter regions presented a variant within a RE which is associated to the TF *IPA1* (Table 3), also known as *SPL9* in *A. thaliana* and *SPL14* in *O. sativa*. *IPA1* has been previously related with the regulation of shoot branching, acting predominantly repressing gene expression, though it has been described to also act in a promoting manner in few cases [69, 70]. In Arabidopsis, it has been reported that *IPA1* downregulates genes involved in responses related to auxin signaling [71]. While *LAZY1* promoter region presents the variant in a TGGGCY motif, *LAZY2* has a mutated GTAC motif (Table 3). *IPA1* has been described to interact with both motifs, and more specifically, directly with the second one [71]. Due to the nature of *IPA1* activity, it would be conceivable that it is acting in a repressive fashion. Therefore, if a mutation obstructs its binding to a RE, *LAZY1* and *LAZY2* would predictably be overexpressed. The mutations described might fit with this predicted outcome, especially in the *LAZY1* promoter region, where 'Garnem' presented the mutation, which displayed a remarkable high *LAZY1*/*TAC1* ratio due to an overexpression of *LAZY1* (Fig 3, Table 3). 'Garfi' also presented a mutation in the *LAZY2* promoter, which could be linked to its elevated *LAZY2*/*TAC1* ratio, though similar levels are observed in *LAZY1*/*TAC1* ratio where no mutation was described (Fig 3, Table 3). Nevertheless, other cultivars also present the variant in this RE without showing high ratio values, indicating that the mutation does not affect gene expression by itself, possibly being affected by other factors, i.e., *IPA1* expression level, protein activity or the interaction of other TFs.

Another mutation of interest was found in the *LAZY1* promoter region, affecting an E-box element, which has been described as a binding region of the transcription factor *RAVL1* (Table 3). The mutation exists in several selected varieties and is present in homozygosis in the cultivar 'Ferragnes' (Table 3), whose *LAZY1*/*TAC1* ratio was low (Fig 3). In rice, *RAVL1* has been described directly promoting genes involved in BRs and ET responses, acting in diverse metabolic processes [72, 73]. BRs act promoting branching and shoot growth [74]. The involvement of *RAVL1* in regulating *LAZY1* and therefore, gravity response, would place this gene at the crossover between both responses. Moreover, an ABRE element described as a binding region for the TF *ABI3* could be also altered by the same mutation. Nevertheless, *ABI3* is mainly involved in ABA signaling and predominantly in processes related to seed germination [75].

The mutations described in *LAZY1* and *LAZY2* promoter might explain the differences in their gene expression through cultivars. In particular, a mutation within a RE related to the TF *IPA1* in the *LAZY1* promoter may cause the high *LAZY1*/*TAC1* ratio observed in 'Garnem'.

Other mutations could also affect the expression profile, though more knowledge is needed to characterize their effect.

Analysis of expression *IPA1* homologues in *P. dulcis*

Due to its possible involvement in the regulation of *LAZY1* and *LAZY2* expression, a BLASTp search for IPA1 homologues in *P. dulcis* was conducted using atIPA1. Three *IPA1* homologues were found: *IPA1-like 1* (Prudul26A025211), *IPA1-like 2* (Prudul26A009750) and *IPA1-like 3* (Prudul26A016898). No non-synonymous mutations were found for any of the homologues. The expression levels of the three genes were analyzed in the shoot tips previously collected at the end of summer, in ten of the previous fourteen cultivars.

The expression profile through the ten cultivars was relatively stable for the three genes. Cultivars 'Vairo', 'Marinada' and 'Diamar' presented the highest expression levels (Fig 4). However, significant differences were only found in *IPA1-like 2*, which is overexpressed in 'Vairo' and repressed in 'Garfi'. In all three homologues, 'Garfi' presented low expression levels compared with the rest of cultivars. A similar profile can be observed in 'Vialfas' (Fig 4). As it is mentioned before, *IPA1* has been previously described acting as a repressor [69–71]. Therefore, the relative high ratio observed in both *LAZ1*/*TAC1* and *LAZY2*/*TAC1* in 'Garfi' might be associated with low *IPA1* activity. Although 'Vialfas' high *LAZY2*/*TAC1* ratio was mostly explained by *TAC1* repression, a similar phenomenon could underlie its profile. Nonetheless, no REs associated to *IPA1* were found in the analysis of the *TAC1* promoter.

'Garnem' showed similar expression levels that other cultivars for all three *IPA1* homologues, while displaying a remarkably high *LAZY1*/*TAC1* ratio. This overexpression could be caused by the mutation previously described in the *LAZY1* promoter, affecting a regulatory element associated to *IPA1* regulatory activity (Table 3). The mutation could disrupt *IPA1* interaction with the *LAZY1* promoter, and hence preventing *LAZY1* inhibition (Figs 3 and 4). Since no alterations were found in the *LAZY2* promoter, *IPA1* would be able to repress its expression, leading to the lower *LAZY2*/*TAC1* ratio observed in 'Garnem'.

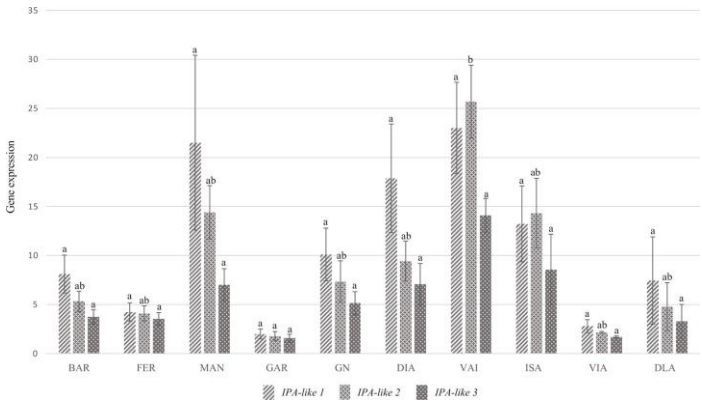

Fig 4. Expression analysis of *IPA1* homologues in *P. dulcis*. Cultivars abbreviatures are as follows: 'Bartre' (BAR), 'Ferragnes' (FER), 'Marinada' (MAN), 'Garfi' (GAR), 'Garnem' (GN), 'Diamar' (DIA), 'Vairo' (VAI), 'Isabelona' (ISA), 'Vialfas' (VIA), 'Desmayo Largueta' (DLA). Statistical analysis was performed for each gene separately. Letters above each bar indicate significance group derived from Nemenyi's Test.

https://doi.org/10.1371/journal.pone.0252001.g004

IPA1 homologues seem to act redundantly, presenting a similar expression profile for the three genes. As it can be observed in 'Garfi' and 'Vialfas', low expression levels may be behind high *LAZY1*/*TAC1* and *LAZY2*/*TAC1* ratios. Therefore, confirming *IPA1* genes as candidate repressors of *LAZY1* and *LAZY2* activity in *P. dulcis*.

Regulatory elements and transcription factors in *LAZY1* and *LAZY2* promoter regions

In order to identify TFs that might interact with REs present in *LAZY1* and *LAZY2* promoter regions, these regions were analyzed using New PLACE and PlantCARE online platforms. Twenty-one TFs were selected as preferred candidates, in addition to the previously described *RAVL1* and *ABI3*, which possible RE variability was noted within the varieties (Table 4). A majority of the TFs are involved in light responses and hormonal regulation. Similar functions have been described in the REs of *LAZY1*, *LAZY2* and *TAC1* in *Malus* x *domestica* [76].

Several TFs are involved in auxin responses. While *ARF1* REs are present in both promoter regions, *ARF2* and *IAA24* REs only are found in *LAZY1* promoter; all of them act as mediators in the auxin signaling pathway [77–82]. Other hormone regulatory pathways are represented among the TFs selected. *RAP2.2* and *RAP2.3* belong to the Group VII of ERF (Ethylene Response Factors) and are involved in various stress responses [83–86]. *RAP2.2* REs can be

Table 4. Localization in the LAZY1 and LAZY2 promoters of identified Transcription Factors (TFs).

Transcription factor	P. dulcis ID	Position *LAZY1*	Position *LAZY2*
ABI3	Prudul26A014736		-1314, -1166, -882, -878, 85
ARF1	Prudul26A011950	-1423	-1138, -474, 222
ARF2	Prudul26A008717	-1298, -344, -343	
ATAF1	Prudul26A030564	-1299, -345, -344	
GATA14	Prudul26A008840	-33	-1569, -129
GBF6	Prudul26A015068	-345	
GTL1	Prudul26A008868	-892, -890	
HB4	Prudul26A018199	-1325, -1152	-1475, -1314, -1102, -882, -878, 85
HB5	Prudul26A009108		-1246, -1011, -758, 115
IAA24	Prudul26A021243	-678	
LEAFY	Prudul26A028984	85	
MYC2	Prudul26A013616	-1474, -1296, -1325, -841, -777, -699, -418, -392, -340, -238, -223, -155	-1413, -908, -672, -304, -284, -164, 404
OBP4	Prudul26A018122	-869, -863	-1475, -1469, -516
PCL1	Prudul26A032278		-1139, -744, -743
phyA	Prudul26A016497		-559
RAP2.2	Prudul26A031706	-1454, -1420, -1374, -1370, -1290, -1203, -1120, -1111, -1046, -1023, -1019, -954, -802, -768, -719, -643, -518, -445, -420, -394, -361, -308, -291, -287, -269, -212, -180, -176, -112, -84, -35, -28, -18, 43, 58, 63, 75, 144, 280, 326'	-1619, -1564, -1267, -1257, -1232, -1113, -1105, -1069, -982, -975, -967, -949, -916, -894, -861, -747, -704, -692, -647, -604, -544, -502, -490, -483, -470, -416, -400, -384, -355, -353, -344, -289, -278, -257, -218, -211, -207, -195, -172, -124, -99, -82, -70, -64, -58, -51, -47, -18, 46, 149, 204, 296, 343, 385, 410
RAP2.3	Prudul26A030616	-1036, 8	-1090, -236
RAVL1	Prudul26A026729	-779, -157, 87, 85	-1439, -1277, 402, 402, 402, 403
SGR5	Prudul26A008399	-1426	
TGA1	Prudul26A032960	-1168	-58
WUS	Prudul26A011412		82

Position is displayed as relative to the start codon.

https://doi.org/10.1371/journal.pone.0252001.t004

found extensively repeated through both promoter regions. *LAZY2* promoter exhibits REs for *HB5*, a positive regulator of ABA and GA responses, and *WUS* a promotor of meristem proliferation in response to ET and auxin [87–89]. The *ATAF1* RE, that falls within the *LAZY1* promoter, is a key regulator of biotic and abiotic stress pathways, promoting ABA biosynthesis and regulating carbon metabolism genes or inducing the expression of genes involved in salt stress and detoxification responses [90–93]. Both promoters have REs for the TF OBP4, which is a negative regulator of cell expansion and root growth in response to ABA [94–96]. *GBF6* with a RE in *LAZY1* promoter, is repressed by sucrose and acts as a mediator between carbohydrates regulation and amino acid metabolism [97]. Sugars have been described as an essential part of branch outgrowth [11]. *TGA4*, with a RE described in both promoters, acts as a regulatory factor that mediate nitrate responses and induce root hair development in Arabidopsis roots [98, 99]. Light response TFs were also included in the selection. Both *LAZY1* and *LAZY2* promoters present a site for *MYC2* and *HB4*, which are involved in R:FR regulation and shade avoidance response [100, 101]. *PCL1 (*RE found in *LAZY2* promoter), is involved in the circadian clock [102, 103]. *GT-1*, found in both promoters, and its family member *GTL1*, only in *LAZY1*, have been described to modulate various metabolic processes in response to light perception [104]. *LAZY2* promoter presents a RE associated to the photoreceptor *phyA*, core regulator of the R:FR ratio light perception [12–15]. REs for *GATA14*, a zing finger TF belonging to the GATA family, are found in both promoters. GATA family of TFs have been described to integrate growth and light perception in several species [105, 106]. Although *LAZY1* and *LAZY2* have been primarily described as regulators of gravity responses, a lack of known TFs related to gravity perception or responses was found. Only *SGR5*, involved in early stages of shoot gravitropism, could be found in the *LAZY1* promoter [107]. LAZY1 promoter present a RE for *LEAFY*, which is a central regulator of inflorescence development [108]. Flower development and tree architecture has been previously linked in studies in *Malus* x *domestica* [109]. Between the TFs identified, there are a prevalence of genes related to several hormones. This points to IGT family genes being affected by numerous regulatory processes, as it could be expected hence their predicted role in a complex trait like tree habit. Gene expression was analyzed for these twenty-one TFs, not observing a connection between their levels and the previously reported *LAZY1*/*TAC1* and *LAZY2*/*TAC1* ratios (S1 Fig). In any case, this TFs collection influence gene expression and act in regulatory pathways differently, therefore, the lack of a wide correlation might be expected.

Conclusions

IGT family proteins are highly conserved in *P. dulcis*, especially within the five conserved regions and a limited number of variations found across all cultivars. Though no correlation with architectural phenotypes was observed, LAZY1 and LAZY2 did exhibit mutations with an expected impact on their functionality. In addition, despite differences in their expression profile, there was no direct relation between the overall tree habit and their expression. Although IGT family members are known to play a role in tree growth habit in other species, we do not see evidence of their influence in tree habit variability for a considerable number of almond cultivars. This is probably because no loss-of-function mutation has been selected in the set of forty-one studied major commercial almond cultivar that favor this trait, while those correlating with phenotype observed in other species alter significantly the protein structure. Until recently tree habit has not been an influential trait in almond breeding and these types of mutations were probably never selected. Furthermore, several of the mutations found in almond cultivars are present in heterozygosis, hence they could alter the phenotype if appear in homozygosis and be a foundation for possible future breeding efforts. Anyway, there are

many mechanisms leading to different tree habit, and even though *LAZY1* and *LAZY2* are not discriminant in current almond commercial cultivars, other families of genes must be involved in the regulation of almond tree habit. However, important aspects of the regulation of the IGT family in almond have been characterized. TFs *IPA1-like 1*, *IPA1-like 2*, *IPA1-like 3* seems to play a role in the regulation of *LAZY1* and *LAZY2* expression in addition to other TFs involved in hormonal regulation and light perception. In conclusion, almond tree habit depends on numerous factors, which outlines the necessity to better characterize the regulation of this trait and molecular mechanisms behind it both in almond orchards and other fruit trees.

Supporting information

S1 File. List of the 41 almond cultivars and wild species. Overall tree habit phenotype for each cultivar is described categorically according UPOV guidelines.
(XLSX)

S2 File. Protein sequences of the six IGT family members in the 41 almond cultivars and wild species. First entry of each cultivar or wild species contains homozygous variants while second entry contains both homozygous and heterozygous variants.
(FASTA)

S3 File. List of mutations affecting the protein sequence for the 41 almond cultivars and wild species. HOM: mutation in both alleles; HET: mutation in only one allele.
(XLSX)

S4 File. List of mutations affecting the promoter sequence of *TAC1*, *LAZY1* and *LAZY2* for the selected 14 almond cultivars. HOM: mutation in both alleles; HET: mutation in only one allele.
(XLSX)

S1 Fig. Heatmap of relative gene expression for identified transcription factors. TFs are separated into three groups, whether they are expected to interact with both promoters or only one of them. Heatmap was constructed in R (https://cran.r-project.org/).
(TIF)

Acknowledgments

The authors thank for technical and human support provided by SGIker of UPV/EHU.

Author Contributions

Conceptualization: Álvaro Montesinos, Chris Dardick, María José Rubio-Cabetas, Jérôme Grimplet.

Formal analysis: Álvaro Montesinos.

Funding acquisition: María José Rubio-Cabetas.

Investigation: Álvaro Montesinos.

Supervision: Chris Dardick, María José Rubio-Cabetas, Jérôme Grimplet.

Writing – original draft: Álvaro Montesinos, María José Rubio-Cabetas, Jérôme Grimplet.

Writing – review & editing: Chris Dardick.

References

1. Socias i Company R, Gomez Aparisi J, Alonso JM, Rubio-Cabetas MJ, Kodad O. Retos y perspectivas de los nuevos cultivares y patrones de almendro para un cultivo sostenible. ITEA Inf Tec Econ Agrar. 2009; 105(2): 99–116.
2. Costes E, Lauri PE, Regnard JL. Analyzing Fruit Tree Architecture: Implications for Tree Management and Fruit Production. Hort. Rev. 2006; 32:, 1–61. https://doi.org/10.1002/9780470767986.ch1
3. Hollender CA, Dardick C. Molecular basis of angiosperm tree architecture. New Phytol. 2015: 541–56. https://doi.org/10.1111/nph.13204 PMID: 25483362
4. Hearn DJ. Perennial Growth, Form and Architecture of Angiosperm Trees. In: Groover A, Cronk Q., editors. Comparative and Evolutionary Genomics of Angiosperm Trees. Plant Genetics and Genomics: Crops and Models, vol 21. Springer, Chams; 2016. pp. 179–204. https://doi.org/10.1007/7397_2016_25
5. Hill JL, Hollender CA. Branching out: new insights into the genetic regulation of shoot architecture in trees. Curr. Opin. Plant Biol. 2019; 47: 73–80. https://doi.org/10.1016/j.pbi.2018.09.010 PMID: 30339931
6. Barbier FF, Dun EA, Kerr SC, Chabikwa TG, Beveridge CA. An Update on the Signals Controlling Shoot Branching. Trends Plant Sci. 2019; 24: 220–236. https://doi.org/10.1016/j.tplants.2018.12.001 PMID: 30797425
7. Bennett T, Liang Y, Seale M, Ward S, Müller D, Leyser O. Strigolactone regulates shoot development through a core signalling pathway. Biol. Open. 2016; 5: 1806–1820. https://doi.org/10.1242/bio.021402 PMID: 27793831
8. Dun EA, Germain A de Saint, Rameau C, Beveridge CA. Antagonistic action of strigolactone and cytokinin in bud outgrowth control. Plant Physiol. 2012; 158: 487–498. https://doi.org/10.1104/pp.111.186783 PMID: 22042819
9. Tanaka M, Takei K, Kojima M, Sakakibara H, Mori H. Auxin controls local cytokinin biosynthesis in the nodal stem in apical dominance. Plant J. 2006; 45: 1028–1036. https://doi.org/10.1111/j.1365-313X.2006.02656.x PMID: 16507092
10. Barbier FF, Lunn JE, Beveridge CA. Ready, steady, go! A sugar hit starts the race to shoot branching. Curr. Opin. Plant Biol. 2015; 25: 39–45. https://doi.org/10.1016/j.pbi.2015.04.004 PMID: 25938609
11. Mason MG, Ross JJ, Babst BA, Wienclaw BN, Beveridge CA. Sugar demand, not auxin, is the initial regulator of apical dominance. Proc. Natl. Acad. Sci. 2014; 111: 6092–6097. https://doi.org/10.1073/pnas.1322045111 PMID: 24711430
12. Casal JJ. Shade Avoidance. Arab. B. 2012; 10, e0157. https://doi.org/10.1199/tab.0157 PMID: 22582029
13. Finlayson SA, Krishnareddy SR, Kebrom TH, Casal JJ. Phytochrome regulation of branching in arabidopsis. Plant Physiol. 2010; 152: 1914–1927. https://doi.org/10.1104/pp.109.148833 PMID: 20154098
14. Rausenberger J, Tscheuschler A, Nordmeier W, Wüst F, Timmer J, Schäfer E, et al. Photoconversion and nuclear trafficking cycles determine phytochrome A's response profile to far-red light. Cell. 2012; 146: 813–825. https://doi.org/10.1016/j.cell.2011.07.023 PMID: 21884939
15. Reddy SK, Finlayson SA. Phytochrome B promotes branching in Arabidopsis by suppressing auxin signaling. Plant Physiol. 2014; 164: 1542–1550. https://doi.org/10.1104/pp.113.234021 PMID: 24492336
16. Walker LM, Sack FD. Amyloplasts as possible statoliths in gravitropic protonemata of the moss Ceratodon purpureus. Planta. 1990; 181: 71–77. https://doi.org/10.1007/BF00202326 PMID: 24196676
17. Berut A, Chauvet H, Legue V, Moulia B, Pouliquen O, Forterre, Y. Gravisensors in plant cells behave like an active granular liquid. Proc Natl Acad Sci USA. 2018; 115(20): 5123–5128. https://doi.org/10.1073/pnas.1801895115 PMID: 29712863
18. Kolesnikov YS, Kretynin SV, Volotovsky I, Kordyum EL, Ruelland E, Kravets VS. Erratum to: Molecular mechanisms of gravity perception and signal transduction in plants. Protoplasma. 2016; 253: 1005. https://doi.org/10.1007/s00709-015-0934-y PMID: 26733389
19. Leitz G, Kang BH, Schoenwaelder MEA. Statolith sedimentation kinetics and force transduction to the cortical endoplasmic reticulum in gravity-sensing Arabidopsis columella cells. Plant Cell. 2009; 21: 843–860. https://doi.org/10.1105/tpc.108.065052 PMID: 19276442
20. Band LR, Wells DM, Larrieu A, Sun J, Middleton AM, French AP, et al. Root gravitropism is regulated by a transient lateral auxin gradient controlled by a tipping-point mechanism. Proc Natl Acad Sci USA. 2012; 109: 4668–4673. https://doi.org/10.1073/pnas.1201498109 PMID: 22393022

21. Kleine-Vehn J, Ding Z, Jones AR, Tasaka M, Morita MT, Friml J. Gravity-induced PIN transcytosis for polarization of auxin fluxes in gravity-sensing root cells. Proc Natl Acad Sci USA. 2010; 107: 22344–22349. https://doi.org/10.1073/pnas.1013145107 PMID: 21135243

22. Schüler O, Hemmersbach R, Böhmer M. A Bird's-Eye View of Molecular Changes in Plant Gravitropism Using Omics Techniques. Front Plant Sci. 2015; 6: 11766. https://doi.org/10.3389/fpls.2015.01176 PMID: 26734055

23. Abe K, Takahashi H, Suge H. Graviresponding sites in shoots of normal and lazy rice seedlings. Physiol Plant. 2004; 92: 371–374. https://doi.org/10.1111/j.1399-3054.1994.tb08823.x

24. Li P, Wang Y, Qian Q, Fu Z, Wang M, Zeng D, et al. LAZY1 controls rice shoot gravitropism through regulating polar auxin transport. Cell Res. 2007; 17: 402–410. https://doi.org/10.1038/cr.2007.38 PMID: 17468779

25. Yoshihara T, Iino M. Identification of the gravitropism-related rice gene LAZY1 and elucidation of LAZY1-dependent and -independent gravity signaling pathways. Plant Cell Physiol. 2007; 48: 678–688. https://doi.org/10.1093/pcp/pcm042 PMID: 17412736

26. Dong Z, Jiang C, Chen X, Zhang T, Ding L, Song W, et al. Maize LAZY1 mediates shoot gravitropism and inflorescence development through regulating auxin transport, auxin signaling, and light response. Plant Physiol. 2013; 163: 1306–1322. https://doi.org/10.1104/pp.113.227314 PMID: 24089437

27. Howard TP, Hayward AP, Tordillos A, Fragoso C, Moreno MA, Tohme J, et al. Identification of the maize gravitropism gene lazy plant1 by a transposon-tagging genome resequencing strategy. PLoS One 2014; 9(1). https://doi.org/10.1371/journal.pone.0087053 PMID: 24498020

28. Yoshihara T, Spalding EP, Iino M. AtLAZY1 is a signaling component required for gravitropism of the Arabidopsis thaliana inflorescence. Plant J. 2013; 74: 267–279. https://doi.org/10.1111/tpj.12118 PMID: 23331961

29. Guseman JM, Webb K, Srinivasan C, Dardick C. DRO1 influences root system architecture in Arabidopsis and Prunus species. Plant J. 2017; 89: 1093–1105. https://doi.org/10.1111/tpj.13470 PMID: 28029738

30. Uga Y, Sugimoto K, Ogawa S, Rane J, Ishitani M, Hara N, et al. Control of root system architecture by DEEPER ROOTING 1 increases rice yield under drought conditions. Nat Genet. 2013; 45: 1097–1102. https://doi.org/10.1038/ng.2725 PMID: 23913002

31. Dardick C, Callahan A, Horn R, Ruiz KB, Zhebentyayeva T, Hollender C, et al. PpeTAC1 promotes the horizontal growth of branches in peach trees and is a member of a functionally conserved gene family found in diverse plants species. Plant J. 2013; 75: 618–630. https://doi.org/10.1111/tpj.12234 PMID: 23663106

32. Yu B, Lin Z, Li H, Li X, Li J, Wang Y, et al. TAC1, a major quantitative trait locus controlling tiller angle in rice. Plant J. 2007; 52: 891–898. https://doi.org/10.1111/j.1365-313X.2007.03284.x PMID: 17908158

33. Nakamura M, Nishimura T, Morita MT. Bridging the gap between amyloplasts and directional auxin transport in plant gravitropism. Curr Opin Plant Biol. 2019; 52: 54–60. https://doi.org/10.1016/j.pbi.2019.07.005 PMID: 31446250

34. Sasaki S, Yamamoto KT. Arabidopsis LAZY1 is a peripheral membrane protein of which the Carboxy-terminal fragment potentially interacts with microtubules. Plant Biotechnol. 2015; 32: 103–108. https://doi.org/10.5511/plantbiotechnology.15.0106a

35. Hollender CA, Hill JL, Waite J, Dardick C. Opposing influences of TAC1 and LAZY1 on Lateral Shoot Orientation in Arabidopsis. Sci Rep. 2020; 10: 1–13. https://doi.org/10.1038/s41598-019-56847-4 PMID: 31913322

36. Taniguchi M, Furutani M, Nishimura T, Nakamura M, Fushita T, Iijima K, et al. The Arabidopsis LAZY1 Family Plays a Key Role in Gravity Signaling within Statocytes and in Branch Angle Control of Roots and Shoots. Plant Cell 2017; 29(8). https://doi.org/10.1105/tpc.16.00575 PMID: 28765510

37. Yoshihara T, Spalding EP. LAZY genes mediate the effects of gravity on auxin gradients and plant architecture. Plant Physiol. 2017; 175(2): 959–969. https://doi.org/10.1104/pp.17.00942 PMID: 28821594

38. Zhang N, Yu Hong, Yu Hao, Cai Y, Huang L, Xu C, et al. A core regulatory pathway controlling rice tiller angle mediated by the LAZY1-dependent asymmetric distribution of auxin. Plant Cell. 2018; 30: 1461–1475. https://doi.org/10.1105/tpc.18.00063 PMID: 29915152

39. Waite JM, Dardick C. TILLER ANGLE CONTROL 1 modulates plant architecture in response to photosynthetic signals. J Exp Bot. 2018; 69(20): 4935–4944. https://doi.org/10.1093/jxb/ery253 PMID: 30099502

40. Hollender CA, Waite JM, Tabb A, Raines D, Chinnithambi S, Dardick C. Alteration of TAC1 expression in Prunus species leads to pleiotropic shoot phenotypes. Hortic Res. 2018; 5: 1–9. https://doi.org/10.1038/s41438-017-0012-z PMID: 29423231

41. Tworkoski T, Webb K, Callahan A. Auxin levels and MAX1–4 and TAC1 gene expression in different growth habits of peach. Plant Growth Regul. 2015; 77: 279–288. https://doi.org/10.1007/s10725-015-0062-x

42. Alioto T, Alexiou KG, Bardil A, Barteri F, Castanera R, Cruz F, et al. Transposons played a major role in the diversification between the closely related almond and peach genomes: results from the almond genome sequence. The Plant J. 2020; 101(2): 455–472. https://doi.org/10.1111/tpj.14538 PMID: 31529539

43. Felipe AJ. El almendro: El material vegetal. Integrum, Lerida; 200.

44. Bolger AM, Lohse M, Usadel B. Trimmomatic: A flexible trimmer for Illumina sequence data. Bioinformatics. 2014; 30: 2114–2120. https://doi.org/10.1093/bioinformatics/btu170 PMID: 24695404

45. Langmead B, Trapnell C, Pop M, Salzberg SL. Ultrafast and memory-efficient alignment of short DNA sequences to the human genome. Genome Biol. 2009; 10(3): 1–10. https://doi.org/10.1186/gb-2009-10-3-r25 PMID: 19261174

46. Langmead B, Salzberg SL. Fast gapped-read alignment with Bowtie 2. Nat Methods. 2012; 9(4): 357–9. https://doi.org/10.1038/nmeth.1923 PMID: 22388286

47. Garrison E, Marth G. Haplotype-based variant detection from short-read sequencing. arXiv:1207.3907 [Preprint] 2012. Available from: https://arxiv.org/abs/1207.3907

48. Chang CC, Chow CC, Tellier LCAM, Vattikuti S, Purcell SM, Lee JJ. Second-generation PLINK: Rising to the challenge of larger and richer datasets. Gigascience. 2015; 4(1): 1–16. https://doi.org/10.1186/s13742-015-0047-8 PMID: 25722852

49. Purcell S, Neale B, Todd-Brown K, Thomas L, Ferreira MAR, Bender D, et al. PLINK: A tool set for whole-genome association and population-based linkage analyses. Am J Hum Genet. 2007; 81(3): 559–75. https://doi.org/10.1086/519795 PMID: 17701901

50. Zuckerkandl E., Pauling L. Evolutionary Divergence and Convergence in Proteins. Evol Genes Proteins. 1965; 97–166. https://doi.org/10.1016/b978-1-4832-2734-4.50017–6

51. Kumar S, Stecher G, Li M, Knyaz C, Tamura K. MEGA X: Molecular evolutionary genetics analysis across computing platforms. Mol Biol Evol. 2018; 35: 1547–1549. https://doi.org/10.1093/molbev/msy096 PMID: 29722887

52. Meisel L, Fonseca B, Gonzalez S, Baeza-Yates R, Cambiazo V, Campos R, et al. A rapid and efficient method for purifying high quality total RNA from peaches (Prunus persica) for functional genomics analyses. Biol Res. 2005; 38(1): 83–8. https://doi.org/10.4067/s0716-97602005000100010 PMID: 15977413

53. Chang S, Puryear J, Cairney J. A simple and efficient method for isolating RNA from pine trees. Plant Mol Biol Rep. 1993; 11: 113–116. https://doi.org/10.1007/BF02670468

54. Salzman RA, Fujita T, Zhu-Salzman K, Hasegawa PM, Bressan RA. An Improved RNA Isolation Method for Plant Tissues Containing High Levels of Phenolic Compounds or Carbohydrates. Plant Mol Biol Report. 1999; 17(1): 11–7. https://doi.org/10.1023/A:1007520314478

55. Zeng Y, Yang T. RNA isolation from highly viscous samples rich in polyphenols and polysaccharides. Plant Mol Biol Report. 2002; 20(4): 417. https://doi.org/10.1007/BF02772130

56. Hosseinpour B, Sepahvand S, Aliabad KK, Bakhtiarizadeh M, Imani A, Assareh R, et al. Transcriptome profiling of fully open flowers in a frost-tolerant almond genotype in response to freezing stress. Mol Genet Genomics. 2018; 293: 151–163. https://doi.org/10.1007/s00438-017-1371-8 PMID: 28929226

57. Untergasser A., Nijveen H, Rao X, Bisseling T, Geurts R, Leunissen JAM. Primer3Plus, an enhanced web interface to Primer3. Nucleic Acids Res. 2007; 35: 71–74. https://doi.org/10.1093/nar/gkm306 PMID: 17485472

58. Lescot M, Dehais P, Thijs G, Marchal K, Moreau Y, Van De Peer Y, et al. PlantCARE, a database of plant cis-acting regulatory elements and a portal to tools for in silico analysis of promoter sequences. Nucleic Acids Res. 2002; 30(1): 325–7. https://doi.org/10.1093/nar/30.1.325 PMID: 11752327

59. Higo K, Ugawa Y, Iwamoto M, Korenaga T. Plant cis-acting regulatory DNA elements (PLACE) database: 1999. Nucleic Acids Res. 1999; 27(1): 297–300. https://doi.org/10.1093/nar/27.1.297 PMID: 9847208

60. Pohlert T. The pairwise multiple comparison of mean ranks package (PMCMR). R package. 2014; 27: 9.

61. Waite JM, Dardick C. The roles of the IGT gene family in plant architecture: past, present, and future. Curr Opin Plant Biol. 2021; 59: 101983. https://doi.org/10.1016/j.pbi.2020.101983 PMID: 33422965

62. Yoshihara T, Spalding EP. Switching the direction of stem gravitropism by altering two amino acids in Atlazy1. Plant Physiol. 2020; 182(2): 1039–51. https://doi.org/10.1104/pp.19.01144 PMID: 31818902

63. Notredame C, Higgins DG, Heringa J. T-Coffee: A novel method for fast and accurate multiple sequence alignment. J Mol Bio. 2000; 302(1): 205–217. https://doi.org/10.1006/jmbi.2000.4042 PMID: 10964570

64. Choi Y, Chan AP. PROVEAN web server: A tool to predict the functional effect of amino acid substitutions and indels. Bioinformatics. 2015; 31(16): 2745–7. https://doi.org/10.1093/bioinformatics/btv195 PMID: 25851949

65. Xu D, Qi X, Li J, Han X, Wang J, Jiang Y, et al. PzTAC and PzLAZY from a narrow-crown poplar contribute to regulation of branch angles. Plant Physiol Biochem. 2017; 118: 571–578. https://doi.org/10.1016/j.plaphy.2017.07.011 PMID: 28787659

66. Felipe AJ. "Felinem", "Garnem", and "Monegro" almond x peach hybrid rootstocks. HortScience. 2009; 44(1): 196–7. https://doi.org/10.21273/HORTSCI.44.1.196

67. Goonetilleke SN, March TJ, Wirthensohn MG, Arus P, Walker AR, Mather DE. Genotyping by Sequencing in Almond: SNP Discovery, Linkage Mapping, and Marker Design. G3 Genes, Genomes, Genetics, 2018; 8(1): 161–172. https://doi.org/10.1534/g3.117.300376 PMID: 29141988

68. Gradziel TM. Almonds: botany, production and uses. Cabi; 2017.

69. Jiao Y, Wang Y, Xue D, Wang J, Yan M, Liu G, et al. Regulation of OsSPL14 by OsmiR156 defines ideal plant architecture in rice. Nat Genet. 2010; 42: 541–544. https://doi.org/10.1038/ng.591 PMID: 20495565

70. Miura K, Ikeda M, Matsubara A, Song XJ, Ito M, Asano K, et al. OsSPL14 promotes panicle branching and higher grain productivity in rice. Nat Genet. 2010; 42: 545–549. https://doi.org/10.1038/ng.592 PMID: 20495564

71. Lu Z, Yu H, Xiong G, Wang J, Jiao Y, Liu G, et al. Genome-wide binding analysis of the transcription activator IDEAL PLANT ARCHITECTURE1 reveals a complex network regulating rice plant architecture. Plant Cell. 2013; 25: 3743–3759. https://doi.org/10.1105/tpc.113.113639 PMID: 24170127

72. Xuan YH, Duan FY, Je B, Kim CM, Li TY, Liu JM, et al. Related to ABI3/VP1-Like 1 (RAVL1) regulates brassinosteroidmediated activation of AMT1;2 in rice (Oryza sativa). J Exp Bot. 2017; 68: 727–737. https://doi.org/10.1093/jxb/erw442 PMID: 28035023

73. Zhu XF, Yuan DP, Zhang C, Li TY, Xuan YH. RAVL1, an upstream component of brassinosteroid signalling and biosynthesis, regulates ethylene signalling via activation of EIL1 in rice. Plant Biotechnol J. 2018; 16: 1399–1401. https://doi.org/10.1111/pbi.12925 PMID: 29604166

74. Rameau C, Bertheloot J, Leduc N, Andrieu B, Foucher F, Sakr S. Multiple pathways regulate shoot branching. Front Plant Sci. 2015; 5: 1–15. https://doi.org/10.3389/fpls.2014.00741 PMID: 25628627

75. Dekkers BJW, He H, Hanson J, Willems LAJ, Jamar DCL, Cueff G, et al. The Arabidopsis Delay of Germination 1 gene affects Abscisic Acid Insensitive 5 (ABI5) expression and genetically interacts with ABI3 during Arabidopsis seed development. Plant J. 2016; 85(4): 451–65. https://doi.org/10.1111/tpj.13118 PMID: 26729600

76. Wang L, Cai W, Du C, Fu Y, Xie X, Zhu Y. The isolation of the IGT family genes in Malus × domestica and their expressions in four idiotype apple cultivars. Tree Genet Genomes. 2018; 14: 1–11. https://doi.org/10.1007/s11295-018-1258-9

77. Guilfoyle TJ. The PB1 Domain in Auxin Response Factor and Aux/IAA Proteins: A Versatile Protein Interaction Module in the Auxin Response. Plant Cell Online. 2015; 27: 33–43. https://doi.org/10.1105/tpc.114.132753 PMID: 25604444

78. Leyser O. Auxin Signaling. Plant Physiol. 2018; 76(1): 465–479. https://doi.org/10.1104/pp.17.00765 PMID: 28818861

79. Li G, Ma J, Tan M, Mao J, An N, Sha G, et al. Transcriptome analysis reveals the effects of sugar metabolism and auxin and cytokinin signaling pathways on root growth and development of grafted apple. BMC Genomics. 2016; 17: 1–17. https://doi.org/10.1186/s12864-015-2294-6 PMID: 26818753

80. Luo J, Zhou JJ, Zhang JZ. Aux/IAA gene family in plants: Molecular structure, regulation, and function. Int J Mol Sci. 2018; 19: 1–17. https://doi.org/10.3390/ijms19010259 PMID: 29337875

81. Okushima Y, Mitina I, Quach HL, Theologis A. AUXIN RESPONSE FACTOR 2 (ARF2): A pleiotropic developmental regulator. Plant J. 2005; 43: 29–46. https://doi.org/10.1111/j.1365-313X.2005.02426.x PMID: 15960614

82. Vert G, Walcher CL, Chory J, Nemhauser JL. Integration of auxin and brassinosteroid pathways by Auxin Response Factor 2. Proc Natl Acad Sci. 2008; 105: 9829–9834. https://doi.org/10.1073/pnas.0803996105 PMID: 18599455

83. Hinz M, Wilson IW, Yang J, Buerstenbinder K, Llewellyn D, Dennis ES, et al. Arabidopsis RAP2.2: An ethylene response transcription factor that is important for hypoxia survival. Plant Physiol. 2010; 153: 757–772. https://doi.org/10.1104/pp.110.155077 PMID: 20357136

84. Papdi C, Perez-Salamo I, Joseph MP, Giuntoli B, Bögre L, Koncz C, et al. The low oxygen, oxidative and osmotic stress responses synergistically act through the ethylene response factor VII genes RAP2.12, RAP2.2 and RAP2.3. Plant J. 2015; 82: 772–784. https://doi.org/10.1111/tpj.12848 PMID: 25847219

85. Nakano T, Suzuki K, Fujimura T, Shinshi H. Genome-wide analysis of the ERF gene family in Arabidopsis and rice. Plant Physiol. 2006; 140(2): 411–432. https://doi.org/10.1104/pp.105.073783 PMID: 16407444

86. Rubio-Cabetas MJ, Pons C, Bielsa B, Amador ML, Marti C, Granell A. Preformed and induced mechanisms underlies the differential responses of Prunus rootstock to hypoxia. J Plant Physiol. 2018; 228: 134–149. https://doi.org/10.1016/j.jplph.2018.06.004 PMID: 29913428

87. Johannesson H, Wang Y, Hanson J, Engstrom P. The Arabidopsis thaliana homeobox gene ATHB5 is a potential regulator of abscisic acid responsiveness in developing seedlings. Plant Mol Biol. 2003; 51: 719–729. https://doi.org/10.1023/a:1022567625228 PMID: 12678559

88. Stamm P, Topham AT, Mukhtar NK, Jackson MDB, Tome DFA, Beynon JL, et al. The transcription factor ATHB5 affects GA-mediated plasticity in hypocotyl cell growth during seed germination. Plant Physiol. 2017; 173: 907–917. https://doi.org/10.1104/pp.16.01099 PMID: 27872245

89. Shi B, Guo X, Wang Y, Xiong Y, Wang J, Hayashi K, et al. Feedback from Lateral Organs Controls Shoot Apical Meristem Growth by Modulating Auxin Transport. Dev Cell. 2018; 44: 204–216. https://doi.org/10.1016/j.devcel.2017.12.021 PMID: 29401419

90. Garapati P, Feil R, Lunn JE, Van Dijck P, Balazadeh S, Mueller-Roeber B. Transcription factor arabidopsis activating factor1 integrates carbon starvation responses with trehalosemetabolism. Plant Physiol. 2015; 169: 379–390. https://doi.org/10.1104/pp.15.00917 PMID: 26149570

91. Jensen MK, Lindemose S, Masi F, Reimer JJ, Nielsen M, Perera V, et al. ATAF1 transcription factor directly regulates abscisic acid biosynthetic gene NCED3 in Arabidopsis thaliana. FEBS Open Bio. 2013; 3: 321–327. https://doi.org/10.1016/j.fob.2013.07.006 PMID: 23951554

92. Liu Y, Sun J, Wu Y. Arabidopsis ATAF1 enhances the tolerance to salt stress and ABA in transgenic rice. J Plant Res. 2016; 129: 955–962. https://doi.org/10.1007/s10265-016-0833-0 PMID: 27216423

93. Zhao J, Missihoun TD, Bartels D. The ATAF1 transcription factor is a key regulator of aldehyde dehydrogenase 7B4 (ALDH7B4) gene expression in Arabidopsis thaliana. Planta. 2018; 248: 1017–1027. https://doi.org/10.1007/s00425-018-2955-1 PMID: 30027414

94. Ramirez-Parra E, Perianez-Rodriguez J, Navarro-Neila S, Gude I, Moreno-Risueno MA, del Pozo JC. The transcription factor OBP4 controls root growth and promotes callus formation. New Phytol. 2017; 213: 1787–1801. https://doi.org/10.1111/nph.14315 PMID: 27859363

95. Rymen B, Kawamura A, Schafer S, Breuer C, Iwase A, Shibata M, et al. ABA suppresses root hair growth via the OBP4 transcriptional regulator. Plant Physiol. 2017; 173: 1750–1762. https://doi.org/10.1104/pp.16.01945 PMID: 28167701

96. Xu P, Chen H, Ying L, Cai W. AtDOF5.4/OBP4, a DOF Transcription Factor Gene that Negatively Regulates Cell Cycle Progression and Cell Expansion in Arabidopsis thaliana. Sci Rep. 2016; 6: 1–13. https://doi.org/10.1038/s41598-016-0001-8 PMID: 28442746

97. Ma J, Hanssen M, Lundgren K, Hernandez L, Delatte T, Ehlert A, et al. The sucrose-regulated Arabidopsis transcription factor bZIP11 reprograms metabolism and regulates trehalose metabolism. New Phytol. 2011; 191: 733–745. https://doi.org/10.1111/j.1469-8137.2011.03735.x PMID: 21534971

98. Alvarez JM, Riveras E, Vidal EA, Gras DE, Contreras-Lopez O, Tamayo KP, et al. Systems approach identifies TGA1 and TGA4 transcription factors as important regulatory components of the nitrate response of Arabidopsis thaliana roots. Plant J. 2014; 80: 1–13. https://doi.org/10.1111/tpj.12618 PMID: 25039575

99. Canales J, Contreras-Lopez O, Alvarez JM, Gutierrez RA. Nitrate induction of root hair density is mediated by TGA1/TGA4 and CPC transcription factors in Arabidopsis thaliana. Plant J. 2017; 92: 305–316. https://doi.org/10.1111/tpj.13656 PMID: 28771873

100. Kazan K, Manners JM. MYC2: The master in action. Mol Plant. 2013; 6: 686–703. https://doi.org/10.1093/mp/sss128 PMID: 23142764

101. Sorin C, Salla-Martret M, Bou-Torrent J, Roig-Villanova I, Martinez-Garcia JF. ATHB4, a regulator of shade avoidance, modulates hormone response in Arabidopsis seedlings. Plant J. 2009; 59: 266–277. https://doi.org/10.1111/j.1365-313X.2009.03866.x PMID: 19392702

102. Helfer A, Nusinow DA, Chow BY, Gehrke AR, Bulyk ML, Kay SA. LUX ARRHYTHMO encodes a nighttime repressor of circadian gene expression in the Arabidopsis core clock. Curr Biol. 2011; 21: 126–133. https://doi.org/10.1016/j.cub.2010.12.021 PMID: 21236673

103. Onai K, Ishiura M. PHYTOCLOCK 1 encoding a novel GARP protein essential for the Arabidopsis circadian clock. Genes to Cells. 2005; 10: 963–972. https://doi.org/10.1111/j.1365-2443.2005.00892.x PMID: 16164597

104. Kaplan-Levy RN, Brewer PB, Quon T, Smyth DR. The trihelix family of transcription factors–light, stress and development. Trends Plant Sci. 2012: 17(3): 163–171. https://doi.org/10.1016/j.tplants.2011.12.002 PMID: 22236699

105. An Y, Zhou Y, Han X, Shen C, Wang S, Liu C, et al. The GATA transcription factor GNC plays an important role in photosynthesis and growth in poplar. J Exp Bot. 2020; 71: 1969–1984. https://doi.org/10.1093/jxb/erz564 PMID: 31872214

106. Luo XM, Lin WH, Zhu S, Zhu JY, Sun Y, Fan XY, et al. Integration of Light- and Brassinosteroid-Signaling Pathways by a GATA Transcription Factor in Arabidopsis. Dev Cell. 2010; 19: 872–883. https://doi.org/10.1016/j.devcel.2010.10.023 PMID: 21145502

107. Morita MT, Sakaguchi K, Kiyose SI, Taira K, Kato T, Nakamura M, et al. A C2H2-type zinc finger protein, SGR5, is involved in early events of gravitropism in Arabidopsis inflorescence stems. Plant J. 2006; 47: 619–628. https://doi.org/10.1111/j.1365-313X.2006.02807.x PMID: 16813575

108. Schultz EA, Haughn GW. LEAFY, a homeotic gene that regulates inflorescence development in arabidopsis. Plant Cell. 1991; 3: 771–781. https://doi.org/10.1105/tpc.3.8.771 PMID: 12324613

109. Foster TM, Watson AE, van Hooijdonk BM, Schaffer RJ. Key flowering genes including FT-like genes are upregulated in the vasculature of apple dwarfing rootstocks. Tree Genet Genomes. 2014; 10: 189–202. https://doi.org/10.1007/s11295-013-0675-z

Annex 6

Montesinos, Á., Thorp, G., Grimplet, J., and Rubio-Cabetas, M. (2021). Phenotyping Almond Orchards for Architectural Traits Influenced by Rootstock Choice. *Horticulturae* 7, 159. doi: 10.3390/horticulturae7070159.

horticulturae

MDPI

Article

Phenotyping Almond Orchards for Architectural Traits Influenced by Rootstock Choice

Álvaro Montesinos [1,2], Grant Thorp [3], Jérôme Grimplet [1,2] and María José Rubio-Cabetas [1,2,*]

[1] Centro de Investigación y Tecnología Agroalimentaria de Aragón (CITA), Unidad de Hortofruticultura, Gobierno de Aragón, Avda. Montañana 930, 50059 Zaragoza, Spain; amontesinos@cita-aragon.es (Á.M.); jgrimplet@cita-aragon.es (J.G.)
[2] Instituto Agroalimentario de Aragón—IA2 (CITA-Universidad de Zaragoza), Calle Miguel Servet 177, 50013 Zaragoza, Spain
[3] Plant & Food Research Australia Pty Ltd., 7 Bevan St, Albert Park, Melbourne, VIC 3206, Australia; grant.thorp@plantandfood.com.au
* Correspondence: mjrubioc@cita-aragon.es

Abstract: The cropping potential of almond (*Prunus amygdalus* (L.) Batsch, syn *P. dulcis* (Mill.)) cultivars is determined by their adaptation to edaphoclimatic and environmental conditions. The effects of scion–rootstock interactions on vigor have a decisive impact on this cropping success. Intensively planted orchards with smaller less vigorous trees present several potential benefits for increasing orchard profitability. While several studies have examined rootstock effects on tree vigor, it is less clear how rootstocks influence more specific aspects of tree architecture. The objective of this current study was to identify which architectural traits of commercially important scion cultivars are influenced by rootstock and which of these traits can be useful as descriptors of rootstock performance in breeding evaluations. To do this, 6 almond cultivars of commercial significance were grafted onto 5 hybrid rootstocks, resulting in 30 combinations that were measured after their second year of growth. We observed that rootstock choice mainly influenced branch production, but the effects were not consistent across the different scion–rootstock combinations evaluated. This lack of consistency in response highlights the importance of the unique interaction between each rootstock and its respective scion genotype.

Keywords: *Prunus dulcis*; branching; tree habit; rootstock-scion interaction; hybrid rootstock; vigor

Citation: Montesinos, Á.; Thorp, G.; Grimplet, J.; Rubio-Cabetas, M.J. Phenotyping Almond Orchards for Architectural Traits Influenced by Rootstock Choice. *Horticulturae* **2021**, *7*, 159. https://doi.org/10.3390/horticulturae7070159

Academic Editor: Alessandra Francini

Received: 4 June 2021
Accepted: 17 June 2021
Published: 22 June 2021

1. Introduction

Since its development, reported around 1800 BCE, grafting has been a crucial part of the propagation process for tree and vine crops [1]. As well as conferring traits of agronomic interest to trees in the orchard, the use of grafting and clonal rootstocks has facilitated the independent selection of scion and rootstock traits, thus improving breeding techniques. Rootstocks can be selected for relevant root system traits, including conferring resistance to pathogens such as root knot nematodes, endowing tolerance of alkaline and calcareous soils and promoting higher yields in non-irrigated soils [2]. Rootstocks can also influence scion phenotype such as fruit quality, yield, flowering time and tree vigor [3–7].

Nowadays, clonal rootstocks are utilized in numerous fruit and nut species of economic significance [7]. Their usage is widespread in almond (*Prunus amygdalus* (L.) Batsch, syn *P. dulcis* (Mill.)) orchards, and varieties are generally graft-compatible with both almond and peach (*P. persica* (L.) Batsch) rootstocks and their interspecific hybrids [2,8]. In the last decade, several new dwarfing rootstocks have been developed, conferring low and medium vigor to establish new more intensive and sustainable cropping systems.

Due to their global significance as a major tree fruit crop, rootstock effects on scion vigor have mostly been studied in apple (*Malus* × *domestica*). In these studies, rootstock effects have mainly been described in generic vigor-related parameters such as scion height,

trunk diameter, shoot length and frequency of branching [9,10]. Apple dwarfing rootstocks can also stimulate flowering in young trees, which indirectly affects shoot production and shoot vigor [11]. Young apple trees on dwarfing rootstocks form more floral buds and thus more axillary bourse shoots compared with the more vigorous terminal shoots produced from purely vegetative buds. Rootstock involvement in more specific aspects of tree architecture is less clear, and there is often a lack of consistency in responses among different cultivars, which highlights the importance of scion–rootstock interactions [10,12]. While previous studies with almond have described rootstock effects on vigor in generic terms [13,14], knowledge of rootstock influence on more specific architectural traits and their wider influence over almond tree architecture is still limited.

First introduced by Halle et al. [15], architectural analysis of trees provided a way to analyze the dynamics of plant development that is applicable to any species. The architectural tree models developed from this work are based on four major features: (i) temporal growth pattern, (ii) branching pattern, (iii) morphological differentiation of axes and (iv) sexual differentiation of meristems [16]. A total of 23 different architectural models were found in nature from all possible combinations of these features [15].

Temporal growth patterns predominantly have two features: rhythmic vs. continuous growth and determinate vs. indeterminate growth [17]. Continuous growth is a rare phenomenon and is not observed in *Rosaceae* species, whose shoots alternate periods of active growth and rest [18]. Determinate growth refers to the abortion or transformation of the terminal bud into a specialized structure [15]. If the apical meristem maintains indefinitely its function, then growth is indeterminate. Branching is a key aspect in defining tree structure. An axillary meristem may develop into a shoot at the same time as the extension of the parent axis, without a period of rest or dormancy, to form a sylleptic shoot [15]. Otherwise, the axillary meristem remains inactive and only develops into a shoot after a period of rest or dormancy, forming a proleptic shoot. Rhythmic (zonal) branching is constituted by groups of branched nodes followed by a succession of unbranched nodes. Diffuse branching is when shoots are disposed uniformly along the main axis [19]. Determinate and indeterminate growth patterns can lead to two different branching patterns, sympodial and monopodial, respectively [17]. Sympodial growth is when continued growth of the primary axis occurs via successive growth of axillary buds in subterminal positions, while monopodial growth occurs via continued extension of a single terminal meristem or bud [15]. The sum of all these features constitutes the architectural tree model.

Markovian models have been used to build general models for describing tree structure [20]. These methods analyze tree architecture as a succession of zones with a different proportion of node types whose arrangement is defined by transition probabilities, using branches as the study subject [16,21–23]. This approach has been applied to almond under different circumstances [24–26]. Although these models are useful for describing and visualizing repetitive patterns in tree architecture and branching formation, they are difficult to incorporate into genomic analyses, such as genome-wide association studies (GWAS). Therefore, accurate and objective measurements are needed. There have been few advancements in the analysis of these kinds of quantitative traits focused on their heritability or on the influence of the environment [27–29]. Recently, high-throughput phenotyping technologies such as T-LiDAR have been used in apple orchards to identify different architectural groups [30]. However, these methods fall short in describing the physiology and control processes determining tree shape and architecture or in distinguishing the nuanced changes that exist between different rootstock/scion combinations. Furthermore, there are considerable difficulties in measuring a substantial number of architectural traits in enough individuals in large trees modified by pruning. It is easier to record these traits of interest on young, unpruned trees.

The objective of the research presented here was to identify which architectural traits of the scion cultivar are influenced by rootstock genotype and which of these traits can be used as reliable descriptors of rootstock performance in breeding evaluations. We

did this by characterizing the genotype-specific effects of a selection of rootstocks on the architecture of a range of important scion cultivars.

2. Materials and Methods

2.1. Plant Material and Growth Conditions

For the experiment, 6 almond cultivars of agronomic interest were grafted onto 5 different commercial rootstocks, resulting in a total of 30 different combinations. The scion cultivars selected were 'Isabelona' (syn. Belona), 'Soleta', 'Guara', 'Vialfas', 'Diamar' (syn. Mardia) and 'Lauranne'. All are important commercial cultivars in Spain. The rootstocks were selected to represent a range of vigor responses in the grafted scion: 'GN-8', 'Densipac' (Rootpac® 20), 'Nanopac' (Rootpac® 40), 'Replantpac' (Rootpac® R) and 'Garnem' (GN15). All were hybrid rootstocks from different origins. 'Garnem' and 'GN-8' are both almond × peach (*P. amygdalus* (L.) Batsch, syn *P. dulcis* (Mill.). × *P. persica* (L.) Batsch) hybrid rootstocks, while the 3 others came from the commercial Rootpac® series including Rootpac® 40 (*P. amygdalus* (L.) Batsch, syn *P. dulcis* (Mill.). × *P. persica* (L.) Batsch), Rootpac® 20 (*P. cerasifera* × *P. besseyi*) and Rootpac® R (*P. cerasifera* × *P. amygdalus* (L.) Batsch, syn *P. dulcis* (Mill.)). Grafted plants were supplied by the Agromillora Iberia S.L. nursery in 2018 (Barcelona, Spain). Trees were planted during October 2018 at the Centro de Investigación y Tecnología Agroalimentaria de Aragón (CITA) experimental orchard El Vedado Bajo el Horno (Zuera, Zaragoza, 41°51′46.5″ N 0°39′09.2″ W). Trees were planted as a single stem and supported by a wooden stake. Trees were then left without pruning so that they could express their natural growth habit unaltered. Conventional orchard practices were used for weed control and drip irrigation. Soil type was calcareous with pH around 7–8.

2.2. Architectural Traits

Data collection was carried out during winter 2020 after two growing seasons from a total of 90 trees with 3 trees per scion–rootstock combination (Figure 1). In total, 24 parameters were considered as possible descriptors of tree architecture, divided into four categories: tree vigor, branching quantity and vigor, branching distribution and branching angle (Table 1). In this context, the primary growth axis of the tree was referred to as the trunk with axillary shoots forming directly on the trunk during the first season's growth. A branch was regarded as a second-order structure comprising multiple axillary shoots present during the second season's growth. The tree vigor category included five parameters. Total trunk length (TL) and number of internodes (Nb_IN) were determined from the graft union to the apex of the tree, and average internode length (IN_L) was calculated from those two measures. Trunk diameter was measured at both 20 mm above the graft union (d_Base) and 20 mm (d_Top) below the apex of the tree. Seven parameters were included in the branch quantity and vigor category. The total number of branches formed directly on the trunk (Nb_B) was recorded as was the number of axillary shoots formed on these branches (B_NbAS). Three categories of shoot length were used to describe branching frequency along the trunk; these categories were short (<10 mm), medium (10–20 mm) and long (>20 mm), denoted as Nb_sB, Nb_mB and Nb_lB, respectively. The ratio of branches by trunk length (BbyL) and trunk internodes (BbyIN) were calculated. Vigor was also recorded as branch diameter measured both at the base (B_dBase) and at the apex (B_dTop) of each branch along the trunk. The branch distribution category included the internode in which each branch was positioned along the trunk. Also determined from this value was the mean distribution of branches along the trunk (Dist_B), as well as the percentage of shoots in each third of the trunk from the basal to middle and distal sections (Dist_Down, Dist_Med and Dist_Up, respectively). Branching angle was recorded for branches formed directly on the trunk as the angle relative to the trunk at the base of the branch and at the branch tip. Three categories were used to describe branching angle: upright (<45°), semi-open (45–65°) and open (>65°), resulting in the following according to their base angle (Base_U, Base_SO and Base_O) and tip angle (Top_U, Top_SO and Top_O).

and Top (°). In total, 17 variables were established directly from measured data, while 7 variables were calculated combining some of the initial measurements.

Figure 1. Scion–rootstock combinations of 2-year-old almond trees show low and high vigor responses: (a) 'Guara' and (b) 'Diamar' grafted onto 'GN15' (left) and 'Garnem' (right) rootstocks, respectively.

Table 1. Parameters used to quantify aspects of almond tree architecture and the corresponding formula if parameters were calculated from other traits. Data were measured on the primary growth axis (trunk) or axillary branches of 2-year-old almond trees for 30–35 scion–rootstock combinations.

Type	Parameter	Formula	Trunk	Branches
Vigor	Number of internodes		Nb_IN	
	Length (mm)		Length	
	Average length of internodes (mm)	Length/Nb_IN	IN_L	
	Base diameter (mm)		d_Base	B_dBase
	Apex diameter (mm)		d_Top	B_dTop
Branch quantity	Number of branches		Nb_B	B_NbAS
	Ratio of branches by trunk internodes	Nb_B/Nb_IN	BbyIN	
	Ratio of branches by trunk length	Nb_B/Length	BbyL	
	Number of short branches (<10 mm)		Nb_sB	
	Number of medium branches (10–20 mm)		Nb_mB	
	Number of long branches (>20 mm)		Nb_lB	
Branch distribution	Mean distribution of branches trought the trunk	SUM(IN)/Nb_IN	Dist_B	
	Percentage of branches in the 1st third of the trunk	NbDown/Nb_B	Dist_Down	
	Percentage of branches in the 2nd third of the trunk	NbMed/Nb_B	Dist_Med	
	Percentage of branches in the 3rd third of the trunk	NbTop/Nb_B	Dist_Up	
Branching habit	Number of upright branches measured at the base (<45°)	NbTop/Nb_B	Base_U	
	Number of semiopen branches measured at the base (45°–65°)		Base_SO	
	Number of open branches measured at the base (>65°)		Base_O	
	Number of upright branches measured at the apex (<45°)		Top_U	
	Number of semiopen branches measured at the apex (45°–65°)		Top_SO	
	Number of open branches measured at the apex (>65°)		Top_O	

2.3. Statistical Analysis

All statistical analyses were carried out in the R platform (https://cran.r-project.org/, accessed on 11 June 2021). To identify which parameters were most influenced by rootstock genotype, a two-way ANOVA test was performed using the R stats package in order to establish which of the 24 measured parameters described in Table 1 were influenced by the rootstock genotype. Although the two-way ANOVA test allowed us to observe the influence on the variability of both the rootstock and the cultivar separately, we limited our focus to the effects of their interaction. Since all data were collected from the scion, the interaction of the two independent variables, rootstock and cultivar, described the extent of rootstock influence in aerial architectural traits. Parameters were selected as being influenced by rootstock choice when the p-value was lower than 0.1. Pearson's correlation coefficients were computed using the Hmisc R package (https://CRAN.R-project.org/package=Hmisc, accessed on 20 December 2020). Parameters correlating with an r value higher than +0.7 or lower than −0.7 were considered redundant, and a single parameter was conserved for analyses. Principal component analysis (PCA) was carried out using the R stats package with default parameters. The rootstock effect on each individual cultivar was evaluated using an ANOVA test to find significant differences. These were assessed with the Tukey's test ($p < 0.05$) using the agricolae R package (https://CRAN.R-project.org/package=agricolae, accessed on 24 January 2021).

3. Results

3.1. Rootstock Influence in Trait Variability

Out of the 24 starting parameters described in Table 1, 15 of these had a p-value lower than 0.10, and of these, 11 had a p-value lower than 0.05 (Table 2). Four scion vigor variables were identified as affected by the rootstock choice: Nb_IN, Length, IN_L and d_Top. However, a scion–rootstock interaction was observed for the diameter at the base of the scion (d_Base), which is equivalent to the trunk cross sectional area (TCSA), even though it could be expected that a more vigorous rootstock should have an effect on this trait. No influence was observed for the vigor parameters measured on the branches, such as B_dBase and B_dTop. All traits representing branch quantity were identified as influenced by the rootstock, suggesting that branching may be strongly affected by rootstock selection. Branch distribution parameters were predominately affected by rootstock genotype, with the exception of Dist_Med. Rootstock did not appear to affect branching angle, since only Top_SO might be characterized as being influenced by the rootstock. All 15 parameters with a p-value lower than 0.1 were considered as possibly influenced by the rootstock and were used in further analyses.

Table 2. Analysis of the effects of 30 almond scion–rootstock combinations on variability in architectural traits as affected by scion and rootstock genotype and the interaction between the two. Refer to Table 1 for abbreviations.

	Trait	Cultivar	Rootstock	Cultivar × Rootstock Interaction
Vigor	Nb_IN	2.21×10^{-6}	0.726	$\mathbf{4.21} \times 10^{-7}$
	Length	0.00263	0.23671	$\mathbf{4.01} \times 10^{-5}$
	IN_L	3.87×10^{-10}	0.000153	**0.080919**
	d_Base	4.06×10^{-10}	7.32×10^{-6}	0.168
	d_Top	8.29×10^{-5}	0.28228	**0.00696**
	B_dBase	8.74×10^{-8}	0.00189	0.23873
	B_dTop	0.0986	0.0686	0.1342

Table 2. *Cont.*

	Trait	Cultivar	Rootstock	Cultivar × Rootstock Interaction
Branch quantity	Nb_B	0.00037	1.14×10^{-12}	**0.01043**
	BbyIN	0.000152	1.20×10^{-7}	**0.001294**
	BbyL	0.001262	8.53×10^{-7}	**0.000649**
	B_NbAS	7.93×10^{-9}	0.00547	**0.05479**
	Nb_sB	3.47×10^{-5}	0.00036	**0.05135**
	Nb_mB	0.00208	8.33×10^{-7}	**0.01555**
	Nb_lB	0.00634	1.65×10^{-9}	**0.00814**
Branch distribution	Dist_B	0.00256	0.08757	**0.00303**
	Dist_Down	0.249	0.7719	**0.0288**
	Dist_Med	0.4682	0.0288	0.2746
	Dist_Up	0.0127	0.0116	**0.0169**
Branching habit	Base_U	0.7449	0.0541	0.9252
	Base_SO	0.182	0.0156	0.6591
	Base_O	0.0643	2.96×10^{-5}	0.3477
	Top_U	0.00336	7.06×10^{-7}	0.11616
	Top_SO	0.2424	0.3178	**0.0845**
	Top_O	0.0247	7.55×10^{-7}	0.6563

[1] Significant variability ($p < 0.1$) for the Cultivar:Rootstock interaction according to the two-way ANOVA test are in bold.

3.2. Identification of Relevant Parameters and Interaction between Different Categories

Correlation values between parameters were analyzed in a two-part approach. Firstly, variables belonging to the same category with a correlation value higher than +0.7 or lower than −0.7 were considered redundant, and a unique representative parameter was selected. Secondly, correlation values above +0.32 or below −0.32 between traits classified among different categories were contemplated as possible interrelated architectural processes.

Vigor parameters Length and Nb_IN were highly correlated, $r = 0.899$ (Table 3), which is not unexpected, since a longer main axis is expected to present a higher number of internodes. In addition, both variables were also negatively correlated with d_Top above the threshold. Length, as well as IN_L, were selected as descriptors of tree vigor.

For branch quantity parameters, BbyL and BbyIN presented a correlation value of +0.887 (Table 3). Both depended on the number of branches (Table 1), describing similar aspects of the phenotype. Despite BbyL having a lower *p*-value (Table 2), BbyIN was chosen as a branch quantity descriptor because it also described the potentiality of a given node to become a branch. Nb_sB and Nb_mB were positively correlated with Nb_B, presenting an $r > 0.7$ (0.722 and 0.801, respectively) (Table 3). Therefore, the amount of short and medium shoots (Nb_sB and Nb_mB) might depend primarily on the total number of branches. The number of long shoots (Nb_lB) appeared to be more independent of the total number of branches, $r = 0.397$. Thus, Nb_lB was kept with Nb_B as a branch quantity descriptor. Finally, B_NbAS, did not show correlation values above the 0.7 threshold with any other parameter, and so, with no reason to discard it, the B_NbAS parameter was added to the list of branch quantity descriptors.

For branch distribution parameters, both Dist_Down and Dist_Up were highly correlated with Dist_B, $r = -0.796$ and $r = 0.914$, respectively (Table 3). Since Dist_B describes the overall distribution of branches along the trunk and not their concentration in a single part of the main axis, it was taken as the unique branch distribution descriptor. As it was the only branching angle parameter at this point, conferring therefore little descriptive value, Top_SO was excluded from subsequent analyses. In summary, seven parameters were selected as representative of three different categories: Length, IN_L, Nb_B BbyIN, B_NbAS, Nb_lB and Dist_B.

Table 3. Pearson's correlation coefficients of variables comparing 30 almond scion–rootstock combinations, classified by which aspect of almond tree architecture they affect and selected by rootstock influence. Refer to Table 1 for abbreviations.

		Vigor				**Branch Quantity**							**Branch Distribution**			**Branch Habit**
		Nb_IN	**Length**	**IN_L**	**d_Top**	**Nb_AS**	**ASbyIN**	**ASbyL**	**ASNb_As**	**Nb_sAS**	**Nb_mAS**	**Nb_lAS**	**Dist_AS**	**Dist_Down**	**Dist_Up**	**Top_soAS**
Vigor	Nb_IN	1.000														
	Length	**0.899**	1.000													
	IN_L	−0.306	0.078	1.000												
	d_Top	**−0.707**	**−0.711**	0.075	1.000											
Branch quantity	Nb_AS	0.323	0.246	−0.169	−0.229	1.000										
	ASbyIN	−0.587	−0.563	0.233	0.472	0.437	1.000									
	ASbyL	−0.490	−0.591	−0.177	0.445	0.489	**0.887**	1.000								
	ASNb_As	−0.483	−0.485	0.067	0.501	−0.268	0.215	0.165	1.000							
Branch vigor	Nb_sAS	0.458	0.366	−0.224	−0.351	**0.722**	0.084	0.148	−0.394	1.000						
	Nb_mAS	0.257	0.219	−0.161	−0.234	**0.801**	0.281	0.361	−0.225	0.359	1.000					
	Nb_lAS	−0.214	−0.220	0.122	0.260	0.397	0.616	0.547	0.211	−0.155	0.186	1.000				
Branch distribution	Dist_AS	−0.656	−0.672	0.084	0.622	−0.088	0.452	0.409	0.393	−0.124	−0.113	0.113	1.000			
	Dist_Down	0.540	0.579	−0.026	−0.480	−0.041	−0.434	−0.398	−0.262	0.031	−0.031	−0.112	**−0.796**	1.000		
	Dist_Up	−0.596	−0.580	0.140	0.602	−0.174	0.362	0.308	0.372	−0.210	−0.190	0.128	**0.914**	−0.584	1.000	
Branch habit	Top_soAS	0.121	0.088	−0.045	−0.034	−0.016	−0.010	0.000	−0.072	−0.050	0.035	−0.007	0.022	−0.078	0.030	1.000

[1] Parameters with an *r* value higher than +0.7 or lower than −0.7 between members of the same category are in bold.

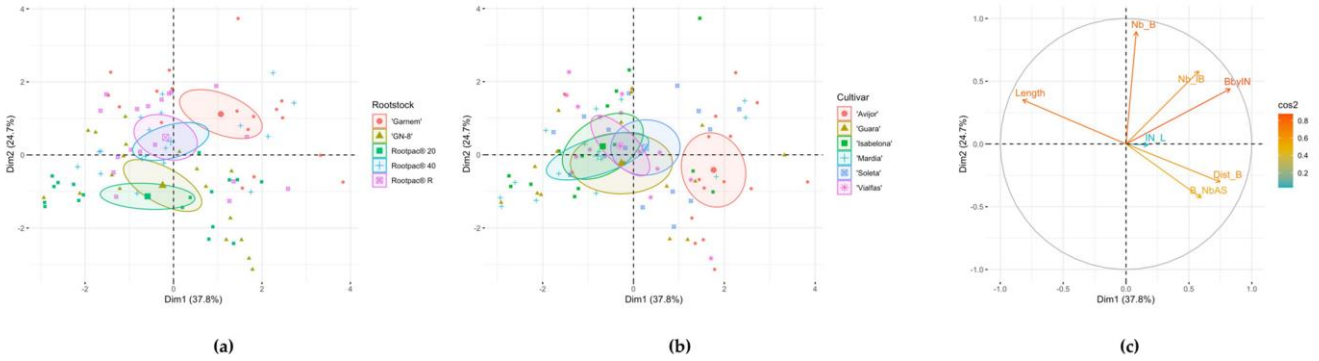

Figure 2. Principal component analysis (PCA) of seven non-redundant variables of 30 almond scion–rootstock combinations. (**a**) Distribution of scion–rootstock combinations classified by rootstock choice as a categorical variable with the first two components (Dim1 and Dim2), with concentration ellipses for each rootstock; (**b**) Distribution of scion–rootstock combinations classified by cultivar choice as a categorical variable with the first two components (Dim1 and Dim2), with concentration ellipses for each cultivar; (**c**) Distribution of the seven non-redundant variables with the first two components (Dim1 and Dim2). Contribution of each parameter to the components is colored from blue to red. Data were collected from 2-year-old trees. Refer to Table 1 for abbreviations.

4. Discussion

Combinations of five rootstocks and six scion varieties were compared in this study to identify a set of representative parameters of tree architecture influenced by rootstock choice. In the first instance, 24 parameters comprising 4 trait categories (Table 1) were sorted by how their variability was affected by rootstock/scion interaction (Table 2). Then, a Pearson's correlation test was performed for the 15 remaining parameters to identify highly correlated parameters from the same category and non-redundant variables. Correlations between parameters from different categories were also analyzed without eliminating parameters (Table 3). Only seven variables were selected after this step, and we studied how the scion–rootstock combinations affected these seven parameters and how different almond cultivars were affected by the rootstock (Table 4). Finally, these seven variables were submitted to a principal component analysis (PCA) to observe differential distributions of scion–rootstock combinations (Figure 2).

The seven parameters selected represented only three of the trait categories. Two of the parameters, Length and IN_L, belong to the category vigor. Branch quantity was represented by four different parameters Nb_B, B_NbAS. Nb_lB and BbyIN. Finally, Dist_B acts as unique representative of the branch distribution category. Practically no influence of the rootstock/scion interaction was detected in the branching angle category. It is of interest that the parameter IN_L and similar variables to Nb_B and B_NbAS were found to be relevant descriptors of apple tree architecture when selected by their genetic variability [29].

A shared trend was observed in the parameters influenced by rootstock genotype, with the majority of traits involved in processes related to the control of branching. It was observed that scion–rootstock combinations were primarily distributed differentially as a function of two opposing traits (Figure 2c). The Length parameter presented a negative value for the Dim1 axis, while all branch quantity (Nb_B, BbyIN, B_NbAS, Nb_lB) parameters had positive values in the Dim1 axis. Moreover, Length was negatively correlated with BbyIN and B_NbAS (Table 3).

Apical meristem maintenance and branching control are driven by the apical dominance exerted by the apex. Apical dominance refers to the suppression of axillary bud outgrowth during and/or after extension of the parent shoot, reducing the number of sylleptic and/or proleptic shoots, respectively. Gradziel [31] has described this feature to classify primary and secondary branching patterns in almond. Apical dominance is controlled by the terminal apical meristem on the parent shoot and by the apical meristems of subordinate axillary shoots [32–34]. Auxin is regarded as the main regulator of apical dominance, while other factors and hormones have been described as participating in branching regulation [35–45]. Specifically, strigolactones (SLs) are a crucial regulator of plant architecture [46,47]. Application of SL analogs has been proven able to reduce branching in tree species such as olive (*Olea europaea*) [48].

Depending on the strength of apical dominance present, we can observe opposing phenotypes as described by Gradziel [31]. If apical dominance is strong, due to the cultivar or the rootstock effect or both, dormancy is imposed, affecting branch quantity parameters and producing low BbyIN, Nb_B and B_NbAS values, while the apical meristem would continue its growth resulting in high Length values. In contrast, with weak apical dominance, the repression of axillary buds is reduced, and more branches will develop, described by high values in branch quantity parameters. Sylleptic shoots are generally formed in the lower portion of the parent shoot, while proleptic shoots are mainly formed from subterminal buds, immediately below the shoot apex, which is consistent with the positive correlation we found between Length and Dist_Down (Table 3). While the redistribution of resources to the formation of these lateral shoots may be expected to slow the growth of the main axis, resulting in determinate growth and low Length values, this effect appears to be mainly constrained to the formation of proleptic shoots formed after a period of rest. This would explain the negative correlation we found between Length and Dist_Up. Furthermore, while the presence of medium (Nb_mB) and short shoots (Nb_sB) correlates with the total number of shoots (Nb_B), we found the development of long shoots (Nb_lB)

to be more independent. This is due to the existence of few long shoots, appearing more predominantly in combination with low apical dominance but not necessarily in those with more branches (Table 4).

There is evidence from studies in peach that within the same genotype, rapid extension of the parent axis is associated with weak apical dominance and thus a high number of sylleptic axillary shoots [49]. Hence, in our study we often found more branches (Nb_B) with the more vigorous rootstocks than with the less vigorous rootstocks (Table 4). Rootpac® 20 and 'GN-8' can be described as dwarfing rootstocks, and their effects on the TCSA have been measured, proving a suppressing influence on tree vigor compared with more vigorous rootstock such as 'Garnem' and Rootpac® 40 [14,50]. We did not record a strong influence of parameters related to trunk diameter, such as d_Base (Table 2). Instead we found a stronger relationship between rootstock vigor and shoot production (Nb_B). We observed that Rootpac® 20 and 'GN-8' seemed to favor apical dominance, not promoting the formation of branches and maintaining an active apical meristem. In contrast, 'Garnem' appeared to negatively affect apical dominance, forming numerous branches, including long shoots (Nb_lB) and ceasing main axis growth earlier than other rootstocks (Table 4). It is possible that this growth response is a forerunner of the strong basitonic growth habit evident in commercial almond orchards. A less intense but similar effect can be observed when grafted onto Rootpac® 40. Rootpac® R presented a medium phenotype, with numerous branches but maintaining an active main axis (Table 4). This distribution can be observed in the PCA, where Rootpac® 20 and 'GN-8' were diametrically opposed to 'Garnem', with Rootpac® 40 and Rootpac® R between them (Figure 2a).

Cultivars grafted onto 'GN-8' showed shorter internodes than when grafted onto more vigorous rootstocks, such as 'Garnem' or Rootpac® 40 (Table 4). Internode elongation, which is mainly regulated by gibberellic acid (GA), has been described as being influenced by rootstock genotype [10,51]. However, SLs are also known to affect internode elongation independent of GA [52].

While there is ample evidence of rootstocks having a strong effect on scion tree architecture, the scion itself plays an essential part in branching regulation. Both 'Diamar' and 'Isabelona' showed a similar phenotype when grafted onto Rootpac® 20, favoring apical dominance, resulting in high Length values and reduced branching, observed through all branch quantity parameters. However, once grafted onto 'Garnem', only 'Isabelona' was able to maintain an active apical meristem, while 'Diamar' ceased growth of the main axis earlier (Table 4). The cultivar 'Lauranne' presented a typical low apical dominance phenotype, developing an elevated number of both branches (BbyIN) and axillary shoots (B_NbAS) and reduced trunk length when grafted onto almost every rootstock (Table 4). Rootpac® R was the only exception, promoting the formation of short horizontal branches (Nb_B) but maintaining an active main axis (Length) (Table 4).

While almond trees in commercial orchards show strong basitonic branching with strong lower limbs dominating the growth of the trunk, at the branch level, new shoot growth can predominate from basal, middle or distal sections of the parent shoot (basitonic, mesotonic and acrotonic branching, respectively) [18,24]. Dist_B, which measures branching distribution, is negatively correlated with Length and positively with BbyIN, connecting apical dominance and branch positioning (Table 3). A desirable ideotype might present the axillary shoots equally distributed through the axis, as described by Gradziel [31], presenting intermediate values for Dist_B, instead of being accumulated in a few internodes. Low apical dominance cultivar 'Lauranne' had consistent high Dist_B values (Table 4). In these combinations, the apical meristem ceases its growth early and long branches from the current season's growth form in the upper part of the trunk. 'Guara' presented a comparable phenotype to 'Lauranne', although the formation of branches from the current season's growth was more impaired by dwarfing rootstocks such as 'GN-8' and Rootpac® 20. A similar effect can be observed when cultivars are grafted onto 'Garnem' (Table 4). 'Soleta' displayed significant differences of Dist_B between rootstock combinations, presenting high values when grafted onto Rootpac® 20. However, this combination

also presented a reduced number of long shoots (Table 4). Thus, the high Dist_B values are due to the accumulation of a few short branches in the apex, not descriptive of a lack of apical dominance.

Although they are not distributed as clearly as in the rootstocks comparison, there is a certain degree of separation between some of the cultivars in the PCA. 'Lauranne' combinations were mildly distanced from the rest of the cultivar combinations. Combinations with 'Isabelona' as the cultivar are located predominantly in the opposite extreme, yet closer to the rest of combinations (Figure 2b). Apical dominance seems to be heavily influenced by rootstock choice in some cultivars, such as 'Diamar' or 'Soleta', but not in those that present a stronger control of this feature, such as 'Lauranne'. A similar phenomenon can be observed with 'Isabelona', where the rootstock effect is more diluted (Table 4). Hence, this illustrates the importance of a correct choice of rootstock when deciding what scion cultivar should be selected for field production.

No clear influence was observed on branch angle by the rootstock choice (Table 2). This could reflect the narrow range of branching angles among the scion cultivars selected for this study. Branch angle is a complex trait regulated by several processes, where light perception and gravity sensing have a main relevance, which are regulated primarily at the aerial part of the plant [36,53–55].

In conclusion, seven parameters were selected as descriptors of rootstock influence in almond scion architecture. The choice of rootstock affected scion cultivar architecture, modifying both apical dominance and branch parameters. 'Garnem' and Rootpac® 20 had an opposite influence on the architecture of the scion, as was observed in parameters such as Length or the number of branches (Nb_B), while mixed results were observed with other rootstocks. However, these processes are regulated by numerous physiological processes, and the final phenotype is not only the result of the interaction between the rootstock and the scion but also the result of rootstock and scion interaction with the environment. Cultivars with a strong or weak display of apical dominance, for example 'Lauranne' and 'Isabelona', were less affected by rootstock influence, while the other scion cultivars in this study were strongly influenced by rootstock choice. This highlights the importance of screening rootstock progeny with a number of scion genotypes, in view of the strong scion–rootstock genotype interactions. Thus, a better understanding of what is happening at the graft union and with other physiological and molecular aspects of scion–rootstock interactions is needed in order to decipher the nuanced changes that determine tree architecture across a range of scion–rootstock combinations.

Author Contributions: Conceptualization, Á.M. and M.J.R.-C.; methodology, Á.M., G.T. and M.J.R.-C.; formal analysis, Á.M.; investigation, Á.M. and M.J.R.-C.; data curation, Á.M.; writing—original draft preparation, Á.M., J.G. and M.J.R.-C.; writing—review and editing, G.T.; supervision, J.G. and M.J.R.-C.; project administration, M.J.R.-C.; funding acquisition, M.J.R.-C. All authors have read and agreed to the published version of the manuscript.

Funding: This research was funded by the Spanish Research State Agency (AEI), grant numbers RTI-2018-094210-R-100 and FPI-INIA CPD2016-0056. Funding for G.T. was provided through the National Tree Crop Intensification in Horticulture Program (AS18000), funded by the Hort Frontiers Advanced Production Systems Fund, part of the Hort Frontiers strategic partnership initiative developed by Hort Innovation (Australia), with co-investment from Plant & Food Research and contributions from the Australian Government.

Institutional Review Board Statement: Not applicable.

Informed Consent Statement: Not applicable.

Data Availability Statement: Not applicable.

Conflicts of Interest: The authors declare no conflict of interest. The funders had no role in the design of the study; in the collection, analyses, or interpretation of data; in the writing of the manuscript; or in the decision to publish the results.

References

1. Mudge, K.; Janick, J.; Scofield, S.; Goldschmidt, E.E. A History of Grafting. *Hortic. Rev.* **2009**, *35*, 437–493. [CrossRef]
2. Rubio-Cabetas, M.J.R.; Felipe, A.J.; Reighard, G.L. Rootstock Development. In *Almonds: Botany, Production and Uses*; Socias i Company, R., Gradizel, T.M., Eds.; CABI: Wallingford, UK, 2017; pp. 209–227.
3. Albacete, A.; Martínez-Andújar, C.; Martínez-Pérez, A.; Thompson, A.J.; Dodd, I.C.; Pérez-Alfocea, F. Unravelling rootstock×scion interactions to improve food security. *J. Exp. Bot.* **2015**, *66*, 2211–2226. [CrossRef] [PubMed]
4. Aloni, B.; Cohen, R.; Karni, L.; Aktas, H.; Edelstein, M. Hormonal signaling in rootstock-scion interactions. *Sci. Hortic.* **2010**, *127*, 119–126. [CrossRef]
5. Foster, T.M.; Celton, J.M.; Chagne, D.; Tustin, D.S.; Gardiner, S.E. Two quantitative trait loci, Dw1 and Dw2, are primarily responsible for rootstock-induced dwarfing in apple. *Hortic. Res.* **2015**, *2*, 9. [CrossRef]
6. Martínez-Ballesta, M.C.; Alcaraz-López, C.; Muries, B.; Mota-Cadenas, C.; Carvajal, M. Physiological aspects of rootstock-scion interactions. *Sci. Hortic.* **2010**, *127*, 112–118. [CrossRef]
7. Warschefsky, E.J.; Klein, L.L.; Frank, M.H.; Chitwood, D.H.; Londo, J.P.; von Wettberg, E.J.B.; Miller, A.J. Rootstocks: Diversity, Domestication, and Impacts on Shoot Phenotypes. *Trends Plant. Sci.* **2016**, *21*, 418–437. [CrossRef]
8. Felipe, A.J. "Felinem", "Garnem", and "Monegro" almond x peach hybrid rootstocks. *HortScience* **2009**, *44*, 196–197. [CrossRef]
9. Tworkoski, T.; Fazio, G. Effects of Size-Controlling Apple Rootstocks on Growth, Abscisic Acid, and Hydraulic Conductivity of Scion of Different Vigor. Int. J. *Fruit Sci.* **2015**, *15*, 369–381. [CrossRef]
10. Tworkoski, T.; Miller, S. Rootstock effect on growth of apple scions with different growth habits. *Sci. Hortic.* **2007**, *111*, 335–343. [CrossRef]
11. Seleznyova, A.N.; Tustin, D.S.; Thorp, T.G. Apple dwarfing rootstocks and interstocks affect the type of growth units produced during the annual growth cycle: Precocious transition to flowering affects the composition and vigour of annual shoots. *Ann. Bot.* **2008**, *101*, 679–688. [CrossRef]
12. Van Hooijdonk, B.M.; Woolley, D.J.; Warrington, I.J.; Tustin, D.S. Initial alteration of scion architecture by dwarfing apple rootstocks may involve shoot-root-shoot signalling by auxin, gibberellin, and cytokinin. *J. Hortic. Sci. Biotechnol.* **2010**, *85*, 59–65. [CrossRef]
13. Balducci, F.; Capriotti, L.; Mazzoni, L.; Medori, I.; Albanesi, A.; Giovanni, B.; Giampieri, F.; Mezzetti, B.; Capocasa, F. The rootstock effects on vigor, production and fruit quality in sweet cherry (*Prunus avium* L.). *J. Berry Res.* **2019**, *9*, 249–265. [CrossRef]
14. Lordan, J.; Zazurca, L.; Maldonado, M.; Torguet, L.; Alegre, S.; Miarnau, X. Horticultural performance of 'Marinada' and 'Vairo' almond cultivars grown on a genetically diverse set of rootstocks. *Sci. Hortic.* **2019**, *256*, 108558. [CrossRef]
15. Hallé, F.; Oldeman, R.A.A.; Tomlinson, P.B.; Hallé, F.; Oldeman, R.A.A.; Tomlinson, P.B. Forests and Vegetation. In *Tropical Trees and Forests*; Springer: Berlin/Heidelberg, Germany, 1978. [CrossRef]
16. Costes, E.; Lauri, P.-E.; Regnard, J.L. Analyzing Fruit Tree Architecture: Implications for Tree Management and Fruit Production. *Hort. Rev.* **2006**, *32*, 1–61. [CrossRef]
17. Barthélémy, D.; Caraglio, Y. Plant architecture: A dynamic, multilevel and comprehensive approach to plant form, structure and ontogeny. *Ann. Bot.* **2007**, *99*, 375–407. [CrossRef]
18. Costes, E.; Crespel, L.; Denoyes, B.; Morel, P.; Demene, M.-N.; Lauri, P.-E.; Wenden, B. Bud structure, position and fate generate various branching patterns along shoots of closely related Rosaceae species: A review. *Front. Plant. Sci.* **2014**, *5*, 666. [CrossRef]
19. Hallé, F. Branching in Plants. In *Branching in Nature*; Centre de Physique des Houches, Fleury, V., Gouyet, J.F., Léonetti, M., Eds.; Springer: Berlin/Heidelberg, Germany, 2001; Volume 14. [CrossRef]
20. Durand, J.B.; Guédon, Y.; Caraglio, Y.; Costes, E. Analysis of the plant architecture via tree-structured statistical models: The hidden Markov tree models. *New Phytol.* **2005**, *166*, 813–825. [CrossRef] [PubMed]
21. Guédon, Y.; Barthélémy, D.; Caraglio, Y.; Costes, E. Pattern analysis in branching and axillary flowering sequences. *J. Theor. Biol.* **2001**, *212*, 481–520. [CrossRef] [PubMed]
22. Costes, E.; Guédon, Y. Modelling branching patterns on 1-year-old trunks of six apple cultivars. *Ann. Bot.* **2002**, *89*, 513–524. [CrossRef] [PubMed]
23. Seleznyova, A.N.; Thorp, T.G.; Barnett, A.M.; Costes, E. Quantitative analysis of shoot development and branching patterns in Actinidia. *Ann. Bot.* **2002**, *89*, 471–482. [CrossRef]
24. Negrón, C.; Contador, L.; Lampinen, B.D.; Metcalf, S.G.; Dejong, T.M.; Guédon, Y.; Costes, E. Systematic Analysis of Branching Patterns of Three Almond Cultivars with Different Tree Architectures. *J. Am. Soc. Hortic. Sci.* **2013**, *138*, 407–415. [CrossRef]
25. Negrón, C.; Contador, L.; Lampinen, B.D.; Metcalf, S.G.; Guédon, Y.; Costes, E.; Dejong, T.M. How different pruning severities alter shoot structure: A modelling approach in young "Nonpareil" almond trees. *Funct. Plant. Biol.* **2015**, *42*, 325–335. [CrossRef] [PubMed]
26. Negrón, C.; Contador, L.; Lampinen, B.D.; Metcalf, S.G.; Guédon, Y.; Costes, E.; Dejong, T.M. Differences in proleptic and epicormic shoot structures in relation to water deficit and growth rate in almond trees (*Prunus dulcis*). *Ann. Bot.* **2014**, *113*, 545–554. [CrossRef] [PubMed]
27. Migault, V.; Pallas, B.; Costes, E. Combining Genome-Wide Information with a Functional Structural Plant Model to Simulate 1-Year-Old Apple Tree Architecture. *Front. Plant. Sci.* **2017**, *7*, 2065. [CrossRef] [PubMed]
28. Segura, V.; Cilas, C.; Costes, E. Dissecting apple tree architecture into genetic, ontogenetic and environmental effects: Mixed linear modelling of repeated spatial and temporal measures. *New Phytol.* **2008**, *178*, 302–314. [CrossRef]

29. Segura, V.; Cilas, C.; Laurens, F.; Costes, E. Phenotyping progenies for complex architectural traits: A strategy for 1-year-old apple trees (Malus x domestica Borkh.). *Tree Genet. Genomes* **2006**, *2*, 140–151. [CrossRef]
30. Coupel-Ledru, A.; Pallas, B.; Delalande, M.; Boudon, F.; Carrié, E.; Martinez, S.; Regnard, J.-L.; Costes, E. Multi-scale high-throughput phenotyping of apple architectural and functional traits in orchard reveals genotypic variability under contrasted watering regimes. *Hortic. Res.* **2019**, *6*, 52. [CrossRef] [PubMed]
31. Gradziel, T.M. The utilization of wild relatives of cultivated almond and peach in modifying tree architecture for crop improvement. *Acta Hortic.* **2012**, *948*, 271–278. [CrossRef]
32. Cline, M.G. Apical dominance. *Bot. Rev.* **1991**, *57*, 318–358. [CrossRef]
33. Dun, E.A.; Ferguson, B.J.; Beveridge, C.A. Apical dominance and shoot branching. Divergent opinions or divergent mechanisms? *Plant. Physiol.* **2006**, *142*, 812–819. [CrossRef] [PubMed]
34. Hollender, C.A.; Dardick, C. Molecular basis of angiosperm tree architecture. *New Phytol.* **2015**, *206*, 541–556. [CrossRef]
35. Barbier, F.F.; Dun, E.A.; Kerr, S.C.; Chabikwa, T.G.; Beveridge, C.A. An Update on the Signals Controlling Shoot Branching. *Trends Plant. Sci.* **2019**, *24*, 220–236. [CrossRef]
36. Casal, J.J. Shade Avoidance. *Arab. B.* **2012**, *10*, e0157. [CrossRef]
37. Dun, E.A.; de Saint Germain, A.; Rameau, C.; Beveridge, C.A. Antagonistic action of strigolactone and cytokinin in bud outgrowth control. *Plant. Physiol.* **2012**, *158*, 487–498. [CrossRef]
38. Mason, M.G.; Ross, J.J.; Babst, B.A.; Wienclaw, B.N.; Beveridge, C.A. Sugar demand, not auxin, is the initial regulator of apical dominance. *Proc. Natl. Acad. Sci. USA* **2014**, *111*, 6092–6097. [CrossRef]
39. Pereira-Netto, A.B.; Roessner, U.; Fujioka, S.; Bacic, A.; Asami, T.; Yoshida, S.; Clouse, S.D. Shooting control by brassinosteroids: Metabolomic analysis and effect of brassinazole on Malus prunifolia, the Marubakaido apple rootstock. *Tree Physiol.* **2009**, *29*, 607–620. [CrossRef]
40. Rameau, C.; Bertheloot, J.; Leduc, N.; Andrieu, B.; Foucher, F.; Sakr, S. Multiple pathways regulate shoot branching. *Front. Plant. Sci.* **2015**, *5*, 741. [CrossRef]
41. Kieber, J.J.; Schaller, G.E. Cytokinin signaling in plant development. *Development* **2018**, *145*, dev149344. [CrossRef] [PubMed]
42. Waldie, T.; McCulloch, H.; Leyser, O. Strigolactones and the control of plant development: Lessons from shoot branching. *Plant. J.* **2014**, *79*, 607–622. [CrossRef]
43. Wang, B.; Smith, S.M.; Li, J. Genetic Regulation of Shoot Architecture. *Annu. Rev. Plant. Biol.* **2018**, *69*, 437–468. [CrossRef] [PubMed]
44. De Jong, M.; Ongaro, V.; Ljung, K. Auxin and Strigolactone Signaling are Required for Modulation of Arabidopsis Shoot Branching by Nitrogen Supply. *Plant. Physiol.* **2014**, *166*, 384–395. [CrossRef]
45. Xu, J.; Zha, M.; Li, Y.; Ding, Y.; Chen, L.; Ding, C.; Wang, S. The interaction between nitrogen availability and auxin, cytokinin, and strigolactone in the control of shoot branching in rice (*Oryza sativa* L.). *Plant. Cell Rep.* **2015**, *34*, 1647–1662. [CrossRef]
46. Napoli, C. Highly branched phenotype of the petunia dad1-1 mutant is reversed by grafting. *Plant. Physiol.* **1996**, *111*, 27–37. [CrossRef]
47. Simons, J.L.; Napoli, C.A.; Janssen, B.J.; Plummer, K.M.; Snowden, K.C. Analysis of the DECREASED APICAL DOMINANCE genes of petunia in the control of axillary branching. *Plant. Physiol.* **2007**, *143*, 697–706. [CrossRef]
48. Chesterfield, R.J.; Vickers, C.E.; Beveridge, C.A. Translation of Strigolactones from Plant Hormone to Agriculture: Achievements, Future Perspectives, and Challenges. *Trends Plant. Sci.* **2020**, *25*, 1087–1106. [CrossRef] [PubMed]
49. Génard, M.; Pagès, L.; Kervella, K. Relationship between sylleptic branching and components of parent shoot development in the peach tree. *Ann. Bot.* **1994**, *74*, 465–470. [CrossRef]
50. Ben Yahmed, J.; Ghrab, M.; Ben Mimoun, M. Eco-physiological evaluation of different scion-rootstock combinations of almond grown in Mediterranean conditions. *Fruits* **2016**, *71*, 185–193. [CrossRef]
51. Hearn, D.J. Perennial Growth, Form and Architecture of Angiosperm Trees. In *Comparative and Evolutionary Genomics of Angiosperm Trees*; Groover, A., Cronk, Q., Eds.; Springer: Cham, Switzerland, 2016; Volume 21, pp. 179–204. [CrossRef]
52. De Saint Germain, A.; Ligerot, Y.; Dun, E.A.; Pillot, J.-P.; Ross, J.J.; Beveridge, C.A.; Rameau, C. Strigolactones Stimulate Internode Elongation Independently of Gibberellins. *Plant. Physiol.* **2013**, *163*, 1012–1025. [CrossRef] [PubMed]
53. Finlayson, S.A.; Krishnareddy, S.R.; Kebrom, T.H.; Casal, J.J. Phytochrome regulation of branching in arabidopsis. *Plant. Physiol.* **2010**, *152*, 1914–1927. [CrossRef] [PubMed]
54. Kolesnikov, Y.S.; Kretynin, S.V.; Volotovsky, I.D.; Kordyum, E.L.; Ruelland, E.; Kravets, V.S. Molecular mechanisms of gravity perception and signal transduction in plants. *Protoplasma* **2016**, *253*, 1005. [CrossRef]
55. Schüler, O.; Hemmersbach, R.; Böhmer, M. A Bird's-Eye View of Molecular Changes in Plant Gravitropism Using Omics Techniques. *Front. Plant. Sci.* **2015**, *6*, 1176. [CrossRef] [PubMed]

cita
CENTRO DE INVESTIGACIÓN Y TECNOLOGÍA AGROALIMENTARIA DE ARAGÓN

GOBIERNO DE ARAGON

GOBIERNO DE ESPAÑA
MINISTERIO DE CIENCIA E INNOVACIÓN

Universidad Zaragoza
1542